University of Alberta

Electrocyclization Reactions: Studies on Torquoselectivity and Application Toward the Total Synthesis of Taxinine

by

Chantel L. Benson

A thesis submitted to the Faculty of Graduate Studies and Research
in partial fulfillment of the requirements for the degree of

Doctor of Philosophy

Department of Chemistry

Edmonton, Alberta
Fall 2007

Your file Votre référence
ISBN: 978-0-494-32918-4
Our file Notre référence
ISBN: 978-0-494-32918-4

Abstract

Electrocyclization reactions are valuable carbon-carbon bond forming transformations. Their inherent stereospecificity makes them applicable to stereoselective synthesis of numerous cyclic molecules. Further, factors that control torquoselectivity in the electrocyclization allow control over absolute stereochemistry providing access to compounds with high enantiomeric and diastereomeric purity.

In chapter two, we report the 6π electrocyclization reaction of 1,3,5-trienes encased in chiral bridged bicyclic skeletons. The requisite trienes were easily prepared by reduction of the corresponding dienynes with activated zinc, and most underwent cyclization *in situ* at ambient temperature. While yields in some cases were moderate, it was found that the electrocyclization took place consistently with complete *exo* selectivity. For the 6π electrocyclization of trienes that were a part of a bicyclo[3.2.1]octadiene system, the observed *exo* selectivity stands in contrast to the complete *endo* preference found in a related study on the 4π electron Nazarov cyclization of this particular system.

In chapter three our continued efforts toward the total synthesis of taxinine are recounted. The completion of the synthesis requires a method for annulation of a six-membered ring to a previously established bicyclo[5.3.1]undecene core. Early attempts to cyclize the six-membered ring via enolate chemistry were thwarted due to unfavorable conformational preferences of the bicyclic ring system. We initially focused on the incorporation of functional substitution at an early stage of the synthesis, hoping to provide a handle for later ring closure, but this approach was not successful in the

ultimate goal. Our efforts toward a second annulation strategy involving late-stage C-H insertion via metal-carbenoid chemistry are also presented.

Tandem reactions are an efficient process to quickly build structural complexity from relatively simple precursors. Our studies toward the development of a tandem Nazarov cyclization/Diels Alder cycloaddition are delineated in chapter four. Conditions have been found to effect each transformation separately, and a complex *cis-trans*-fused-5-6-5-tricyclic product is readily obtained from a simple acyclic precursor. Efforts to elaborate this tricyclic product to an angular triquinane structure are also reported.

Acknowledgement

First and foremost I would like to thank my supervisor Dr. Frederick West. His mentorship over the years has been outstanding, and I have learned so much from him about what it takes to do well in research. I am indebted to him for his guidance with respect to the writing of this thesis, and for his support when it came to fellowship and job applications.

I would also like to thank the members of supervisory committee, specifically Drs. Dennis Hall and Todd Lowary for the role that their support has played in the evaluation of my achievements for fellowships and job applications.

I would also like to thank various members of the staff at the University of Alberta, especially Drs. Albin Otter and Michael Ferguson. Their assistance was outstanding and vital to the progression of many projects.

I extend a lot of gratitude to the members of my research group for making the last few years so enjoyable - for their valuable discussions on chemistry, as well as their friendship. In particular I would like to thank Tina Grant, Dr. Hayley Wan, Nina Vo, Graham Murphy and Lei Li.

Finally, I would like to thank my family for always being there to support me over the last few years. Thank you to my little sister for so patiently awaiting "my return home after I'm done school." Thank you to my mother for her encouragement and guidance and to my father for his inspirational eternal optimism. I would also like to thank Neil for his continued support and patience.

Financial assistnce provided by the Natural Sciences and Engineering Research Council of Canada is gratefully acknowledged.

Table of Contents

1. Stereoselective Electrocyclizations 1

1.1. Introduction 1

1.2. Stereocontrol in cationic 4π electron cyclizations 3

1.2.1. Torquoselectivity induced via tetrahedral chirality 4

1.2.2. Torquoselectivity induced via axial chirality 12

1.2.3. Torquoselectivity induced via chiral auxiliary 15

1.2.4. Torquoselectivity induced via chiral Lewis or Brønsted acid 21

1.3. Stereocontrol in 6π electron cyclizations 26

1.3.1. Torquoselectivity in the all carbon 6π electrocyclization 27

1.3.2. Torquoselectivity in the aza 6π electrocyclization 28

1.4. Stereocontrol in 8π, 6π cascade electrocyclizations 32

1.5. Stereocontrol in 8π electrocyclizations 35

1.6. Conclusion 38

1.7. References 39

2. Torquoselectivity in the 6π Electrocyclization of Bridged Bicyclic Trienes 42

2.1. Introduction 42

2.2. Background 43

2.3. Results and Discussion 43

2.4. Conclusion 52

2.5. Experimental 52

2.5.1. General 52

2.5.2. Substrate syntheses and characterization 54

2.6. References 71

3. Approach to the Total Synthesis of Taxinine 73

3.1. Introduction 73

3.1.1. Oxidative fragmentation approach to the taxane core 77

3.1.2. Biological significance of taxinine 80

3.2. Background 81

3.2.1. The first approach to taxinine (Giese) 82

3.2.2. The second approach to taxinine (Mazzola) 86

3.3. Results and Discussion 91

3.3.1. The third approach to taxinine 91

3.3.2. The fourth approach to taxinine 101

3.4. Conclusion and Future work 113

3.5. Experimental 116

3.5.1. General 116

3.5.2. Substrates syntheses 117

3.6. References 139

4. Studies Toward a Tandem Nazarov Cyclization/Diels-Alder Cycloaddition Reaction 143

4.1. Introduction 143

4.2. Background 144

4.3. Results and discussion 146

4.4. Conclusions and Future work 159

4.5. Experimental 160

4.5.1. General 160

4.5.2. Substrate syntheses and characterization 161

4.6. References 167

5. Conclusion 169

Appendices 172

Appendix A: Selected NMR Spectra (Chapter 2) 173

Appendix B: Selected NMR Spectra (Chapter 3) 190

Appendix C: Selected NMR Spectra (Chapter 4) 210

Appendix D: X-ray crystallographic data for compound 58a (Chapter 3) 216

List of Tables

Table 1.1. Denmark's comparison of substituent effects on diastereoselectivity in the silyl-directed Nazarov cyclization. 5

Table 1.2. Prigden's use of a chiral auxiliary in the Nazarov cyclization. 16

Table 1.3. Aggarwal's chiral Lewis acid promoted Nazarov cyclization. 22

Table 1.4. Catalytic asymmetric proton transfer in the Nazarov cyclization 24

Table 1.5. Rueping's use of chiral Brønsted acid in the Nazarov cyclization. 25

Table 2.1. Preparation of dienynes **3a-h**. 44

Table 2.2. Reduction/cyclization of dienynes **3a-h**. 47

Table 3.1. Attempted Mukaiyama aldol of siloxydiene **66** 100

Table 4.1. Lewis acid screen for the Diels-Alder cycloaddition of **5** in refluxing solvent. 151

Table 4.2. Optimization of oxidative cleavage of **6**. 157

List of Figures

Figure 1.1. Depiction of the Woodward and Hoffmann rules (thermal electrocyclizations). 2

Figure 1.2. Proposed explanation for the stereochemical outcome in Nazarov cyclizations promoted by copper(II) pybox complexes. 22

Figure 1.3. Proposed catalytic cycle of the chiral Brønsted acid catalyzed Nazarov cyclization. 26

Figure 2.1. Relative stereochemical assignments of **5a-c**. 49

Figure 2.2. Selected ^{1}H NMR chemical shift data of bridgehead methyls of **5a**,**b** and hydrogens of **5c**. 49

Figure 3.1. Representative examples of members of the taxane family. 74

Figure 3.2. Taxol numbering and ring designations. 75

Figure 3.3. Activation of a δ-C-H bond toward C-H insertion by adjacent heteroatom substitution. 102

Figure 3.4. C-H insertion at a δ-benzylic position. 102

Figure 3.5. δ-Lactone formation via C-H insertion. 103

Figure 3.6. Target diazo compound. 104

Figure 3.7. Proposed equilibrium of **78** with a hemi-ketal. 107

Figure 4.1. Representative natural products containing angularly fused triquinane cores 146

Figure 4.2. Transition states leading to *exo* and *endo* diastereomers 152

Figure 4.3. Selected ^{1}H and ^{13}C resonances in **19** 154

Figure 4.4. Resonance contribution to the structure of **19**. 154

Figure 4.5. NOE interactions in **19**. 155

List of Schemes

Scheme 1.1. The classic Nazarov cyclization. 3

Scheme 1.2. Effect of β'-Si stereocenters on the Nazarov cyclization. 6

Scheme 1.3. Nazarov cyclization of heteroatom substituted conjugated alkoxy trienes. ... 6

Scheme 1.4. Effect of substituent position in the Nazarov cyclization. 7

Scheme 1.5. Nazarov cyclization of 2-substituted pyrroline analogs. 8

Scheme 1.6. Nazarov cyclization of substituted dihydropyran derivatives. 9

Scheme 1.7. Formation of spirocyclic enones via the Nazarov cyclization. 10

Scheme 1.8. Possible modes of rotation in formation of spirocyclic enones. 11

Scheme 1.9. Nazarov cyclization of bridged bicyclic dienones. 12

Scheme 1.10. Chirality transfer in the allenyl Nazarov reaction. 13

Scheme 1.11. Explanation for the observed stereochemical outcome in the chiral allenyl-Nazarov cyclization. 14

Scheme 1.12. Nazarov cyclization of allenyl dioxolanes. 15

Scheme 1.13. Flynn's use of Evans' oxazolidinone in the Nazarov cyclization. 17

Scheme 1.14. Tius' use of a glucose derived auxiliary in the Nazarov cyclization. 18

Scheme 1.15. Tius' second generation chiral auxiliary. 19

Scheme 1.16. Tius' camphor derived auxiliary. 20

Scheme 1.17. Tius' modified pyranose-derived chiral auxiliary. 21

Scheme 1.18. Trauner's chiral Lewis acid catalyzed Nazarov cyclization 23

Scheme 1.19. Axial to tetrahedral chirality transfer in the 6π electrocyclization 27

Scheme 1.20. Magomedov's torquoselective 6π electrocyclization 28

Scheme 1.21. Use of a chiral auxiliary in the aza-6π electrocyclization. 29

Scheme 1.22. Explanation for observed stereoselectivity in Katsumura's asymmetric aza-6π electrocyclization. 30

Scheme 1.23. Hsung's torquoselective aza-6π electrocyclization. 31

Scheme 1.24. Hsung's revised torquoselective aza-6π electrocyclization. 32

Scheme 1.25. 8π, 6π Cascade: proposed biosynthesis to the bicyclo[4.2.0]octadiene core. 33

Scheme 1.26. 8π, 6π Cascade in the synthesis of SNF4435 compounds. 34

Scheme 1.27. Recently discovered non-racemic bicyclo[4.2.0]octane natural products.. 35

Scheme 1.28. Paquette's squarate ester cascade. 36

Scheme 1.29. Paquette's theory of torquoselectivity in the 8π electrocyclization. 37

Scheme 1.30. Paquette's torquoselective 8π electrocyclization. 37

Scheme 2.1. Reduction and *in situ* electrocyclization of **3a**. 45

Scheme 2.2. Steric factors in electrocyclization reactions. 51

Scheme 2.3. Aromatization of **5d**,**e**. 52

Scheme 3.1. Trost's oxidative cleavage strategy. 78

Scheme 3.2. Blechert's oxidative cleavage strategy. 79

Scheme 3.3. Little's oxidative cleavage strategy. 80

Scheme 3.4. Retrosynthesis of taxinine: first approach. 82

Scheme 3.5. Preparation of ketone **27** and its conjugate reduction. 83

Scheme 3.6. Preparation of **30** by selenoxide elimination and subsequent methylation.. 84

Scheme 3.7. Elaboration of **30** to the tricyclic taxane core. 85

Scheme 3.8. Retrosynthesis of taxinine: second approach. 86

Scheme 3.9. Carbonylative Stille coupling, Nazarov cyclization and methylation..... 87

Scheme 3.10. Elaboration of ketone **46** to diketone **51**. 89

Scheme 3.11. Attempt to form the tricyclic taxinine core. 90

Scheme 3.12. Retrosynthesis of taxinine: third approach..... 92

Scheme 3.13. Installation of the C3 isopropenyl group to **45**..... 93

Scheme 3.14. Attempted conversion of **58** to selenide **59**..... 94

Scheme 3.15. Vinylation of **45** and attempted selenylation..... 96

Scheme 3.16. Attempted selenylation of ketone **63**..... 97

Scheme 3.17. Attempted reversal in functionalization of **45**..... 98

Scheme 3.18. Generation of siloxy diene **66**. 99

Scheme 3.19. Attempted MOM deprotection of **51**..... 105

Scheme 3.20. Reduction of diketone **51**. 106

Scheme 3.21. Preparation of monoacetate **80**..... 107

Scheme 3.22. Attempted elaboration of **83** to a β-Keto ester..... 109

Scheme 3.23. Preparation of allylic acetate **84**..... 110

Scheme 3.24. Preparation of diketone **90**. 111

Scheme 3.25. Preparation of β-keto ester **94.** 112

Scheme 3.26. Elaboration of **94** to β-keto diazo ester **95** and attempted diazo decomposition. 113

Scheme 3.27. Future plans: accessing the C3 enolate via conformational change induced by C10 reduction..... 115

Scheme 3.28. Future plans: accessing the C3 enolate via conformational change induced by C11-C12 pyramidalization..... 115

Scheme 4.1. Trapping of the Nazarov intermediate by [4+3] cycloaddition..... 144

Scheme 4.2. Possible reaction pathways after Nazarov cyclization of tetraenone **3**..... 145

Scheme 4.3. Preparation of tetraenone **3**. 147

Scheme 4.4. Nazarov cyclization of **3**. 148

Scheme 4.5. Optimized microwave irradiated Diels Alder cycloaddition of **5**. 149

Scheme 4.6. Optimized Lewis acid promoted Diels-Alder cycloaddition of **5**. 151

Scheme 4.7. Methylation of diastereomeric **6**. 153

Scheme 4.8. Oxidative cleavage and aldol condensation of **6**..... 156

Scheme 4.9. Attempted aldol condensation of **20**..... 158

Standard List of Abbreviations

Ac	acetyl
Ar	aryl
app	apparent (spectral)
aq	aqueous
Bn	benzyl
br	broad (spectral)
i-Bu	*iso*-butyl
n-Bu	butyl
t-Bu	*tert*-butyl
°C	degrees Celcius
calcd	calculated
Cbz	benzloxycarbonyl
CSA	(1*S*)-camphorsulphonic acid
d	day(s); doublet (spectral)
DBU	1,8-diazabicyclo[5.4.0]undec-7-ene
dd	doublet of doublets (spectral)
DDQ	2,3-dichloro-5,6-dicyano-1,4-benzoquinone
DHP	dihydropyran
DIBALH	diisobutylaluminum hydride
DIPA	diisopropylamine
DMAP	4-dimethylaminopyridine
DMP	Dess-Martin periodinane

DMSO	dimethyl sulfoxide
dr	diastereomeric ratio
EDA	ethyl diazoacetate
ee	enantiomeric excess
EI	electron impact (mass spectrometry)
eq	equivalents
ESI	electrospray ionization (mass spectrometry)
EtOAc	ethyl acetate
g	gram(s)
h	hour(s)
HFIP	hexafluoroisopropyl alcohol
HMPA	hexamethylphosphoramide
HRMS	high resolution mass spectrum
Hz	Hertz
IBX	*o*-iodoxybenzoic acid
IR	infrared
J	coupling constant (NMR)
LDA	lithium diisopropylamine
L-Selectride	lithium tri-*sec*-butylborohydride
LTMP	lithium tetramethylpiperidide
M	moles per liter
m	multiplet (spectral)
m-CPBA	*m*-chloroperoxybenzoic acid

Me	methyl
MHz	megahertz
min	minute(s)
mol	mol(s)
MOM	methoxy methyl
mmol	millimole(s)
m.p.	melting point
MS	molecular sieves
m/z	mass to charge ratio (mass spectrometry)
NMO	*N*-methylmorpholine-*N*-oxide
NMR	nuclear resonance spectroscopy
Nu	nucleophile
Ph	phenyl
ppm	parts per million (NMR)
pyr	pyridine
q	quartet (spectral)
R_f	retention factor (chromatography)
rt	room temperature
s	singlet (spectral); second(s)
t	triplet (spectral)
TBAF	tetra-*n*-butylammonium fluoride
TBDPS	*tert*-butyldiphenylsilyl
TBS	*tert*-butyldimethylsilyl

Tf	trifluoromethanesulfonyl
TFE	2,2,2-trifluoroethanol
THF	tetrahydrofuran
THP	tetrahydropyran
TIPS	triisopropylsilyl
TLC	thin layer chromatography
TMS	trimethylsilyl
TPAP	tetra-*n*-propylammonium perruthenate
Ts	tosyl; *p*-toluenesulfonyl
p-TsOH	*p*-toluenesulfonic acid

1. Stereoselective Electrocyclizations

1.1. Introduction

Electrocyclic transformations constitute a class of reactions that are characterized by sigma bond formation between the termini of linear conjugated *n* π systems. The converse process, sigma bond cleavage in a cyclic system containing (*n*-2) π electrons may also be categorized under this heading.[1] Over 40 years ago, reports of opposing stereochemical results observed in thermal and photochemical electrocyclizations by others as well as themselves prompted Woodward and Hoffmann to develop and disclose their now famous conservation of orbital symmetry theory.[2] The simplicity of the theory is stunning, as is the accuracy with which it predicts the stereochemical outcome in electrocyclic transformations. One has only to consider the symmetry of the highest occupied molecular orbital (HOMO) in the acyclic component to understand the process. For bond formation to occur, the phase relations of the terminal molecular orbitals must be in harmony. Therefore, during bond formation (or cleavage), the termini must rotate in a synchronous or asynchronous fashion to fulfill this requirement. The terms conrotatory and disrotatory have been invoked to describe this sense of directionality. For

thermal electrocyclizations, the Woodward and Hoffman rules state that *reactions involving 4n electrons are allowed if they proceed by conrotatory paths*, while those *involving 4n+2 electrons are allowed if they proceed by disrotatory paths* (Figure 1.1). As a result, stereochemical relationships between the terminal substituents in the electrocyclic products are preordained by the geometry of the starting material, a concept known as stereospecificity.

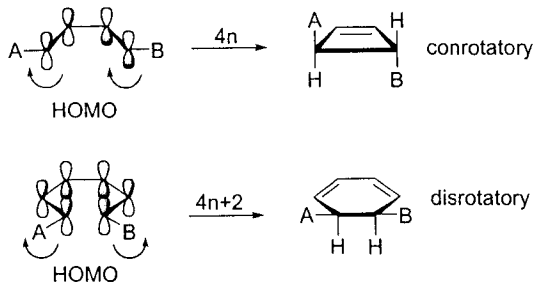

Figure 1.1. Depiction of the Woodward and Hoffmann rules (thermal electrocyclizations).

From the above discussion, it can be seen how stereospecificity arises in the given products of a particular electrocyclization. However, in the absence of influencing factors, there is an equal probability for the direction of con- or disrotation to proceed in either clockwise or counterclockwise fashion. In simple achiral substrates, this is of little consequence, but in more complex systems it becomes relevant as lack of rotational selectivity may lead to diastereoisomerism. A term known as torquoselectivity was invented by Houk to describe electrocyclization reactions that are, for a variety of possible reasons, biased towards a particular rotational mode.[3] Houk has since performed detailed computational studies on torquoselectivity in 4π,[4,5] 6π,[6] and 8π[7] electrocyclizations to determine the effect that the electronic and steric nature of

substituents attached to the forming and breaking bonds might have. This is one possible way to invoke torquoselection, but there are numerous others. A discussion of relevant examples of torquoselectivity in 4π, 6π, and 8π thermal electrocyclization reactions follows.

1.2. Stereocontrol in cationic 4π electron cyclizations

The 4π electrocyclization of oxy-pentadienyl cations has been termed the Nazarov cyclization.[8] In its most frequently encountered form, a divinyl ketone (**1**, Scheme 1.1) is subjected to acidic conditions (Brønsted or Lewis) to generate a pentadienyl cation, which then undergoes conrotatory 4π electron cyclization. After deprotonation and reprotonation of the allyl cation intermediate, substituted cyclopentenone products **3** result. As such, this is an excellent method for the generation of functionalized cyclopentenones and has received much attention in recent years.[9]

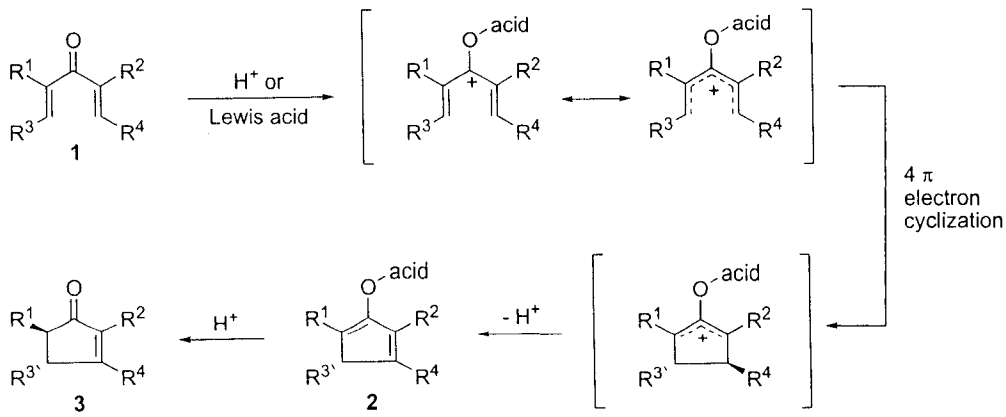

Scheme 1.1. The classic Nazarov cyclization.

Torquoselectivity in the Nazarov cyclization has been studied in some detail. One drawback of this process, however, is the necessary obliteration of one of the newly formed stereocenters by deprotonation of the oxy-allyl intermediate to give alkene **2** (Scheme 1.1). An additional stereocenter is created by reprotonation of **2** to give **3**. Providing this transformation takes place with some selectivity, products with high diastereomeric purity result. On the other hand, one way to avoid loss of the original stereocenter in the first place, is via the "interrupted" Nazarov process, whereby the intermediate allyl cation is intercepted via nucleophilic capture in either inter- or intramolecular fashion. This extension of the Nazarov cyclization has been reviewed elsewhere, and for that reason will not be discussed here.[9] What follows is a brief summary of methods that have been developed for induction of chirality in the simple Nazarov cyclization.

1.2.1. Torquoselectivity induced via tetrahedral chirality

Advancements in the torquoselective Nazarov cyclization began as early as 1986 when Denmark and coworkers reported that silicon-directed Nazarov cyclization of dienones bearing substituted cyclohexenyl moieties (**4**, Table 1.1) led to predominant formation of *trans* isomers **5** with exclusive *cis* stereochemistry at the ring fusion positions.[10] This preference was attributed to a steric effect of the R substituent, which forces the direction of conrotation to the less hindered face of the cyclohexyl unit. Thus, for more bulky R groups (entries 2 and 3), the ratio of **5** relative to **6** greatly increases.

The authors also found that steric bulk on the silyl substituent could be used to favor the formation of **5** (entry 4).

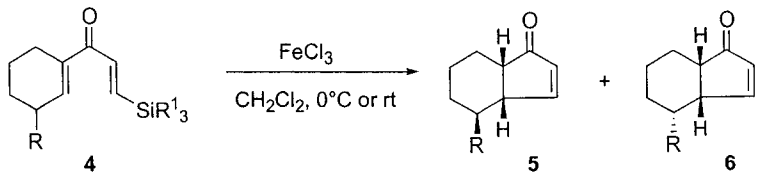

entry	R^1	R	Yield / %	ratio of 5:6
1	CH_3	CH_3	99	78:22
2	CH_3	C_6H_5	76	94:6
3	CH_3	$C(CH_3)_3$	63	94:6
4	*i*-Pr	CH_3	70	90:10

Table 1.1. Denmark's comparison of substituent effects on diastereoselectivity in the silyl-directed Nazarov cyclization.

In later work, Denmark found an effect of β'-silicon stereocenters on the stereochemistry of the cyclization.[11] When either of the corresponding *R* or *S* enantiomers of dienone **7** was treated with $FeCl_3$ to effect Nazarov cyclization, the products formed had retained the enantiomeric purity of the starting material (Scheme 1.2). The original silyl-bearing stereogenic center was destroyed, but its stereochemical information was transcribed to three new stereocenters via chirality transfer. The preferred sense of conrotation in each case was said to be a result of the beneficial continuous overlap of silicon with the forming allyl cation that is permitted through only one direction of conrotation.

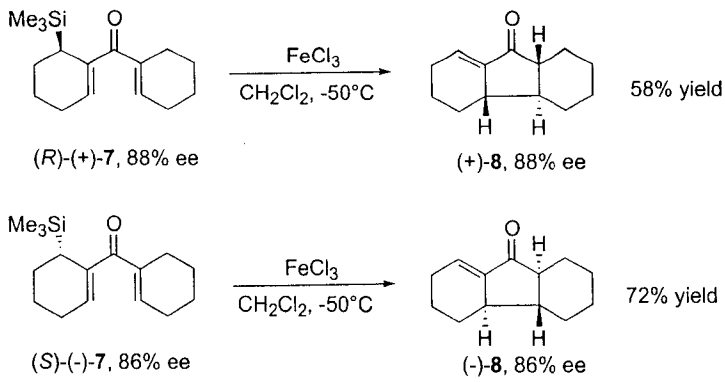

Scheme 1.2. Effect of β'-Si stereocenters on the Nazarov cyclization.

Occhiato and Prandi have studied in some detail substituent effects on torquoselectivity in Nazarov cyclizations of conjugated alkoxy trienes in which one of the double bonds is embedded in a heterocyclic moiety.[12] These substrates provide an alternative entry to the Nazarov oxy-cyclopentadienyl cation. They react under much milder conditions than analogous non-heteroatom substituted dienone substrates. The reaction proceeds by protonation of the ethoxy ether **9** at the terminal alkene position, followed by Nazarov cyclization of the resulting pentadienyl cation, and is completed by hydrolysis to the ketone **10** (Scheme 1.3).

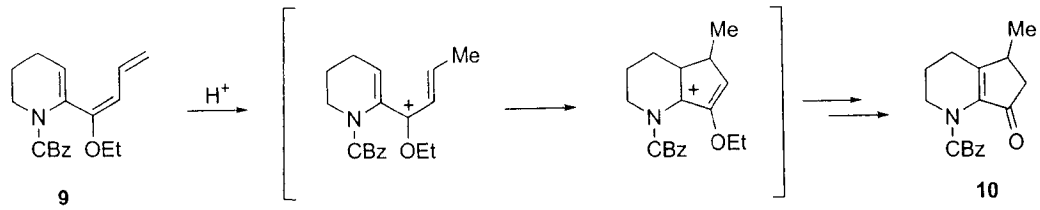

Scheme 1.3. Nazarov cyclization of heteroatom substituted conjugated alkoxy trienes.

When 2-, and 4-, substituted trienes **11a** and **b** were subjected to hydrolysis with Amberlyst-15, 67% and 46% yields of cyclized products were obtained each as only one

diastereomer (**12a**, **b**, Scheme 1.4). However, in the case of 3-substituted **11c**, the cyclization occurred to give a 2:1 ratio of **12c** diastereomers. The formation of products **12a** and **12b** was explained primarily based on steric effects, which favor an approach of the pentadienyl terminus to the less hindered face of the endocyclic olefin. For **12b**, additional stabilization is conferred via a chair-like conformation of the six-membered ring in the transition state. This is not the case for **12a**, however. The 2-Me substituent is said to prefer a pseudo-axial orientation to reduce allylic strain with the Cbz group on the nitrogen atom. The transition state resembles a twist-boat, but proceeds to the observed product despite this. In this case, the formation of **12a** likely takes place only under steric control. Finally, the low diastereoselectivity observed in the cyclization of **11c** was explained by poor steric differentiation of the two faces of the endocyclic olefin due to the equatorial disposition of the 3-Me substituent, and its distance from the reacting center.

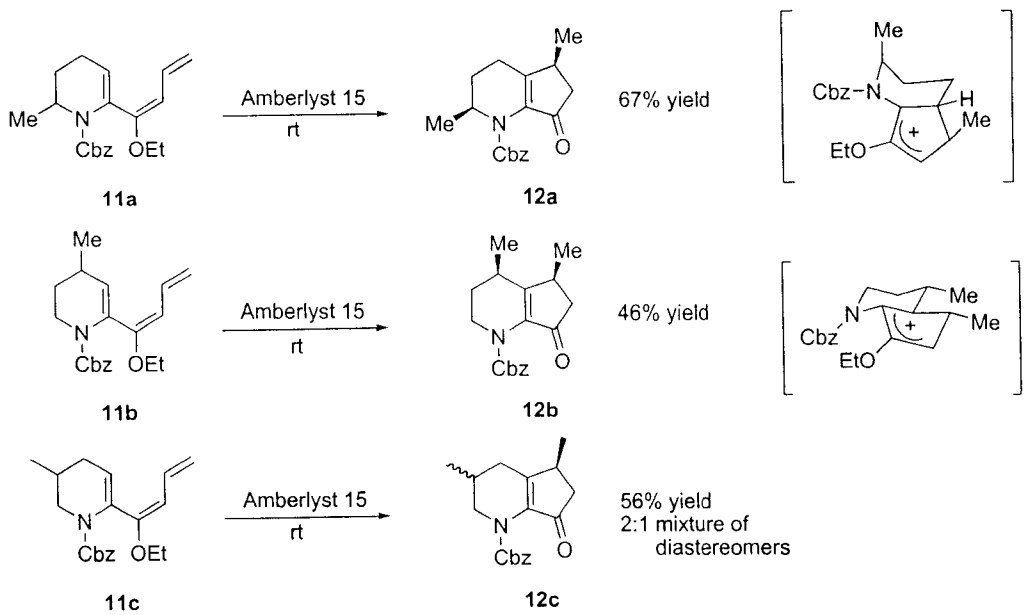

Scheme 1.4. Effect of substituent position in the Nazarov cyclization.

In a subsequent publication, Occhiato and Prandi elaborated on the scope of this stereoselective cyclization.[13] The reaction was attempted with 2-substituted pyrroline analog **13** (Scheme 1.5). Due to the strain associated with a 5-5 fused system, enol ether **13** did not go directly to the Nazarov product **15** on treatment with Amberlyst 15, and the intermediate dienone **14** was isolated instead. It was necessary to treat **14** in a separate step with a stronger protic acid – neat TFA, to promote its cyclization. This provided **15** in 50% yield as one diastereomer. The stereochemical outcome is consonant with the results obtained in the analogous substituted-piperidine cyclization (Scheme 1.4). The same group has applied this methodology to a nonracemic synthesis of roseophilin.[14]

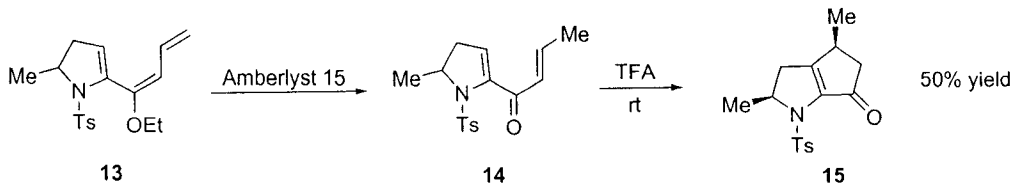

Scheme 1.5. Nazarov cyclization of 2-substituted pyrroline analogs.

The viability of the corresponding series of substituted oxacycles remained to be tested in the torquoselective Nazarov cyclization. Therefore, 1- and 4-substituted dihydropyrans **16a**, **b** were prepared and subsequently treated with Amberlyst 15 at room temperature (Scheme 1.6). In the case of **16a**, *trans*-**17a** was observed as the major product (in addition to small amounts of spirocyclized product **18a**), while **16b** gave *cis*- and *trans*-**17b** in a ratio of 2:1 along with significant amounts of **18b**. The reasons for the divergent *trans* selectivity in the cyclization of **16a** remain unclear, but the authors postulate that it may be due to a stereoelectronic effect. In the transition state, the pyran

ring must adopt a boat-like conformation to give the resulting stereochemical relationship and this may provide better orbital overlap during the formation of the new bond.

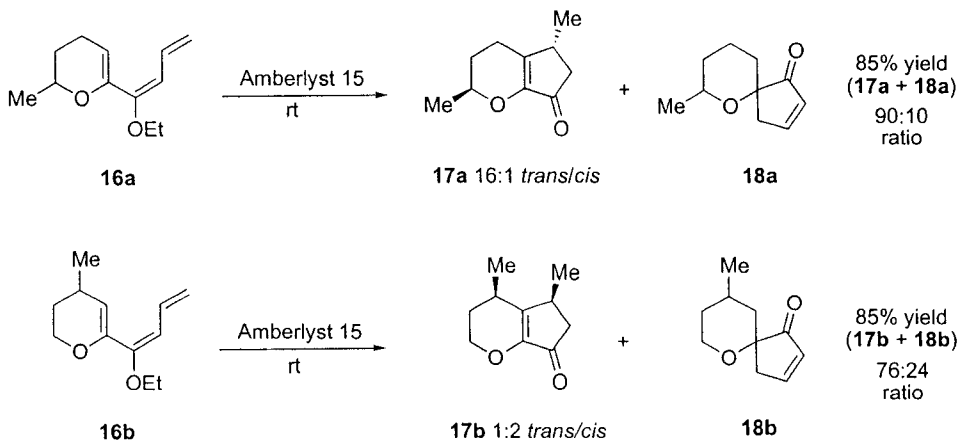

Scheme 1.6. Nazarov cyclization of substituted dihydropyran derivatives.

The unexpected formation of spirocyclic products **18a, b** (Scheme 1.6) prompted an investigation into the mechanism and stereoselectivity of this process, as this functional group is present in many biologically active compounds.[15] Initially, conditions were sought to maximize the yield of these interesting by-products. It was found that for trienes in which the dienyl moiety is terminally disubstituted (**19**, Scheme 1.7), Amberlyst 15 promoted exclusive cyclization to the spiro ketones **20**. The *geminal* dimethyl center is thought to stabilize the intermediate positive charge that develops on protonation of the dihydropyran, and cyclization then proceeds entirely through the spirocyclic pathway.

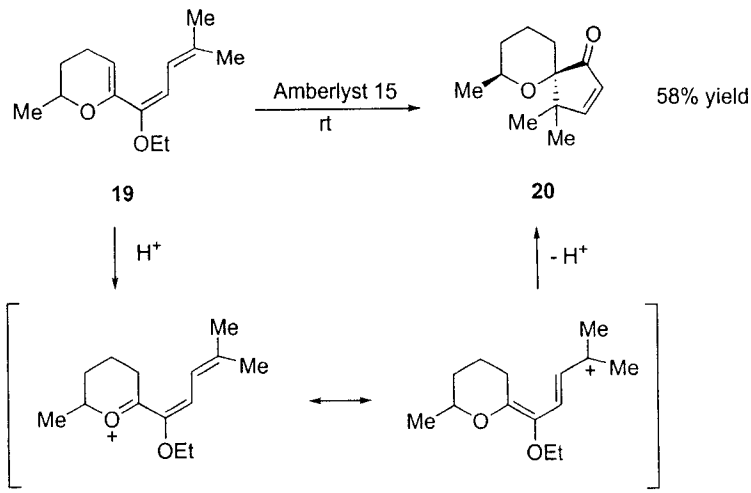

Scheme 1.7. Formation of spirocyclic enones via the Nazarov cyclization.

In order to explain the stereochemical outcome observed in the spirocyclization, the authors examined putative intermediates in the transition states leading to each of the two potential diastereomeric products (Scheme 1.8). The diastereomeric spirocycles would arise from either clockwise or counterclockwise rotation of the intermediate pentadienyl cation termini (mode a or b respectively). Clockwise rotation (mode a) would result in the formation of an unfavorable twist-boat intermediate **A**, and the isomer expected from this rotation was therefore not observed. Instead, counterclockwise rotation (mode b), which proceeds through a chair-like transition state (**C**), led to the formation of **20**.

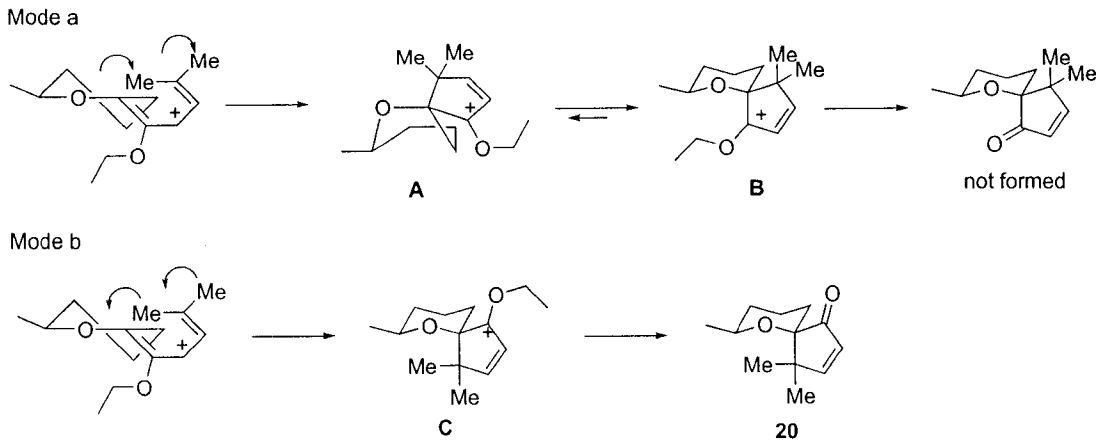

Scheme 1.8. Possible modes of rotation in formation of spirocyclic enones.

West and coworkers have reported a torquoselective Nazarov cyclization of dienones that are embedded in bridged bicyclic structures.[16] They found that camphor-derived dienone **21** cyclized in the presence of $BF_3{\cdot}OEt_2$ to *exo* **22**, as the only diastereomer (Scheme 1.9). Other bicyclic systems investigated gave similar selectivity. However, in the case of bicyclo[3.2.1]octadiene **23**, the product **24** demonstrated a complete reversal in torquoselectivity, as the product was found to have an *endo* orientation of the cyclopentenone moiety. The selectivity of *exo*-cyclized **22** was rationalized based on analogy to the thoroughly studied electrophilic addition to norbornene, where reaction occurs preferentially from the *exo*-face of the bicycle. The complete *endo* selectivity resulting from cyclization of **23** was unexpected, and not fully understood. Further studies indicated that the presence of the remote olefin in the 3-carbon bridge of the bicyclic moiety is required for the prevailing *endo* selectivity, as $BF_3{\cdot}OEt_2$ induced cyclization of reduced derivatives of **23** resulted in formation of *exo* products.

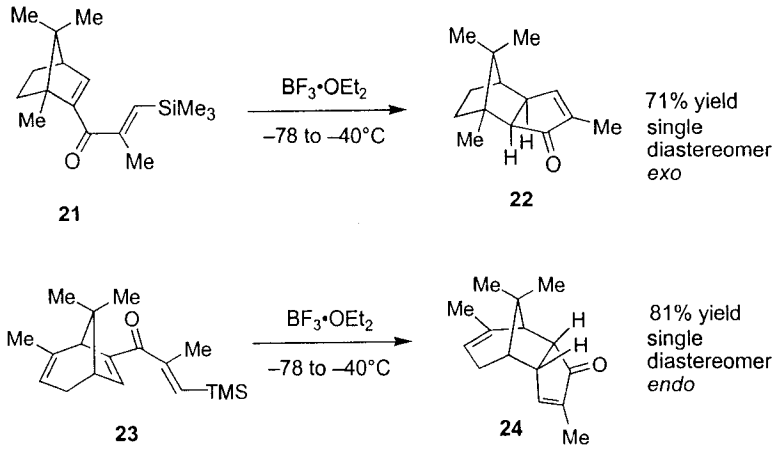

Scheme 1.9. Nazarov cyclization of bridged bicyclic dienones.

1.2.2. Torquoselectivity induced via axial chirality

In his studies on the allenyl-Nazarov reaction,[17] Tius discovered the effect that an axially chiral allene can have on the preferred conrotation of the cyclization.[18] Morpholino amides **25a,b** (Scheme 1.10) were prepared independently as racemic mixtures, then separated into their enantiomeric counterparts via chiral HPLC resolution. Individual treatment of (-)-**25a** with vinyl lithium species **26** produced allenyl vinyl ketone **27a**, which cyclized during work-up to cyclopentenone (+)-**28a** accompanied by a small amount of diastereomeric (-)-**29**. Compound **28a** was formed with 84% chirality transfer demonstrating the effect the chiral allene has on directing the cyclization. The effect is even more pronounced when *t*-Bu substituted morpholino amide (+)-**25b** participated in the cyclization. The product, **27b**, was obtained with >95% chirality transfer, and none of the other diastereomer was detected in this case. Grimme[19] and Hoppe,[20] reported a similar outcome in their application of easily prepared,[21] optically active allene carbamates to the cyclization.

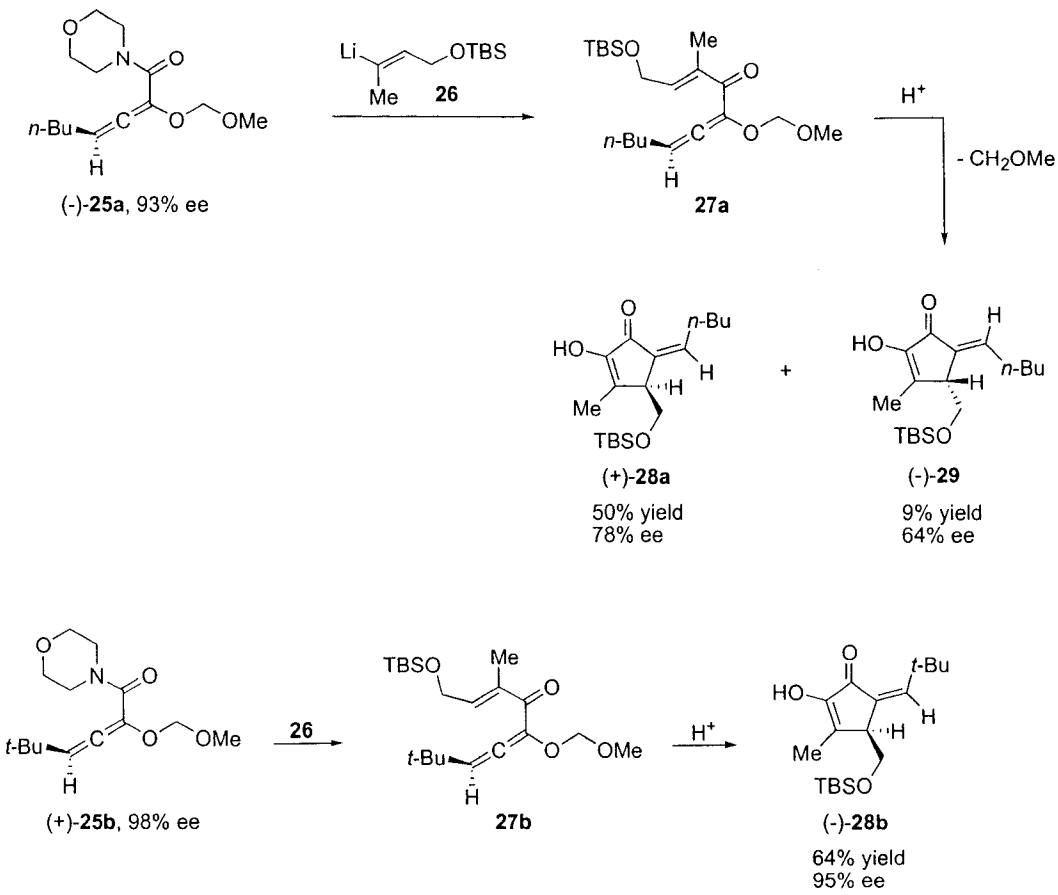

Scheme 1.10. Chirality transfer in the allenyl Nazarov reaction.

Tius offered an explanation for the axial to tetrahedral chirality transfer in the allenyl Nazarov cyclization. Essentially, the bulky allenyl substituent R^3 prefers to rotate away form the alkene (mode a, Scheme 1.11) in a clockwise direction to give the product with *Z* geometry about the exocyclic olefin. Rotation in the opposite direction (mode b, counterclockwise) gives rise to the corresponding *E* diastereomer and is disfavored by developing steric congestion between R^3 and R^2.

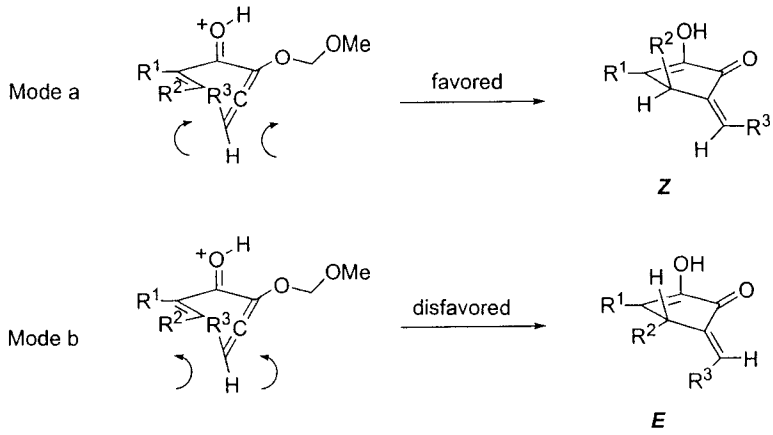

Scheme 1.11. Explanation for the observed stereochemical outcome in the chiral allenyl-Nazarov cyclization.

De Lera and coworkers have performed related studies on the acid-catalyzed rearrangement of (2-*Z*)-hexa-2,4,5-trienal acetals **29** to tetrahydroalkylidenecyclopenta-1,4-dioxins **30** (Scheme 1.12).[22] This reaction can be considered to occur through a Nazarov-like process, and as such, the stereochemical outcome should be subject to influence by the chirality of the allene. In preliminary studies, de Lera found evidence for the exclusive formation of expected kinetic product *E*-**30** at low temperatures. This is in agreement with Tius' finding, where the product arises from outward rotation of the allenyl R substituent (Scheme 1.11). However, at room temperature, the only product isolated in 99% yield was thermodynamic product *Z*-**30**. This presumably arises through equilibration of *E*-**30** to avoid unfavorable interactions between the *t*-Bu and R substituents. The thermodynamic selectivity was not found to be general, as when other R groups were employed, near 1:1 ratios of *Z* to *E* products were isolated.

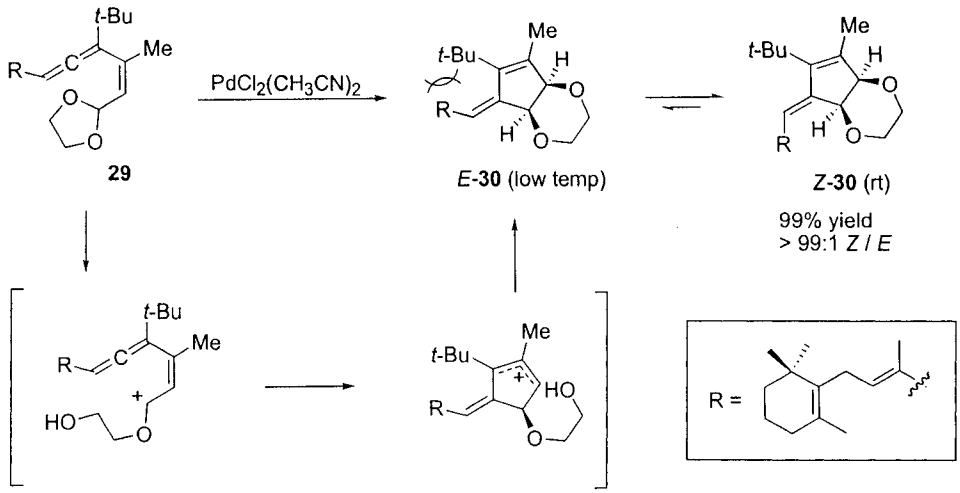

Scheme 1.12. Nazarov cyclization of allenyl dioxolanes.

1.2.3. Torquoselectivity induced via chiral auxiliary

Pridgen was the first to implement the use of chiral auxiliaries in the traditional Nazarov reaction.[23] The influence of Evans' oxazolidinone and 8-phenyl menthol were compared in the acid catalyzed cyclization of **31** (Table 1.2). It was observed that both auxiliaries furnished the major diastereomer **32** in good yield and diastereoselectivity. Small amounts of diastereomer **33** were also isolated in each case. It appeared that chelation through the auxiliary in the usual sense was not necessary for chiral induction in this case because of the observation that 8-phenyl menthol (entry 2) was as effective as the oxazolidinone (entry 1). Further studies indicated that the cyclization could be carried out just as efficiently with non-chelating protic acid CH_3SO_3H (entry 3). Evidence from X-ray data of **31** led Prigden to believe that the structure exists with a highly transoid geometry (see Table 1.2), but the steric influence of the auxiliary remains strong nonetheless.

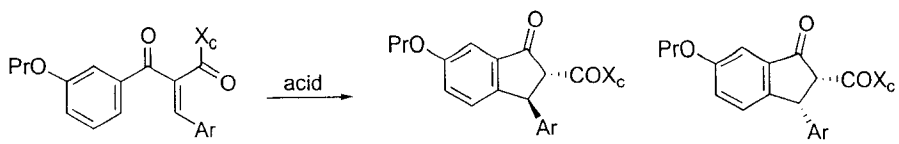

31 32 33

entry	acid	yield	product ratio 32:33:other
1	$SnCl_4$	85	88:12:0
2	$SnCl_4$	90	92:4:4
3	CH_3SO_3H	88	85:15:0

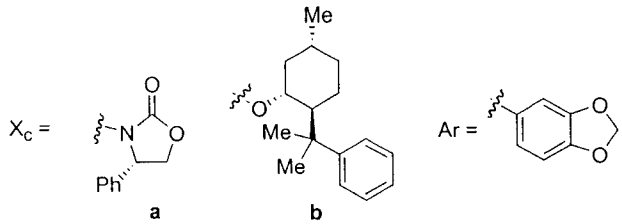

Table 1.2. Prigden's use of a chiral auxiliary in the Nazarov cyclization.

Flynn has recently developed an efficient two step protocol for the synthesis of cyclopentenones via Nazarov cyclization beginning with simple starting materials. Within this, he has reported an asymmetric variant employing Evans' oxazolidinone (Scheme 1.13).[24] Palladium mediated *syn*-hydrostannylation of alkyne **34** gave a vinyl stannane that was directly coupled with acyl chloride **35** using CuCl to furnish the requisite dienone **36**. Subsequent treatment of the resulting dienone product **36** with $MeSO_3H$ followed by either low temperature or room temperature quench, led to 73 or 76% yield of kinetic *cis*-**37** or thermodynamic *trans*-**37**. Given that both enantiomers of the chiral auxiliary are available, this protocol provides access to all four possible stereoisomers of the cyclopentenone.

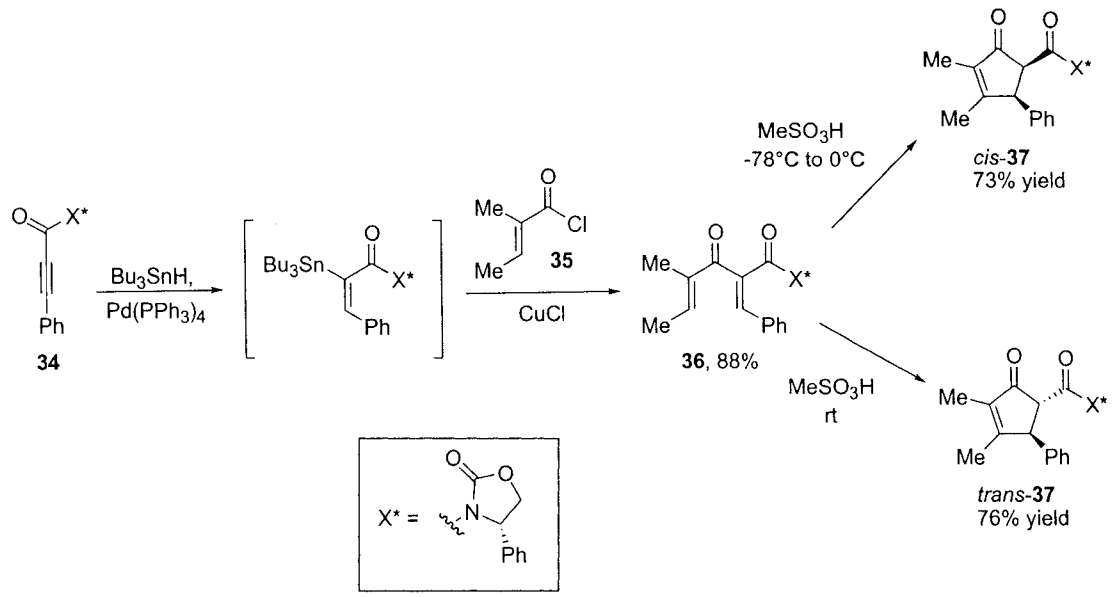

Scheme 1.13. Flynn's use of Evans' oxazolidinone in the Nazarov cyclization.

Tius and coworkers have devoted much effort to find an ideal chiral auxiliary for use in the allene ether Nazarov cyclization. The previously described chiral allenyl Nazarov relies on the inherent chirality of the allene to influence the stereochemical course of the cyclization (Scheme 1.10). By necessity, this route provides products where the exocyclic alkene is substituted. To allow for the formation of cyclopentenones with an unsubstituted exocyclic alkene, an alternate, cleavable chirality source was required. Tius' initial work focused on the use of glucose- derived auxiliaries located on the allene (**38**, Scheme 1.14).[25] To test its influence on the cyclization, allene **38** was lithiated, then added to morpholino amide **39** in the presence of LiCl (to allow for efficient addition to the amide). As before, the cyclization occurred *in situ*, and the auxiliary was cleaved during the course of the reaction. The yields of the transformation at this stage were moderate, as were ee's. However, an interesting finding was that the α- and β-anomers of the auxiliary each promoted conrotation in opposing directions, thus

affording access to either enantiomer of the product. Although no reason was offered at the time, the β-anomer of **38** gave products with greater optical purity than α-**38**.

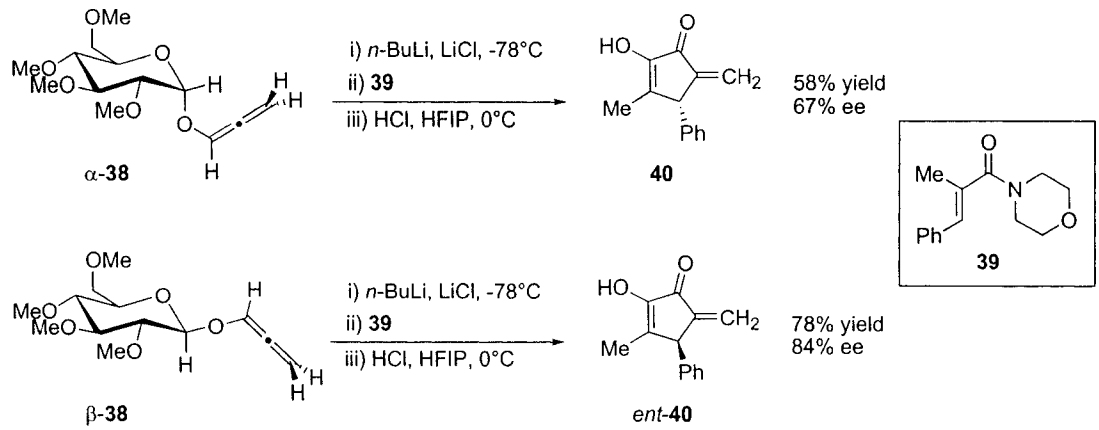

Scheme 1.14. Tius' use of a glucose derived auxiliary in the Nazarov cyclization.

Though the protocol developed by Tius implementing a glucose derivative as chiral auxiliary provided acceptable yields and ee's of the cyclopentenone products, significant erosion in enantioselectivity was experienced on attempted scale up. Therefore, a second generation auxiliary was developed based on camphor (Scheme 1.15).[26] When allene **41** was reacted with **39** (no LiCl necessary), the product **42** was formed in moderate yield with 77% ee. Though there was not much improvement in yield or ee with this protocol, it was amenable to scale up, and therefore constitutes a much better approach. As a testament to its worth, this protocol has been utilized in the key step of the group's asymmetric total synthesis of roseophilin.[27]

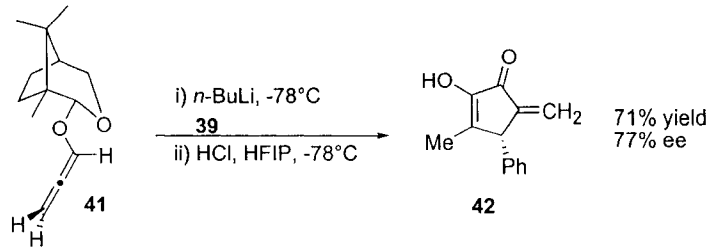

Scheme 1.15. Tius' second generation chiral auxiliary.

With the establishment of a suitable auxiliary to effect torquoselection in the Nazarov cyclization, the Tius group wondered what effect an intrinsically chiral allene might have in competition with the auxiliary. Therefore, examples where the allene moiety bore a terminal substituent were investigated as well (Scheme 1.16). Under the reaction conditions, allene **43** gave predominantly *Z*-**45** with the highest ee observed at that point. A small amount of isomerized *E*-**45** was also isolated. It would appear that the excellent ee observed is a result of matched chirality of the auxiliary and allene, which doubly enforces conrotation in a single direction. However, with substrate **46** (9:1 ratio of allenyl epimers), kinetic product *Z*-**47** was formed with much reduced ee. In this case, the chirality of the auxiliary and allene are mismatched, and the intrinsic chirality of the allene completely overwhelms that of the auxiliary as indicated by the fact that *Z*-**47** is enantiomeric to *Z*-**45**. The stereochemical rationale for the matched case is highlighted in Scheme 1.16. The conformation of the pentadienyl cation is restricted due to its coordination with the pyranyl oxygen. The auxiliary influences conrotation in a counterclockwise motion to bring the terminal Me group of the pentadienyl cation away from the steric bulk of the auxiliary. The allene enforces this direction of rotation by having its *t*-Bu substituent rotate away from this same methyl group.

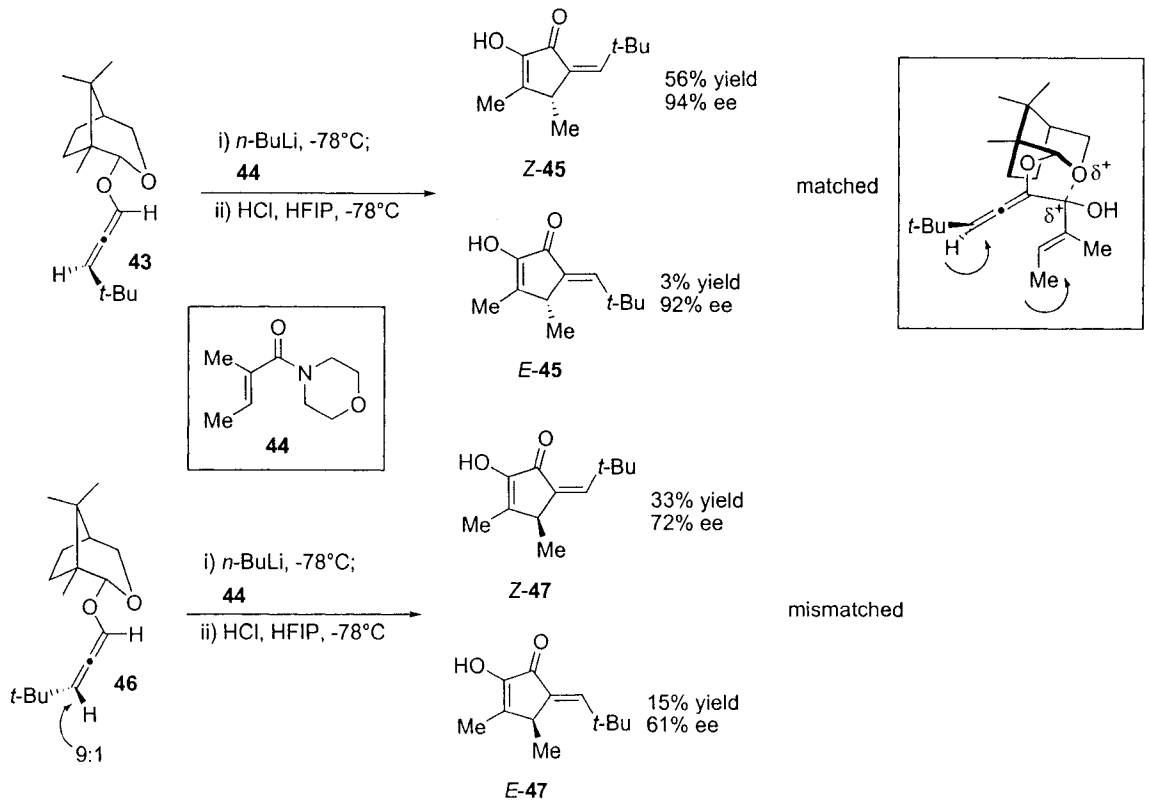

Scheme 1.16. Tius' camphor derived auxiliary.

Recently, Tius has reinvestigated the use of the glucose-derived auxiliary described in Scheme 1.14. He has found that a modified version, where the Me protecting groups have been exchanged for TBS, as well as removal of the glycosyl C-2 substituent, gives far superior results to those obtained in both the previous examples (Scheme 1.17).[28] When the lithium anion of α-**48** was added to morpholino amide **39** (see Scheme 1.15), the product **49** was obtained in excellent yield and good enantioselectivity. In addition, they have shown that this methodology can be extended to include the formation of chiral quaternary centers by reaction of lithiated α-**48** with tetrasubstituted morpholino amide **50** to give highly substituted cyclopentenone **51** in moderate yield and ee. The selectivity is brought about by a conformational change of the pyranose auxiliary

during the stereochemical-determining step, which places the C3 and C4 OTBS groups in pseudoaxial positions. Steric shielding by the OTBS group at C4 ultimately controls the stereochemical outcome of the cyclization.[29]

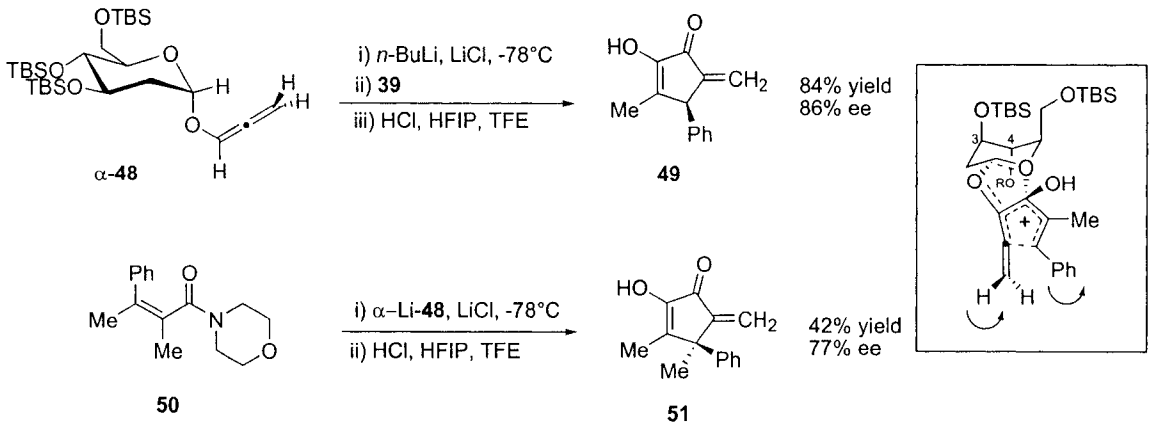

Scheme 1.17. Tius' modified pyranose-derived chiral auxiliary.

1.2.4. Torquoselectivity induced via chiral Lewis or Brønsted acid

In 2003, Aggarwal reported the first use of a chiral Lewis acid complex to promote an asymmetric Nazarov cyclization (Table 1.3).[30] For divinyl ketones bearing α-ester substituents (**52**), copper(II) pyridyl bisoxazoline complex **54** was found to effectively promote the cyclization with acceptable asymmetric induction, although it was required in stoichiometric or near stoichiometric amounts. It was observed that bulky substituents at R^1 and R^2 promote catalyst turnover as well as enantioselectivity (entries 1 and 3 vs entry 2). α-Amide substituted substrates were unreactive with complex **54**, but other bisoxazoline complexes were found to promote reaction with these substrates in moderate yields and ee's. To explain the observed stereochemical outcome,

Aggarwal reasoned that distortion in the plane of the pentadienyl cation by the steric bulk of the chiral ligand favors one direction of conrotation by having the divinyl ketone predisposed to rotate in one particular direction (Figure 1.2).

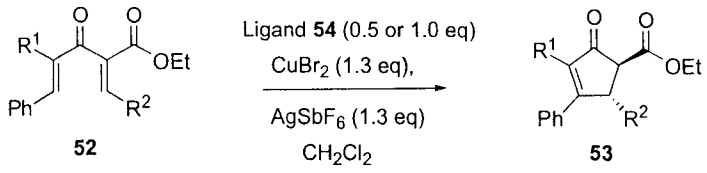

entry	R^1	R^2	ligand eq.	yield (%)	ee (%)
1	Me	Ph	1.0	73	76
2	Ph	Ph	0.5	96	86
3	Ph	Me	0.5	86	35

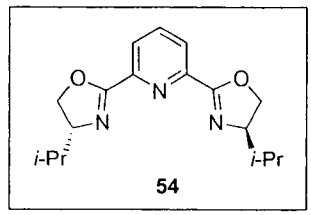

Table 1.3. Aggarwal's chiral Lewis acid promoted Nazarov cyclization.

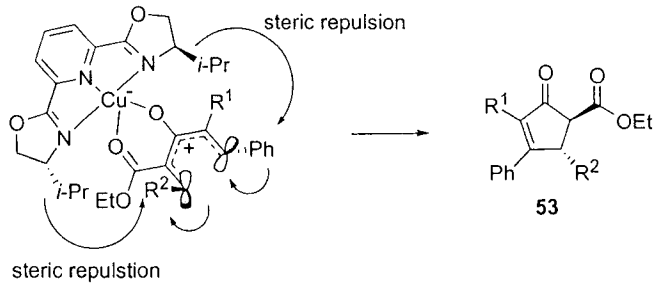

Figure 1.2. Proposed explanation for the stereochemical outcome in Nazarov cyclizations promoted by copper(II) pybox complexes.

Around the same time that Aggarwal reported the asymmetric Nazarov cyclization promoted by chiral Lewis acid complexes, Trauner published a similar finding for asymmetric catalysis in the Nazarov cyclization of 2-alkoxy-1,4-pentadien-3-ones (Scheme 1.18).[31] When treated with 20 mol% of chiral scandium-pybox complex

57, divinyl ketone **55** underwent asymmetric 4π electrocyclization to afford tricyclic product **56** in moderate yield and ee.

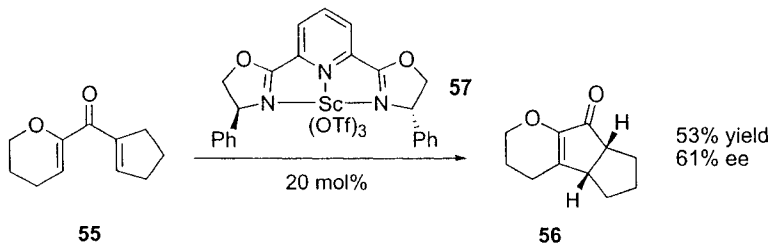

Scheme 1.18. Trauner's chiral Lewis acid catalyzed Nazarov cyclization.

Trauner investigated this idea more thoroughly in a subsequent publication, where he disclosed a truly catalytic asymmetric Nazarov cyclization that involves catalytic asymmetric proton transfer.[32] When optimizing conditions for the cyclization, it was found that the best yields and enantioselectivites were obtained on terminally unsubstituted substrates **58** using scandium-pybox complex **60** (Table 1.4). Therefore, the only stereocenter present in the product **59** results from an asymmetric reprotonation step after the cyclization has already occurred. Presumably, the catalyst complex influences this proton transfer resulting in moderate to excellent enantioselectivities. Following similar trends as observed in Aggarwal's work, bulkier substituents at R were found to give the highest yields and ee's of **59** (entry 3, R = *t*-Bu).

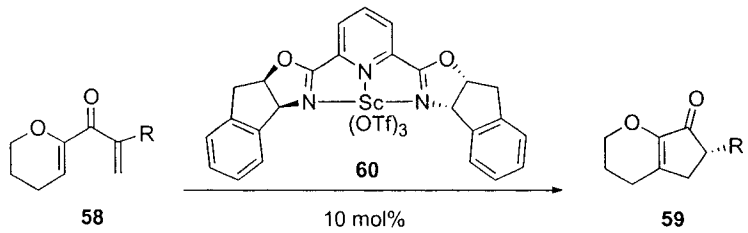

entry	R	yield (%)	ee (%)
1	Me	65	85
2	*i*-Pr	88	95
3	*t*-Bu	94	97

Table 1.4. Catalytic asymmetric proton transfer in the Nazarov cyclization.

In a recent publication, Rueping disclosed the use of a chiral Brønsted acid in the catalytic asymmetric Nazarov reaction.[33] After some optimization, the best catalyst was found to be binol N-trifyl phosphoramide **63**, (Table 1.5). In the presence of only 2.5 mol% **63**, substituted dienones **61** provided Nazarov products **62** in excellent yields and ee's. It should be noted that this procedure gives predominantly the kinetic product *cis*-**62**, which could be quantitatively converted to corresponding *trans*-**62** by isomerization in basic alumina without any loss in optical purity. Because both enantiomers of **63** are available, it is possible to selectively access all four stereoisomers of **62** with this protocol.

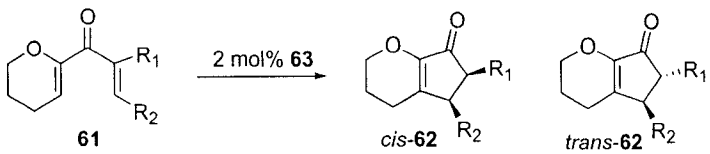

entry	R_1	R_2	yield (%)	*cis/trans*	ee (*cis/trans*)
1	Me	Ph	88	6:1	87, 95
2	Et	Ph	61	4.3:1	92, 96
3	*n*-Pr	Ph	85	3.2:1	93, 91

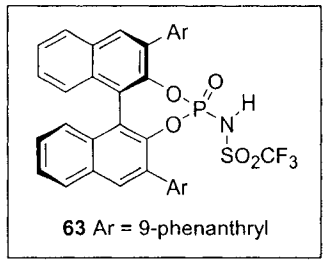

Table 1.5. Rueping's use of chiral Brønsted acid in the Nazarov cyclization.

The proposed mechanism for the cyclization is shown in Figure 1.3. The reaction is initiated by catalytic protonation of dienone **A** by the binol phosphate (*BH) and results in the formation of cationic intermediate **B**, which is complexed with the chiral conjugate base. The conjugate base would then influence the direction of conrotation in the subsequent 4π electron cyclization to give oxyallyl cation **C**. Deprotonation of **C** results in the formation of enol **D**, which then undergoes tautomerization to furnish chiral cyclopentenone **E**, and the chiral Brønsted acid is released for subsequent catalysis.

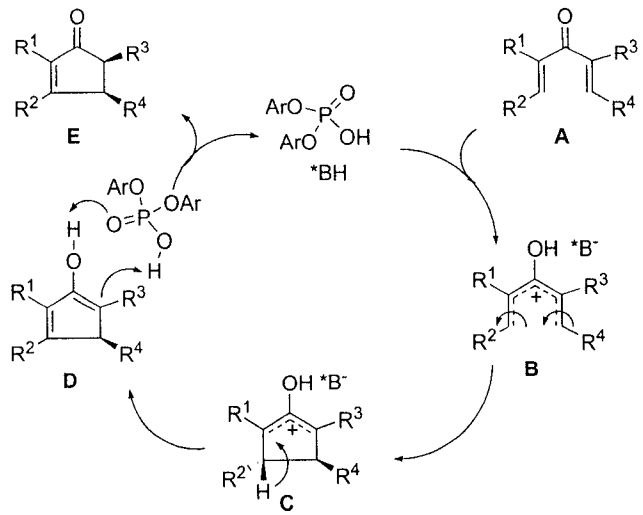

Figure 1.3. Proposed catalytic cycle of the chiral Brønsted acid catalyzed Nazarov cyclization.

1.3. Stereocontrol in 6π electron cyclizations

The typical 6π electrocyclization involves conversion of 1,3,5-hexatrienes to 1,3-cyclohexadienes, with rotation of the bond forming centers occurring in a disrotatory fashion. In contrast to the Nazarov cyclization, there have been far fewer systematic studies on torquoselectivity in the 6π electrocyclization. This is not to say that it is not possible, or even difficult for that matter, to induce chirality in the reaction. In fact, stereoselective 6π reactions are observed quite frequently in specialized intermediates *en route* to natural products.[34] For the most part, these reports of selectivity are a result of steric effects inherent within a particular system and thus will not be discussed here. That being said, there have been a few general studies reported on torquoselectivity in this reaction, as well as the aza-6π analog, and these will be reviewed in the following section.

1.3.1. Torquoselectivity in the all carbon 6π electrocyclization

Work done by Okamura and coworkers in 1985 demonstrated the application of axial to tetrahedral chirality transfer in the 6π electrocyclization.[35] Ketone **64** was reduced stereoselectively using $LiAlH_4$ in the presence of Chirald. The resultant allylic alcohol **65**, formed in 84% ee, then underwent *E/Z* isomerization on triplet sensitized photolysis to give **66**. Subsequent reaction with PhSCl gave **67**, an intermediate that immediately rearranged to allene **68** via stereospecific [2,3]-sigmatropic rearrangement, then cyclized at room temperature to a mixture of two diastereomers **69** and **69'** that were epimeric at sulfur. Through the entire sequence, the stereochemical information of the starting material **65** was retained and ultimately transferred to **69** via sp^3 to axial to sp^3 chirality transmission.

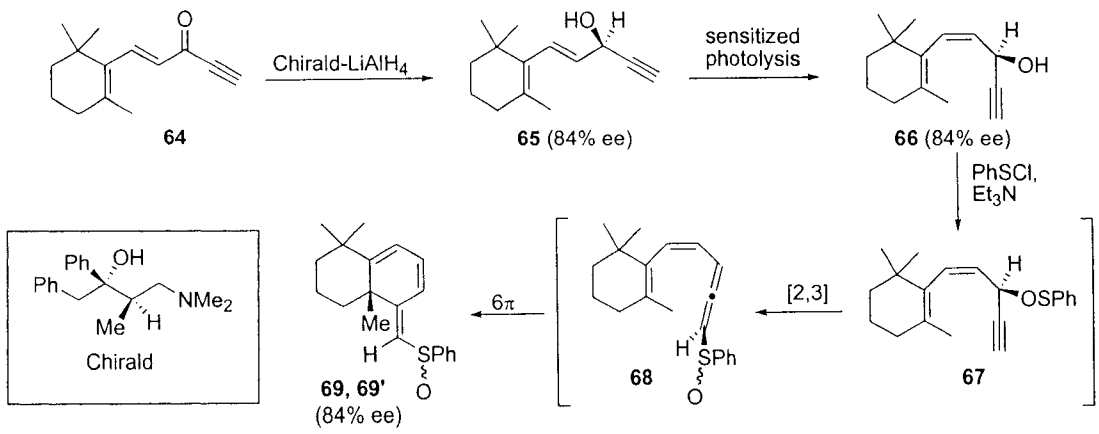

Scheme 1.19. Axial to tetrahedral chirality transfer in the 6π electrocyclization.

Similar to West's study on the Nazarov cyclization of bridged bicyclic dienones (Scheme 1.9), Magomedov and co-workers found a related stereoselective 6π

electrocyclization of *in situ* generated trienes that are embedded in a camphor skeleton.[36] The cyclization is initiated by γ-deprotonation of dienone **70** in the presence of the Lewis acid, MAD (Scheme 1.20). The resulting 1,3,5-hexatriene **71** then immediately cyclizes at room temperature to give 91% yield of cyclohexenone **72** after protonation. The diastereoselectivity in this case is consistent with electrocyclization involving the *exo* face of the intermediate enolate.

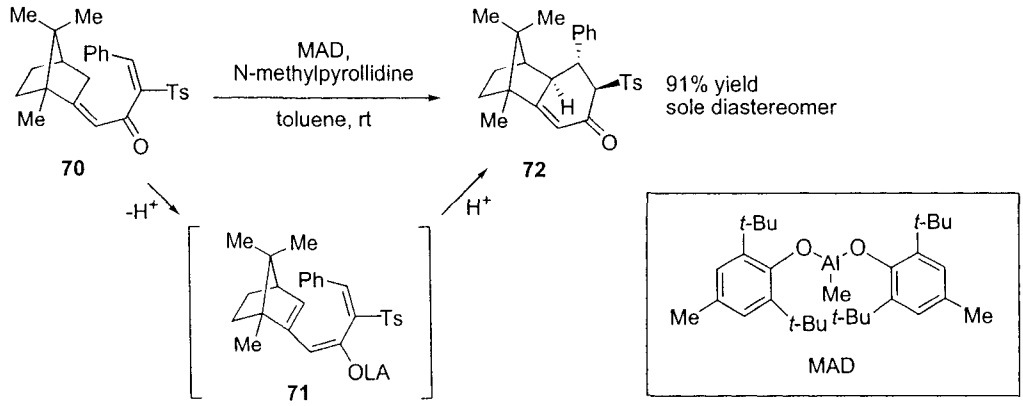

Scheme 1.20. Magomedov's torquoselective 6π electrocyclization.

1.3.2. Torquoselectivity in the aza 6π electrocyclization

Contrary to the all carbon-based 6π electrocyclization, the stereoselectivity of the corresponding aza-electrocyclization has been investigated in more detail. The first example of a highly stereoselective 6π aza-electrocyclization was reported and systematically studied by Katsumura.[37] A representative example is shown in Scheme 1.21. The sequence begins with initial imine formation between **73** and *cis*-aminoindanol **74** to give an aza-triene that undergoes cyclization at room temperature to **75**. This

product was not isolated, as it was immediately trapped intramolecularly by the free indanol hydroxyl to furnish **76** in excellent yield as one stereoisomer. The chiral auxiliary could then be cleaved by reduction with $LiAlH_4$ to the corresponding diol, followed by oxidation of the nitrogen atom to an intermediary N-oxide on treatment with MnO_2. During chromatography with silica gel, a Polonovski-type reaction occurs releasing **77** in 74% yield. This protocol was applied to the asymmetric synthesis of (-)-dendroprimine.[36a]

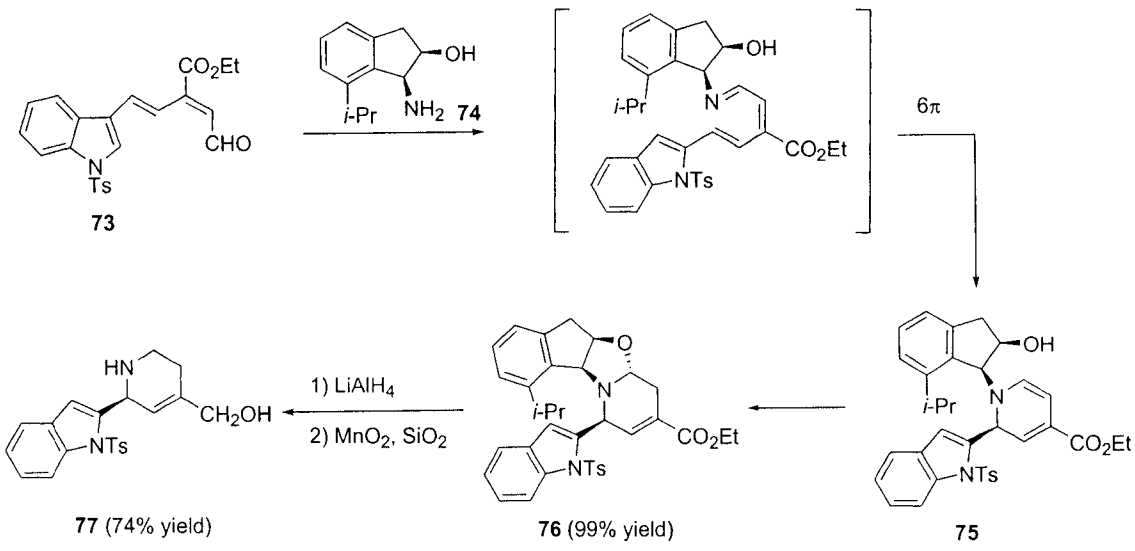

Scheme 1.21. Use of a chiral auxiliary in the aza-6π electrocyclization.

To explain the stereochemical outcome, the authors invoked hydrogen bonding of the imine nitrogen with the hydroxyl group of the indan moiety to stabilize the reacting conformers (Scheme 1.22). Cyclization with inward disrotatory motion would proceed through intermediate **A** (mode a) in which there are no destabilizing interactions, and gives rise to the observed diastereomer **76**. On the other hand, outward disrotatory motion (mode b) would proceed through intermediate **B**, in which steric interaction is

encountered between the imine hydrogen and the indan isopropyl group. For this reason, mode b is disfavored and the resulting product *diast*-**76** is not observed.

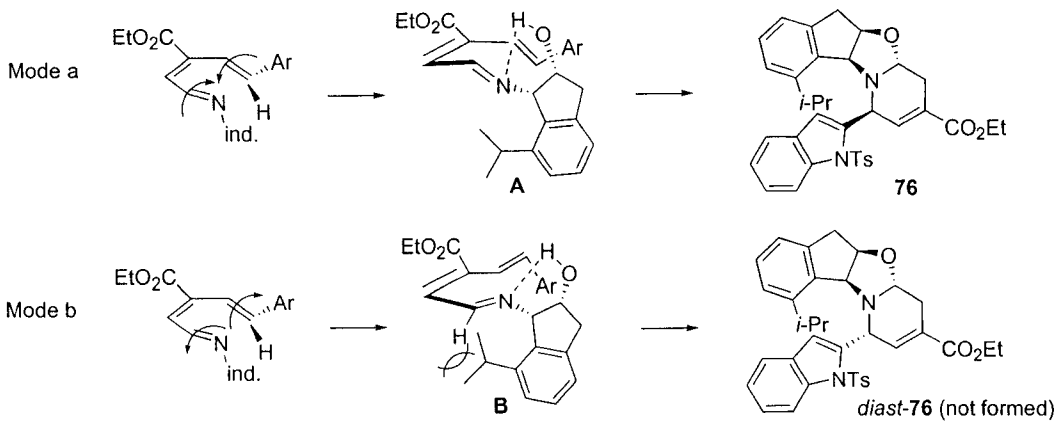

Scheme 1.22. Explanation for observed stereoselectivity in Katsumura's asymmetric aza-6π electrocyclization.

Hsung reported the use of an acyclic chiral auxiliary on nitrogen for use in the stereoselective aza-6π electrocyclization (Scheme 1.23).[38] The reaction proceeds through condensation of **78** with iminium ion **79** to give aza-triene **80**. This undergoes electrocyclic ring closure to the product **81** as a 96:4 ratio of diastereomers. The authors propose that the linear auxiliary adopts a conformation that allows π-stacking between the C2′ Ph of the auxiliary and the C5-C6 alkene. Through favored disrotatory motion a, which reduces steric hindrance between the C6 R and C2′ Ph substituents during the transition state, the product is formed. The authors have also found evidence for reversibility in the 6π electrocyclization, and suggest that the observed selectivity may also be explained by a thermodynamic equilibrium favoring the more stable product.

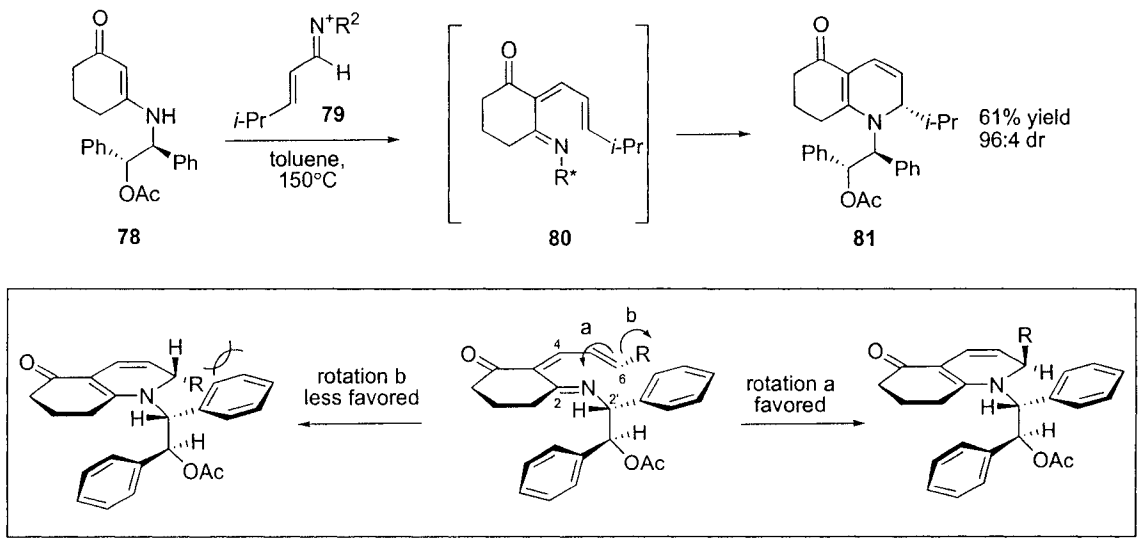

Scheme 1.23. Hsung's torquoselective aza-6π electrocyclization.

Recently, these same authors have reported a modification of the asymmetric aza-6π electrocyclization discussed above where the source of chirality is located at the carbon-terminus of the aza-triene.[39] Achiral enamine **82** reacts with chiral iminium salt **83** to give aza-triene **84**, which cyclizes to furnish **85** in modest yield, but excellent diastereoselectivity (Scheme 1.24). Though the chiral auxiliary potentially has a high degree of rotational freedom, the bulky nitrogen protecting group was expected to restrict its rotation so that high levels of diastereoselectivity could be achieved. The cyclization takes place predominantly through mode a, which decreases steric interactions between the benzhydryl group on nitrogen and the C-terminus allylic substituent. These interactions are magnified in the transition state in rotation b, which is thus disfavored.

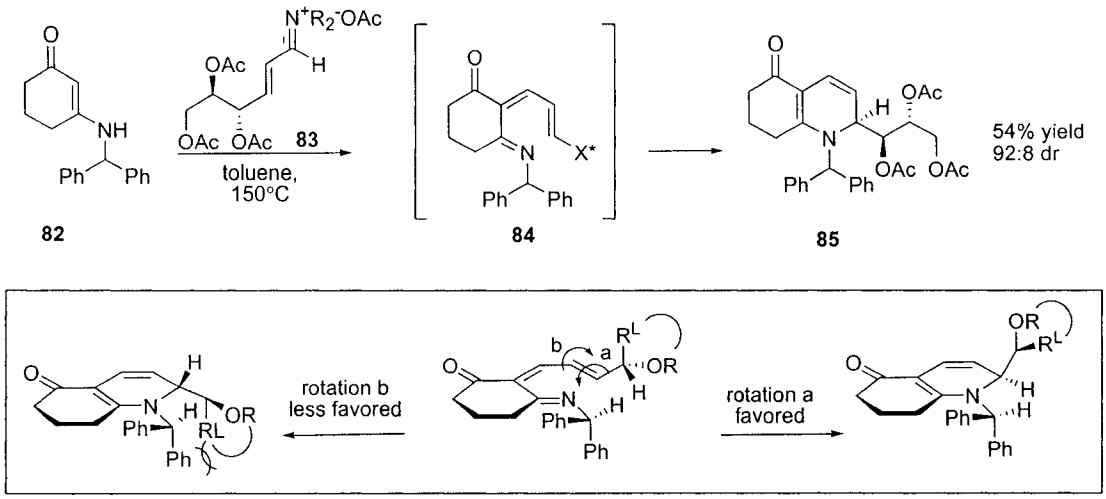

Scheme 1.24. Hsung's revised torquoselective aza-6π electrocyclization.

1.4. Stereocontrol in 8π, 6π cascade electrocyclizations

There have been many relevant reports in the domain of 8π, 6π cascade cyclizations in syntheses of molecules containing a unique substituted bicyclo[4.2.0]octadiene core.[40] Interest in these molecules first began in the 1980's when Black proposed a hypothesis for the biogenesis of a series of these compounds known as the endiandric acids. These compounds are present in nature in racemic form, a somewhat unusual phenomenon, and Black therefore proposed that they were made from achiral precursors through a series of nonenzymatic electrocyclizations, namely, the cascade 8π, 6π electrocyclization.[41] Based on this hypothesis, Nicolaou devised and implemented a synthetic strategy to a number of the endiandric acid compounds using the electrocyclization approach.[42] The products were formed with ease and perfect stereoselectivity, providing support for the feasibility of Black's biogenesis theory. There are other products containing this core that have been recently isolated. Their

syntheses have been undertaken along with studies into a more in depth understanding of the stereoselectivity with which these processes occur.

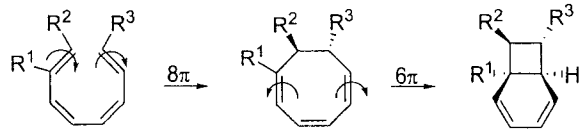

Scheme 1.25. 8π, 6π Cascade: proposed biosynthesis to the bicyclo[4.2.0]octadiene core.

In recent years, much effort has been devoted to the syntheses of (-)SNF4435 C and (+)SNF4435 D, two bicyclo[4.2.0]octadiene products isolated from nature in enantiopure form (Scheme 1.26).[43] At the outset of these studies, factors that control torquoselectivity in tetraene-cylcooctatriene-bicyclooctadiene transformations were not completely understood.[34c] An undertaking of the synthesis of the SNF4435 compounds by three independent groups provided some insight into these issues, and their findings all concur. Each synthesis hinged on the preparation of octatetraene **86**, or one of its derivatives. Once formed, **86** can cyclize via either of two helical conformers, a or b. Conrotatory cyclization from conformer a should be facile, while that in b would be slowed due to steric interactions between the pyrone and nitrophenyl groups. The resulting enantiomeric cyclooctatriene products **87** should go on to a stereospecific 6π electrocyclization, where cyclization takes place in a manner that avoids interaction between the nitrophenyl group and the adjacent methyl. From here, the products SNF4435 C and D would be formed. Each of the synthetic studies carried out found that the cascade reaction proceeded predictably as above. Interestingly, SNF compounds are isolated in nature in approximately a 3:1 ratio (C:D), which is close to the observed ratios

in the synthetic studies. Because the ratio of the products is determined in the 8π electrocyclization, the steric argument that favors cyclization through conformer a seems likely.

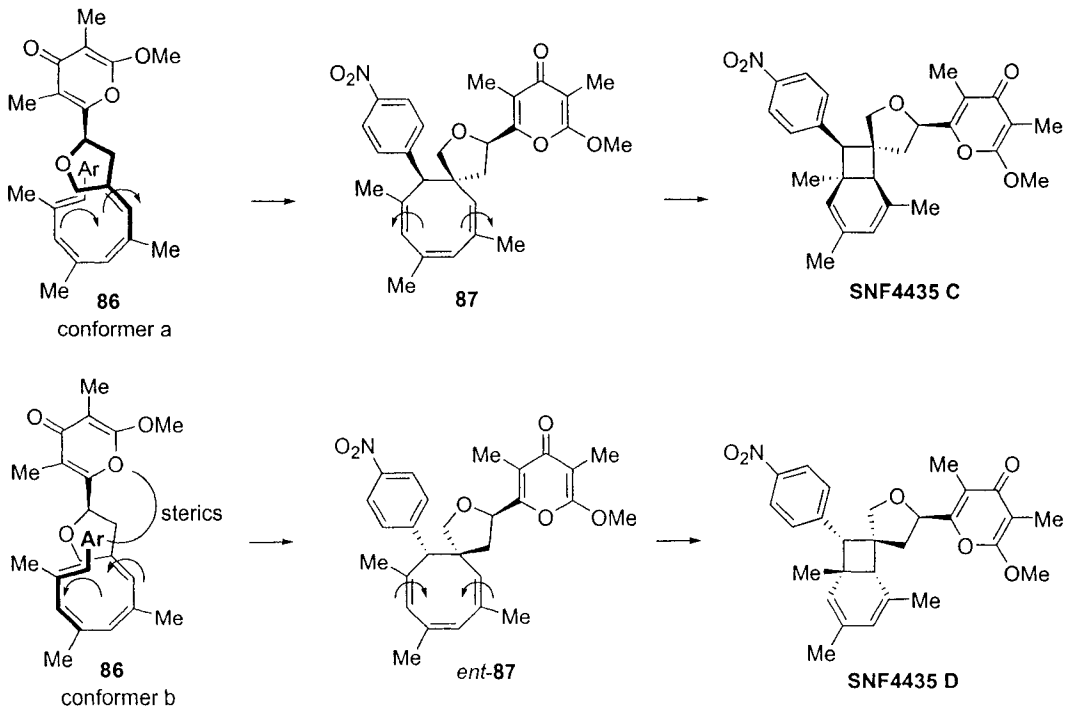

Scheme 1.26. 8π, 6π Cascade in the synthesis of SNF4435 compounds.

Recently, some new optically active bicyclo[4.2.0]octane natural products have been isolated and characterized (Scheme 1.27).[44] In their proposed biosyntheses, a role for an enzyme has been invoked. For the purpose of a nonracemic laboratory synthesis, an external chirality source would therefore be necessary. Work is underway in the Parker group to find an effective auxiliary for use in these cascade cyclizations to direct the initial 8π ring closure.[45] The results thus far have not led to an ideal chiral auxiliary to effect the transformation with high diastereoselectivity, but investigations are ongoing.

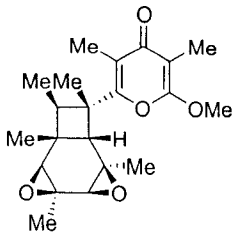

Elysiapyrone A

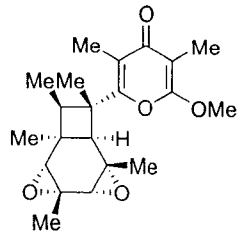

Elysiapyrone B

Scheme 1.27. Recently discovered non-racemic bicyclo[4.2.0]octane natural products.

1.5. Stereocontrol in 8π electrocyclizations

The conrotatory 8π electrocyclization of linear 1,3,5,7-octatetraenes to 1,3,5-cyclooctatrienes is not as frequently encountered in the literature as its corresponding 6π and 4π counterparts. Nevertheless, there are some examples to be found in synthesis of specific natural products that utilize a stereoselective 8π electrocyclization.[46] Paquette has thoroughly studied torquoselectivity in 8π electrocyclizations during his investigations into cascade reactions with squarate esters (Scheme 1.28).[47] In its simplest form, this astonishing cascade reaction is initiated by the *trans*-addition of 2 equivalents of a vinyl lithium species **89** to squarate ester **88**. This is followed by a stereospecific 4π conrotatory electrocyclic ring opening of the cyclobutene **90** to give a tetra-ene **91** that is geometrically predisposed to undergo a conrotatory 8π electrocyclization. The resulting cyclooctatriene **92** then participates in a transannular aldol reaction furnishing complex polycyclic product **94** in excellent yield.

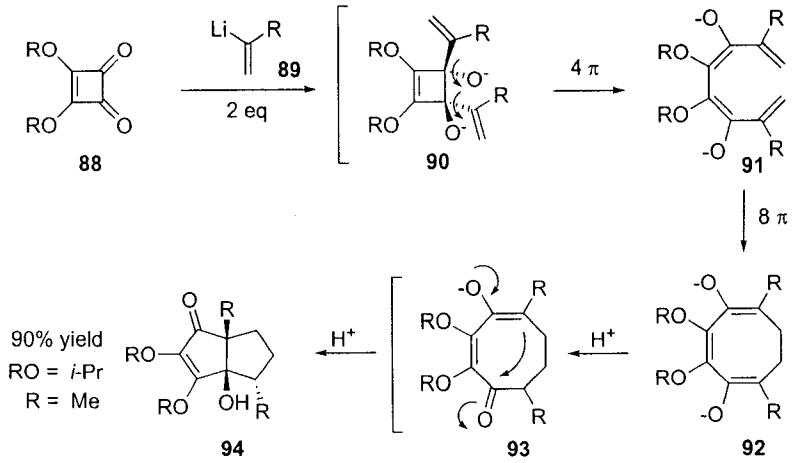

Scheme 1.28. Paquette's squarate ester cascade.

Paquette suspected that the stereochemical course of the cascade cyclization could be controlled via chiral induction at the stage of 8π electrocyclic ring closure, and devised an experiment to test this theory (Scheme 1.29). He reasoned that addition of 1 equivalents of a chiral alkenyl anion **96** to **95** would lead to an approximate 1:1 mixture of diastereomers **97** and **98**, which, on addition of a second equivalent of achiral alkenyl anion **99** would lead to diastereomeric dialkoxides **100** and **101**. Upon electrocyclic ring opening, octatetraenes **102** and **103** arise. Paquette ventured that these two could be distinct species due to helical chirality transferred from the starting materials. The 8π electrocyclization of **102** was predicted to be slow because of steric interactions between the *i*-Pr substituent and the upper portion of the helix, while that of **103** should be facile because of the exterior location of the *i*-Pr group. Paquette surmised that if chiral induction were indeed possible at this stage, then hindered helix **102** would be required to equilibrate to more stable **103**, thus eroding any "handedness" present from the starting material. The stereochemical outcome of the 8π electrocyclization would therefore be controlled solely by the chiral isopropenyl center.

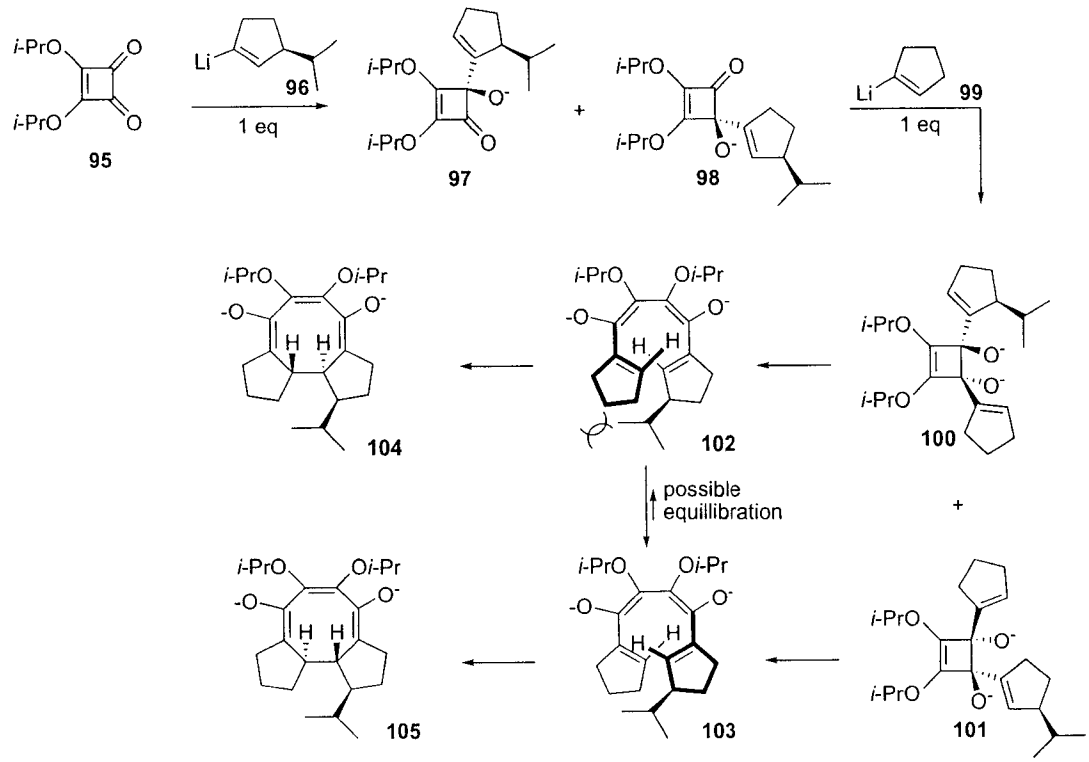

Scheme 1.29. Paquette's theory of torquoselectivity in the 8π electrocyclization.

In the event, the reaction of **95** with vinyl anions **96** and **99** followed by trapping of the oxidoanion with TMSCl led to isolation of tricycle **106** in 64% yield as the only detectable product. This preliminary result provided evidence for the feasibility of chiral induction in the 8π electrocyclization in the squarate ester cascade. Further in depth studies indicated that this theory was indeed correct.[45a]

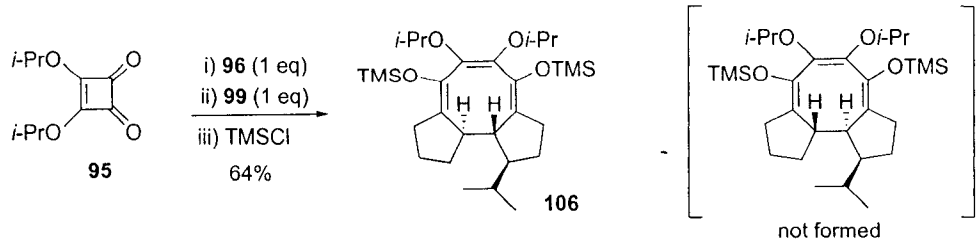

Scheme 1.30. Paquette's torquoselective 8π electrocyclization.

1.6. Conclusion

Electrocyclization reactions are valuable C-C bond forming transformations. Their inherent stereospecificity makes them useful for construction of complex systems in a stereoselective manner. Additionally, the potential for control over absolute stereochemistry through torquoselectivity makes them indispensable tools for annulations to complex polycycles. Further investigation into factors that control the torquoselectivity in these cyclizations is necessary to broaden the scope of the methods in existence and to develop new protocols for use in organic synthesis. In Chapter 2, developments from this group in the torquoselective 6π electrocyclization will be detailed. Chapter 3 will discuss the progress towards the total synthesis of taxinine using a key stereoselective Nazarov cyclization of a dienone encased in a bicyclo[3.2.1]octadiene core. In the final chapter, our efforts towards the development of a tandem Nazarov cyclization/Diels Alder cycloaddition will be reported.

1.7. References

[1] Woodward, R. B.; Hoffman, R. *J. Am. Chem. Soc.* **1965**, *87*, 395.

[2] Woodward, R. B.; Hoffmann, R. *The Conservation of Orbital Symmetry*; Verlag Chemie: Weinheim, Germany, 1970.

[3] Dolbier, W. R., Jr.; Koroniak, H.; Houk, K. N.; Sheu, C. *Acc. Chem. Res.* **1996**, *29*, 471.

[4] Houk, K. N.; Rondan, N. *J. Am. Chem. Soc.* **1985**, 2099.

[5] Kallel, E. A.; Houk, K. N. *J. Am. Chem. Soc.* **1989**, 6006.

[6] Evanseck, J. D.; Thomas, B. E., IV; Spellmeyer, D. C.; Houk, K. N. *J. Org. Chem.* **1995**, *60*, 7134.

[7] Thomas, B. E., IV; Evanseck, J. D.; Houk, K. E. *J. Am. Chem. Soc.* **1993**, *115*, 4165.

[8] Nazarov, I. N.; Zaretskaya, I. I. *Izv. Akad. Nauk. SSSR, Ser. Khim.* **1941**, 211.

[9] For recent reviews see: a) Tius, M. A. *Eur. J. Org. Chem.* **2005**, 2193. b) Pellissier, H. *Tetrahedron.* **2005**, *61*, 6479. c) Frontier, A. J.; Collison, C. *Tetrahedron.* **2005**, *61*, 7577.

[10] Denmark, S. E.; Habermas, K. L.; Hite, G. A.; Jones, T. D. *Tetrahedron* **1986**, *42*, 2821.

[11] Denmark, S. E.; Wallace, M. A.; Walker, C. B., Jr. *J. Org. Chem.* **1990**, *55*, 5543.

[12] Occhiato, E. G.; Prandi, C.; Ferrali, A.; Guarna, A.; Ventuello, P. *J. Org. Chem.* **2003**, *68*, 9728.

[13] Prandi, C.; Ferrali, A.; Guarna, A.; Venturello, P.; Occhiato, E. G. *J. Org. Chem.* **2004**, *69*, 7705.

[14] Occhiato, E. G.; Prandi, C.; Ferrali, A.; Guarna, A. *J. Org. Chem.* **2005**, *70*, 4542.

[15] Prandi, C.; Deagostino, A.; Venturello, P.; Occhiato, E. G. *Org. Lett.* **2005**, *7*, 4345.

[16] a) Mazzola, R. D., Jr.; White, T. D.; Vollmer-Snarr, H. R.; West, F. G. *Org. Lett.* **2005**, *7*, 2799. b) White, T. D.; West, F. G. *Tetrahedron Lett.* **2005**, *46*, 5629. c) Giese, S.; Mazzola, R. D., Jr.; Amann, C. M.; Arif, A. M.; West, F. G. *Angew. Chem. Int. Ed.* **2005**, *44*, 6546.

[17] Tius, M. A. *Acc. Chem. Res.*, **2003**, *36*, 284.

[18] Hu, H.; Smith, D.; Cramer, R. E.; Tius, M. A. *J. Am. Chem. Soc.* **1999**, *121*, 9895.

[19] Schultz-Fademrecht, C.; Tius, M. A.; Grimme, S. G.; Wibbeling, B.; Hoppe, D. *Angew. Chem. Int. Ed.* **2002**, *41*, 1532.

[20] Zimmermann, M.; Wibbeling, B.; Hoppe, D.; *Synthesis* **2004**, 765.

[21] Shultz-Fademrecht, C.; Wibbeling, B.; Frohlich, R.; Hoppe, D. *Org. Lett.* **2001**, *3*, 1221.

[22] Iglesias, B.; de Lera, A. R.; Rodríguez-Otero, J.; López, S. *Chem. Eur. J.* **2000**, *6*, 4021.

[23] Pridgen, L. N.; Huang, K.; Shilcrat, S.; Tickner-Eldridge, A.; DeBrosse, C.; Haltiwanger, R. C. *Synlett* **1999**, 1612.

[24] Kerr, D. J.; Metje, C.; Flynn, B. L. *Chem. Commun.* **2003**, 1380.

[25] Harrington, P. E.; Tius, M. A. *Org. Lett.* **2000**, *2*, 2447.

[26] Harrington, P. E.; Murai, T.; Chu, C.; Tius, M. A. *J. Am. Chem. Soc.* **2002**, *124*, 10091.

[27] Harrington, P. E.; Tius, M. A. *J. Am. Chem. Soc.* **2001**, *123*, 8509.

[28] d. Santos, D. B.; Banaag, A. R.; Tius, M. A. *Org. Lett.* **2006**, *8*, 2579.

[29] Banaag, A. R.; Tius, M. A. *J. Am. Chem. Soc.* **2007**, *129*, 5238.

[30] Aggarwal, V. K.; Belfield, A. J. *Org. Lett.* **2003**, *5*, 5075.

[31] Liang, G.; Gradi, S. N.; Trauner, D. *Org. Lett.* **2003**, *5*, 4931.

[32] Liang, G.; Trauner, D. *J. Am. Chem. Soc.* **2004**, *126*, 9544.

[33] Rueping, M.; Ieawsuwan, W.; Antonchick, A. P.; Nachtsheim, B. J. *Angew. Chem. Int. Ed.* **2007**, *46*, 2097.

[34] a) Tambar, U. K.; Kano, T.; Stoltz, B. M. *Org. Lett.*, **2005**, *7*, 2413. b) Hsung, R. P.; Cole, K. P.; Zehnder, L. R.; Wang, J.; Wei, L.; Yang, X.; Coverdale, H. *Tetrahedron* **2003**, *59*, 311. c) Suffert, J.; Salem, B.; Klotz, P. *J. Am. Chem. Soc.* **2001**, *123*, 12107.

[35] Okamura, W. H.; Peter, R.; Reisch, I. W. *J. Am. Chem. Soc.* **1985**, *107*, 1034.

[36] Magomedov, N. A.; Ruggiero, P. L.; Tuchen, T. *Org. Lett.* **2004**, *6*, 3373.

[37] a) Kobayashi, T.; Hasegawa, F.; Tanaka, K.; Katsumura, S. *Org. Lett.* **2006**, *8*, 3813. b) Kobayashi, T.; Nakashima, M.; Hakogi, T.; Tanaka, K.; Katsumura, S. *Org Lett.* **2006**, *8*, 3809. c) Tanaka, K.; Kobayashi, T.; Mori, H.; Katsumura, S. *J. Org. Chem.* **2004**, *69*, 5906. d) Tanaka, K.; Katsumura, S. *J. Am. Chem. Soc.* **2002**, *124*, 9660.

[38] Sklenicka, H. M.; Hsung, R. P.; McLaughlin, M. J.; Wei, L.; Gerasyuto, A. I.; Brennessel, W. B. *J. Am. Chem. Soc.* **2002**, *124*, 10435.

[39] Sydorenko, N.; Hsung, R. P.; Vera, E. L. *Org. Lett.* **2006**, *8*, 2611.

[40] Beaudry, C. M.; Malerich, J. P.; Trauner, D. *Chem. Rev.* **2005**, *105*, 4757.

[41] Bandaranayake, W. M.; Banfield, J. E.; Black, D. St. C. *J. Chem. Soc., Chem. Commun.* **1980**, 902.

[42] a) Nicolaou, K. C.; Petasis, N. A.; Uenishi, J.; Zipkin, R. E. *J. Am. Chem. Soc.* **1982**, *104*, 5557. b) Nicolaou, K. C.; Petasis, N. A.; Zipkin, R. E. *J. Am. Chem. Soc.* **1982**, *104*, 5560. c) Nicolaou, K. C.; Petasis, N. A.; Zipkin, R. E.; Uenishi, J. *J. Am. Chem. Soc.* **1982**, *104*, 5555.

[43] a) Beadry, C. M.; Trauner, D. *Org. Lett.* **2005**, *7*, 4475. b) Jacobsen, M. F.; Moses, J. E.; Adlington, R. M.; Baldwin, J. E. *Org. Lett.* **2005**, *7*, 2473. c) Parker, K. A.; Lim, Y. H. *J. Am. Chem. Soc.* **2004**, *126*, 15968.

[44] Cueto, M.; D'Croz, L.; Maté, J. L.; San-Martin, A.; Darias, J. *Org. Lett.* **2005**, *7*, 415.

[45] Parker, K. A.; Wang, Z. *Org. Lett.* **2006**, *8*, 3553.

[46] a) Salem, B.; Suffert, J. *Angew. Chem. Int. Ed.* **2004**, *43*, 2826. b) Hayashi, R.; Fernández, S.; Okamura, W. H. *Org. Lett.* **2002**, *4*, 851.

[47] a) Paquette, L. A. *Eur. J. Org. Chem.* **1998**, 1709. b) Paquette, L. A.; Hamme, A. T., II; Kuo, L. H.; Doyon, J.; Kreuzholz, R. *J. Am. Chem. Soc.* **1997**, *119*, 1242. c) Paquette, L. A.; Morwick, T. M. *J. Am. Chem. Soc.* **1997**, *8*, 1230.

2. Torquoselectivity in the 6π Electrocyclization of Bridged Bicyclic Trienes

2.1. Introduction

Electrocyclization reactions offer a powerful ring-forming strategy, with the possibility for simultaneous creation of one or two new stereocenters. An overview of the recent progress towards asymmetric induction in 4π, 6π and 8π electrocyclizations was included in Chapter 1. Therein, a report recently published by our group on 4π Nazarov electrocyclizations of facially biased bridged bicyclic dienones was briefly discussed (Scheme 1.9).[1] In this study, high diastereoselectivity for cyclization from the *exo* face of the bicyclic system was seen in most cases; however, some bicyclo[3.2.1]octadiene systems displayed complete *endo* selectivity in their cyclizations. Although the origins of this stereochemical reversal are obscure, the presence of the remote olefin was found to be critical for *endo* cyclization to be observed. As a cationic process, the Nazarov cyclization is expected to be sensitive to electronic effects. We wondered whether the corresponding disrotatory 6π electrocyclization of neutral trienes would display the same stereodivergence as a function of different bicyclic skeletons.

2.2. Background

Electrocyclizations of conjugated trienes containing the bornene system are known. Magomedov and co-workers' report of a 6π electrocyclization of a camphor-based dienone in the presence of the Lewis acid MAD was discussed in Chapter 1 (Scheme 1.20).[2] In this particular example, a single (*exo*) diastereomeric cyclohexenone product was obtained. Fallis and coworkers also described the generation and cyclization of several bicyclic trienes via vinylmagnesiation of propargyl alcohols, including one possessing the bornene nucleus.[3] However, in those cases the stereochemical outcome was not considered, because the cyclized products were immediately oxidized to the corresponding aromatic systems. In the present study, we aimed to examine the stereoselective 6π electrocyclization of conjugated trienes containing several different bridged bicyclic ring systems to afford complex polycyclic cyclohexadiene products.[4]

2.3. Results and Discussion

Although Magomedov's enolization method and Fallis' carbometallation approach proved effective in generating the required 3,4-*cis*-trienes, both strategies required the presence of very specific groups along the triene chain. To limit the conformational variables in our investigation of the stereochemical outcomes of these cyclizations, we sought to prepare a series of trienes with minimal substitution. Specifically, we wanted to vary the bicyclic system containing C1 and C2, as well as the substituent at the other terminus (C6), while keeping the other three carbons unsubstituted. *Cis* reduction of the corresponding 1,5-dien-3-ynes seemed to be the most

straightforward method to accomplish this. Thus, initial efforts focused on the construction of the necessary dienynes via Sonogashira or Negishi cross-coupling[5] of bicyclic vinyl triflates **1a-c**[6] with enynes **2a-c**[7] (Table 2.1). In the event, Sonogashira conditions afforded **3a-c** in excellent yields. However, with enynes **2b,c**, Sonogashira reactions were complicated by undesired homocoupling pathways. In these cases, use of the Zn-acetylide was effective, affording **3d-f** in good to excellent yields, and **3g,h** in acceptable yields.

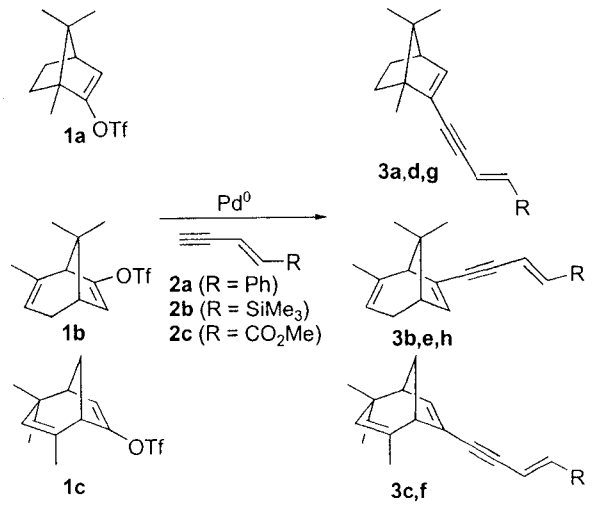

entry	vinyl triflate	enyne	conditions[a]	product	yield (%)[b]
1	**1a**	**2a**	A	**3a**	87
2	**1b**	**2a**	A	**3b**	100
3	**1c**	**2a**	A	**3c**	94
4	**1a**	**2b**	B	**3d**	80
5	**1b**	**2b**	B	**3e**	100
6	**1c**	**2b**	B	**3f**	100
7	**1a**	**2c**	B	**3g**	57
8	**1b**	**2c**	B	**3h**	63

[a]Condition A: Vinyl triflate **1**, THF/Et_2NH, $Pd(PPh_3)_2Cl_2$, CuI, reflux. Condition B: Alkyne **2**, THF, BuLi (**2b**) or LDA (**2c**); then $ZnCl_2$; then vinyl triflate **1**, $Pd(PPh_3)_4$, -78°C to rt or reflux. [b]Yields given are for isolated product after purification.

Table 2.1. Preparation of dienynes 3a-h.

With the dienynes **3a-h** in hand, methods for partial acetylene reduction were examined. Initial attempts focused on semi-hydrogenation using the Lindlar catalyst, conditions that were employed effectively in Nicolaou's elegant biomimetic synthesis of the endriandric acids,[8] as well as in the construction of 1α,25-dihydroxyvitamin D3 analogues by Okamura[9] and Gotor.[10] Although this method produced small amounts of the desired trienes, over-reduced products predominated. This problem has been noted in several other examples involving attempted partial reduction of alkynes in systems with extended conjugation.[11] Inclusion of additives[12] such as 1-octene or pyridine led only to recovery of starting dienyne.

We next turned to a protocol using Zn activated by successive treatment with $Cu(OAc)_2$, and $AgNO_3$,[13] which has been used for reduction of conjugated alkynes with high *Z*-selectivity and with little accompanying isomerization or over-reduction.[14] When dienyne **3a** was stirred in the presence of the activated Zn for 11 days at room temperature, a 67% yield of the product **5a** was obtained as a single (*exo*) diastereomer (Scheme 2.1). This compound is presumed to result from half-reduction to **4a**, followed by room temperature electrocyclization. The high *exo* selectivity is consonant with the stereochemical course of Nazarov cyclizations of camphor-derived dienones,[1a] as well as the observations of Magomedov and coworkers.[2]

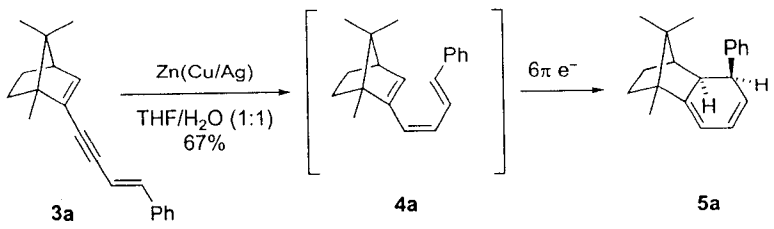

Scheme 2.1. Reduction and *in situ* electrocyclization of 3a.

The activated zinc conditions were then applied to the other dienyne substrates, with mixed success (Table 2.2). Dienynes **3b,c** (entries 2 and 3) furnished significant quantities of the undesired (*E*)-trienes, along with the desired cyclohexadienes **5b,c**. Though evidence for the formation of an analogous (*E*)-triene was occasionally found during reaction of substrate **3a**, it was much easier to minimize its formation by careful exclusion of any isomerization agents in the reaction conditions. Specifically, all solvents used during the reduction/cyclization sequence were of high purity and when necessary, they were filtered through basic alumina before use to remove any trace acid. Despite these precautions, isolation of the (*E*)-trienes was unavoidable in the conversion of **3b,c** to **5b,c**. Low yields of **5c** may be attributed to its ready decomposition under the reaction conditions. While all the cyclization products were prone to decomposition on storage, derivatives containing the **1c** nucleus were found to be especially sensitive.

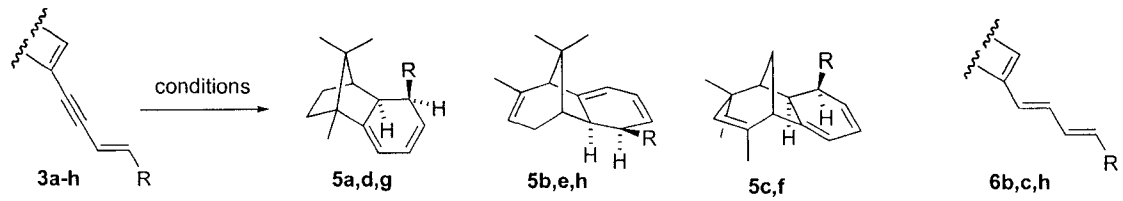

entry	dienyne	conditions[a]	cyclization product	yield (%)[b]	other products (% yield)
1	**3a**	A	**5a**	67	--
2	**3b**	A[c]	**5b**	50	**6b** (36)
3	**3c**	A[c]	**5c**	20	**6c** (4)
4	**3d**	B	**5d**	90	--
5	**3e**	B	**5e**	55	--
6	**3f**	B	**5f**	--	--
7	**3g**	C	**5g**	45	--
8	**3h**	C	**5h**	27[d]	**6h** (13)[d]

[a]Condition A: Activated Zn, H_2O/THF, **3**, rt. Condition B: Activated Zn, H_2O/THF, 45°C. Condition C: Compound **3**, CH_2Cl_2, quinoline, Lindlar catalyst, H_2 gas, rt; then argon gas, rt. [b]Yields given are for isolated product after purification. [c]After consumption of **3**, the crude reduction product **5** was redissolved in THF (**3b**) or $PhCH_3$ (**3c**) and stirred at reflux to effect electrocyclization. [d]**5h** and **6h** were isolated as an inseparable mixture.

Table 2.2. Reduction/cyclization of dienynes **3a-h.**

Treatment of silyl-substituted substrates **3d-f** with the activated Zn conditions at room temperature gave only recovered starting material. It was found that higher temperatures were needed to reduce the dienyne substrates. When the reaction was conducted at 45 °C, camphor-derived substrate **3d** was efficiently converted to **5d**, while **5e** was formed in moderate yield with some decomposition (entries 4 and 5, Table 2.2). As in the case of **3c**, **3f** and/or its reduction products were extremely sensitive and underwent rapid decomposition to a complex mixture and none of the cyclized product was obtained in this case (entry 6).

Substitution of the dienynes with an electron withdrawing group (**3g,h**) presented a challenge when trying to reduce the alkyne with the activated Zn conditions. Though the starting material was evidently consumed in the reaction, a number of products were formed that did not resemble the cyclized dienes (**5g,h**) or the intermediate trienes (*E* or *Z*). Moderate success was achieved, however, with the Lindlar reduction conditions (entries 7 and 8, Table 2.2). In these cases, partial reduction occurred quickly, and electrocyclization was effected by continued stirring at room temperature. Use of higher temperatures caused triene isomerization and rearrangement of cyclohexadiene products presumably by 1,5-hydride shift.

The stereochemical outcome of the electrocyclization was determined by 2D TROESY analysis of the products **5a-h**. This technique allows observation of close through-space interactions between non-equivalent proton sets through the nuclear Overhauser effect (NOE). The presence of cross-peaks in the TROESY spectrum between substituents at or near the newly generated stereocenters was noted. In Figure 2.1, the important NOE interactions for a representative series of compounds are shown (**5a-c**). For camphor derived cyclohexadiene **5a**, clear through space interactions were noted between the series of protons on the *endo* face of the molecule (H7 and H5, H9, H10). Similar cross-peaks were observed for the *endo* oriented protons of **5b** (H2 and H3, H11). An additional correlation was noted between the outside C12 methyl with *exo* H11. In the last example (**5c**), *endo* protons H6 and H7 correlated with one another, and H7 shared a cross peak with the *endo* C9 methyl. The corresponding *exo* C9 methyl correlated with the outside bridgehead H12, while the inside H12 showed a cross-peak to

the aromatic protons of the Ph substituent. The other cyclized products (**5d-g**) shared similar telling NOE interactions in their 2D-TROESY spectra.

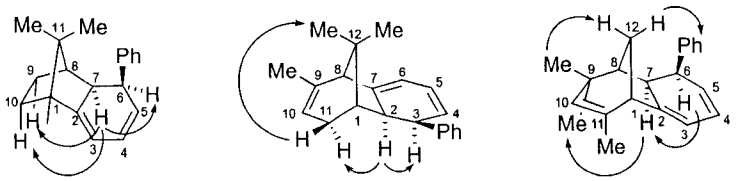

Figure 2.1. Relative stereochemical assignments of **5a-c.**

For some of the products (**5a-c**), distinctive chemical shifts in the ^{1}H NMR spectra offered further evidence for *exo* diastereoselectivity. In the spectra of **5a** and **b**, the inward pointing C11 and C12 methyls resonate significantly further upfield (-0.80 and –0.05 ppm) than the corresponding outward pointing C11 and C12 methyls (0.70 and 0.82 ppm). In these compounds, the *exo* disposed aromatic ring shields the nearby bridgehead substituents through anisotropic effects. A similar situation is observed for compound **5c** where the inside H12 resonates ~1 ppm further upfield than the outer H12 (0.69 versus 1.61 ppm).

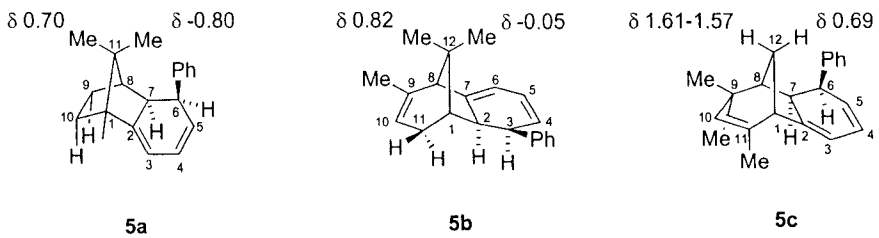

Figure 2.2. Selected ^{1}H NMR chemical shift data of bridgehead methyls of **5a,b** and hydrogens of **5c**.

In all cases involving successful conversion to cyclohexadienes **5**, exclusive formation of the product of cyclization from the *exo* face of the bicyclic olefin was observed, regardless of terminal substituent (R) or bicyclic ring system. The propensity for norbornene systems and related compounds to undergo various addition processes with high or complete *exo* selectivity has been addressed extensively. Proposed explanations for this phenomenom include torsional strain,[15] steric crowding,[16] nonequivalent orbital extension[17] as well as alkene pyramidalization[18] and transition state allylic bond staggering.[19] These arguments are relevant to the present study and were also applied to the *exo*-selective Nazarov cyclizations seen previously.[1a]

Importantly, the disrotatory electrocyclization leads to a *cis* relationship for the hydrogen atoms on the two newly formed adjacent stereocenters (Scheme 2.2). The transition state for 6π cyclization from the *endo* face may entail significant energetic penalties resulting from movement of the terminal R group into a sterically demanding location within the concave portion of the tricyclic skeleton. As a result, even substrates possessing the bicyclo[3.2.1]octadiene nucleus of **1b** undergo *exo* cyclization. In contrast, the corresponding conrotatory Nazarov cyclization of these substrates permits cyclization from the *endo* face, since the bulky terminal group will rotate outward. In addition, the greater polar character of the Nazarov cyclization may render it more sensitive to perturbation by the remote alkene. Cyclization in the *endo* mode could be favored because it permits continued homoconjugative overlap between the developing cyclopentenyl cation and the neighboring alkene; the formation of products resulting from apparent interrupted Nazarov reaction in some of these systems[1c] offers support for

such an interaction. In contrast, no significant benefit is expected from overlap in the charge-neutral 6π cyclization.

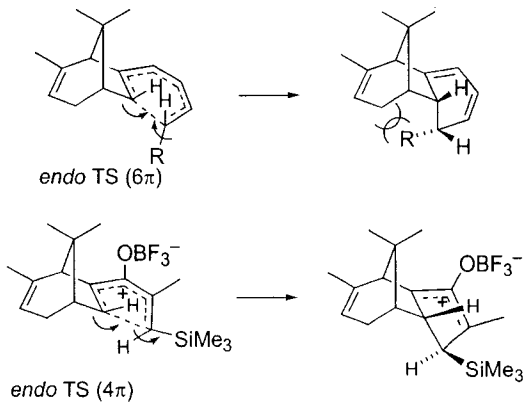

Scheme 2.2. Steric factors in electrocyclization reactions.

We were interested in pursuing further stereoselective elaboration of the tricyclic products, and dienyl silanes **5d**,**e** were prepared with this in mind. We believed that these cyclohexadienes should be amenable to functionalization by nucleophilic attack on a variety of electrophiles to provide products with high stereoselectivity.[20] In preliminary experiments, both compounds were treated with benzaldehyde or isobutyraldehyde in the presence of Lewis acids (Scheme 2.3). To our surprise, the major products in all cases were aromatic compounds **7d**,**e**, resulting from an apparent dehydrogenation process. Related oxidative aromatizations of cyclohexadienes have been observed previously.[21] The identity of the oxidant is not clear, as the reactions were carried out under an inert atmosphere. Although the Lewis acid-complexed aldehyde may serve as a possible hydride acceptor, it should be noted that **7d**,**e** were also formed to varying extents during the reductive cyclization of **3d**,**e**.

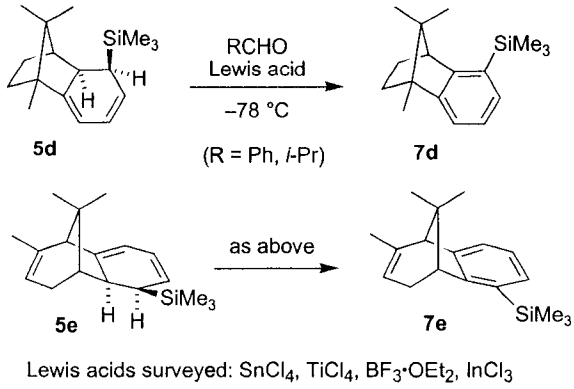

Scheme 2.3. Aromatization of **5d,e.**

2.4. Conclusion

As with the Nazarov cyclization, the 6π electrocyclization of bridged bicyclic trienes has been shown to be highly stereoselective. Selectivity for cyclization from the *exo* face was seen in all cases, even those involving the bicyclic skeleton found to undergo *endo*-selective cyclization in the Nazarov process. Substrates were readily prepared by a two-step alkynylation/half-reduction sequence. The resulting products possess unique and complex skeletons, which may be subject to a variety of stereoselective functionalization. Preliminary attempts to carry out allylation reactions with aldehydes resulted in a surprising aromatization pathway.

2.5. Experimental

2.5.1. General

Reactions were conducted in oven-dried (120°C) or flame-dried glassware under a positive argon atmosphere unless otherwise stated. Transfer of anhydrous solvents or

mixtures was accomplished with oven dried syringes or cannula. Solvents were distilled before use: dichloromethane (CH_2Cl_2) from calcium hydride; toluene from sodium; and tetrahydrofuran (THF) from sodium benzophenone ketyl. For reactions involving preparation and use of activated Zn, solvents used were of reagent grade purity and were filtered through basic alumina before use. Chloroform-*d* was filtered through basic alumina before use. Commercial reagents were used as received unless otherwise stated. Thin layer chromatography (TLC) was performed on glass plates precoated with 0.25 mm Kieselgel 60 F_{254} (Merck). Flash chromatography columns were packed with 230-400 mesh silica gel (Silicycle), or ~150 mesh, 58Å, activated neutral Brockmann I, standard grade alumina (Aldrich) as indicated.

Proton nuclear magnetic resonance spectra (^{1}H NMR) were recorded at 500 MHz, and the chemical shifts are reported on the δ scale (ppm) upfield from deuterochloroform (δ = 7.27 ppm). Coupling constants (*J*) are reported in Hertz (Hz). Splitting patterns are designated as s, singlet; d, doublet; t, triplet; q, quartet; m, multiplet; br, broad; dd, doublet of doublets, etc. Carbon nuclear magnetic resonance spectra (^{13}C NMR) were obtained at 125 MHz. Chemical shifts are reported (ppm) relative to the center line of the triplet for deuterochloroform (δ = 77.23 ppm). Infrared (IR) spectra were measured with a Mattson Galaxy Series FT-IR 3000 spectrophotometer. Mass spectra were determined on a Kratos Analytical MS-50 (EI).

2.5.2. Substrate syntheses and characterization

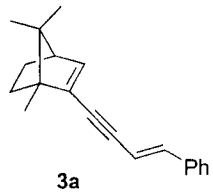

3a

Dienyne **3a**: To a solution of vinyl triflate **1a** (196 mg, 0.72 mmol) in THF (21 mL) and Et_2NH (21 mL) was added CuI (14 mg, 0.072 mmol), and $Pd(PPh_3)_2Cl_2$ (25 mg, 0.036 mmol). The mixture was flushed with argon at rt for 20 min. The alkyne **2a** (110 mg, 0.86 mmol), dissolved in THF (2 mL), was then added via cannula and the resulting solution was heated to reflux, and stirred 12 h. The mixture was cooled to rt and then concentrated directly. Purification was achieved by column chromatography using neutral alumina eluting with 100% hexanes and gave 165 mg (87%) of dienyne **3a** as a clear colorless oil: R_f 0.52 (20:1 hexanes/EtOAc); IR (CH_2Cl_2 film) 3059, 2955, 2871, 2176 cm^{-1}; ^1H NMR (500 MHz, $CDCl_3$) δ 7.42-7.24 (m, 5H), 6.94 (d, J = 16.1 Hz, 1H), 6.36 (d, J = 16.2 Hz, 1H), 6.32 (d, J = 3.3 Hz, 1H), 2.39 (dd, J = 3.6, 3.6 Hz, 1H), 1.92 (dddd, J = 12.3, 7.3, 3.7, 3.7 Hz, 1H), 1.59 (ddd, J = 12.0, 9.0, 3.5 Hz, 1H,), 1.17-1.11 (m, 4H), 1.05 (ddd, J = 12.1, 9.3, 3.4 Hz, 1H), 0.84 (s, 3H), 0.82 (s, 3H); ^{13}C NMR (125 MHz, $CDCl_3$) δ 141.0, 140.3, 136.6, 132.2, 128.7, 128.3, 126.2, 108.6, 92.7, 88.4, 56.5, 55.8, 52.2, 31.2, 24.9, 19.6, 19.5, 12.0; HRMS for $C_{20}H_{22}$ (M^+) calcd 262.1723, found 262.1728.

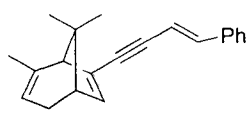

3b

Dienyne **3b**: To a solution of vinyl triflate **1b** (220 mg, 0.74 mmol) in THF (19 mL) and Et_2NH (19 mL) was added CuI (20 mg, 0.11 mmol), and $Pd(PPh_3)_2Cl_2$ (25 mg, 0.036 mmol). The mixture was flushed with argon at rt for 20 min. The alkyne **2a** (114 mg, 0.89 mmol), dissolved in THF (2 mL), was then added via cannula and the resulting solution was heated to reflux, and stirred 12 h. The mixture was cooled to rt and then concentrated directly. Purification was achieved by column chromatography using neutral alumina eluting with 100% hexanes and gave 203 mg (100%) of dienyne **3b** as a clear colorless oil: R_f 0.23 (100% hexanes); IR (CH_2Cl_2 film) 3059, 2955, 2875, 2177 cm^{-1}; ^1H NMR (500 MHz, $CDCl_3$) δ 7.42-7.24 (m, 5H), 6.94 (d, J = 16.2 Hz, 1H), 6.34 (d, J = 16.2 Hz, 1H), 5.94 (d, J = 3.1 Hz, 1H), 5.02 (s, 1H), 2.32-2.23 (m, 1H), 2.17-2.12 (m, 2H), 1.84-1.77 (m, 4H), 1.11 (s, 3H), 1.08 (s, 3H); ^{13}C NMR (125 MHz, $CDCl_3$) δ 140.5, 140.2, 136.9, 136.5, 134.1, 128.7, 128.4, 126.2, 116.6, 108.5, 92,0, 89.2, 59.0, 47.9, 44.2, 27.1, 26.8, 24.1, 20.7; HRMS for $C_{21}H_{22}$ (M^+) calcd 274.1723, found 274.1720.

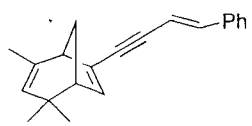

3c

Dienyne **3c**: To a solution of vinyl triflate **1c** (128 mg, 0.43 mmol) in THF (12 mL) and Et_2NH (12 mL) was added CuI (8 mg, 0.042 mmol), and $Pd(PPh_3)_2Cl_2$ (15 mg, 0.021 mmol). The mixture was flushed with argon at rt for 20 min. The alkyne **2a** (66 mg, 0.51 mmol), dissolved in THF (1 mL), was then added via cannula and the resulting solution was heated to reflux, and stirred 12 h. The mixture was cooled to rt and then

concentrated directly. Purification was achieved by column chromatography using neutral alumina eluting with 100% hexanes and gave 111 mg (94%) of dienyne **3c** as a clear colorless oil: R_f 0.70 (10:1 hexanes/EtOAc); IR (neat) 3059, 2962, 2863, 2178 cm^{-1}; ^1H NMR (500 MHz, $CDCl_3$) δ 7.41-7.25 (m, 5H), 6.93 (d, J = 16.1 Hz, 1H), 6.34 (d, J = 16.2 Hz, 1H), 6.09 (d, J = 3.3 Hz, 1H), 4.73 (s, 1H), 2.54 (d, J = 4.1 Hz, 1H), 2.47 (br s, 1H), 2.04 (ddd, J = 9.8, 4.7, 4.7 Hz, 1H), 1.98 (d, J = 9.9 Hz, 1H), 1.80 (s, 3H), 1.12 (s, 3H), 0.88 (s, 3H); ^{13}C NMR (125 MHz, $CDCl_3$) δ 140.5, 138.9, 138.6, 136.4, 134.5, 128.7, 128.5, 128.4, 126.2, 108.4, 92.8, 88.6, 50.5, 48.6, 39.8, 35.1, 30.3, 25.0, 23.5; HRMS for $C_{21}H_{22}$ (M^+) calcd 274.1723, found 274.1718.

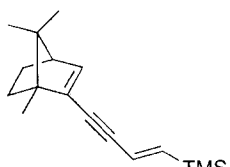

3d

Dienyne **3d**: To a solution of the alkyne **2b** (45 mg, 0.37 mmol) in THF (0.5 mL) at –78°C was added *n*-BuLi (0.225 mL, 1.6 M in hexanes, 0.37 mmol). The resulting mixture was allowed to stir at this temperature for 0.5 h, whereupon a solution of $ZnCl_2$ (49 mg, 0.37 mmol) in THF (0.5 mL) was added via cannula. The solution was warmed to 0°C, and left to stir for another 0.5 h. Following this, vinyl triflate **1a** (50 mg, 0.18 mmol) in THF (0.5 mL) was added via cannula, and $Pd(PPh_3)_4$ (6 mg, 0.005 mmol) was subsequently added in one solid portion. The mixture was warmed to rt and left to stir overnight. The reaction was quenched by the addition of saturated aq NH_4Cl (1.5 mL). The aqueous layer was extracted with Et_2O (2 x 5 mL), and the combined organic layers were dried over $MgSO_4$, filtered, and concentrated. Gravity column chromatography

using silica treated with 1% Et_3N/hexanes and eluting with 100% hexanes afforded 38 mg (80%) of dienyne **3d** as a yellow oil: R_f 0.58 (100% hexanes); IR (neat) 3060, 2956, 2873, 2179,1556 cm^{-1}; ^1H NMR (500 MHz, $CDCl_3$) δ 6.41 (d, J = 19.2 Hz, 1H), 6.28 (d, J = 3.3 Hz, 1H), 6.13 (d, J = 19.2 Hz, 1H), 2.36 (dd, J = 3.6, 3.6 Hz, 1H), 1.90 (dddd, J = 12.1, 7.6, 3.7, 3.7 Hz, 1H), 1.56 (ddd, J = 12.2, 9.0, 3.5 Hz, 1H), 1.13-1.06 (m, 4H), 1.06 (ddd, J = 11.8, 9.3, 3.1 Hz, 1H), 0.81 (s, 3H), 0.80 (s, 3H), 0.09 (s, 9H); ^{13}C NMR (125 MHz, $CDCl_3$) δ 144.5, 141.2, 132.1, 123.6, 93.6, 86.4, 56.4, 55.7, 52.2, 31.1, 24.9, 19.6, 19.5, 11.9, -1.6; HRMS for $C_{17}H_{26}Si$ (M^+) calcd 258.1805, found 258.1805.

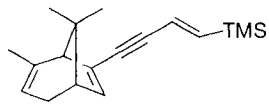

3e

Dienyne **3e**: To a solution of the alkyne **2b** (42 mg, 0.34 mmol) in THF (0.5 mL) at –78°C was added *n*-BuLi (0.215 mL, 1.6 M in hexanes, 0.34 mmol). The resulting mixture was allowed to stir for 0.5 h, whereupon a solution of $ZnCl_2$ (46 mg, 0.34 mmol) in THF (0.5 mL) was added via cannula. The solution was warmed to 0°C, and left to stir for another 0.5 h. Following this, the vinyl triflate **1b** (50 mg, 0.17 mmol) in THF (0.5 mL) was added via cannula, and $Pd(PPh_3)_4$ (6 mg, 0.005 mmol) was subsequently added in one solid portion. The mixture was then heated to reflux for 2 h. The reaction was quenched by the addition of saturated aq NH_4Cl (1.5 mL). The aqueous layer was extracted with Et_2O (2 x 5 mL), and the combined organic layers were dried over $MgSO_4$, filtered, and concentrated. Gravity column chromatography using silica treated with 1% Et_3N/hexanes and eluting with 100% hexanes afforded 46 mg (100%) of dienyne **3e** as a

yellow oil: R_f 0.52 (100% hexanes); IR (CH_2Cl_2 film) 2955, 2925, 2181,1559 cm^{-1}; ^1H NMR (500 MHz, $CDCl_3$) δ 6.41 (d, J = 19.2 Hz, 1H), 6.15 (d, J = 19.2 Hz, 1H), 5.88 (d, J = 2.8 Hz, 1H), 4.99 (s, 1H), 2.24 (d, J = 16.6 Hz, 1H), 2.11 (app. s, 2H), 1.80-1.74 (m, 4H), 1.08 (s, 3H), 1.05 (s, 3H), 0.09 (s, 9H); ^{13}C NMR (125 MHz, $CDCl_3$) δ 144.8, 140.1, 137.1, 134.0, 123.5, 116.5, 92.7, 87.2, 58.9, 47.8, 44.2, 27.2, 26.7, 24.1, 20.6, -1.6; HRMS for $C_{18}H_{26}Si$ (M^+) calcd 270.1805, found 270.1808.

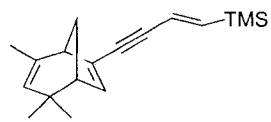

3f

Dienyne **3f**: To a solution of the alkyne **2b** (32 mg, 0.26 mmol) in THF (0.5 mL) at –78°C was added *n*-BuLi (0.165 mL, 1.6 M in hexanes, 0.26 mmol). The resulting mixture was allowed to stir for 0.5 h, whereupon a solution of $ZnCl_2$ (35 mg, 0.26 mmol) in THF (0.5 mL) was added via cannula. The solution was warmed to 0°C, and left to stir for another 0.5 h. Following this, the vinyl triflate **1c** (50 mg, 0.17 mmol) in THF (0.5 mL) was added via cannula, and $Pd(PPh_3)_4$ (6 mg, 0.005 mmol) was subsequently added in one solid portion. The mixture was then heated to reflux for 2 h. The reaction was quenched by the addition of saturated aq NH_4Cl (1.5 mL). The aqueous layer was extracted with Et_2O (2 x 5 mL), and the combined organic layers were dried over $MgSO_4$, filtered, and concentrated. Gravity column chromatography using silica treated with 1% Et_3N/hexanes and eluting with 100% hexanes afforded 47 mg (100%) of dienyne **3f** as a yellow oil: R_f 0.50 (100% hexanes); IR (neat) 2957, 2864, 2183, 1597 cm^{-1}; ^1H NMR (500 MHz, $CDCl_3$) δ 6.42 (d, J = 19.2 Hz, 1H), 6.12 (d, J = 19.2 Hz, 1H), 6.05 (d, J = 3.1

Hz, 1H), 4.70 (s, 1H), 2.49 (d, J = 4.4 Hz, 1H), 2.45 (br s, 1H), 2.01 (ddd, J = 12.2, 4.3, 4.3 Hz, 1H), 1.96 (d, J = 10.7 Hz, 1H), 1.77 (d, J = 1.6 Hz, 3H), 1.10 (s, 3H), 0.86 (s, 3H), 0.09 (s, 9H); ^{13}C NMR (100 MHz, $CDCl_3$) δ 144.8, 138.9, 138.4, 134.2, 128.3, 123.4, 93.5, 86.5, 50.4, 48.5, 39.6, 34.9, 30.2, 24.9, 23.3, -1.7; HRMS for $C_{18}H_{26}Si$ (M^+) calcd 270.1805, found 270.1807.

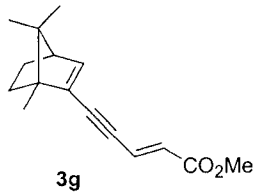

3g

Dienyne **3g**: *n*-BuLi (130 μL, 2.4 M in hexanes, 0.31 mmol) was added to a –78°C solution of DIPA (43 μL, 0.31 mmol) in THF (0.5 mL). The solution was warmed to 0°C and stirred for 20 min before being cooled back to –78°C. The alkyne **2c** (30mg, 0.28 mmol) in THF (0.3 mL) was then added via cannula to the cooled base solution and stirred at this temperature for 30 min. Next, a THF (0.5 mL) solution of $ZnCl_2$ (42 mg, 0.31 mmol) was added via cannula and the mixture was warmed to 0°C and stirred for 30 min. A solution of the vinyl triflate **1a** (50 mg, 0.18 mmol) in THF (0.3 mL) was then added via cannula to the reaction mixture followed by addition of solid $Pd(PPh_3)_4$ (3 mg, 0.005 mmol). After warming to rt, the solution was heated to reflux until TLC showed consumption of the vinyl triflate (~1.5 h). The mixture was cooled to rt and quenched by the addition of H_2O (2.5 mL). The aqueous layer was extracted with Et_2O (2 x 5 mL), and the combined Et_2O washings were dried over anhydrous $MgSO_4$, filtered, and concentrated. The crude residue was purified by flash column chromatography (neutral alumina) eluting with 50:1 hexanes/Et_2O and gave 25 mg (57%) of dienyne **3g** as a

colorless oil: R_f 0.5 (20:1 hexanes:EtOAc); IR (CH_2Cl_2 film) 2956, 2873, 2180, 1725, 1620, 1566 cm^{-1}; ^1H NMR (500 MHz, $CDCl_3$) δ 6.95 (d, J = 15.8 Hz, 1H), 6.44 (d, J = 3.3 Hz, 1H), 6.19 (d, J = 15.7 Hz, 1H), 3.79 (s, 3H), 2.41 (dd, J = 3.7, 3.7 Hz, 1H), 1.92 (dddd, J = 15.2, 7.8, 3.4, 3.4 Hz, 1H), 1.60 (ddd, J = 12.1, 9.2, 3.5 Hz, 1H), 1.13-0.99 (m, 5H), 0.81 (s, 6H); ^{13}C NMR (125 MHz, $CDCl_3$) δ 166.5, 144.2, 131.6, 128.4, 125.8, 95.5, 90.5, 56.7, 55.9, 52.5, 51.7, 31.1, 24.6, 19.5, 19.4, 11.8; HRMS for $C_{16}H_{20}O_2$ (M^+) calcd 244.1464, found 244.1465.

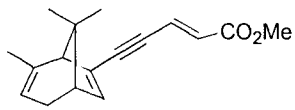

3h

Dienyne **3h**: *n*-BuLi (130 μL, 2.4 M in hexanes, 0.31 mmol) was added to a –78°C solution of DIPA (43 μL, 0.31 mmol) in THF (0.5 mL). The solution was warmed to 0°C and stirred for 20 min before being cooled back to –78°C. The alkyne **2c** (32mg, 0.29 mmol) in THF (0.3 mL) was then added via cannula to the cooled base solution and stirred at this temperature for 30 min. Next, a THF (0.5 mL) solution of $ZnCl_2$ (42 mg, 0.31 mmol) was added via cannula and the mixture was warmed to 0°C and stirred for 30 min. A solution of the vinyl triflate **1b** (50 mg, 0.17 mmol) in THF (0.3 mL) was then added via cannula to the reaction mixture followed by addition of solid $Pd(PPh_3)_4$ (3 mg, 0.005 mmol). After warming to rt, the solution was heated to reflux until TLC showed consumption of the vinyl triflate (~1.5 h). The mixture was cooled to rt and quenched by the addition of H_2O (2.5 mL). The aqueous layer was extracted with Et_2O (2 x 5 mL), and the combined Et_2O washings were dried over anhydrous $MgSO_4$, filtered, and

concentrated. The crude residue was purified by flash column chromatography (neutral alumina) using a gradient elution consisting of 60:1, 50:1, 40:1, 30:1, 20:1 hexanes/Et_2O and gave 28 mg (63% yield) of dienyne **3h** as a colorless oil: R_f 0.4 (20:1 hexanes:EtOAc); IR (CH_2Cl_2 film) 2952, 2924, 2182, 1725, 1622, 1574 cm^{-1}; ^1H NMR (500 MHz, $CDCl_3$) δ 6.94 (d, J = 15.7 Hz, 1H), 6.19 (d, J = 15.8 Hz, 1H), 6.06 (d, J = 3.2 Hz, 1H), 5.00 (br s, 1H), 3.77 (s, 3H), 2.32-2.22 (m, 1H), 2.18-2.12 (m, 2H), 1.84-1.74 (m, 4H), 1.08 (s, 3H), 1.06(s, 3H); ^{13}C NMR (125 MHz, $CDCl_3$) δ 166.4, 140.1, 139.9, 133.3, 128.7, 125.6, 116.7, 96.0, 89.6, 58.7, 51.8, 48.1, 44.3, 27.0, 26.5, 24.0, 20.5; HRMS for $C_{17}H_{20}O_2$ (M^+) calcd 256.1464, found 256.1465.

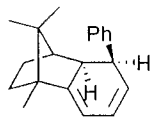

5a

Cyclohexadiene **5a**: Activated Zn dust was prepared as described by Boland et al.[12] Argon was bubbled through a suspension of Zn dust (1.5 g) in distilled H_2O (6 mL) for 15 min. $Cu(OAc)_2$ (0.15 g) was added and the flask was immediately sealed. The mixture was vigorously stirred for 15 min. $AgNO_3$ (0.15 g) was then added, and the solution was stirred for 30 min. The activated Zn was then filtered and washed successively with H_2O, MeOH, acetone, and Et_2O. The moist activated Zn was transferred immediately to a flask containing the reaction solvents H_2O (2 mL) and THF (1.5 mL). Compound **3a** (140 mg, 0.53 mmol) in THF (0.5 mL) was added to this mixture and was vigorously stirred at rt in the dark for 11 d. The Zn dust was removed by filtration on a sintered glass funnel and washed with large amounts of Et_2O and H_2O. The organic phase was separated, dried over $MgSO_4$, filtered and concentrated. After

purification by flash chromatography using silica gel eluting with 100% hexanes, 94 mg (67%) of cyclohexadiene **5a** was obtained as a yellow oil: R_f 0.38 (100% hexanes); IR (neat) 3026, 2985, 2954, 2888 cm^{-1}; ^1H NMR (500 MHz, $CDCl_3$) δ 7.28-7.15 (m, 5H), 6.26 (ddd, J = 9.8, 1.2, 0.6 Hz, 1H), 5.68 (dd, J = 9.7, 5.5 Hz, 1H), 5.48 (dd, J = 5.1, 3.2 Hz, 1H), 3.77 (dd, J = 12.5, 5.4 Hz, 1H), 2.91(dd, J = 13.0, 3.1 Hz, 1H), 2.03 (d, J = 3.9 Hz, 1H), 1.94 (dddd, J = 12.0, 12.0, 4.9, 4.9 Hz, 1H), 1.64 (ddd, J = 12.3, 12.3, 3.3 Hz, 1H), 1.52-1.47 (m, 1H), 1.38 (ddd, J = 12.1, 9.1, 3.4 Hz, 1H), 0.82 (s, 3H), 0.70 (s, 3H), -0.20 (s, 3H); ^{13}C NMR (125 MHz, $CDCl_3$) δ 153.7, 142.2, 130.6, 127.7, 126.2, 126.0, 124.4, 107.7, 50.3, 50.2, 50.0, 45.7, 39.8, 33.6, 31.8, 20.8, 20.1, 11.5; HRMS for $C_{20}H_{24}$ (M^+) calcd 264.1879, found 264.1876.

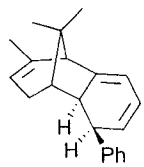

5b

Cyclohexadiene **5b**: Activated Zn dust was prepared as described above for the preparation of compound **5a**. Zn dust (0.5 g), distilled H_2O (3 mL), $Cu(OAc)_2$ (0.05 g), and $AgNO_3$ (0.05 g) were combined, then filtered. The moist activated Zn was transferred immediately to a flask containing the reaction solvents H_2O (2 mL) and THF (1.5 mL). Compound **3b** (21 mg, 0.076 mmol) in THF (0.5 mL) was added to this mixture and was vigorously stirred at rt in the dark for 6 d. The Zn dust was removed by filtration on a sintered glass funnel and washed with large amounts of Et_2O and H_2O. The organic phase was separated, dried over $MgSO_4$, filtered and concentrated. The crude residue was then redissolved in THF and heated to reflux for 6 h. The mixture was

concentrated under reduced pressure. After purification by flash chromatography using silica gel eluting with 100% hexanes, 11 mg (50%) of cyclohexadiene **5b** was obtained as a yellow oil: R_f 0.50 (100% hexanes); IR (CH_2Cl_2 film) 3026, 2985, 2924, 2882 cm^{-1}; ^1H NMR (500 MHz, $CDCl_3$) δ 7.23-7.15 (m, 5H), 6.22 (dd, J = 9.6, 5.1 Hz, 1H), 5.74 (dd, J = 9.6, 5.6 Hz, 1H), 5.66 (dd, J = 5.1, 3.0 Hz, 1H), 5.16 (s, 1H) 3.69 (dd, J = 11.8, 5.7 Hz, 1H), 3.06 (d, J = 12.2 Hz, 1H), 2.47-2.37 (m 1H), 2.01 (s, 1H), 1.99-1.93 (m, 1H), 1.75 (s, 1H), 1.64 (s, 3H), 0.82 (s, 3 H), -0.05 (s, 3H); ^{13}C NMR (125 MHz, $CDCl_3$) δ 150.6, 140.8, 138.1, 130.8, 127.7, 126.5, 126.1, 125.6, 117.7, 110.4, 57.3, 50.2, 41.0, 40.7, 40.6, 35.8, 25.6, 22.6, 21.9; HRMS for $C_{21}H_{24}$ (M^+) calcd 276.1879, found 276.1883.

Partial data for *trans*-hexatriene **6b**: Slightly impure, 8 mg (36%); R_f 0.32 (100% hexanes); ^1H NMR (500 MHz, $CDCl_3$) δ 7.40 (d, J = 7.2 Hz, 2H), 7.31 (dd, J = 7.4, 7.4 Hz, 2H), 7.20 (dd, J = 7.4, 7.4 Hz, 1H), 6.86 (dd, J = 15.7, 9.8 Hz, 1H), 6.58 (d, J = 15.4 Hz, 1H), 6.52-6.41 (m, 2H), 5.65 (d, J = 3.2 Hz, 1H), 5.01 (br s, 1H), 2.37 (s, 1H), 2.32-2.24 (m, 1H), 2.14-2.10 (m, 1H), 1.84-1.76 (m, 4H), 1.09 (s, 3H), 1.05 (s, 3H); ^{13}C NMR (125 MHz, $CDCl_3$) δ 153.2, 140.4, 137.6, 131.7, 131.1, 130.0, 129.7, 129.4, 128.6, 127.3, 126.2, 117.2, 53.7, 47.6, 44.4, 27.7, 27.3, 24.3, 20.9.

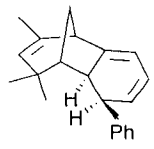

5c

Cyclohexadiene **5c**: Activated Zn dust was prepared as described above for the preparation of compound **5a**. Zn dust (2.4 g), distilled H_2O (18 mL), $Cu(OAc)_2$ (0.24 g),

and $AgNO_3$ (0.24 g) were combined, then filtered. The moist activated Zn was transferred immediately to a flask containing the reaction solvents H_2O (20 mL) and THF (15 mL). Compound **3c** (36 mg, 0.13 mmol) in THF (5 mL) was added to this mixture and was vigorously stirred at rt in the dark for 2 d. The Zn dust was removed by filtration on a sintered glass funnel and washed with large amounts of Et_2O and H_2O. The organic phase was separated, dried over $MgSO_4$, filtered and concentrated. The crude residue was then dissolved in toluene and heated to reflux for 1.5 h. The mixture was concentrated under reduced pressure. After purification by flash chromatography using silica gel eluting with 100% hexanes, 7 mg (20%) of cyclohexadiene **5c** was obtained as a yellow oil: R_f 0.55 (100% hexanes, ran twice); IR (CH_2Cl_2 film) 3082, 2963, 2925 cm^{-1}; ^1H NMR (500 MHz, $CDCl_3$) δ 7.27-7.18 (m, 5H), 6.14 (dd, J = 9.5, 4.9 Hz, 1H), 5.78 (dd, J = 9.6, 5.8 Hz, 1H), 5.67 (dd, J = 4.8, 2.8 Hz, 1H), 4.83 (s, 1H) 3.35 (dd, J = 10.2, 5.8 Hz, 1H), 3.23 (d, J = 8.6 Hz, 1H), 2.44 (d, J = 3.6 Hz, 1H), 1.62 (d, J = 1.4 Hz, 3H), 1.61-1.57 (m, 2H), 1.05 (s, 3H), 0.80 (s, 3H), 0.69 (ddd, J = 9.5, 5.3, 3.9 Hz, 1H); ^{13}C NMR (125 MHz, $CDCl_3$) δ 149.0, 138.4, 136.5, 129.8, 129.1, 127.8, 127.7, 126.7, 125.6, 110.0, 46.1, 44.8, 43.3, 42.6, 38.3, 34.2, 30.3, 26.0, 22.2; HRMS for $C_{21}H_{24}$ (M^+) calcd 276.1879, found 276.1880.

Partial data for *trans*-hexatriene **6c**: R_f 0.44 (100% hexanes, ran twice); ^1H NMR (500 MHz, $CDCl_3$, partial data) δ 7.42-7.18 (m, 5H), 6.86 (ddd, J = 15.3, 7.5, 3.0 Hz, 1H), 6.58 (d, J = 15.3 Hz, 1H), 6.50-6.42 (m, 2H), 5.80 (d, J = 3.4 Hz, 1H), 4.72 (s, 1H).

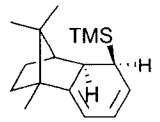

5d

Cyclohexadiene **5d**: Activated Zn dust was prepared as previously described above for the preparation of compound **5a**. Zn dust (4.0 g), distilled H_2O (30 mL), $Cu(OAc)_2$ (0.40 g), and $AgNO_3$ (0.40 g) were combined, then filtered. The moist activated Zn was transferred immediately to a flask containing the reaction solvents H_2O (40 mL) and THF (25 mL). Compound **3d** (78 mg, 0.30 mmol) in THF (5 mL) was added to this mixture and was vigorously stirred at 45°C in the dark for 6 d. The Zn dust was removed by filtration on a sintered glass funnel and washed with large amounts of Et_2O and H_2O. The organic phase was separated, dried over $MgSO_4$, filtered and concentrated. After purification by flash chromatography using alumina eluting with 1% Et_3N/hexanes, 70 mg (90%) of cyclohexadiene **5d** was obtained as a yellow oil: R_f 0.58 (100% hexanes); IR (CH_2Cl_2 film) 3027, 2955, 2899, 1663, 1583 cm^{-1}; ^1H NMR (500 MHz, $CDCl_3$) δ 5.81 (ddd, J = 9.8, 5.0, 2.0 Hz, 1H), 5.60 (dd, J = 9.8, 5.5 Hz, 1H), 5.28 (dd, J = 5.0, 3.1 Hz, 1H), 3.09 (dd, J = 14.1, 3.2 Hz, 1H), 2.21 (ddd, J = 14.0, 5.4, 2.1 Hz, 1H), 1.96 (d, J = 3.9 Hz, 1H), 1.87 (ddd, J = 16.8, 12.2, 4.0 Hz, 1H), 1.62 (ddd, J = 12.5, 12.5, 3.3 Hz, 1H), 1.39 (ddd, J = 14.5, 9.2, 5.3 Hz, 1H) 1.23 (ddd, J = 12.2, 9.3, 3.3 Hz, 1H) 1.08 (s, 3H), 0.92 (s, 3 H), 0.90 (s, 3H), 0.05 (s, 9H); ^{13}C NMR (125 MHz, $CDCl_3$) δ 152.8, 125.7, 122.3, 108.0, 50.0, 49.9, 47.9, 47.3, 32.8, 32.6, 31.7, 22.6, 20.8, 11.7, 0.0; HRMS for $C_{17}H_{28}Si$ (M^+) calcd, 260.1961, found 260.1960.

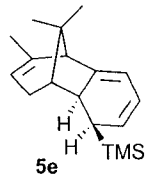

5e

Cyclohexadiene **5e**: Activated Zn dust was prepared as previously described. Zn dust (2.2 g), distilled H_2O (17 mL), $Cu(OAc)_2$ (0.22 g), and $AgNO_3$ (0.22 g) were combined, then filtered. The moist activated Zn was transferred immediately to a flask containing the reaction solvents H_2O (20 mL) and THF (15 mL). Compound **3e** (42 mg, 0.16 mmol) in THF (5 mL) was added to this mixture and was vigorously stirred at 45°C in the dark for 3 d. The Zn dust was removed by filtration on a sintered glass funnel and washed with large amounts of Et_2O and H_2O. The organic phase was separated, dried over $MgSO_4$, filtered and concentrated. After purification by flash chromatography using alumina eluting with 1% Et_3N/hexanes, 23 mg (55%) of cyclohexadiene **5e** was obtained as a yellow oil: R_f 0.50 (100% hexanes); IR (CH_2Cl_2 film) 3092, 2953, 2927, 1656, 1578 cm^{-1}; ^1H NMR (500 MHz, $CDCl_3$) δ 5.82 (dddd, J = 9.8, 4.9, 1.7, 0.6 Hz, 1H), 5.67 (dddd, J = 9.8, 5.8, 0.8, 0.8 Hz, 1H), 5.49 (dd, J = 4.9, 3.1 Hz, 1H), 5.12-5.07 (m, 1H) 3.24 (br. d, J = 12.5 Hz, 1H), 2.39-2.31 (m, 1H), 2.18 (dddd, J = 12.5, 5.8, 1.0, 1.0 Hz, 1H), 2.07 (s, 1H), 1.85-1.76 (m, 2H), 1.62 (dd, J = 3.8, 1.5 Hz, 3H), 1.20 (s, 3H), 1.06 (s, 3 H), 0.07 (s, 9H); ^{13}C NMR (125 MHz, $CDCl_3$) δ 150.5, 137.5, 126.7, 123.4, 117.3, 111.1, 57.4, 48.3, 43.2, 41.3, 35.8, 32.7, 29.3, 22.5, 22.0, -0.2; HRMS for $C_{18}H_{28}Si$ (M^+) calcd 272.1961, found 272.1962.

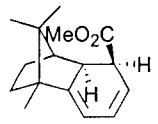

5g

Cyclohexadiene **5g**: The dienyne **3g** (25 mg, 0.10 mmol) was dissolved in CH_2Cl_2 (5 mL) at rt. Quinoline (7 μL, 0.06 mmol) was added, followed by Lindlar catalyst (21 mg, 5% Pd on $CaCO_3$ poisoned with Pb, 0.01 mmol). H_2 (balloon) was bubbled through the solution until TLC showed consumption of starting material (0.5 h). The reaction vessel was then flushed with Argon, and left to stir at rt for 6 d to allow the cyclization to occur. Filtration through Celite removed the spent catalyst, and the solution was then concentrated and purified by flash column chromatography (60:1 hexanes:Et_2O, silica treated with 1% Et_3N) to give 12 mg (45%) of cyclohexadiene **5g** as a yellow oil: R_f 0.56 (20:1 hexanes:EtOAc, ran twice); IR (CH_2Cl_2 film) 3039, 2953, 2871, 1731, 1597 cm^{-1}; ^1H NMR (500 MHz, $CDCl_3$) δ 6.12 (ddd, J = 9.8, 5.2, 1.1 Hz, 1H), 5.52 (dd, J = 10.2, 5.4 Hz, 1H), 5.46 (dd, J = 5.1, 3.0 Hz, 1H), 3.62 (s, 3H), 3.27 (ddd, J = 13.7, 5.4, 1.3 Hz, 1H), 2.77 (dd, J = 13.6, 2.8 Hz, 1H), 2.34 (d, J = 3.9 Hz, 1H), 1.96 (dddd, J = 12.0, 12.0, 4.9, 4.9 Hz, 1H), 1.68 (ddd, J = 12.5, 12.5, 3.5 Hz, 1H), 1.48 (ddd, J = 14.5, 9.3, 5.3 Hz, 1H) 1.33 (ddd, J = 12.3, 9.2, 3.4 Hz, 1H) 0.93 (s, 3H), 0.90 (s, 3 H), 0.65 (s, 3H); ^{13}C NMR (125 MHz, $CDCl_3$) δ 173.8, 153.3, 126.2, 119.7, 108.4, 51.7, 50.8, 50.7, 46.7, 45.9, 40.0, 32.8, 31.3, 20.7, 20.6, 11.8; HRMS for $C_{16}H_{22}O_2$ (M^+) calcd 246.1621, found 246.1620.

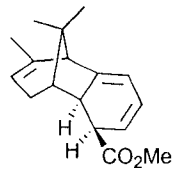

5h

Cyclohexadiene **5h**: The dienyne **3h** (15 mg, 0.06 mmol) was dissolved in CH_2Cl_2 (3 mL) at rt. Quinoline (5 μL, 0.04 mmol) was added, followed by Lindlar catalyst (15 mg, 5% Pd on $CaCO_3$ poisoned with Pb, 0.01 mmol). H_2 (balloon) was bubbled through the solution until TLC showed consumption of starting material (2 h). The reaction vessel was then flushed with Argon, and left to stir at rt for 5 d to allow the cyclization to occur. Filtration through Celite removed the spent catalyst, and the solution was then concentrated and purified by flash column chromatography (80:1 hexanes:Et_2O, silica treated with 1% Et_3N) to give 6 mg (40%) of an inseparable mixture of 2:1 cyclohexadiene **5h**:*trans*-hexatriene **6h** as a yellow oil.

Partial data for **5h**: R_f 0.50 (20:1 hexanes/EtOAc, ran twice); ^{1}H NMR (500 MHz, $CDCl_3$) δ 6.11 (dd, J = 9.2, 5.1 Hz, 1H), 5.65 (dd, J = 5.2, 3.1 Hz, 1H), 5.56 (dd, J = 10.3, 6.0 Hz, 1H), 5.18 (br s, 1H), 3.63 (s, 3H), 3.28 (dd, J = 12.1, 5.6 Hz, 1H), 2.95 (d, J = 12.5 Hz, 1H), 2.48-2.40 (m, 1H), 2.16-2.11 (m, 2H), 1.64 (app. q, J = 1.5 Hz, 3H), 1.04 (s, 3H), 0.80 (s, 3H).

Partial data for *trans*-hexatriene **6h**: R_f 0.50 (20:1 hexanes/EtOAc, ran twice); ^{1}HNMR (500 MHz, $CDCl_3$, partial data) δ 7.36 (dd, J = 15.2, 11.3 Hz, 1H), 6.70 (d, J = 15.3 Hz, 1H), 6.34 (dd, J = 15.3, 11.3 Hz, 1H), 5.90 (d, J = 15.2 Hz, 1H), 5.84 (d, J = 3.3 Hz, 1H), 5.0 (br s, 1H).

Attempted Sakurai Reactions of 3d and 3e—Preparation of Arenes 7d and 7e

To a solution of the aldehyde (1 eq) in CH_2Cl_2 (0.2 M) at –78°C was added the Lewis acid (1 eq). The mixture was allowed to stir for 10 min before the allylic silane (1 eq) in CH_2Cl_2 was added via cannula. The reaction was allowed to stir at this temperature until TLC showed consumption of the allyl silane (~ 20 – 120 min). The mixture was then quenched with saturated aq $NaHCO_3$. The aqueous layer was extracted with CH_2Cl_2, and the combined organic extracts were dried over $MgSO_4$, filtered, and concentrated. The crude reaction mixture was purified using gravity silica gel chromatography (100% hexanes).

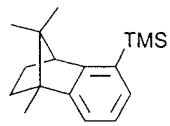

7d

Clear colorless oil; Yield ~50%; R_f 0.50 (100% hexanes); IR (CH_2Cl_2 film) 3054, 2955, 2871, 1407 cm^{-1}; ^1H NMR (500 MHz, $CDCl_3$) δ 7.21 (dd, J = 7.3, 1.2 Hz, 1H), 7.10 (dd, J = 7.3, 7.3 Hz, 1H), 7.04 (dd, J = 7.2, 1.2 Hz, 1H), 2.93 (d, J = 4.1 Hz, 1H), 2.14-2.01 (m, 1H), 1.87-1.79 (m, 1H), 1.25 (s, 3H), 1.15-1.05 (m, 2H), 0.98 (s, 3H), 0.51 (s, 3H), 0.29 (s, 9H); ^{13}C NMR (125 MHz, $CDCl_3$) δ 153.7, 149.7, 131.2, 130.2, 124.6, 120.1, 57.2, 53.5, 52.1, 33.2, 26.0, 20.0, 19.3, 11.6, -0.3; HRMS for $C_{17}H_{26}Si$ (M^+) calcd 258.1805, found 258.1803.

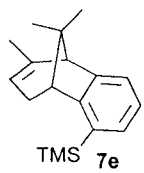

7e

Clear colorless oil; Yield ~50%; R_f 0.41 (100% hexanes); IR (CH_2Cl_2 film) 3021, 2954, 2921, 1446 cm^{-1}; ^1H NMR (500 MHz, $CDCl_3$) δ 7.25 (dd, J = 9.1, 3.8 Hz, 1H), 7.09-7.03 (m, 2H), 4.89 (br s, 1H), 2.74 (d, J = 2.5 Hz, 1H), 2.50 (s, 1H), 2.45 (dddd, J = 18.0, 5.3, 2.8, 2.8 Hz, 1H), 1.94 (dddd, J = 17.5, 3.7, 2.0, 2.0 Hz, 1H), 1.73 (dd, J = 4.0, 2.3 Hz, 3H), 1.20 (s, 3H), 0.89 (s, 3H), 0.28 (s, 9H); ^{13}C NMR (125 MHz, $CDCl_3$) δ 152.2, 150.6, 139.4, 134.8, 131.3, 125.1, 121.1, 116.3, 56.1, 49.3, 44.9, 30.0, 27.4, 23.1, 21.1, 0.06; HRMS for $C_{18}H_{26}Si$ (M^+) calcd 270.1805, found 270.1800.

2.6. References

[1] a) Mazzola, R. D., Jr.; White, T. D.; Vollmer-Snarr, H. R.; West, F. G. *Org. Lett.* **2005**, *7*, 2799. b) White, T. D.; West, F. G. *Tetrahedron Lett.* **2005**, *46*, 5629. c) Giese, S.; Mazzola, R. D., Jr.; Amann, C. M.; Arif, A. M.; West, F. G. *Angew. Chem. Int. Ed.* **2005**, *44*, 6546.

[2] Magomedov, N. A.; Ruggiero, P. L.; Tang, Y. *Org. Lett.* **2004**, *6*, 3373.

[3] Tessier, P. E.; Nguyen, N.; Clay, M. D.; Fallis, A. G. *Org. Lett.* **2005**, *7*, 767.

[4] A version of this chapter has been submitted for publication.

[5] For a review of Pd-catalyzed alkynylation chemistry, see: Negishi, E.; Anastasia, L. *Chem. Rev.* **2003**, *103*, 1979.

[6] Mazzola, R. D., Jr.; Giese, S.; Benson, C. L.; West, F. G. *J. Org. Chem.* **2004**, *69*, 220.

[7] a) **2a**: Michel, P.; Gennet, D.; Rassat, A. *Tetrahedron Lett.* **1999**, *40*, 8575. b) **2b**: Fiandanese, V.; Marchese, G.; Punzi, A.; Ruggieri, G. *Tetrahedron Lett.* **1996**, *37*, 8455. c) **2c**: Wei, X.; Taylor, R. J. K. *Tetrahedron Lett.* **1998**, *39*, 3815.

[8] Nicolaou, K. C.; Petasis, N. A.; Zipkin, R. E. *J. Am. Chem. Soc.* **1982**, *104*, 5560.

[9] Hayashi, R.; Fernandez, S.; Okamura, W. H. *Org. Lett.* **2002**, *4*, 851.

[10] Oves, D.; Ferrero, M.; Fernandez, S.; Gotor. V. *J. Org. Chem.* **2003**, *68*, 1154.

[11] a) Marvell, E. N.; Tashiro, J. *J. Org. Chem.* **1965**, *30*, 3991. b) Paquette, L. A.; Chang, J.; Liu, Z. *J. Org. Chem.* **2004**, *69*, 6441. c) Kumar, P.; Naidu, S. V.; Gupta, P. *J. Org. Chem.* **2005**, *70*, 2843.

[12] a) Nicolaou, K. C.; Ladduwahetty. T.; Taffer, I. M.; Zipkin, R. E. *Synthesis* **1986**, 344. b) Overman, L. E.; Thompson, A. S. *J. Am. Chem. Soc.* **1998**, *110*, 2248.

[13] Boland, W.; Schroer, N.; Sieler, C.; Feigel, M. *Helv. Chim. Acta* **1987**, *70*, 1025.

[14] a) Alami, M.; Crousse, B.; Linstrumelle, G. *Tetrahedron Lett.* **1994**, *35*, 3543. b) Borhan, B.; Souto, M. L.; Um, J. M.; Zhou, B.; Nakanishi, K. *Chem. Eur. J.* **1999**, *5*, 1172. c) Nesnas, N.; Rando, R. R.; Nakanishi, K. *Tetrahedron* **2002**, *58*, 6577.

[15] Schleyer, P. V. R. *J. Am. Chem. Soc.* **1967**, *89*, 701.

[16] Brown, H. C.; Kawakami, J. H.; Liu, K.-T. *J. Am. Chem. Soc.* **1973**, *95*, 2209.

[17] Inagaki, S.; Fujimoto, H.; Fukui, K. *J. Am. Chem. Soc.* **1976**, *98*, 4054.

[18] Rondan, N. G.; Paddon-Row, M. N.; Caramella, P.; Houk, K. N. *J. Am. Chem. Soc.* **1981**, *103*, 2436.

[19] Rondan, N. G.; Paddon-Row, M. N.; Caramella, P.; Mareda, J.; Mueller, P. H.; Houk, K. N. *J. Am. Chem. Soc.* **1982**, *104*, 4974.

[20] Masse, C. E.; Panek, J. S. *Chem. Rev.* **1995**, *95*, 1293.

[21] a) Suffert, J.; Salem, B. Klotz, P. *J. Am. Chem. Soc.* **2001**, *123*, 12107. b) von Essen, R.; Frank, D.; Sünnemann, H. W.; Vidovic, D.; Magull, J.; de Meijere, A. *Chem. Eur. J.* **2005**, *11*, 6583.

3. Approach to the Total Synthesis of Taxinine

3.1. Introduction

There are currently hundreds of taxane diterpenes that have been isolated and characterized from various species of the yew tree. Chemical studies on constituents of this plant had been carried out as early as 1856, when a mixture of highly toxic taxoid alkaloids was isolated from the European yew (*Taxus baccata*) and collectively called taxine by Lucas.[1] One component of this mixture is shown in Figure 3.1. The first taxane diterpene whose structure was fully elucidated was taxinine in 1963.[2] However, the most famous member of this family of compounds is Taxol® (paclitaxel),[3] currently a billion plus dollar per year drug used for the treatment of certain breast and ovarian cancers.

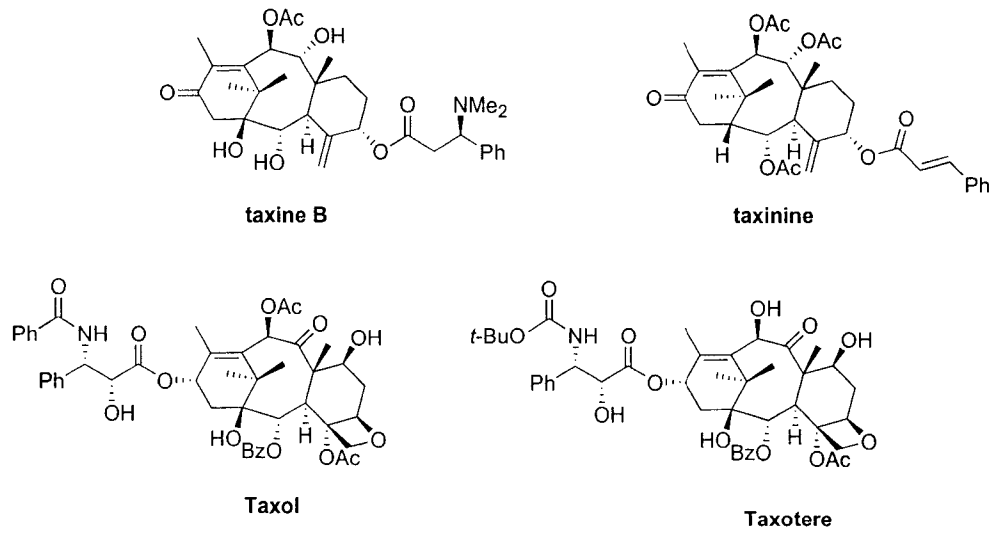

Figure 3.1. Representative examples of members of the taxane family.

Taxol was first harvested in its natural form from the bark of the slow growing pacific yew tree (*Taxus brevifolia*). It was quickly identified as a potent anti-cancer agent, though progress in its eventual development as a widely used drug was hampered due to problems associated with its low aqueous solubility, in addition to low natural abundance (0.02% isolated yield). Years later, the unique mechanism of action responsible for taxol's activity was elucidated, and fostered a renewed interest in its capabilities. The compound was found to disrupt the dynamic cell microtubule polymerization-depolymerization process necessary for chromosome segregation during cell division.[4] By binding to the tubulin polymer, taxol promotes polymerization and prevents microtubule disassembly, which is necessary for completion of mitosis. This ultimately leads to cell death. Other anti-tumour agents that were known to exert their action through microtubule binding had the opposite effect: they were microtuble destabilizers. This new realization, coupled with the effective formulation of taxol in ethanol and Cremophor EL to solve its solubility issues, fueled further investigations into

its development: taxol was enrolled in Phase I clinical trials and shortly thereafter, progressed into Phase II. The later development of an efficient semi-synthesis of the compound from readily and substantially available 10-deacetyl-baccatin III, addressed the issue of its supply.[5] Finally, some 30 years after its initial discovery, taxol was approved for the treatment of refractory ovarian and breast cancer as well as non-small cell lung cancer. A close semisynthetic relative, Taxotere® (docetaxel), was granted approval as well (Figure 3.1).[6]

The unique and challenging structure of taxol elicited great interest within the synthetic community. Taxol is comprised of a basic 6-8-6 tricyclic core in which the conformation of the ring system adopts a cage-like appearance, a feature that must be taken into consideration in any synthetic undertaking. Further, the challenges associated with the construction of entropically and enthalpically disfavored eight-membered rings have been noted, and much effort has been devoted in recent years to the development of efficient methods for their formation.[7] That, coupled with the presence of a bridgehead olefin embedded within the six-membered A-ring, as well as the mulititude of oxygenated stereocenters (Figure 3.2), presented a unique opportunity to showcase some clever synthetic approaches to this new class of compounds.

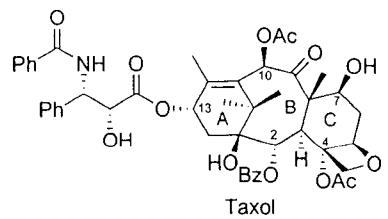

Taxol

Figure 3.2. Taxol numbering and ring designations.

To date, there have been six total syntheses of the natural product spanning the years 1994 to 1999, and these have recently been reviewed.[8] Numerous approaches to the taxane 6-8-6 ring system have also been published and subsequently reviewed.[3a] While a convergent synthesis would suggest higher efficiency in terms of greater material throughput, this strategy is much less commonly employed in the many synthetic approaches to the tricyclic core of the taxanes. This is perhaps due to the difficulty that ensues on closure of the eight-membered ring following union of functionalized A and C ring precursors. Nevertheless, three of the six total synthesis of taxol successfully utilize this method,[9,10,11] and numerous approaches to the taxane skeleton have adopted this strategy as well.[12] On the other hand, the great majority of syntheses of the taxane core proceed via a linear sequence.[13] One of the more popular strategies utilizes an intramolecular Diels Alder cycloaddition as a key bond forming reaction, a particularly effective route, as two of the taxane rings are usually formed simultaneously (A/B or B/C).[14]

Another linear strategy commonly employed involves fragmentative opening of two conjoined rings to reveal the central cyclooctane core equipped with varying degrees of functionalization. This approach has been very popular in accessing the taxane nucleus, likely because the ease with which the eight-membered ring can be formed by fragmentation of a strained bicyclic precursor. There are numerous fragmentation strategies one could conceivably apply, but the retro-aldol reaction has been one of the more popular methods.[15] The Grob fragmentation has also received significant attention.[16] A particular variant of the Grob reaction, involving epoxy alcohol fragmentation, was used by both Holton[17] and Wender[18] in their syntheses of taxol.

3.1.1. Oxidative fragmentation approach to the taxane core

Fragmentation via oxidative cleavage of vicinal diols or alkenes has been investigated in taxane synthesis by numerous groups. The utility of this approach stems from its ability to incorporate additional oxygen functionality while simultaneously revealing the cyclooctane. Our group was particularly interested in this strategy with respect to our own taxane approach. Therefore, it is worth discussing to a greater extent the details of such studies that exploit this methodology for taxane synthesis.

In 1984, Trost disclosed a straightforward, three step sequence to a simplified A/B taxoid ring skeleton via oxidative fragmentation (Scheme 3.1).[19] Enediol silyl ether **2** was reacted with allylic chloride **1** under Lewis acidic conditions to give α-trimethylsilyloxy ketones **3** and **3′** as a separable mixture of diastereomers. The diastereomers were then independently exposed to $EtAlCl_2$, to promote an intramolecular allylation reaction giving rise to diols **4** and **4′** in good yield. The diastereomeric diols converged to the same bicyclo[5.3.1]undecane ring system **5** on oxidative cleavage with $NaIO_4$ in excellent yield.

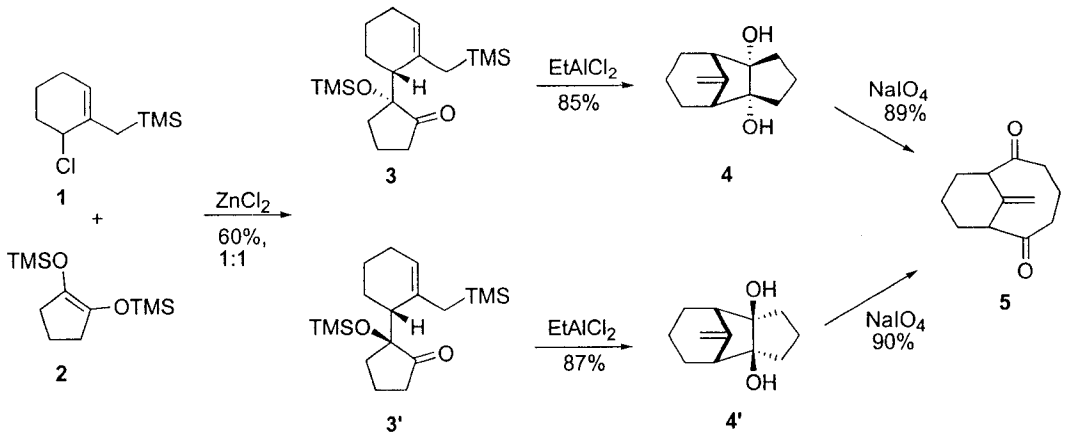

Scheme 3.1. Trost's oxidative cleavage strategy.

In addition to a retro-aldol strategy, Blechert also devised a ring-opening oxidative fragmentation approach to the taxane nucleus (Scheme 3.2).[20] Exploiting the ease with which cycloaddition reactions build up structural complexity, Blechert coupled enone **6** with cyclohexene via [2+2] photochemistry to provide **7** after carbonate cleavage and hydrolysis to reveal the ketone. Prior to ring cleavage with ozone, the C10 and C13 carbonyls of **7** were each reduced and protected in separate steps. Treatment of the resulting diacetate **9** with ozone in CH_2Cl_2 and MeOH resulted in formation of **10** in good yield.

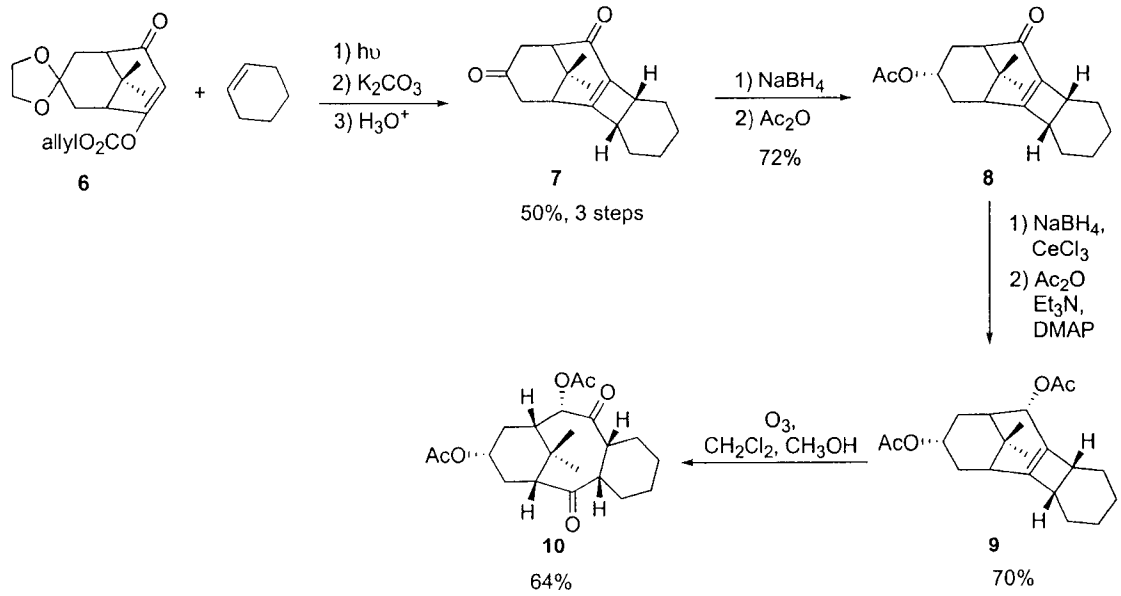

Scheme 3.2. Blechert's oxidative cleavage strategy.

In Little's approach, a unique diyl trapping reaction of diazene **11** was used to prepare bridged cycloadduct **12**, which was formed as a 1:1 mixture of diastereomers (Scheme 3.3).[21] In principle, either diastereomer could be advanced in the synthesis, but in practise, only one of them proved to be useful. Therefore, treatment of appropriate diastereomer **12** with phenylselenyl trifluoroacetate and KOH gave **13**, which was oxidized under Moffat-Swern conditions to α-selenyl-ketone **14**. Oxidation of **14** with *m*-CPBA followed by selenoxide *syn*-elimination furnished enone **15**. Next, the side chain that was to eventually become the C-ring was introduced by treatment of **15** with LDA and the appropriate electrophile. Subsequent ketone protection followed by oxidative cleavage of the alkene using RuO_2 and $NaIO_4$ afforded bicyclic diketone **16**. The C-ring was installed via intramolecular alkylation of **17** (prepared from **16** in three steps) culminating in the synthesis of tricyclic taxane precursor **18**.

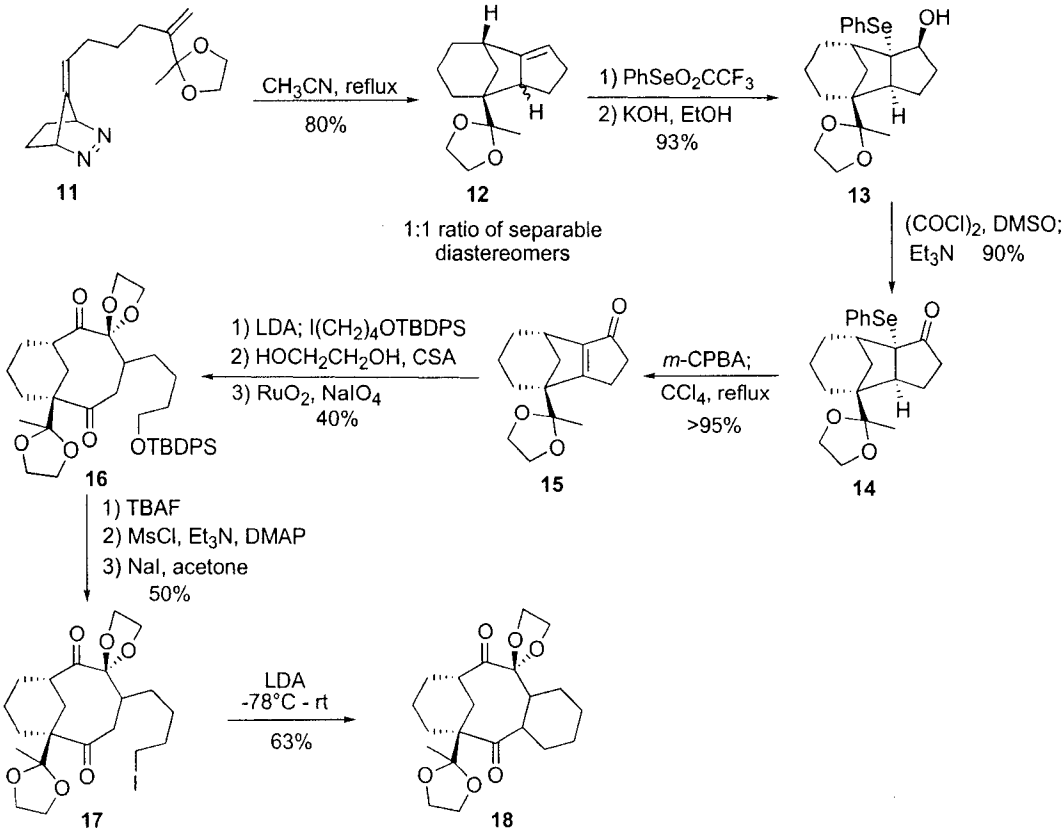

Scheme 3.3. Little's oxidative cleavage strategy.

3.1.2. Biological significance of taxinine

The natural product taxinine (Figure 3.1), isolated from the leaves of the Japanese yew (*Taxus cuspidata*), bears a structure similar to that of Taxol, though the biological activity it exhibits is remarkably different. While Taxol displays highly effective anti-cancer activity via a mechanism of action involving cell microtubule polymerization, taxinine shows little promise as an anti-proliferative agent.[22] It has been identified as an inhibitor of the cell membrane transporter P-glycoprotein, over-expression of which can lead to a rapid efflux of cytotoxic agents from within the cancerous cell.[23] It is through

this mechanism that multi-drug resistance (MDR) most commonly develops within a cell. MDR is a serious problem in cancer therapy, as once initiated, the cancerous cell gains resistance to a wide range of cytotoxic drugs, not just those involved in the treatment. In fact, for patients undergoing therapy with taxol, this is a common occurrence. For that reason, compounds that display MDR reversal activity are highly sought after. While taxinine itself has modest P-glycoprotein inhibitory activity, some of its unnatural analogs may show more promise.[24] An efficient and flexible synthetic route to this compound could allow access to some unnatural analogs that would otherwise be very difficult to obtain. To date, taxinine has yet to succumb to total synthesis, although numerous approaches to the natural product have been published.[25]

3.2. Background

The West group has previously initiated studies into the total synthesis of taxinine. Work done by Giese[26] and Mazzola[27] has culminated in the development of two routes to the natural product that provide access to highly advanced intermediates and address many of the challenging structural features associated with this class of compounds. However, within each approach there are particular drawbacks that prevented completion of the synthesis. In the next section, a summary of the two routes will be presented.

3.2.1. The first approach to taxinine (Giese)

In the retrosynthesis of the first approach, diketone **19** was proposed as a key intermediate (Scheme 3.4). From this compound, the bridgehead C11-C12 olefin could be revealed by base induced elimination of the epoxide. Further oxidation state adjustments and protective group manipulations would furnish taxinine. It was thought that β-epoxy diketone **19** should be available via oxidative cleavage of the C2-C10 olefin in substrate **20**, which would in turn be formed by a Nazarov cyclization of dienone **21**. This was envisioned to arise from a carbonylative Stille cross coupling of vinyl stannane **22** and enol triflate **23**. This enol triflate derives from α-pinene, and thus serves as an inexpensive source of chiral non-racemic starting material for the synthesis.

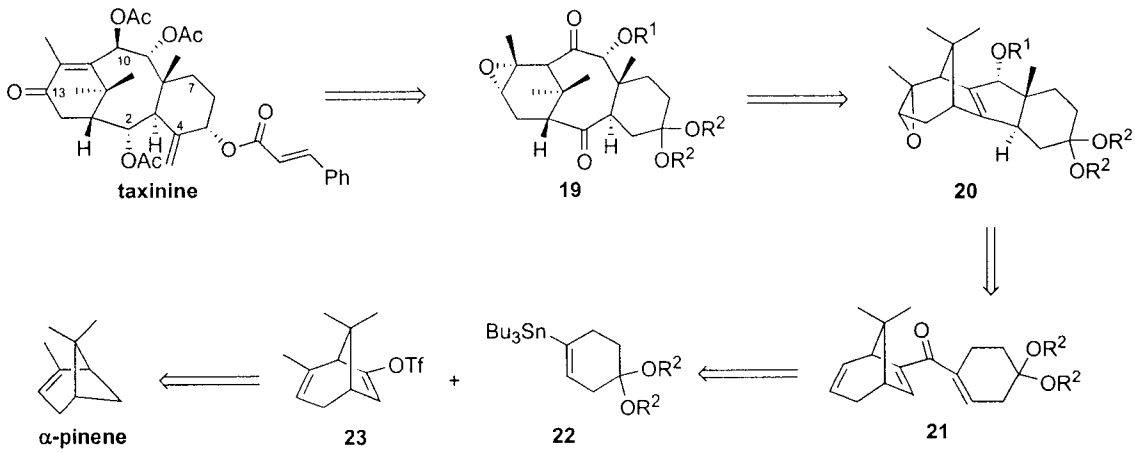

Scheme 3.4. Retrosynthesis of taxinine: first approach.

The first key step of the synthesis began with the carbonylative Stille cross coupling of **23** and **24** (Scheme 3.5).[28] This afforded dienone **25** in excellent yield, and permitted investigation into its subsequent Nazarov cyclization. When **25** was subjected

to low-temperature treatment with $BF_3{\cdot}OEt_2$, surprisingly, the product isolated from the reaction turned out to be cyclopropyl ketone **26**.[29] The seemingly remote olefin at C12-C13 is in close enough proximity to the intermediate allyl cation to react. This apparently occurs faster than straightforward deprotonation of the allyl cation to give the expected product. Fortunately, it was found that heating compound **26** in EtOH led to the rearranged ketone **27**, which could be carried forward in the synthesis. This reaction sequence provided **27** as one diastereomer. The next step of the synthesis aimed to reduce **27** via 1,4-hydride addition and to set the C8 quaternary center by reaction with MeI. However, on treatment with a host of reducing agents, either the product of 1,2-reduction, or recovered starting material were isolated. It was eventually found that dissolving metal conditions provided the desired reduced compound, but this intermediate could not be methylated at C8. With the intent to postpone the introduction of this substituent to a later intermediate in the synthesis, the sequence was carried on.

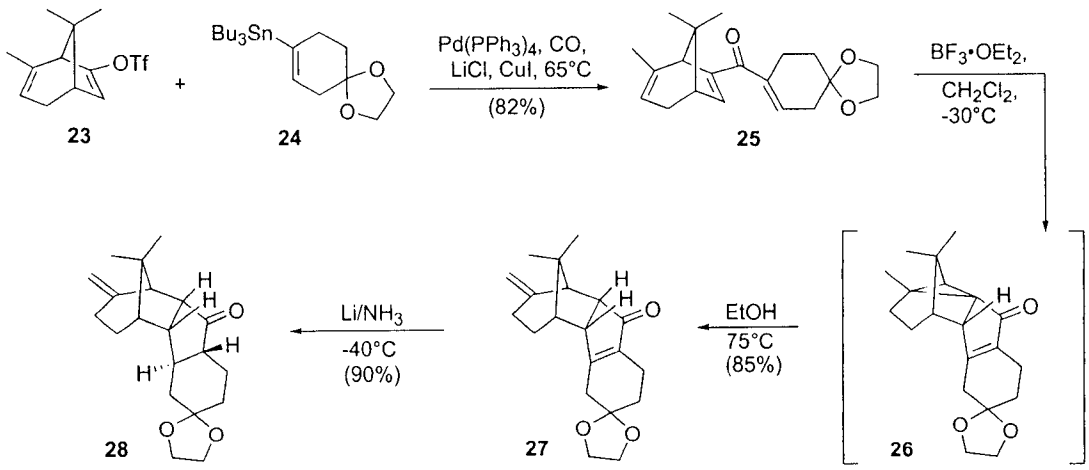

Scheme 3.5. Preparation of ketone **27** and its conjugate reduction.

At this stage, the exocyclic double bond in ketone **28** was isomerized by reaction with iodine in hot benzene (Scheme 3.6). The next step was to install the C2-C10 olefin required for later oxidative cleavage, and was accomplished by a two step selenoxide elimination. The phenylselenyl group was introduced selectively to C10 by reaction of PhSeCl with the TMS enol ether prepared from kinetic deprotonation of ketone **29** with LTMP. Subsequent oxidation to the selenoxide took place on treatment with *m*-CPBA, and this was immediately transferred to a refluxing solution of Et_3N in CH_2Cl_2/CCl_4 to effect elimination furnishing **30** in good yield. Methylation of this intermediate (LDA, then MeI) provided an excellent yield of **31**, where the methyl group was incorporated with high stereoselectivity, but with incorrect stereochemistry.

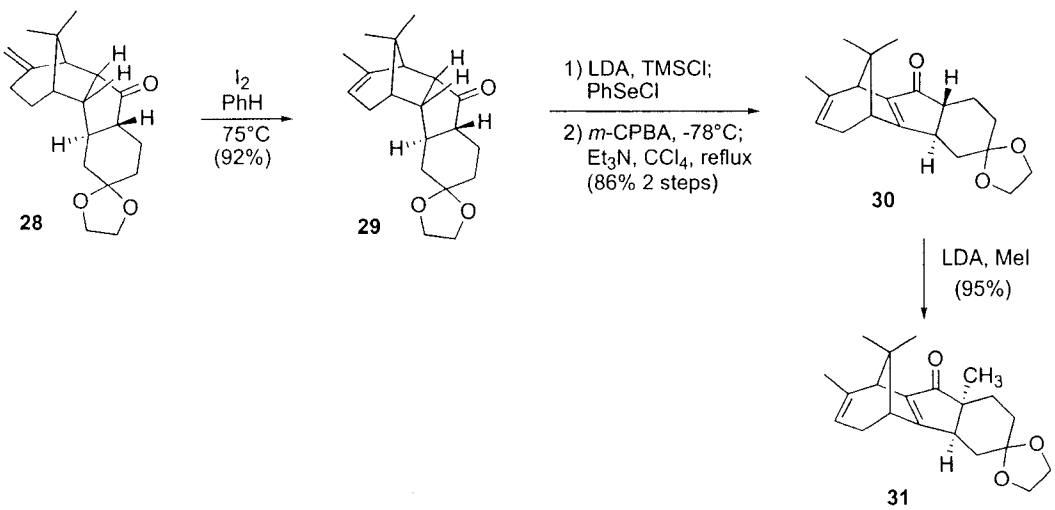

Scheme 3.6. Preparation of **30** by selenoxide elimination and subsequent methylation.

Non-methylated enone **30** was carried forward to the key oxidative ring opening step. Reduction with DIBALH afforded a separable 4:1 α:β mixture of allylic alcohol **32**. The major diastereomer was protected with MOMCl, then subjected to oxidation

with *m*-CPBA to effect epoxidation of the C12-C13 olefin providing **34**. The key ring fragmentation reaction took place without difficulty using RuO_2 in the presence of $NaIO_4$ as the oxidant and furnished the 6-8 bicyclic diketone **35** in excellent yield. Unfortunately, all attempts to open the A-ring epoxide by treatment with a range of basic conditions resulted in complex reaction mixtures. The problem was speculated to arise from a particular conformational preference of the eight-membered ring that moves the C11 proton out of proper alignment with the adjacent carbonyl, significantly lowering its acidity.

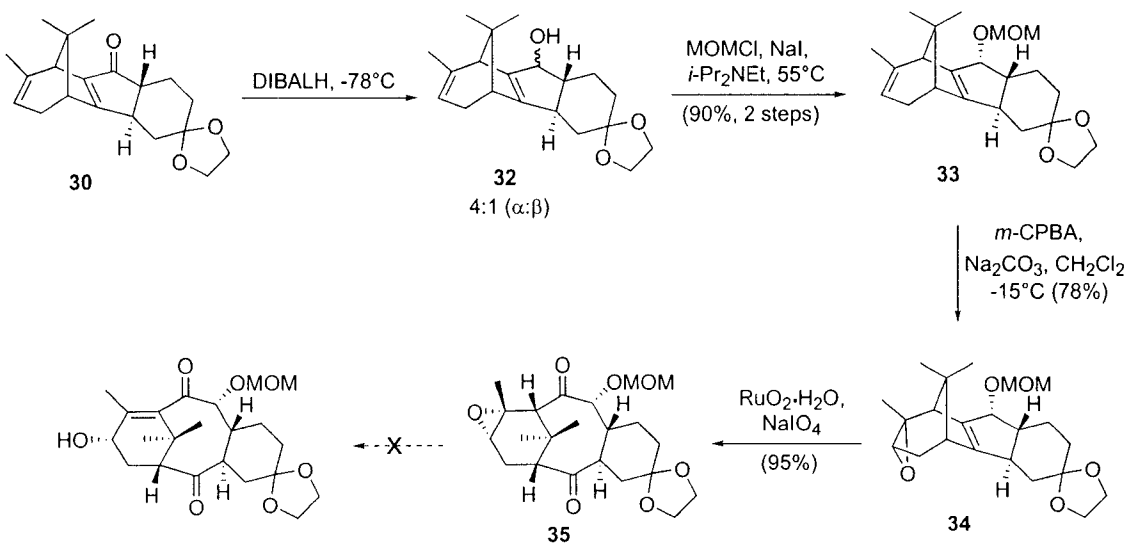

Scheme 3.7. Elaboration of **30** to the tricyclic taxane core.

Though this initial route was successful in establishing the complete tricyclic core of taxinine, two major problems prevented further studies along this avenue. First was the inability to position the C8 methyl at the correct center with the correct stereochemistry. Second was the inability to open the A-ring epoxide of diketone **35** to reveal the bridgehead olefin, a key structural element of the taxane core. Despite this,

valuable information was obtained about conformational and reactivity preferences in a system such as this one. In addition, the Nazarov cyclization/oxidative fragmentation approach was proven to be a viable strategy. This new knowledge was then applied in a second route to taxinine.

3.2.2. The second approach to taxinine (Mazzola)

Outlined in the retrosynthesis below are the key features of the second route to taxinine (Scheme 3.8). The proposed strategy involved a late stage annulation of the C-ring from an intermediate such as **36**. This would be revealed by oxidative cleavage of **37**. The installation of the C8 methyl group would be attempted in the same manner as planned in the first approach. Finally, this intermediate would derive, as before, from a Nazarov cyclization of dienone **38**, which would be prepared by a carbonylative Stille coupling of enol triflate **23** and new vinyl stannane **39** (from **40**).

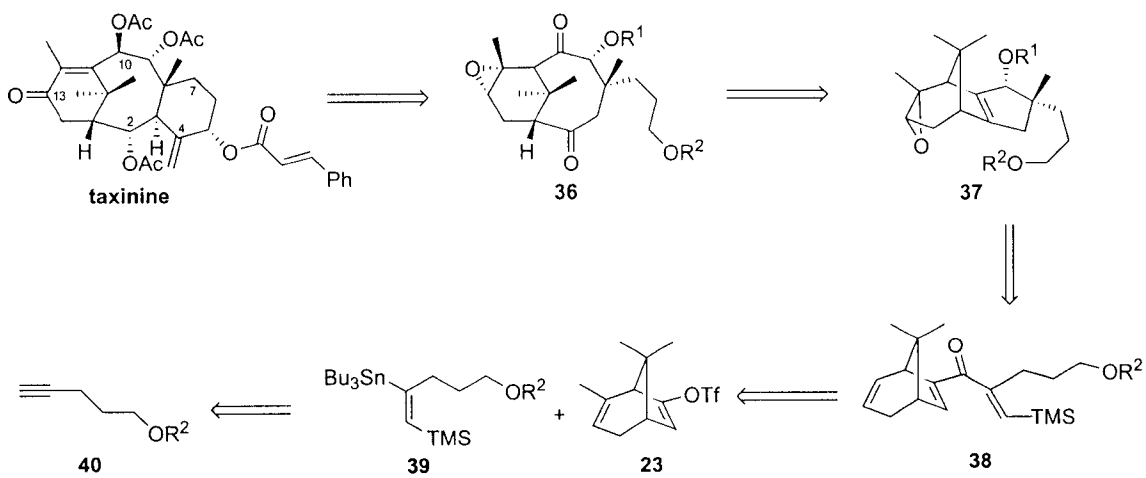

Scheme 3.8. Retrosynthesis of taxinine: second approach.

Stille coupling partner **42** was prepared via a Mo-catalyzed hydrostannylation reaction of 5-trimethylsilyl-4-pentynol **41** (available from 4-pentynol) (Scheme 3.9). It was found that the subsequent cross coupling reaction benefited from the presence of the free alcohol functionality, as its protection resulted in decreased yields of the product. Thus, vinyl triflate **23** was directly reacted with **42** in the presence of catalytic $Pd(PPh_3)_4$, LiCl and CuI and afforded dienone **43** in 72% yield. At this point, it was necessary to protect the primary alcohol, as the subsequent conditions for Nazarov cyclization were found to be incompatible with the free hydroxyl. When TBDPS protected dienone **44** was then treated with $FeCl_3$, a 74% yield of the desired product **45** was obtained with complete *endo* selectivity.[30] In contrast to the analogous reaction in the previous route where the C12-C13 olefin interfered with the cationic Nazarov intermediate, this substrate provided only the expected product. This is presumably due to the presence of the cation-stablizing trimethyl silyl moiety, which directs termination of the cyclization.

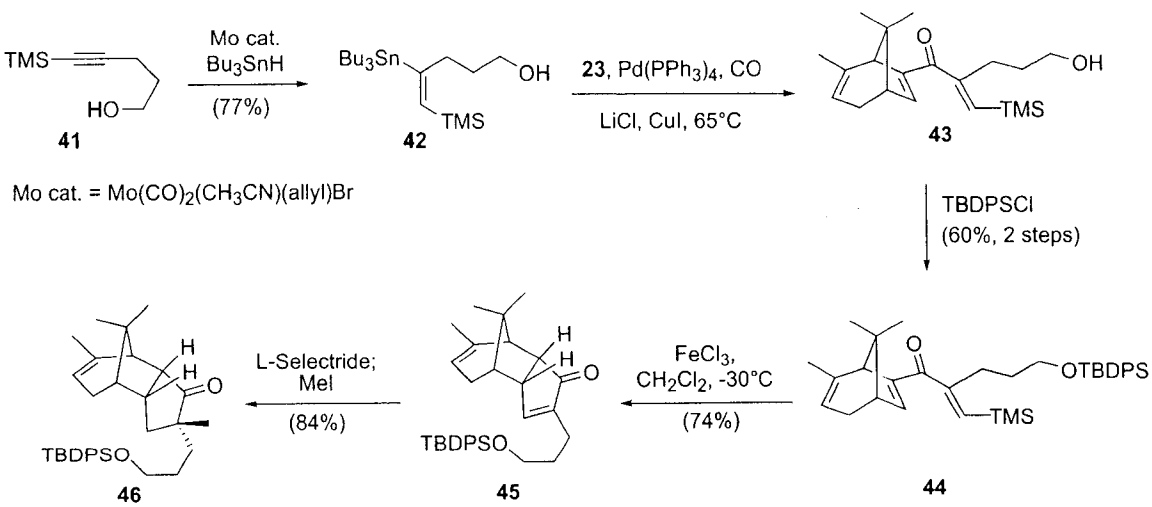

Scheme 3.9. Carbonylative Stille coupling, Nazarov cyclization and methylation.

The crucial investigation into the conjugate reduction and methylation of **45** followed. Contrary to the cyclohexane-fused case described earlier, when **45** was treated with L-Selectride, then MeI, reductive alkylation product **46** was obtained in high yield. Further, the quaternary center was set without difficulty and with the correct stereochemistry. It was surmised that methylation occurs exclusively from the β-face of the intermediate enolate due to severe steric hindrance on the α-face resulting from the cage-like structure of the tricyclic system.

The tetrasubstituted olefin required for later oxidative cleavage was introduced in the same manner as previously discussed. Conversion of ketone **46** to an α-selenide occurred readily and its oxidation was followed by a highly efficient *syn*-elimination furnishing enone **47** in 91% overall yield from **46** (Scheme 3.10). Selective 1,2 reduction of the enone **47** was accomplished by treatment with DIBALH, and the resulting crude allylic alcohol was directly protected as a MOM ether giving compound **48** in 87% yield. The reduction took place solely from the more accessible β-face of the molecule setting the C9 oxygenated stereocenter with correct stereochemistry. Next, an epoxide, which was to provide a means for the later installation of the bridgehead olefin and C13 oxygen of taxinine, was introduced. The less sterically encumbered alkene was thus epoxidized on treatment with *m*-CPBA, affording compound **49** in good yield. Prior to oxidative cleavage, exchange of the TBDPS protective group on the primary alcohol for an alternative siloxy group that did not contain aromatic functionality was found to be necessary in order to avoid a low yielding, sluggish reaction in the oxidative cleavage step. Therefore, TBDPS ether **49** was deprotected with TBAF and the resultant crude alcohol was then treated with TBSCl to furnish **50**. Substrate **50** was subsequently

oxidized with $RuO_2 \cdot 2H_2O$ and $NaIO_4$ to reveal the bicyclo[5.3.1]undecane ring system in excellent yield. In this case, base induced opening of the epoxide with *t*-BuOK to the allylic alcohol occurred readily and was followed immediately by protection with TIPSOTf providing diketone **51** in high yield.

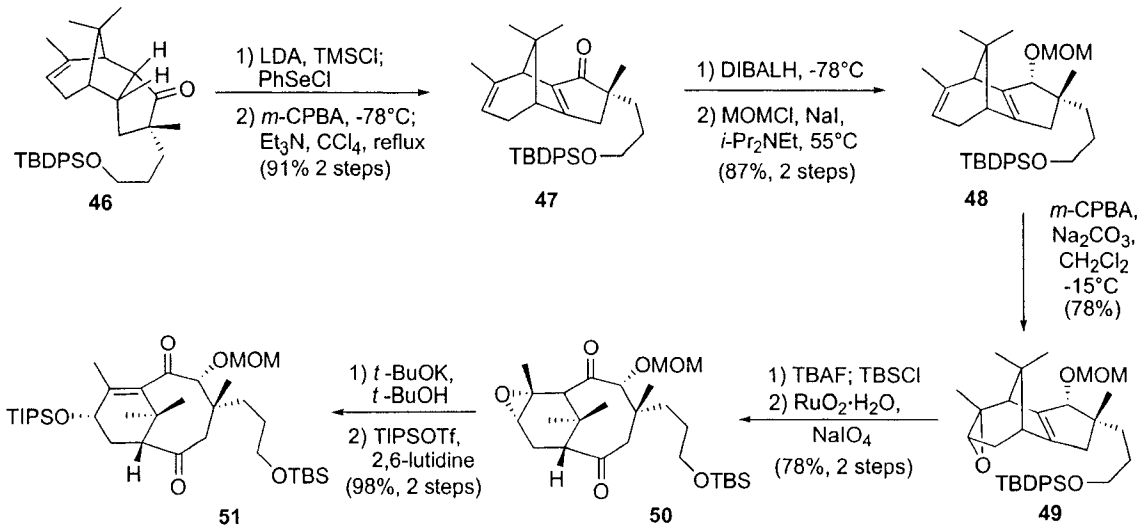

Scheme 3.10. Elaboration of ketone **46** to diketone **51**.

With an efficient strategy devised for the preparation of the A/B bicyclic ring system of taxinine that incorporates the A-ring bridgehead olefin and sets stereocenters at C8 and C9, a method for its elaboration to the tricyclic skeleton was next pursued. To that end, compound **51** was converted to aldehyde **52** in a four step sequence beginning with deprotection and subsequent oxidation of the primary alcohol to the corresponding 3-carbon aldehyde side chain. Homologation of the side chain was achieved by reaction with a Wittig reagent, $Ph_3PCHOMe$, followed by hydrolysis of the resultant enol ether with HCl and NaI providing aldehyde **52** in 62% yield over the four steps. Attempts aimed at closure of the C-ring via an aldol reaction were next investigated. It was found

that exposure of **52** to a range of relevant basic conditions resulted in recovered starting material or decomposition. Acidic conditions delivered a similar outcome. Further, no progress was achieved in trying to access a silyl enol ether by C3 deprotonation and silyl trapping of a protected aldehyde derivative of **52**. This lack of reactivity was attributed to particular conformational preferences of the eight-membered ring that rendered deprotonation at C3 unfavorable despite the presence of an adjacent carbonyl - a similar event led to the demise of the first approach to taxinine. This phenomenon has been observed in other syntheses or approaches to taxane diterpenes.[31]

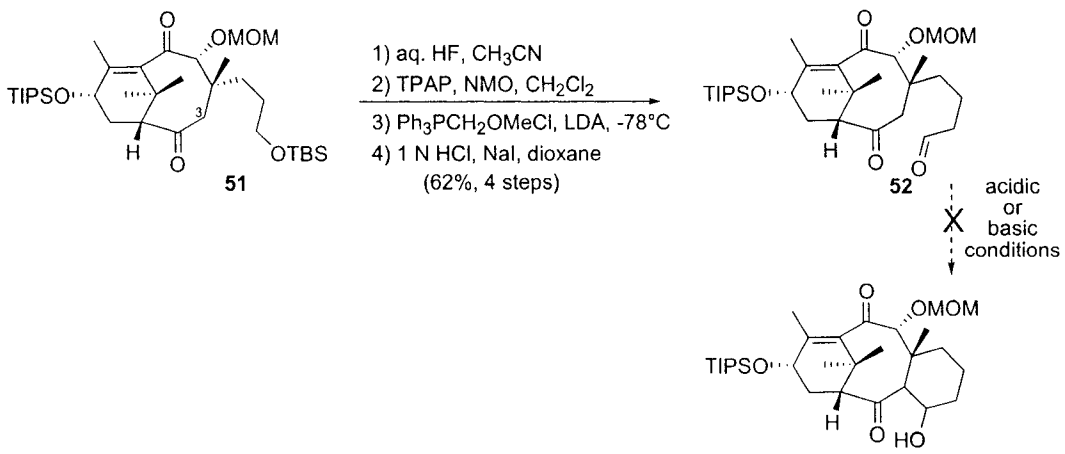

Scheme 3.11. Attempt to form the tricyclic taxinine core.

All of the early steps in the second approach progressed as planned with only minor modifications to adjust reactivity. Unfortunately, this route failed to enable the critical C-ring closure because of the inability to functionalize the C3 position and thus was not carried on to the final product.

3.3. Results and Discussion

3.3.1. The third approach to taxinine

A new route to taxinine was envisioned based on the two approaches previously devised by Giese and Mazzola. We considered that a potential solution to the problem of C-ring closure as well as C8 methylation might involve functionalization of C3 prior to oxidative fragmentation with an acyclic, carbon-based substituent. In essence, a handle for later C-ring formation would be installed at an early stage of the synthesis. Problems experienced with the first approach to taxinine could conceivably be overcome because of the additional conformational flexibility that would be granted to the system by no longer having the C3 substituent locked into a ring. After revelation of the cyclooctane, this group could aid the ring closure by two different pathways, dependent on the identity of the substituent. In one, the group might act to further acidify the remaining C3 proton, allowing C-ring closure via the originally planned aldol reaction. In the other, the group may serve to migrate the point of ring-closure away from the problematic eight-membered ring, an approach that could lend itself to a multitude of different ring closure strategies.

The idea behind this new strategy is shown as a retrosynthesis in Scheme 3.12. We planned the early functionalization of C3 via conjugate addition into Nazarov product **56**. A simultaneous methyl trapping of the enolate generated therein was further envisioned. From there, we hoped to prepare epoxide **55** following previously established protocols. On fragmentation, this would reveal the A/B ring system in **54**. At

that stage, C-ring closure should be facile and the synthesis would be well on its way to completion.

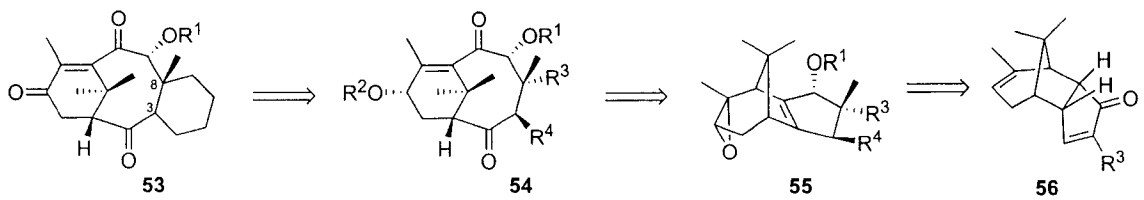

Scheme 3.12. Retrosynthesis of taxinine: third approach.

As a first attempt, we decided to explore the utility of a C3 isopropenyl substituted derivative, with the hope that this perturbation would not affect the viability of the subsequent chemical transformations. We believed that this group would provide us with a number of feasible ring closing strategies to consider when the time came.

We considered introducing the isopropenyl group by conjugate addition to **45** (Scheme 3.13). In the event, the most straightforward method employing a simple Gilman-type cuprate, lithium [bis(1-propen-2-yl)cuprate], did not provide a species that was active enough to achieve the desired transformation. After some experimentation, it was found that the Lipshutz cuprate, lithium [cyano(1-propen-2-yl)(2-thienyl)cuprate] **57**,[32] provided a competent nucleophile for the 1,4-addition. With these conditions, the conjugate addition and subsequent methylation occurred in excellent yield to give C3 substituted ketone **58** as one stereoisomer. The high stereoselectivity of this tandem reaction derives from geometrical features inherent to this particular structure, and is a direct consequence of the *endo* selective Nazarov cyclization. In the end, both the nucleophile and the electrophile react from the more accessible β-face of the molecule,

despite the steric repulsion that is created with the two groups *cis* to one another. An X-ray crystal structure of the alcohol **58a** provided proof of the supposed stereochemistry of the addition.

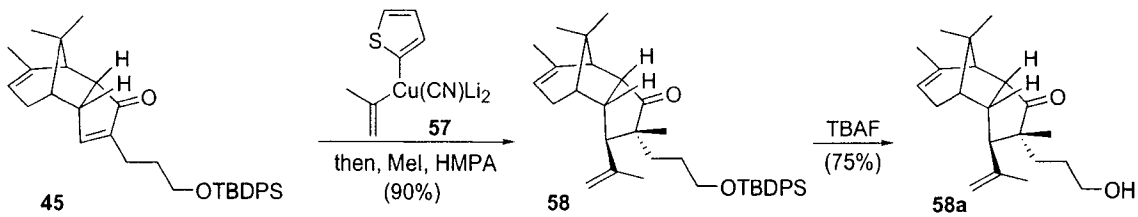

Scheme 3.13. Installation of the C3 isopropenyl group to **45**.

With the C3-substituted ketone **58** in hand, the next step was to explore its oxidation to the tetra-substituted enone that was required for fragmentation (Scheme 3.14). Attempts to introduce the phenyl selenyl moiety to be oxidized were met with much resistance, however. After an extremely sluggish reaction of the TMS enol ether of **58** (formed in *situ*) with PhSeCl, a product was obtained in a yield of 64%. At the time, this compound was thought to be desired α-selenide **59**. The MS data showed a molecular ion peak consistent with the proposed structure ($[M - t\text{-Bu}]^+$), and the ^1H NMR showed an increase in integral ratios of aromatic protons to aliphatic (however, they were slightly less than expected). When this compound was subjected to oxidation conditions with *m*-CPBA, then thermal elimination in refluxing CCl_4, no reaction occurred. In addition, other oxidation conditions including $NaIO_4$ and H_2O_2, returned the starting material unchanged. It was finally found that after treatment with excess CH_3CO_3H over one week at room temperature, the starting material was consumed in part (11% recovered). The only identifiable products isolated were diastereomers of the α-chloro

epoxide **61** in 16% and 19% yield (a complex mixture of more polar material was also obtained). No evidence of a product containing a tetrasubstituted olefin was found.

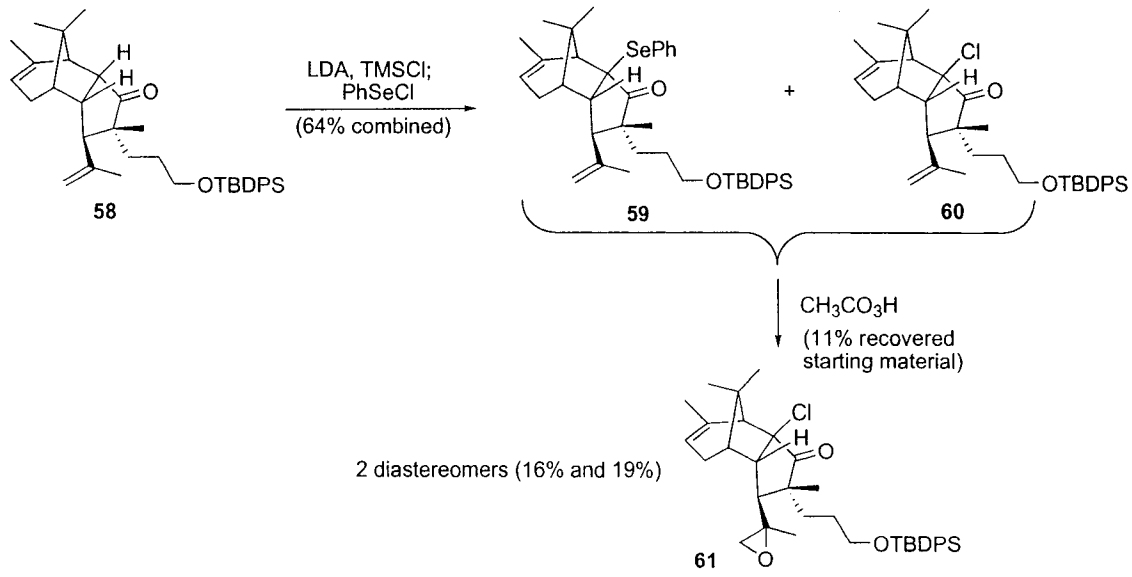

Scheme 3.14. Attempted conversion of **58** to selenide **59**.

At this point, we were curious as to when and how the chloride had been introduced into the product **61**. On closer inspection of the MS data of what was originally thought to be the starting α-selenide **59**, a second peak at a smaller *m/z* was noted which was consistent with α-chloride **60**. In retrospect, it appears that the original selenated compound actually consisted of a mixture of desired selenide **59** and undesired chloride substituted product **60**, the ratio of which remains uncertain. It would appear that the reagent PhSeCl is able to function as a source of electrophilic chlorine in instances where steric bulk precludes reaction with the Se center. The α-selenide **59**, if formed to an appreciable extent at all, is extremely resistant to oxidation and elimination conditions presumably due to steric factors. From the X-ray structure of intermediate

58a, one can observe the severe steric crowding of the C10 position by the presence of the bridgehead methyl as well as the flanking C8 methyl and C3 isopropenyl substituents, rendering this position highly inaccessible to incoming reagents of a certain size.

While great adversity was encountered on attempted α-selenylation of **58**, it was noted that the formation of the silyl enol ether precursor occurred with relative ease, though a bit sluggish. This compound could be isolated by careful non-aqueous work-up, and the crude ^{1}H NMR spectrum provided evidence for its formation (presence of a TMS group, loss of the C-10 proton). There are a number of dehydrogenation protocols known that utilize a pre-formed silyl enol ether as a substrate, such as the Saegusa oxidation with $Pd(OAc)_2$.[33] When the TMS enol ether of ketone **58** was isolated and subsequently treated with $Pd(OAc)_2$ in CH_3CN, only ketone starting material was recovered after work-up. We surmised that once again steric hinderance was to blame for lack of reactivity. Other silyl enol ether oxidations employing IBX[34] or DDQ[35] are widely regarded by the synthetic community as being useful for the formation of simple unhindered enones. Their application to the formation of highly substituted, sterically congested α,β-unsaturated ketones has not been noted, and for that reason were not investigated. Instead, it was thought that through structural modification of the substrate, or via alternative sequencing of steps, the selenoxide elimination might show more promise.

In an attempt to modify the reactivity of the sterically congested ketone **58**, the 3-carbon isopropenyl group was replaced with a slightly smaller vinyl group (Scheme 3.15). This substituent was easily introduced to enone **45** using MgBr(diethenylcuprate), and the intermediate enolate generated could once again be trapped by MeI to furnish

vinyl-substituted ketone **62** in moderate yield and with excellent stereoselectivity. When the silyl enol ether of **62** was treated with PhSeCl a complex mixture was obtained with no discernable products. The $Pd(OAc)_4$ oxidation protocol of the intermediate silyl enol ether, discussed earlier, gave only recovered ketone starting material.

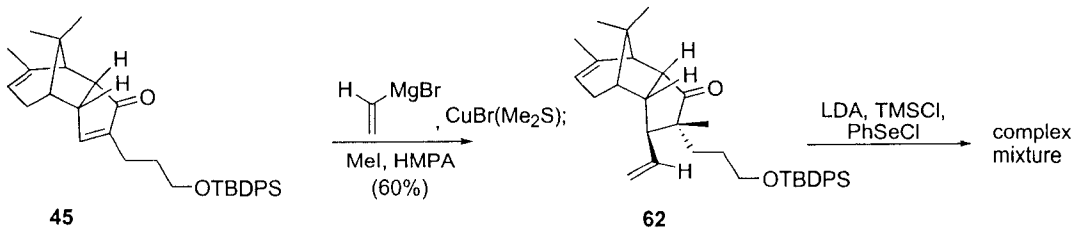

Scheme 3.15. Vinylation of **45** and attempted selenylation.

To further sterically decongest the ketone and to determine if formation of the enone was possible in any way with substitution at C3, an analog of compound **62** lacking the C8 methyl group was prepared. This strategy is reminiscent of the earlier preformed C-ring approach, where, without the C8 methyl, the chemical transformations required to prepare the oxidative fragmentation precursor occurred with ease. In the event, vinyl magnesium bromide cleanly underwent 1,4-addition to the enone in the presence of catalytic $CuBr{\cdot}SMe_2$ (Scheme 3.16). Following direct aqueous work-up and purification, ketone **63** was obtained in 97% yield. The ketone was then treated with LTMP, followed by TMSCl, and after a brief period, PhSeCl. The product of this sequence, phenyl selenyl-substituted cyclopropane **64**, though interesting, quickly put an end to this latest investigation. In quantitative yields, the kinetic deprotonation apparently occurs at C8 as opposed to C10, the reverse of what was observed in the intact C-ring approach. Expected reaction of the intermediate silyl enol ether with PhSeCl to

give the C8 substituted α-selenyl ketone does not occur either. We presume that **64** arises from initial complexation of $PhSe^+$ to the vinyl group, followed by attack on the resulting selenonium ion by the nearby silyl enol ether.

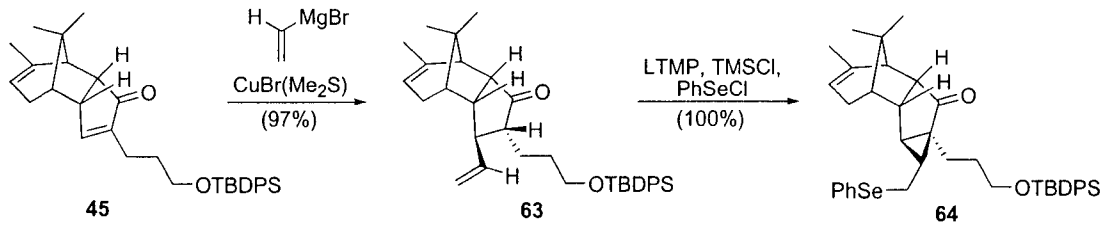

Scheme 3.16. Attempted selenylation of ketone **63**.

Because steric hinderance in the C3-substituted taxane analogs had proven to be detrimental to the subsequent functionalization of C10, we next addressed the possibility of reversing the order that the required substituents were introduced with the hope of gaining access to a selenylated derivative of **62** or **63**. Enone **45** was therefore reacted with LDA and PhSeCl to generate α-selenyl enone **65** in 40% yield. The moderate yield obtained in this case can be attributed to sluggish deprotonation of the ketone. Because of the additional unsaturation present in the five-membered ring, formation of the enolate results in a near planar cyclopentadiene fused through an sp^3 carbon to a rigid bicyclic scaffold, a very strained intermediate. Nevertheless, enough of the substituted ketone was obtained for the subsequent conjugate addition to be attempted (it should also be noted that none of the α-chloro ketone was observed in this case). Unfortunately, when this compound was treated with vinyl magnesium bromide in the presence of catalytic copper, a complex reaction mixture developed. The starting material was evidently consumed by TLC, but reacted to give a large number of products, and perhaps some

decomposition, as the crude ^{1}H NMR spectrum was quite messy and demonstrated broadening of peaks. Further, the vinyl group appeared not to have been incorporated into any part of the molecule for there were no peaks present in the expected region of 5.8 – 5.0 ppm.

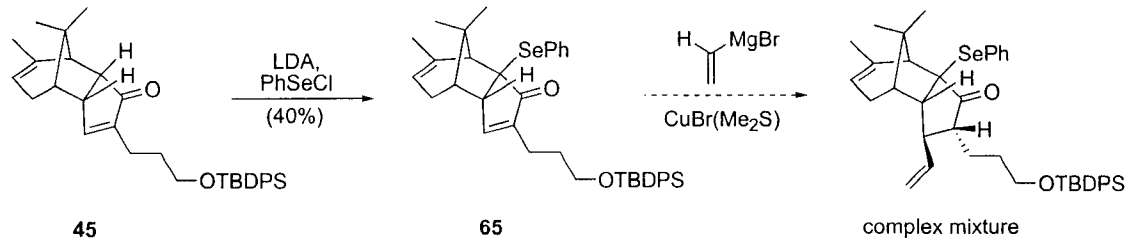

45 65 complex mixture

Scheme 3.17. Attempted reversal in functionalization of **45**.

Because it seemed that simultaneous C10, C8 and C3 substitution was a lot to ask of this sterically encumbered cyclopentanone, we next sought to position the C3 substituent after the C2-C10 olefin had already been installed. In this approach, we planned to use enone **47** to gain reactivity at C3 via dienolate chemistry. Initially, we explored the vinylogous Mukaiyama aldol reaction employing a siloxy diene and an aldehyde activated by complexation with Lewis acid.[36] To generate the requisite vinylogous enoxy silane we explored a variety of conditions. Weak base (Et_3N) in the presence of TMSCl at room temperature did not provide the dienolsilane. Use of strong bases such as LDA, LTMP, or KHMDS were a better alternative, and the resultant dienolate could be trapped with TMSCl, although not quantitatively (Scheme 3.18). The siloxy diene was extremely sensitive to aqueous work-up and almost immediately returned the starting ketone **47** upon exposure to water. Better success was achieved by using non-aqueous conditions, involving treatment with Et_3N, dilution with pentane, and

filtration of the resulting precipitate. After concentration, the extremely labile siloxy diene **66** was taken directly to the next step without purification.

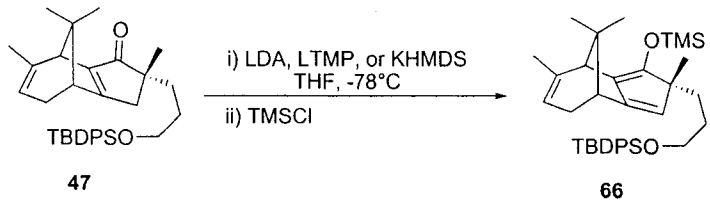

Scheme 3.18. Generation of siloxy diene **66**.

With **66** in hand, its aldol reaction with propanal and benzaldehyde promoted by either $BF_3{\cdot}OEt_2$ or $TiCl_4$ was investigated (Table 3.1). At low temperature, all trials resulted in reversion of the TMS dienol ether to starting material (entries 1,2). Interestingly, when the reaction of **66** with propanal and $BF_3{\cdot}OEt_2$ was allowed to warm to room temperature and stirred overnight, the starting enone was converted to a new, more polar product in a yield of 50% by weight (entry 3). It is not clear what this compound is, but its spectral data does not fit with that expected for the product of the aldol reaction or its condensation product. In fact, the aldehyde does not appear to have been incorporated at all. In the final entry, a more stable TBS dienol ether was subjected to the reaction conditions, but after warming to room temperature only the siloxy diene and ketone **47** were obtained.

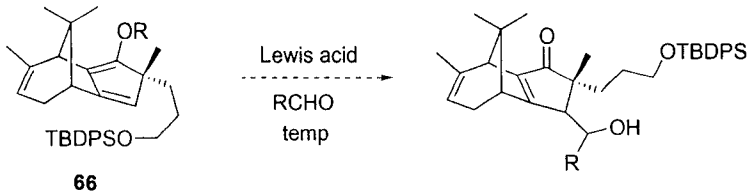

66

entry	R	aldehyde	Lewis acid	temp (°C)	result
1	TMS	PhCHO	$BF_3{\cdot}OEt_2$	-78 to rt	---[a]
2	TMS	CH_3CH_2CHO	$BF_3{\cdot}OEt_2$	-78	---[a]
3	TMS	CH_3CH_2CHO	$BF_3{\cdot}OEt_2$	-78 to rt	---[b]
4	TBS	CH_3CH_2CHO	$TiCl_4$	-78 to rt	N/R[c]

[a] Recovered ketone **47** was obtained. [b] Unidentified product was obtained (50% by weight). [c] Unreacted **66** was obtained along with **47**.

Table 3.1. Attempted Mukaiyama aldol of siloxydiene **66**.

It seemed that **66** was too poor a nucleophile to participate in the aldol reaction. We considered the use of a "free carbanion" in place of the silyl-dienol ether, intending to provide a more reactive nucleophile for the reaction.[37] Combining **47** with benzaldehyde in the presence of $BF_3{\cdot}OEt_2$ followed by the addition of LDA at –78°C gave no reaction. Even with warming to room temperature, the starting material still did not react. Milder conditions using Et_3N with or without Lewis acid at room temperature and at reflux also gave recovered **47**.

We believe that the poor nucleophilicity of the dienolate of **47** at both potential reactive sites (α and γ) is a result of steric congestion in the vicinity of these positions. The linearity imposed on the structure of the dienolate brings the inner methyl of the bridging geminal dimethyl group into closer proximity to the C2 position, hindering the approach of an electrophile. At C3, the presence of an adjacent fully substituted carbon may be responsible for the lack of reactivity observed there.

From the results of the above studies, it seemed unlikely that the C-ring closure strategy involving early incorporation of a non-hydrogen substituent at C3 was going to be successful. Steric intolerance of the substituted intermediates precluded formation of the necessary precursor to oxidative fragmentation. For that reason, a fourth approach to the formation of the taxinine C-ring was considered, and will be detailed in the next section.

3.3.2. The fourth approach to taxinine

C-H insertion reactions of metal-stabilized carbenes generated by decomposition of α-diazo ketones or β-keto diazo esters with transition metal catalysts have been extensively studied.[38] Ultimately, the reaction allows the formation of new C-C bonds between two sp^3 centers via activation of a C-H bond in a saturated hydrocarbon. It is well known that intramolecular carbenoid C-H insertion reactions of acyclic, non-constrained alkyl chains exhibit an overwhelming preference for the formation of five-membered rings. In the absence of any directing effects, the reaction proceeds through a low energy six-membered transition state forming substituted cyclopentanones (as well as γ-lactones and lactams) with ease. Exceptions to this general trend have been noted in cases where steric, electronic, or conformational factors override this kinetic preference and lead to the formation of alternate ring sizes. In two reports of six membered ring formation via C-H insertion,[39,40] the presence of an adjacent heteroatom (O, or N) activates a δ-C-H bond toward cyclohexane formation (Figure 3.3, **67** to **68** and **69** to **70**). Despite the fact that the benzylic position has been shown to be less active towards C-H

insertion than simple methine hydrocarbons,[41] Ghatak and coworkers have reported preferential cyclohexanone formation by C-H insertion to a benzylic position (Figure 3.4, **71** to **72**).[42] The alternate methine C-H insertion pathway was uncompetitive. While no explanation was offered for this selectivity, it would seem logical that the *trans* diaxial relationship between the simple methine C-H and the diazo ester prevents their interaction leading to bond formation. In a final example of C-H insertion to form six-membered rings, Cane *et al* have reported the formation of a δ-lactone in their synthesis of dl-Pentalenolactones E and F (Figure 3.5, **73** to **74**).[43] They postulate that the δ-lactone forms preferentially on the basis of steric and conformational considerations.

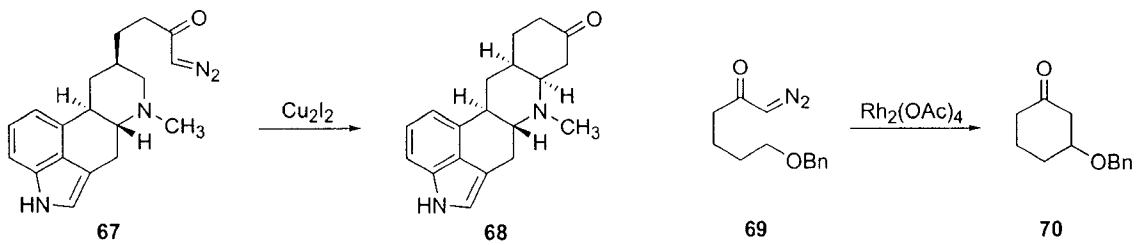

67 68 69 70

Figure 3.3. Activation of a δ-C-H bond toward C-H insertion by adjacent heteroatom substitution.

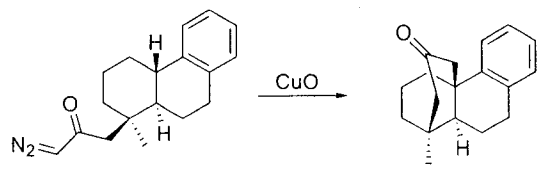

71 72

Figure 3.4. C-H insertion at a δ-benzylic position.

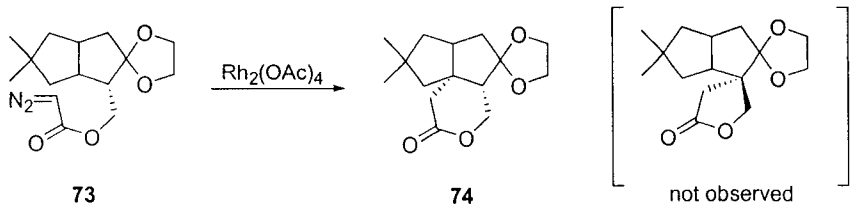

73 74 not observed

Figure 3.5. δ-Lactone formation via C-H insertion.

Application of the C-H insertion strategy to the synthesis of taxinine seemed a feasible route. In the target diazo compound, competitive five-membered ring formation was not a consideration due to the presence of a quaternary center at the γ position (Figure 3.6). In addition, Stork and Nakatani have shown that the presence of an electron withdrawing carbonyl substituent one, or even two carbons away tends to deactivate targeted C-H bonds.[44] From this observation, we expected the β-position to be inert towards C-H insertion, thus preventing competitive four-membered ring formation. Particular attention would need to be given to the identity of the protecting group of the C9 hydroxyl, as activation of adjacent C-H bonds toward insertion occurs on substitution with oxygen.[45] To discourage reaction at the C9 methine (γ′-position), the hydroxyl would have to be protected with an electron withdrawing acetate, shown to disfavor adjacent C-H insertion.[46] Finally, it has been observed that the ease of insertion into targeted C-H bonds increases as the reactive carbon becomes more highly substituted ($CH_3 < CH_2 < CH$).[41] In fact, C-H insertion rarely occurs with methyl groups, and we hoped this would hold true in our system. All of these factors taken together should leave the most reactive site for insertion at C3 (γ-position). However, should the desired reaction be sluggish, carbene dimerization might become a competing processes.

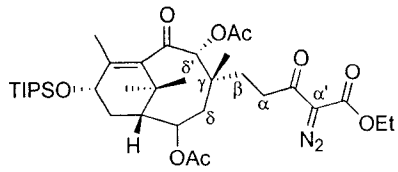

75

Figure 3.6. Target diazo compound.

To that end, diketone **51** was synthesized as previously described (Scheme 3.10). At this stage, advancement towards the targeted diazo compound **75** required exchange of the MOM-ether protecting group in **51** for an acetate. Conditions to effect this desired transformation were thus explored (Scheme 3.19). Treatment of MOM-ether **51** with either TMSBr or *B*-bromocatechol borane led to complex reaction mixtures where it appeared that both the TBS and MOM groups were lost resulting in formation of compound **76**. Lewis acidic conditions ($AlCl_3$, NaI) cleanly furnished **76**. Attempted removal under protic acid conditions (HCl, THF, rt or 50°C) gave **77**, resulting from clean deprotection of the TBS ether. It appeared that selective deprotection of the MOM group in the presence of the more labile primary TBS ether was not going to be possible. To circumvent this difficulty, the acetate group could be used in place of the MOM ether upon initial reduction of C9. This approach will be discussed at a later stage. At this point, it was decided to continue on with the steps needed to prepare β-keto diazoester **75** to determine their feasibility, and to deprotect the MOM ether at a later stage.

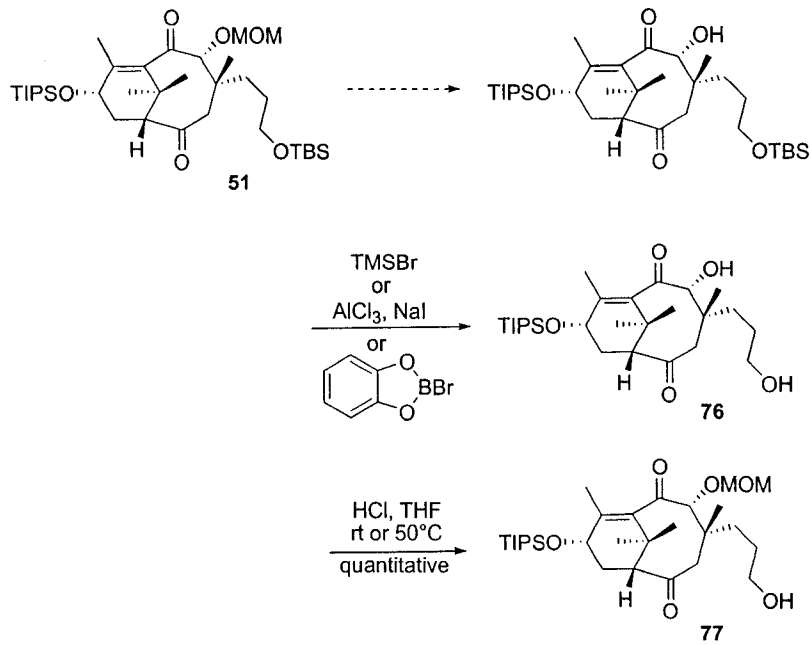

Scheme 3.19. Attempted MOM deprotection of **51.**

The first step towards preparation of the β-keto ester was the selective reduction of the C2 carbonyl (to avoid deactivation of the adjacent C3 position towards later C-H insertion). When diketone **51** was treated with DIBALH (slight excess), the formation of two new compounds was observed by TLC (Scheme 3.20). After work-up, purification/separation, and characterization, the two products were tentatively assigned as mono- and di-reduced compounds **78** and **79**. Mass spectral data for the two products displayed molecular ion peaks consistent with the proposed structures. IR spectral data were also in agreement, indicating the presence of a hydroxyl moiety for both compounds. A medium intensity carbonyl peak was observed for **78**, and was absent in the spectrum of **79**. Surprisingly, the ^{1}H NMR spectra of both of the products were complicated due to peak broadening. In fact, some of the peaks were broadened to the extent that they appeared to blend in with the baseline. This strange phenomenon is

presumed to arise from conformational equilibria of the eight-membered ring, and has previously been observed in other ring systems.[47]

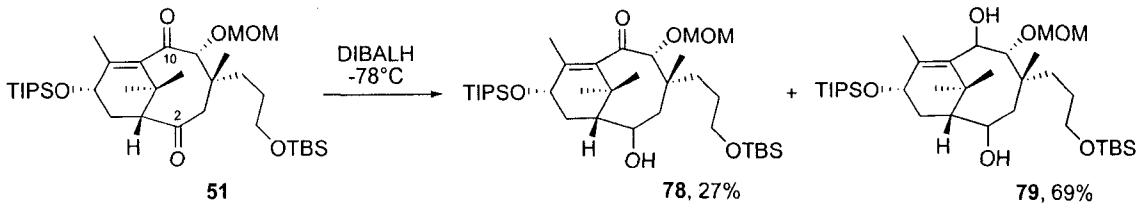

51 78, 27% 79, 69%

Scheme 3.20. Reduction of diketone **51.**

Regardless, some important observations from the data could be made, particularly regarding **78**. In the ^{1}H NMR spectrum of diketone **51**, signals were readily observed for the C3 and C9 protons at the expected chemical shifts (~2-3 ppm and ~4.2 ppm respectively). However, once the compound was singly reduced, neither of these peaks were present. This could indicate that the initially formed alcohol **78** may be undergoing a transannular hemi-ketalization (Figure 3.7). Because these characteristic peaks were absent, it was not readily apparent which of the two carbonyls had been reduced. ^{13}C NMR data also showed broadening and disappearance of signals, and was therefore not useful for characterization of the compounds. At this point, the tentative assignment of **78** as the C2 reduced compound is based solely on the fact that it could still be visualized by UV irradiation on TLC plates, presumably because of enone conjugation. The di-reduced product **79** was only visible on staining the TLC plate with anisaldehyde. The stereoselectivity of the reduction is also unknown, but there does appear to be only one diastereomer formed for each of the compounds by ^{1}H NMR.

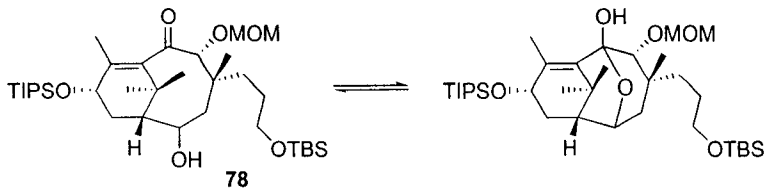

Figure 3.7. Proposed equilibrium of **78** with a hemi-ketal.

In an attempt to gain further insight into the structure of **78**, which could be formed exclusively by reduction of **51** with $NaBH_4$, the compound was treated with Ac_2O to give **80** (Scheme 3.21). It was hoped that some resolution in the ^1H NMR signals might be observed if either the alcohol or the corresponding hemi-ketal could be trapped. Unfortunately, the resulting spectrum provided no further insight as it remained very similar to that of the parent alcohol with respect to peak broadening. A new 3H singlet was observed in the appropriate region for the acetate methyl, and HRMS data provided a molecular ion peak corresponding to that expected for **80**. Apart from that, it was not possible to obtain any other relevant information about the structures of **78** or **80**. Attempts were made to grow X-ray quality crystals of **78** and **80**, but were to no avail.

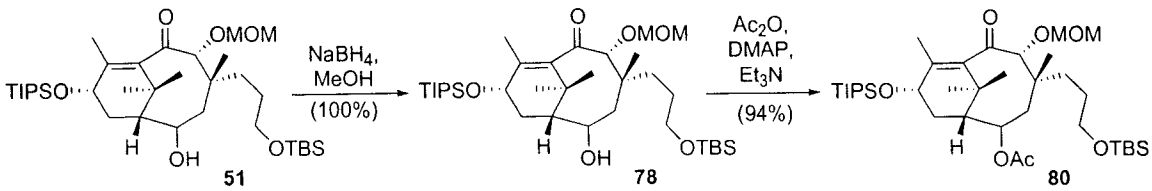

Scheme 3.21. Preparation of monoacetate **80**.

At any rate, it was decided to advance diol **79** through the rest of the study (the uncertain identification of **78** was worrisome in light of the deactivating effect the C2 carbonyl, should it be present, would have on the later C-H insertion at C3). Though

characterization of the subsequent intermediates would be difficult, it was hoped that on successful C-H insertion to form the fused cyclohexane, a more rigid conformation of the resulting molecule would be invoked and the ^{1}H NMR spectral data would resolve. To that end, **79** was treated with Ac_2O and Et_3N to yield diacetate **81**, the formation of which was supported by MS, IR (loss of OH stretch), and to some extent ^{1}H NMR (presence of two acetate methyls at ~ 2 ppm). Compound **81** was subsequently treated with a solution of HF / pyridine in CH_3CN at room temperature to selectively remove the primary TBS protective group (alternatively, HCl could be used as discussed earlier). The resultant alcohol **82** was cleanly oxidized to the corresponding aldehyde **83** by treatment with TPAP and NMO at room temperature (^{1}H NMR, RCHO = 9.8 ppm). Elaboration to the β-keto ester was attempted using the Roskamp reaction[48] with mild $NbCl_5$[49] as a Lewis acid catalyst in the presence of ethyl diazo acetate. A messy reaction developed from which no clear evidence for the formation of the desired product could be found. It appeared that the MOM and possibly also the TIPS protective groups were removed during the transformation, but the MS data did not corroborate any proposed structure.

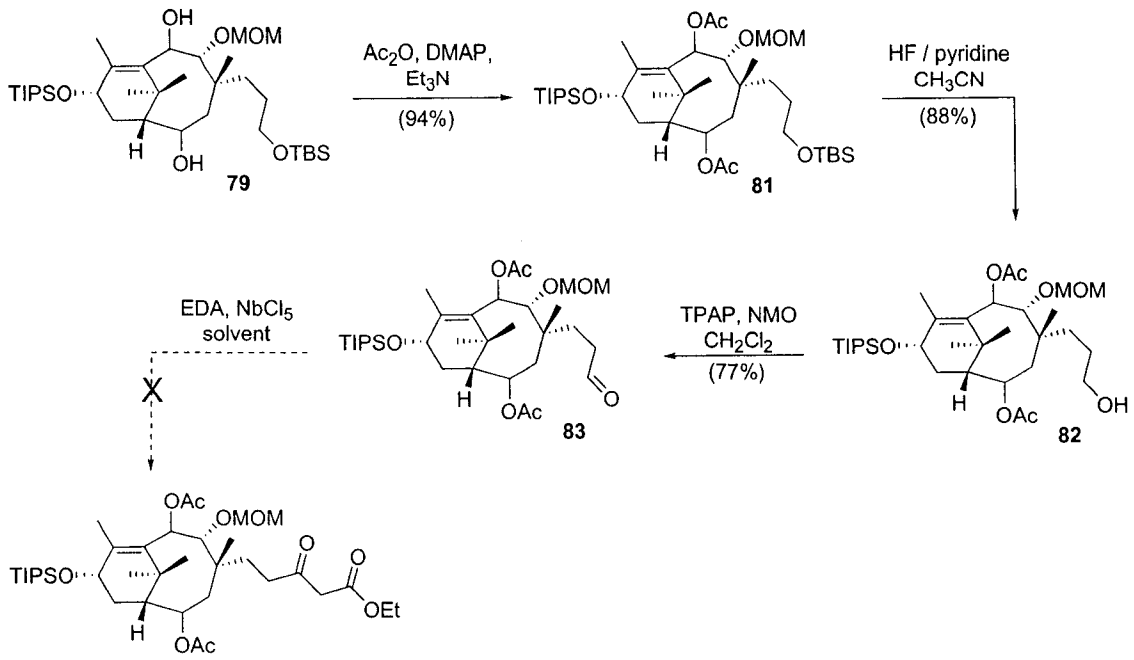

Scheme 3.22. Attempted elaboration of **83** to a β-Keto ester.

We hypothesized that the origin of this disappointing outcome arose as a result of incompatibility of the acid-sensitive MOM ether with the reaction conditions. Because of this, it would be necessary to attempt the sequence of reactions once more on a C9 acetate protected intermediate. Because selective MOM deprotection of **51** was not possible in the presence of the more labile primary TBS ether, it was decided to introduce the acetate directly following reduction of the C9 carbonyl in enone **47** (Scheme 3.23). In practice, it was found that allylic acetate **84** was prone to elimination, and frequently gave significant conversion to diene **85** under the reaction conditions as well as during purification and storage. At this stage, we were not interested in optimizing this sequence, and only wanted to gain access to the C9 acetate analog of **51** in order to quickly verify its viability in the C-H insertion reaction. Therefore, the synthesis was continued as planned.

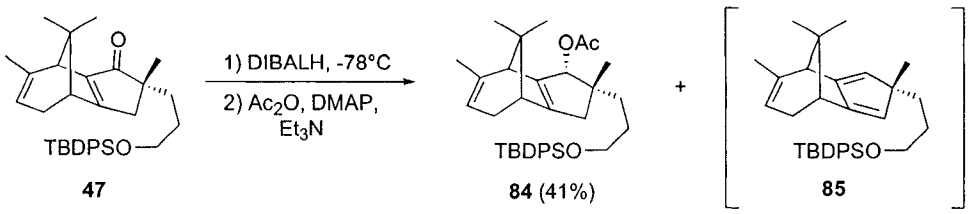

Scheme 3.23. Preparation of allylic acetate **84**.

The labile allylic acetate in **84** caused concern for its survival through the subsequent steps required for elaboration to the ring-opened product. In particular, the basic fluoride conditions necessary for deprotection of the TBDPS ether to allow for its exchange to a RuO_4-compatible protective group were worrisome. To circumvent this issue, it was decided to perform the TBDPS exchange prior to reduction and acetylation of **47**. Therefore, **47** was deprotected by treatment with TBAF, and immediately reacted with TIPSCl to give enone **86** in 90% yield over 2 steps (Scheme 3.24). This was reduced with DIBALH, and the crude reaction mixture was acetylated to furnish **87** in 41% yield after careful chromatography using deactivated silica gel. The acetate was immediately epoxidized in moderate yield using *m*-CPBA. The product (**88**) was then treated with RuO_2 in the presence of $NaIO_4$ to cleanly give diketone **89**. On exposure of **89** to catalytic *t*-BuOK, the epoxide was readily opened, and the resulting allylic alcohol was protected with TIPSOTf, furnishing **90** in excellent yield.

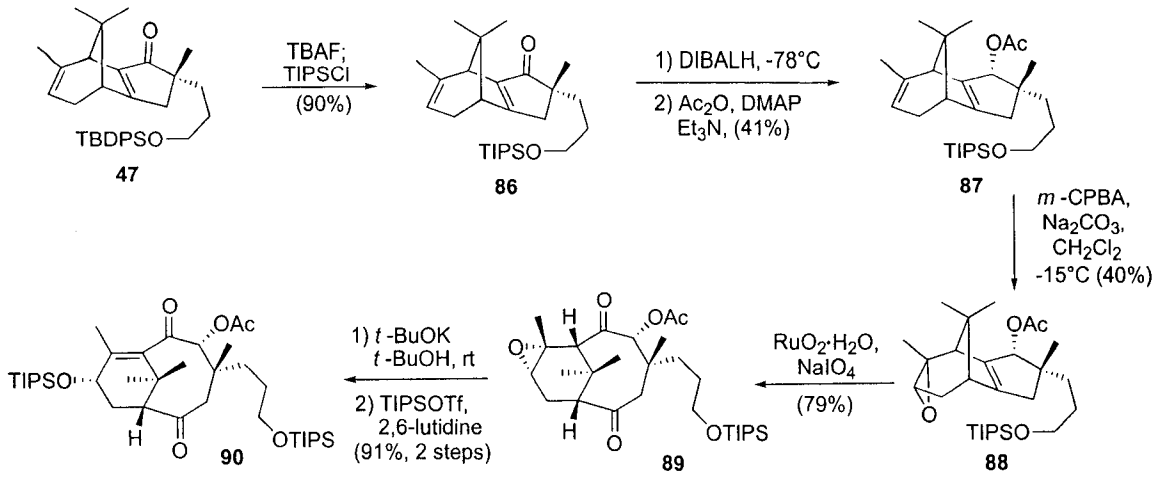

Scheme 3.24. Preparation of diketone **90**.

Treatment of **90** with DIBALH gave triol **91** as the major product, which was accompanied by simultaneous reductive removal of the acetate protecting group (Scheme 3.25). As in the series of C9-MOM analogs previously described, the ^{1}H NMR spectra for this reduced compound also showed severe broadening of peaks. Thus, no new information could be obtained regarding the regio- and stereoselectivity of the reduction. Nevertheless, the triol **91** was carried through the sequence of transformations required for elaboration to the key diazo compound. The triol was first treated with excess Ac_2O to provide triacetate **92** in good yield. Next, the TIPS group was removed by exposure to TBAF, and the resulting alcohol was cleanly oxidized to the corresponding aldehyde **93** in 72% yield over two steps. Elaboration of **93** to β-keto ester **94** via the Roskamp protocol appeared to be a success this time. The ^{1}H NMR spectrum, though very dilute, indicated the presence of an ethyl ester moiety. More importantly, the HRMS data displayed a molecular ion peak that matched the formula for the proposed structure of **94**.

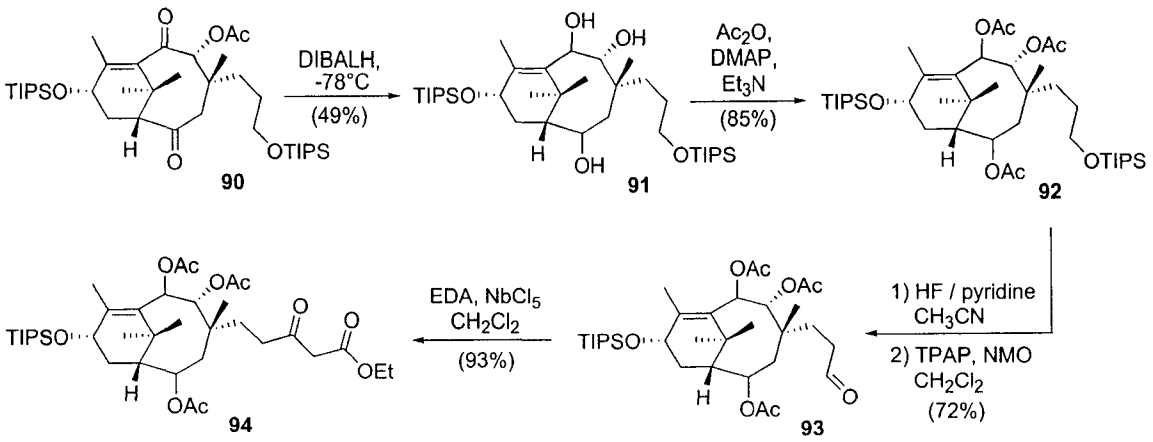

Scheme 3.25. Preparation of β-keto ester **94**.

With only milligram quantities of **94** in hand, its conversion to β-keto diazo ester **95**, and subsequent C-H insertion reaction was going to be difficult to evaluate. Nevertheless, β-Keto ester **94** was carefully subjected to diazo transfer conditions using TsN_3 and Et_3N (Scheme 3.26). After direct concentration and chromatographic purification using deactivated silica gel, a new compound of lower polarity than the starting material was isolated. A peak in the IR spectrum of this compound at 2133 cm^{-1} gave evidence for successful incorporation of the diazo functionality. However, when this material was exposed to $Rh_2(OAc)_4$, a catalyst commonly used to effect C-H insertion of diazo substrates, the results shed some doubt onto the assignment of compound **95** as the β-keto diazo ester. A very dilute ^1H NMR spectrum taken of the crude reaction product closely resembled that of the starting material **94**. The MS data also gave a molecular ion peak matching the molecular formula of **94**. It is possible that the diazo compound **95** was not prepared in the first place, and that the peak in the IR spectrum was a result of TsN_3 impurity, although by TLC there were no other UV active compounds present in the purified diazo ester **95** to indicate contamination.

Unfortunately, due to the small quantity of material and its potential sensitivity, no other spectral data was obtained for **95**. At this stage, the viability of the C-H insertion strategy was unknown as the result of the investigation was inconclusive.

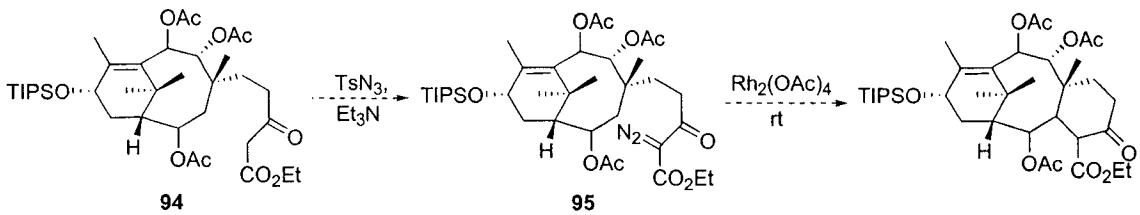

Scheme 3.26. Elaboration of **94** to β-keto diazo ester **95** and attempted diazo decomposition.

3.4. Conclusion and Future work

Our efforts towards the synthesis of taxinine have been presented. At the outset, the impending goal was to achieve reactivity at C3 of the taxane skeleton to allow closure of the C-ring. Previous studies had attempted both an early incorporation of the six-membered ring, and a late stage annulation. While the former method created serious reactivity challenges in key synthetic intermediates, the latter provided a straightforward route to the A/B bicyclic ring system. Because of the conformational preference of the central eight-membered B ring, it was not possible to gain reactivity at the C3 position for C-ring closure via enolate chemistry.

The third strategy described here involved early C3 functionalization of the taxane core, but was complicated because of steric encumbrance in the resulting intermediates. All efforts to prepare the C2-C10 tetrasubstituted olefin required for

oxidative cleavage with simultaneous C3 substitution failed. Further, a strategy involving introduction of the C3 substituent to an intermediate already containing the central alkene also did not provide the desired product.

With the demise of the above strategy, we next elected to investigate a late stage functionalization of C3 via intramolecular carbenoid C-H insertion chemistry. This route was particularly attractive because it does not necessarily require prior activation of the targeted C-H bond. It was found that the choice of protecting groups was critical in the preparation of the requisite β-keto ester. Unfortunately, it was not clear if the subsequent diazo transfer reaction was successful, which made it impossible to draw any conclusions about its following metal catalyzed diazo decomposition. The presence of the diazo functionality needs to be ascertained with confidence before subjecting it once again to $Rh_2(OAc)_4$ or other metal catalysts.

Should the above approach fail to give the desired product then it will be necessary to explore other alternatives for C3 functionalization. It may be possible to institute a conformational change within the eight-membered ring of our late-stage intermediates through modification of substituents around the periphery of the ring. From one of these compounds we may then be able to form the elusive C3 enolate, which would allow advancement to the tricyclic taxane core. We have shown that reduction of the C2 and/or C-10 carbonyls results in significant conformational changes in the molecule as evidenced by broadening of peaks in the ^1H NMR spectra of these intermediates. If it were possible to gain access to a C-10 mono-reduced compound, then we could test the effect that this change would have on the acidity of the C3 protons. A preliminary investigation could access this compound by di-reduction of the C2 and C10

carbonyls. By taking advantage of differing reactivity at the C2 and C10 positions (we have shown that there is a reactivity distinction between the positions, at least in terms of the initial reduction), the C2 alcohol could be selectively re-oxidized, or the C10 alcohol could be selectively protected and C2 subsequently oxidized (Scheme 3.27). From here, the generation and subsequent trapping of the C3 enolate could be explored.

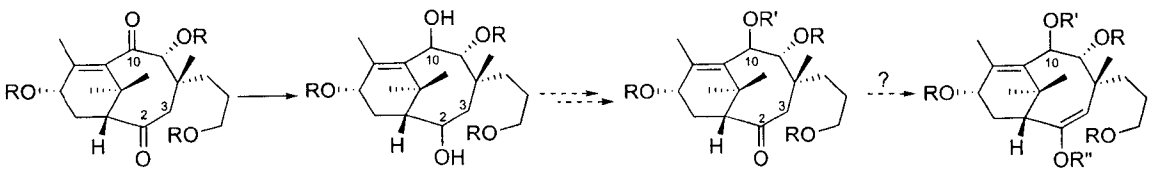

Scheme 3.27. Future plans: accessing the C3 enolate via conformational change induced by C10 reduction.

Alternatively, it should be possible to induce conformational change within the eight-membered ring by pyramidalizing the bridgehead C11-C12 olefin through reduction. While the targeted natural product requires the presence of this olefin, this strategy would simply serve to test the conformational effect of this moiety. Should positive results be obtained, it may be possible to annulate the C-ring before installation of the bridghead olefin to allow for a streamlined route to taxinine (Scheme 3.28).

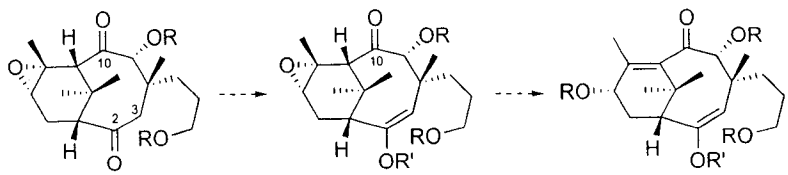

Scheme 3.28. Future plans: accessing the C3 enolate via conformational change induced by C11-C12 pyramidalization.

3.5. Experimental

3.5.1. General

Reactions were conducted in oven-dried (120°C) or flame-dried glassware under a positive argon atmosphere unless otherwise stated. Transfer of anhydrous solvents or mixtures was accomplished with oven dried syringes or cannula. Solvents were distilled before use: CH_2Cl_2 and HMPA from calcium hydride; toluene from sodium metal; THF and Et_2O from sodiumbenzophenone ketyl. Commercial reagents were used as received unless otherwise stated. Lithium 2-thienylcyano cuprate was obtained from Aldrich and used immediately. Thin layer chromatography (TLC) was performed on glass plates precoated with 0.25 mm Kieselgel 60 F_{254} (Merck). Flash chromatography columns were packed with 230-400 mesh silica gel (Silicycle) unless otherwise indicated.

Proton nuclear magnetic resonance spectra (^{1}H NMR) were recorded at 500 MHz, and the chemical shifts are reported on the δ scale (ppm) upfield from deuterochloroform (δ = 7.27 ppm). Carbon nuclear magnetic resonance spectra (^{13}C NMR) were obtained at 125 MHz. Chemical shifts are reported (ppm) relative to the center line of the triplet for deuterochloroform (δ = 77.23 ppm). Infrared (IR) spectra were measured with a Mattson Galaxy Series FT-IR 3000 spectrophotometer. Mass spectra were determined on a Kratos Analytical MS-50 (EI) or Applied Biosystems Mariner Biospectrometry Workstation (ESI).

3.5.2. Substrates syntheses

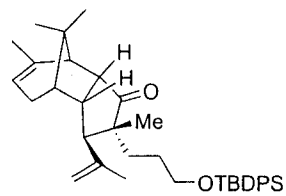

58

Ketone **58**: 2-Bromopropene (266 μL, 3.0 mmol) was dissolved in Et_2O (10 mL) and cooled to –78°C. *t*-BuLi (0.99 M, 6.0 mL, 6.0 mmol) was added and the mixture was subsequently stirred at this temperature for 1 h. Lithium 2-thienylcyano cuprate (freshly opened) (0.25 M, 12.8 mL, 3.2 mmol) was then added via syringe and the mixture was stirred for 15 min. To the resulting red colored homogeneous solution was then added enone **45** (1.13 g, 2.0 mmol) as a solution in Et_2O (2 mL). The reaction was stirred over 2 h with gradual warming to -60°C. The yellow solution was cooled back to -78°C, and treated with HMPA (1.5 mL), followed by MeI (1.5 mL, 24 mmol), then warmed gradually to rt and stirred overnight. The mixture was quenched with saturated aqueous NH_4Cl (12 mL), and the aqueous layer was extracted with Et_2O (3 x 10 mL). The combined organic fractions were then dried over $MgSO_4$, filtered and concentrated under reduced pressure. Purification by column chromatography (silica gel, gradient elution: 120:1, 110:1, 100:1, 90:1, 80:1 hexanes/EtOAc) gave 1.0 g, (90%) of ketone **58** as a clear colorless oil: R_f 0.54 (10:1 hexanes/EtOAc); IR (neat) 3071, 2930, 1732, 1640 cm^{-1}; ^1H NMR (500 MHz, $CDCl_3$) δ 7.94-7.89 (m, 4H), 7.69-7.59 (m, 6H), 5.38 (br s, 1H), 5.23 (s, 1H), 5.05 (s, 1H), 3.95 (m, 1H), 3.84 (m, 1H), 3.54 (dd, J = 11.6, 6.3 Hz, 1H), 3.35 (ddd, J = 11.2, 11.2, 7.3 Hz, 1H), 3.02 (d, J = 10.9 Hz, 1H), 2.49 (d, J = 17.4 Hz, 1H), 2.23 (d, J = 6.3 Hz, 1H), 2.16 (d, J = 18.9 Hz, 1H), 2.04-2.00 (m, 4H), 1.94-1.80 (m, 5H), 1.73-

1.65 (m, 1H), 1.62-1.50 (m, 1H), 1.36-1.27 (m, 15H), 1.11 (s, 3H); ^{13}C NMR (125 MHz, $CDCl_3$) δ 221.7, 144.0, 139.8, 135.6, 134.1, 129.4, 127.5, 119.7, 113.3, 64.5, 57.5, 57.3, 50.2, 48.4, 44.9, 42.9, 42.4, 31.6, 28.5, 27.3, 26.8, 26.6, 25.0, 23.8, 22.1, 21.4, 19.2; HRMS for $C_{33}H_{41}O_2Si$ ($M-C_4H_9^+$) calcd 497.2877, found 497.2882 ($M-C_4H_9^+$).

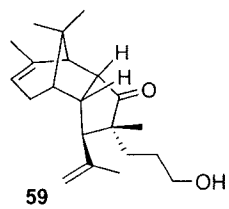

59

Alcohol **59**: TBAF (1.0 M in THF, 1.0 mL, 1.0 mmol) was added to a 0°C solution of the ketone **58** (110 mg, 0.20 mmol) in THF (3 mL). The mixture was allowed to warm to rt and left to stir for 2 h. Workup was achieved by the addition of H_2O (3 mL), then extraction of the aqueous layer with Et_2O (3 x 3 mL). The combined organic fractions were then dried over $MgSO_4$, filtered and concentrated under reduced pressure. Purification by column chromatography (silica gel, 20:1 hexanes/EtOAc) gave 47 mg (75%) of **59** as an oil which crystallized on standing: Mp 68-70°C; R_f 0.34 (10:1 hexanes/EtOAc); IR (neat) 3449, 3075, 2910, 1711, 1454 cm^{-1}; ^1H NMR (500 MHz, $CDCl_3$, missing OH) δ 5.16 (br s, 1H), 5.01 (dd, J = 1.5, 1.5 Hz, 1H), 4.83 (br s, 1H), 3.66-3.54 (m, 2H), 3.34 (dd, J = 11.7, 6.3 Hz, 1H), 3.12 (ddd, J = 11.1, 11.1, 7.1 Hz, 1H), 2.76 (d, J = 10.7 Hz, 1H), 2.26 (br d, J = 16.7 Hz, 1H), 1.99 (dd, J = 6.3, 1.1 Hz, 1H), 1.91 (br d, J = 16.9 Hz, 1H), 1.85-1.78 (m, 4H), 1.72 (ddd, J = 12.7, 11.0, 3.7 Hz, 1H), 1.67 (ddd, J = 2.4, 1.6, 1.6 Hz, 3H), 1.65-1.56 (m, 1H), 1.41 (ddd, J = 12.7, 11.5, 3.7 Hz, 1H), 1.37-1.29 (m, 1H), 1.09 (s, 3H), 1.05 (s, 3H), 0.90 (s, 3H); ^{13}C NMR (125 MHz, $CDCl_3$) δ 222.1, 143.7, 140.0, 119.7, 113.6, 63.2, 57.5, 57.4, 50.1, 48.4, 44.9, 42.9, 42.5,

31.1, 28.5, 27.5, 26.6, 25.1, 23.7, 22.1, 21.4; HRMS for $C_{21}H_{32}O_2$ (M^+) calcd 316.2404, found 316.2400 (M^+).

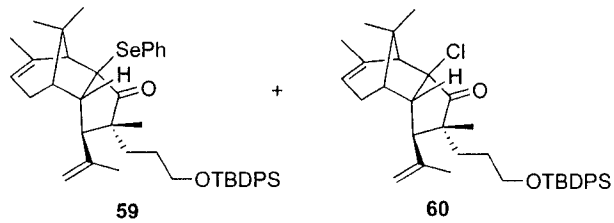

59 **60**

Attempted preparation of selenide **59**: To a –78°C solution of DIPA (126 μL, 0.90 mmol) in THF (1 mL) was added *n*-BuLi (1.3 M in hexanes, 675 μL, 0.90 mmol). The solution was warmed to –20°C and stirred for 5-10 min, then cooled back to –78°C. A solution of the ketone **58** (121 mg, 0.22 mmol) in THF (0.5 mL) was added via cannula, and the resulting mixture was left to stir at –78°C for 1.5 h, whereupon TMSCl (130 μL, 1.02 mmol) was added via syringe. This mixture was then allowed to slowly warm to rt and left to stir overnight. The next day, the solution was cooled back to –78°C for the addition of PhSeCl (200 mg, 1.02 mmol) in THF (0.5 mL) via cannula. Again, the mixture was allowed to warm to rt and stirred overnight. The next morning it was quenched by the addition of 0.3 M HCl (2 mL). The layers were separated and the aqueous layer was extracted with Et_2O (3 x 3 mL). The combined organic fractions were then dried over $MgSO_4$, filtered and concentrated under reduced pressure. Purification by column chromatography (silica gel, gradient elution: 100% hexanes, 120:1, 100:1 hexanes/EtOAc) gave 100 mg (64%) of a mixture of **59** and **60** as a clear colorless oil: R_f 0.60 (10:1 hexanes/EtOAc); ^{1}H NMR (500 MHz, $CDCl_3$) δ 7.68-7.64 (m, 5H), 7.44-7.36 (m, 8H), 5.19 (br s, 1H), 5.02 (br s, 1H), 4.82 (br s, 1H), 3.69 (ddd, J = 11.5, 6.2, 5.3 Hz, 1H), 3.60 (ddd, J = 13.6, 7.1, 6.4 Hz, 1H), 3.46 (dd, J = 8.9, 7.2 Hz, 1H), 2.64 (d, J =

10.0 Hz, 1H), 2.25-2.17 (m, 2H), 2.05 (br s, 1H), 1.90 (br d, J = 18.1 Hz, 1H), 1.81 (s, 3H), 1.72-1.55 (m, 5H), 1.50-1.42 (m, 4H), 1.34-1.22 (m, 1H), 1.85 (s, 3H), 1.09 (s, 3H), 1.07 (s, 9H); ^{13}C NMR (125 MHz, $CDCl_3$) δ 213.2, 142.8, 137.6, 135.5, 134.0, 131.5, 130.8, 129.5, 129.3, 129.1, 127.5, 122.6, 114.0, 79.1, 64.3, 58.4, 55.8, 54.7, 48.5, 45.6, 32.6, 28.8, 28.1, 27.3, 26.8, 25.5, 24.8, 23.4, 23.0, 22.6, 19.2; HRMS for $C_{39}H_{45}O_2SeSi$ ($M-C_4H_9^+$) calcd 653.3191, found 653.2354 ($M-C_4H_9^+$) and $C_{33}H_{40}ClO_2Si$ ($M-C_4H_9^+$) calcd 531.2488, found 531.2469 ($M-C_4H_9^+$).

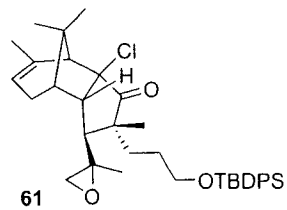

61

Attempted oxidation of selenide **59**: The mixture of ketones **59** and **60** (99 mg, 0.14 mmol) were dissolved in CH_2Cl_2 (1 mL) at rt. To the solution was added H_2O (1 mL), and CH_3CO_3H (32% weight solution in dilute acetic acid, 70 μL, 0.28 mmol). The reaction was stirred for a period of 7 d, with the periodic addition of more CH_3CO_3H until most of the starting material was consumed by TLC. The reaction was quenched with a saturated aqueous solution of $NaHCO_3$ (1 mL). The organic layer was then separated, and washed with 10% HCl (1 x 1 mL), then dried over $MgSO_4$, filtered and concentrated. Purification by column chromatography (silica gel, gradient elution: 50:1, 20:1 hexanes/EtOAc) and gave 11 mg of recovered **60** (11%), 13 mg (16%) and 15 mg (19%) of diastereomers of **61**. The rest of the material consisted of polar unidentifiable byproducts.

Diastereomer **61**: White solid; Mp 92-93°C; R_f 0.33 (10:1 hexanes/EtOAc); ^{1}H NMR (500 MHz, $CDCl_3$) δ 7.68-7.64 (m, 4H), 7.45-7.35 (m, 6H), 5.18 (br s, 1H), 3.69 (ddd, *J* = 10.3, 5.5, 5.5 Hz, 1H), 3.61 (ddd, *J* = 10.0, 6.0, 6.0 Hz, 1H), 2.96 (d, *J* = 3.8 Hz, 1H), 2.72 (dd, *J* = 8.0, 8.0 Hz, 1H), 2.65 (d, *J* = 3.4 Hz, 1H), 2.49 (d, *J* = 8.9 Hz, 1H), 2.30-2.22 (m, 1H), 2.15 (br s, 1H), 2.09-2.02 (m, 2H), 1.80 (ddd, *J* = 14.4, 14.4, 5.4 Hz, 1H), 1.65 (br s, 3H), 1.57-1.48 (m, 2H), 1.41 (s, 3H), 1.37 (s, 3H), 1.28 (s, 3H), 1.27-1.16 (m, 1H), 1.06 (m, 12H); ^{13}C NMR (125 MHz, $CDCl_3$) 213.1, 137.7, 135.6, 134.0, 129.6, 127.6, 122.6, 78.8, 64.2, 58.4, 55.7, 55.0, 52.3, 50.2, 47.4, 45.4, 45.1, 33.8, 28.5, 28.3, 27.6, 26.9, 25.6, 24.8, 23.7, 22.3, 19.2; HRMS for $C_{33}H_{40}ClO_3Si$ ($M-C_4H_9^+$) calcd 547.2437, found 547.2439 ($M-C_4H_9^+$).

Diastereomer **61′**: Clear colorless oil; R_f 0.28 (10:1 hexanes/EtOAc); ^{1}H NMR (500 MHz, $CDCl_3$) δ 7.62-7.58 (m, 4H), 7.42-7.35 (m, 6H), 5.19 (br s, 1H), 3.69 (ddd, *J* = 9.9, 5.9, 4.9 Hz, 1H), 3.64-3.57 (m, 1H), 3.13 (dd, *J* = 8.9, 8.9 Hz, 1H), 2.61 (d, *J* = 2.1 Hz, 1H), 2.46 (d, *J* = 4.5 Hz, 1H), 2.29-2.21 (m, 1H), 2.20-2.15 (m, 2H), 2.10-2.00 (m, 2H), 1.80 (ddd, *J* = 13.5, 13.5, 4.1 Hz, 1H), 1.65 (s, 3H), 1.61-1.52 (m, 2H), 1.45 (s, 3H), 1.42 (s, 3H), 1.41 (s, 3H), 1.24-1.16 (m, 1H), 1.06 (m, 12H); ^{13}C NMR (125 MHz, $CDCl_3$) 213.2, 137.8, 135.6, 134.0, 129.6, 127.6, 122.3, 78.8, 64.1, 58.3, 55.8, 55.5, 51.9, 51.6, 47.3, 45.6, 45.5, 33.7, 28.8, 28.2, 27.6, 26.9, 26.1, 24.8, 22.4, 21.9, 19.2; HRMS for $C_{33}H_{40}ClO_3Si$ ($M-C_4H_9^+$) calcd 547.2437, found 547.2439 ($M-C_4H_9^+$).

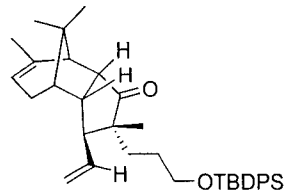

62

Ketone **62**: To a –78°C solution of CuBr·Me_2S (330 mg, 1.6 mmol) in THF (2.2 mL) was added vinylmagnesium bromide (1.0 M solution in THF, 3.2 mL, 3.2 mmol). The solution was stirred at –78°C for 1 h, whereupon the enone **45** (156 mg, 0.31 mmol) in THF (0.6 mL) was added via cannula. Stirring was continued at this temperature for 2.5 h, then MeI (498 μL, 8.0 mmol) and HMPA (1.4 mL, 8.0 mmol) were added. The solution was allowed to slowly warm to rt and left to stir overnight. The reaction was quenched by the addition of saturated aqueous NH_4Cl (5 mL). The aqueous layer was extracted with Et_2O (3 x 5 mL). The combined organic fractions were then dried over $MgSO_4$, filtered and concentrated under reduced pressure. Purification by column chromatography (silica gel, 30:1 hexanes/EtOAc) gave 101 mg (60%) of **62** as a clear colorless oil, along with 38 mg (24%) recovered **45**: R_f 0.50 (10:1 hexanes/EtOAc); IR (CH_2Cl_2 film) 3071, 2930, 1734, 1456 cm^{-1}; ^1H NMR (500 MHz, $CDCl_3$) δ 7.72-7.62 (m, 4H), 7.45-7.35 (m, 6H), 5.77 (ddd, J = 17.4, 10.4, 7.3 Hz, 1H), 5.18-5.02 (m, 3H), 3.75-3.63 (m, 1H), 3.62-3.55 (m, 1H), 3.32 (dd, J = 11.4, 6.4 Hz, 1H), 2.90 (ddd, J = 10.0, 10.0, 7.2 Hz, 1H), 2.71 (dd, J = 7.7, 7.7 Hz, 1H), 2.28 (br d, J = 18.1 Hz, 1H), 2.07-1.97 (m, 2H), 1.84 (br s, 1H), 1.65 (s, 3H), 1.56-1.47 (m, 2H), 1.42-1.33 (m, 2H), 1.10-1.02 (m, 15H), 0.90 (s, 3H); ^{13}C NMR (125 MHz, $CDCl_3$) δ 221.6, 140.0, 138.5, 135.6, 134.2, 129.5, 127.6, 119.5, 116.3, 64.5, 58.8, 56.9, 50.1, 47.3, 45.0, 44.1, 43.0, 30.7, 28.5, 27.1, 26.9, 26.6, 25.1, 21.4, 21.1, 19.2; HRMS for $C_{32}H_{39}O_2Si$ ($M-C_4H_9^+$) calcd 483.2721, found 483.2719 ($M-C_4H_9^+$).

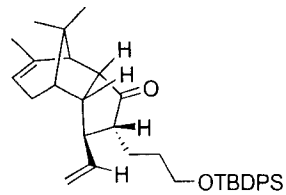

63

Ketone **63**: $CuBr{\cdot}Me_2S$ (3.0 mg, 0.01 mmol) was dissolved in THF/DMS (50:200 μL) and cooled to –55°C. Enone **45** (52 mg, 0.10 mmol) in THF (150 μL) was added via cannula and the resulting mixture was stirred for 5 min before the slow addition of ethylmagnesium bromide (1.0 M solution in THF, 200 μL, 0.20 mmol) via syringe. The reaction was left to stir for 1 h, keeping the temperature between –50°C and –40°C. The reaction was quenched by the addition of saturated aqueous NH_4Cl (2 mL). The aqueous layer was extracted with Et_2O (3 x 5 mL). The combined organic fractions were then dried over $MgSO_4$, filtered and concentrated under reduced pressure. Purification by column chromatography (silica gel, 30:1 hexanes/EtOAc) gave 53 mg (97%) of **63** as a clear colorless oil: R_f 0.47 (5:1 hexanes/EtOAc); ^{1}H NMR (500 MHz, $CDCl_3$) δ 7.70-7.62 (m, 4H), 7.42-7.38 (m, 6H), 5.74 (ddd, J = 18.3, 10.4, 8.0 Hz, 1H), 5.13 (br s, 1H), 5.06 (dd, J = 8.6, 1.5, 1.5 Hz, 1H), 5.03 (d, J = 0.8 Hz, 1H), 3.65 (app. t, J = 6.0 Hz, 2H), 3.21 (ddd, J = 11.8, 6.2, 1.6 Hz, 1H), 2.75 (ddd, J = 11.8, 8.4, 7.2 Hz, 1H), 2.45 (ddd, J = 12.6, 8.7, 8.7 Hz, 1H), 2.33-2.18 (m, 2H), 2.10-2.02 (m, 1H), 1.95 (d, J = 6.2 Hz, 1H), 1.83 (br s, 1H), 1.68 (s, 3H), 1.60-1.49 (m, 4H), 1.09-1.00 (m, 15H); ^{13}C NMR (125 MHz, $CDCl_3$) δ 217.7, 142.1, 140.4, 135.6, 134.2, 129.4, 127.5, 118.9, 114.9, 64.1, 59.3, 57.0, 50.1, 47.2, 46.9, 44.9, 42.9, 29.3, 28.8, 26.9, 26.5, 25.0, 22.7, 21.3, 19.2.

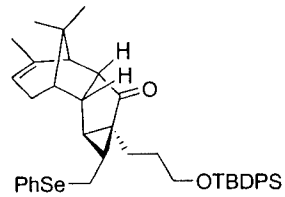

64

Selenide **64**: To a –78°C solution of TMP (67μL, 0.40 mmol) in THF (0.6 mL) was added *n*-BuLi (1.6 M solution in hexanes, 250 μL, 0.40 mmol). The solution was warmed to –20°C and stirred for 5-10 min, then cooled back to –78°C. A solution of ketone **63** (42 mg, 0.08 mmol) in THF (0.4 mL) was added by cannula, and the resulting mixture was left to stir at –78°C for 2 h, whereupon TMSCl (60 μL, 0.48 mmol) was added via syringe. This mixture was then allowed to slowly warm to rt over 2 h, then cooled back to –78°C for the addition of a solution of PhSeCl (92 mg, 0.48 mmol) in THF (0.4 mL) via cannula. Again, the mixture was allowed to warm to rt and stirred overnight. The next morning it was quenched by the addition of H_2O (2 mL). The layers were separated and the aqueous layer was extracted with Et_2O (3 x 3 mL). The combined organic fractions were then dried over $MgSO_4$, filtered and concentrated under reduced pressure. Purification by column chromatography (silica gel, gradient elution: 100% hexanes, 60:1, 50:1, 40:1 hexanes/EtOAc) gave 54 mg (100%) of **64** as one diastereomer as a clear colorless oil: R_f 0.48 (5:1 hexanes/EtOAc); IR (CH_2Cl_2 film) 3069, 2928, 1713, 1473 cm^{-1}; ^1H NMR (500 MHz, $CDCl_3$) δ 7.79-7.63 (m, 4H), 7.59-7.50 (m, 2H), 7.43-7.35 (m, 6H), 7.30-7.22 (m, 3H), 5.06 (br s, 1H), 3.72-3.59 (m, 2H), 3.07 (dd, J = 12.1, 4.9 Hz, 1H), 2.90 (dd, J = 8.7, 8.7 Hz, 1H), 2.78-2.68 (m, 2H), 2.24-2.05 (m, 2H), 1.97 (d, J = 7.6 Hz, 1H), 1.86 (ddd, J = 11.5, 9.0, 7.4 Hz, 1H), 1.71 (br s, 1H), 1.65-1.54 (m, 5H), 1.48-1.39 (m, 2H), 1.12-1.03 (10H), 1.01 (s, 3H), 0.99 (s, 3H); ^{13}C NMR (125 MHz, $CDCl_3$) δ 215.2, 137.7, 135.6, 134.1, 134.0, 133.8, 129.6, 129.1, 127.6, 127.6,

120.4, 64.1, 57.3, 50.8, 46.9, 45.6, 44.7, 44.4, 34.1, 30.6, 30.4, 28.0, 27.4, 26.9, 26.2, 25.1, 21.4, 20.2, 19.2; HRMS for $C_{37}H_{41}O_2SeSi$ ($M-C_4H_9^+$) calcd 625.2477, found 625.2052 ($M-C_4H_9^+$).

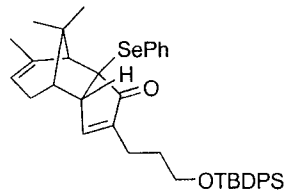

65

Selenide **65**: To a –78°C solution of DIPA (77 μL, 0.55 mmol) in THF (1.5 mL) was added *n*-BuLi (1.6 M in hexanes, 345 μL, 0.55 mmol). The solution was warmed to 0°C, stirred for 30 min, then subsequently cooled back to –78°C. A solution of enone **45** (133 mg, 0.27 mmol) in THF (0.5 mL) was added by cannula, and the resulting mixture was left to stir at –78°C for 1.5 h, whereupon a solution of PhSeCl (157 mg, 0.82 mmol) in THF (1 mL) was added via cannula. The mixture was slowly allowed to warm to –15°C over a 3 h period, and was quenched by the addition of 10% HCl (2 mL). The layers were separated and the aqueous layer was extracted with Et_2O (3 x 5 mL). The combined organic fractions were then dried over $MgSO_4$, filtered and concentrated under reduced pressure. Purification by column chromatography (silica gel, gradient elution: 100% hexanes, 50:1, 40:1, 30:1, 20:1, 10:1, 5:1 hexanes/EtOAc) gave 70 mg (39%) of **65** as a yellow oil: R_f 0.47 (10:1 hexanes/EtOAc); IR (CH_2Cl_2 film) 3070, 2930, 1698, 1428 cm^{-1}; ^1H NMR (500 MHz, $CDCl_3$) δ 7.67-7.63 (m, 4H), 7.58-7.54 (m, 2H), 7.46-7.36 (m, 6H), 7.27-7.22 (m, 1H), 7.20-7.15 (m, 2H), 6.70 (s, 1H), 4.82 (br s, 1H), 3.54-3.45 (m, 3H), 2.10 (br d, J = 18.5 Hz, 1H), 2.05-1.94 (m, 4H), 1.59 (s, 3H), 1.57-1.53 (m, 4H),

1.52-1.45 (m, 2H), 1.05 (s, 12H); ^{13}C NMR (125 MHz, $CDCl_3$) δ 204.7, 153.8, 145.4, 140.8, 137.2, 135.6, 134.0, 129.5, 128.8, 128.5, 127.8, 127.6, 119.2, 64.5, 63.1, 58.0, 54.3, 45.6, 44.6, 30.4, 29.8, 28.4, 27.1, 25.2, 23.2, 21.3, 19.2; HRMS for $C_{35}H_{37}O_2SeSi$ ($M-C_4H_9^+$) calcd 597.2164, found 597.1728 ($M-C_4H_9^+$).

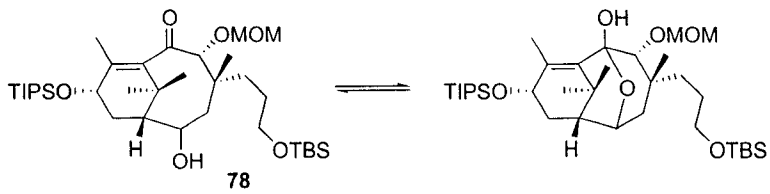

78

Alcohol **78**: To a solution of diketone **51** (42 mg, 0.066 mmol) dissolved in MeOH (0.7 mL) and cooled to 0°C was added $NaBH_4$ (2.5 mg, 0.066 mmol). The mixture was allowed to warm to rt and stirred for 2 h. The reaction was quenched by the addition of saturated aqueous Na_2SO_4 and diluted with CH_2Cl_2. The aqueous layer was then extracted with CH_2Cl_2 (3 x 3 mL), and the combined organic extracts were dried over $MgSO_4$, filtered and evaporated. The crude residue was purified by column chromatography (silica gel, gradient elution from 13:1 to 8:1 hexanes/EtOAc), and gave 42 mg (100%) of **78** as a white solid: R_f 0.42 (2:1 hexanes/EtOAc, UV active); IR (CH_2Cl_2 film) 3486, 2928, 1683 (medium intensity), 1463 cm^{-1}; ^1H NMR (500 MHz, $CDCl_3$, broadened signals, some peaks missing) δ 4.75 (d, J = 7.6 Hz, 1H), 4.68 (d, J = 7.1 Hz, 1H), 4.64 (br s, 1H), 3.52-3.40 (m, 5H), 2.78 (br s, 1H), 1.90-1.82 (m, 4H), 1.52-1.08 (m, 9H), 1.60 (br s, 3H), 1.30-1.02 (m, 22H), 1.00 (br s, 3H), 0.89 (s, 9H), 0.00 (2, 6H); HRMS for $C_{35}H_{67}O_6Si_2$ ($M-H^+$) calcd 639.4478, found 639.4426 ($M-H^+$).

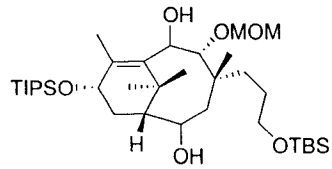

79

Diol **79**: To a solution of diketone **51** (35 mg, 0.055 mmol) dissolved in CH_2Cl_2 (0.5 mL) and cooled to –78°C was added DIBALH (1.0 M solution in CH_2Cl_2, 65 μL, 0.065 mmol). The reaction was stirred at this temperature for 1.5 h. Solid $Na_2SO_4 \cdot 7H_2O$ (100 mg) was then added, and stirring was continued for 2 h. The mixture was subsequently filtered, the solvent removed under reduced pressure, and the crude residue purified by column chromatography (silica, gradient elution from 12:1 to 7:1 hexanes/EtOAc) and gave a mixture of **79** and **78** (69% and 27% yield respectively). Compound **78** could be re-subjected to the reaction conditions to give additional amounts of **79**, or alternatively, excess DIBALH could be added to the reaction mixture to get exclusive formation of the **79** (27 mg, 77%): Clear colorless oil that crystallizes on standing; R_f 0.49 (2:1 hexanes/EtOAc, non-UV active); IR (CH_2Cl_2 film) 3480, 2944, 1464 cm^{-1}; ^1H NMR (500 MHz, $CDCl_3$, broadened signals, some peaks missing) δ 4.88 (br s, 1H), 4.74 (d, J = 6.6 Hz, 1H), 4.72 (d, J = 6.5 Hz, 1H), 4.53 (br s, 1H), 3.60-3.50 (m, 2H), 3.45 (s, 3H), 2.68 (br s, 1H), 2.21 (s, 3H), 1.72-1.36 (m, 9H), 1.32-1.20 (m, 1 or 2H), 1.19-1.10 (m, 25H), 1.01 (br s, 3H), 0.92 (s, 9H), 0.05 (s, 6H); HRMS for $C_{35}H_{70}O_6Si_2$ (M^+) calcd 642.4713, found 642.4704 (M^+).

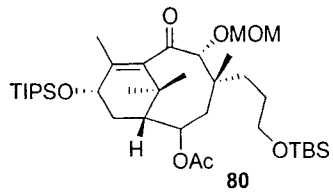

80

Acetate **80**: The alcohol **78** (38 mg, 0.059 mmol) was dissolved in CH_2Cl_2 (0.2 mL). DMAP (0.4 mg, 0.003 mmol) was then added, followed by Ac_2O (75 μL, 0.71 mmol) and Et_3N (165 μL, 1.18 mmol). The mixture was allowed to stir for 12 h, then quenched by the addition of 0.3 M HCl (1 mL). The aqueous layer was extracted with CH_2Cl_2 (3 x 2 mL). The combined organic fractions were then dried over $MgSO_4$, filtered, and concentrated. Purification was achieved by chromatography (silica gel, 10:1 hexanes/EtOAc) and gave 38 mg (94%) of **80** as a white solid: R_f 0.39 (5:1 hexanes/EtOAc); IR (CH_2Cl_2 film) 2948, 2867, 1742, 1694 (med. Intensity), 1463 cm^{-1}; ^1H NMR (500 MHz, $CDCl_3$, broadened signals, some peaks missing) δ 5.20 (br s, 1H), 5.07 (br s, 1H), 4.72 (d, J = 7.2 Hz, 1H), 4.70-4.65 (m, 2H), 3.52-3.42 (m, 5H), 2.82 (br ddd, J = 14.0, 8.5, 8.5 Hz, 1H), 2.13-1.98 (m, 4H), 1.93-1.86 (m, 4H), 1.58-1.34 (m, 5H), 1.19 (s, 3H), 1.15-1.06 (m, 22H), 1.01 (s, 3H), 0.86 (s, 9H), 0.01 (s, 6H); ^{13}C NMR (500 MHz, $CDCl_3$, some peaks missing) δ 203.3, 169.7, 141.2, 96.6, 78.2, 67.5, 64.1, 56.5, 44.3, 41.8, 37.1, 36.3, 32.5, 27.5, 27.0, 26.0, 21.6, 18.3, 18.2, 18.1, 16.6, 12.7, -5.3, -5.4; HRMS for $C_{37}H_{70}O_7Si_2$ (M^+) calcd 682.4662, found 682.4595 (M^+).

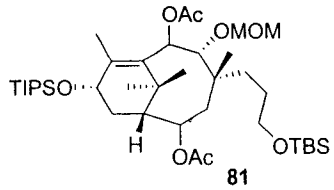

81

Diacetate **81**: Diol **79** (28 mg, 0.044 mmol) was dissolved in CH_2Cl_2 (0.5 mL). DMAP (0.2 mg, 0.002 mmol) was then added, followed by Ac_2O (30 μL, 0.32 mmol) and Et_3N (75 μL, 0.54 mmol). The mixture was allowed to stir for 12 h, then quenched by the addition of 1 mL of 0.3 M HCl. The aqueous layer was extracted with CH_2Cl_2 (3 x 2 mL). The combined organic fractions were then dried over $MgSO_4$, filtered, and concentrated. Purification was achieved by chromatography (silica gel, 10:1 hexanes/EtOAc) and gave 30 mg (94%) of **81** as a white solid: R_f 0.65 (2:1 hexanes/EtOAc); IR (CH_2Cl_2 film) 2945, 2866, 1742, 1464 cm^{-1}; ^1H NMR (500 MHz, $CDCl_3$, broadened signals, some peaks missing) δ 6.04 (br s, 1H), 5.14 (br s, 1H), 4.78 (d, J = 7.2 Hz, 1H), 4.63-4.48 (m, 3H), 3.58 (t, J = 6.1 Hz, 2H), 3.37 (s, 3H), 2.74 (ddd, J = 18.4, 9.0, 9.0 Hz, 1H), 2.15 (s, 3H), 2.08 (s, 3H), 2.05 (s, 3H), 1.88-1.80 (m, 2H), 1.60-1.48 (m, 5H), 1.36-1.29 (m, ~1H), 1.14-1.06 (m, 24H), 1.03 (s, 3H), 0.92-0.85 (m, 11H); HRMS (ESI) for $C_{39}H_{74}O_8Si_2$ (M+Na) calcd 749.4924, found 749.4815 (M+Na).

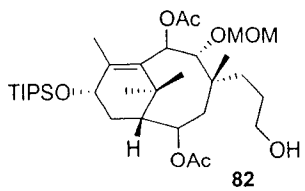

82

Alchol **82**: The diacetate **81** (30 mg, 0.041 mmol) was dissolved in CH_3CN (0.5 mL) at rt in a polypropylene vial. To this was added 180 μL of a 1.1 M solution of HF/pyridine (0.16 mmol). The mixture was allowed to stir for 3 d and was quenched by the addition

of saturated aqueous $NaHCO_3$ (1 mL). The aqueous layer was extracted with Et_2O (3 x 5 mL) and the combined organic layers were then dried over $MgSO_4$, filtered and concentrated under reduced pressure. The crude residue was purified by column chromatography (silica gel, gradient elution: 5:1 to 1:1 hexanes/EtOAc) and gave 22 mg of **82** (88%) as a white solid: R_f 0.23 (2:1 hexanes/EtOAc); ^{1}H NMR (500 MHz, $CDCl_3$, broadened signals, some peaks missing) δ 6.01 (br s, 1H), 5.10 (br s, 1H), 4.78 (d, J = 7.0 Hz, 1H), 4.58-4.43 (m, 3H), 3.60 (br m, 2H), 3.37 (s, 3H), 2.80-2.63 (br m, 1H), 2.11 (s, 3H), 2.05 (s, 3H), 2.01 (s, 3H), 1.90-1.78 (m, 2H), 1.62-1.42 (m, 5H), 1.18-0.80 (m, ~29H).

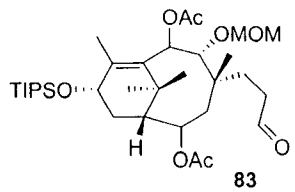

83

Aldehyde **83**: To a solution of alcohol **82** (22 mg, 0.015 mmol) in CH_2Cl_2 (0.4 mL) was added 4Å molecular sieves and NMO (12.7 mg, 0.11 mmol), followed by TPAP (0.6 mg, 0.001 mmol). The mixture was stirred at rt for 15-20 min, and was subsequently filtered through a plug of silica with the aid of 35% EtOAc/hexanes. The crude residue was purified by column chromatography (silica gel, 4:1 hexanes/EtOAc) and gave 17 mg (77%) of **83** as a white solid: R_f 0.33 (2:1 hexanes/EtOAc); ^{1}H NMR (500 MHz, $CDCl_3$, broadened signals, partial data) δ 9.78 (s, 1H), 6.01 (br s, 1H), 5.12 (br s, 1H), 4.78-4.42 (m, ~5H), 3.37 (s, 3H), 2.80-2.63 (br m, 1H), 2.62-2.42 (m, 1H), 2.41-2.32 (m, 1H), 2.13 (s, 3H), 2.05 (s, 3H), 2.01 (s, 3H), 1.90-1.78 (m, 2H).

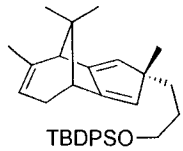

85

Diene **85**: During DIBALH reduction of **47** and subsequent acetylation, varying amounts of diene **85** resulting from elimination were obtained (0-100%): R_f 0.69 (10:1 hexanes/EtOAc); IR (neat) 3051, 2928, 1472 cm^{-1}; ^1H NMR (500 MHz, $CDCl_3$) δ 7.72-7.65 (m, 4H), 7.47-7.35 (m, 6H), 5.58 (s, 1H), 5.40 (s, 1H), 5.01 (br s, 1H), 3.58 (t, J = 7.9 Hz, 2H), 2.40 (br d, J = 17.4 Hz, 1H), 2.24-2.20 (m, 2H), 1.92 (br d, J = 17.2 Hz, 1H), 1.67 (ddd, J = 1.7, 1.7, 1.7 Hz, 3H), 1.64-1.59 (m, 2H), 1.43-1.33 (m, 2H), 1.18 (s, 3H), 1.10 (s, 3H), 1.05 (s, 9H), 0.91 (s, 3H); ^{13}C NMR (125 MHz, $CDCl_3$) δ 153.7, 152.7, 138.3, 135.6, 134.3, 131.3, 129.4, 127.6, 125.7, 117.3, 64.8, 60.9, 51.2, 44.8, 42.7, 33.7, 32.0, 28.2, 27.6, 26.9, 22.6, 22.2, 19.8, 19.2; HRMS for $C_{34}H_{44}OSi$ (M^+) calcd 496.3163, found 496.3165 (M^+).

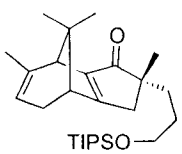

86

Enone **86**: To a solution of TBDPS enone **47** (334 mg, 0.65 mmol) dissolved in THF (6.5 mL) and cooled to 0°C was added TBAF (1.0 M, 850 μL, 0.85 mmol). The mixture was warmed to rt and stirred for 2 h. The reaction was quenched by the addition of H_2O (5 mL) and diluted with Et_2O (5 mL). The layers were separated and the aqueous layer was extracted with Et_2O (3 x 3 mL). The organic layer was then dried over $MgSO_4$, filtered, and concentrated to reveal a clear colorless oil that was taken on crude to the next step.

The crude alcohol was dissolved in CH_2Cl_2 (1.5 mL) at rt and was treated with DMAP (4.0 mg, 0.03 mmol), imidazole (111 mg, 1.6 mmol) and TIPSCl (210 μL, 1.0 mmol). The reaction was stirred overnight at rt and was quenched the next day by the addition of H_2O (1.5 mL). The aqueous layer was extracted with CH_2Cl_2 (3 x 2 mL), and the combined organic extracts were dried over $MgSO_4$, filtered, and concentrated. The crude residue was purified by column chromatography (silica gel, 30:1 hexanes/EtOAc) and gave 252 mg (90%, 2 steps) of the TIPS enone **86** as a clear colorless oil: R_f 0.32 (10:1 hexanes/EtOAc); ^{1}H NMR (500 MHz, $CDCl_3$) δ 4.92 (s, 1H), 3.62-3.52 (m, 2H), 2.53 (d, $J_{A/B}$ = 18.9 Hz, 1H), 2.34-2.27 (m, 3H), 2.24 (d, $J_{A/B}$ = 19.0 Hz, 1H), 1.86-1.78 (m, 1H), 1.72 (s, 3H), 1.56-1.44 (m, 2H), 1.36-1.19 (m, 2H), 1.13 (s, 3H), 1.11 (s, 3H), 1.04-1.01 (m, 24H); ^{13}C NMR (125 MHz, $CDCl_3$) δ 206.9, 182.0, 155.3, 140.4, 134.8, 116.2, 63.6, 52.5, 49.4, 48.6, 48.3, 38.6, 34.7, 27.9, 25.4, 24.5, 23.5, 20.7, 18.0, 12.0.

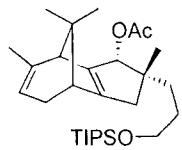

87

Allylic acetate **87**: Enone **86** (280 mg, 0.65 mmol) was dissolved in CH_2Cl_2 (6.5 mL) and cooled to –78°C. DIBALH (1.0 M solution in CH_2Cl_2, 670 μL, 0.67 mmol) was added and the mixture was allowed to stir at this temperature for 40 min. The reaction was quenched by the addition of solid $Na_2SO_4 \cdot 7H_2O$ (250 mg), and left to stir over 2 h. The mixture was then filtered and concentrated under reduced pressure to yield the allylic alcohol, which was immediately taken on crude to the next step.

To a solution of the crude alcohol from above in Et_3N (900 μL, 6.5 mmol) and CH_2Cl_2 (6.5 mL) at rt was added DMAP (4.0 mmol, 0.03 mmol) followed by freshly distilled Ac_2O (370 μL, 3.9 mmol). The reaction was stirred at rt for 2.5 h and subsequently quenched by the addition of 0.3 M HCl (2 mL). The aqueous layer was extracted with CH_2Cl_2 (3 x 5 mL), and the combined organic extracts were dried over $MgSO_4$, filtered, and concentrated. The crude residue was purified by column chromatography (silica gel, 1% Et_3N/hexanes) and gave 126 mg (41%, 2 steps) of allylic acetate **87** along with 134 mg (48% yield) of recovered enone **86**: R_f 0.58 (10:1 hexanes/EtOAc); ^1H NMR (500 MHz, $CDCl_3$) δ 5.38 (s, 1H), 4.99 (br s, 1H), 3.65 (t, J = 8.3 Hz, 2H), 2.29 (dd, J = 15.6, 2.1 Hz, 1H), 2.14-2.05 (m 2H), 2.01 (s, 3H), 1.96 (br s, 1H), 1.90 (dd, J = 15.8, 1.1 Hz, 1H), 1.83 (br d, J = 18.0 Hz, 1H), 1.60 (br s, 3H), 1.53-1.42 (m, 5H), 1.39-1.25 (m, 2H), 1.15 (s, 3H), 1.10-1.01 (m, 24H).

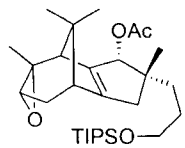

88

Epoxide **88**: Allylic acetate **87** (50 mg, 0.11 mmol) was dissolved in CH_2Cl_2 (1.5 mL) and cooled to –20°C. Na_2CO_3 (128 mg, 1.2 mmol) followed by *m*-CPBA (50%, 30 mg, 0.11 mmol) were then added and the reaction was allowed to warm to 0°C and left to stir 2.5 h. The reaction was quenched by the addition of aqueous $Na_2S_2O_3$ (1 M, 1 mL), and extracted with CH_2Cl_2 (3 x 2 mL). The combined organic fractions were then washed with saturated aqueous $NaHCO_3$ (1 x 5 mL), dried over anhydrous K_2CO_3, filtered, and

concentrated. Purification was achieved by column chromatography (silica gel, 0.5% Et_3N/hexanes) and gave 37 mg (40%) of epoxide **88** as a clear colorless oil: R_f 0.65 (2:1 hexanes/EtOAc); ^1H NMR (500 MHz, $CDCl_3$) δ 4.80 (dd, J = 1.5, 1.5 Hz, 1H), 3.68 (t, J = 6.5 Hz, 2H), 2.85 (d, J = 4.3 Hz, 1H), 2.45 (d, J = 16.9 Hz, 1H), 2.29 (br s, 1H), 2.03 (s, 3H), 1.87-1.70 (m, 3H), 1.67-1.50 (m, 5H), 1.25 (s, 3H), 1.18 (s, 3H), 1.09-1.04 (m, 27H); ^{13}C NMR (125 MHz, $CDCl_3$) δ 171.5, 157.5, 143.8, 83.3, 64.3, 57.9, 54.8, 52.9, 51.2, 48.7, 44.3, 41.6, 32.4, 28.9, 27.9, 26.4, 23.4, 22.7, 21.5, 21.4, 18.0, 12.0.

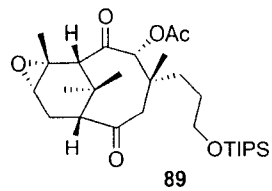

89

Diketone **89**: To a solution of **88** (37 mg, 0.075 mmol) in a biphasic solvent system consisting of $CCl_4/CH_3CN/H_2O$ (2:2:3 mL) was added $NaIO_4$ (20 mg, 0.090 mmol). $RuO_2 \cdot H_2O$ (1 mg, 0.01 mmol) was then added, and the resulting mixture was allowed to stir at rt for 1 h 15 min. The reaction was diluted with H_2O (3 mL) and CH_2Cl_2 (3 mL), and the aqueous layer separated and extracted with CH_2Cl_2 (3 x 3 mL). The CH_2Cl_2 extracts were then combined, dried over $MgSO_4$, filtered, and concentrated. Purification was achieved by pipette chromatography (silica gel, 10:1 hexanes/EtOAc and gave 31 mg (79 %) of **89** as a clear colorless oil: R_f 0.52 (2:1 hexanes/EtOAc); ^1H NMR (500 MHz, $CDCl_3$) δ 4.88 (s, 1H), 3.72-3.56 (m, 3H), 3.10 (d, J = 3.7 Hz, 1H), 2.63 (d, J = 1.3 Hz, 1H), 2.37-2.29 (m, 2H), 2.20 (ddd, J = 17.1, 8.7, 4.0 Hz, 1H), 2.06 (s, 3H), 1.88 (dd, J = 12.5, 1.6 Hz, 1H), 1.73-1.62 (m, 4H), 1.57-1.48 (m, 1H), 1.42 (s, 3H), 1.38-1.30 (m, 1H), 1.22 (s, 3H), 1.16 (s, 3H), 1.12-1.00 (m, 22H).

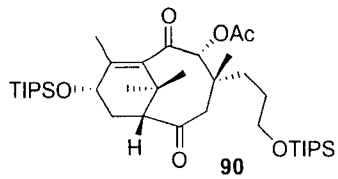

90

Diketone **90**: To a solution of **89** (31 mg, 0.059 mmol) in *t*-BuOH (1 mL) at ~30°C was added *t*-BuOK (0.30 mg, 0.003 mmol). The pale yellow mixture was stirred for 2 h, then quenched by the addition of H_2O (1 mL). The reaction was extracted with Et_2O (3 x 2 mL), dried over $MgSO_4$, filtered and concentrated to reveal a yellow oil that was taken on crude to the next step.

The crude alcohol was dissolved in CH_2Cl_2 (0.3 mL) and cooled to 0°C. 2,6-Lutidine (50 μL, 0.19 mmol) was added, followed by TIPSOTf (50 μL, 0.43 mmol) and the resulting mixture was warmed to rt and stirred overnight. The reaction was quenched by the addition of saturated aqueous $NaHCO_3$ (1 mL). The aqueous layer was extracted with CH_2Cl_2 (3 x 2 mL), and the combined organic layers were dried over $MgSO_4$, filtered and concentrated under reduced pressure. The crude residue was purified by chromatography using a pipette (silica gel, 15:1 hexanes/EtOAc) and gave 37 mg (91%) of **90** as a white solid: R_f 0.59 (2:1 hexanes/EtOAc); ^{1}H NMR (500 MHz, $CDCl_3$) δ 5.30 (s, 1H), 4.88 (br s, 1H), 3.65-3.55 (m, 2H), 2.81 (d, J = 12.4 Hz, 1H), 2.74 (ddd, J = 15.3, 9.5, 8.8 Hz, 1H), 2.57 (d, J = 8.4 Hz, 1H), 2.18 (s, 3H), 2.03 (d, J = 12.3 Hz, 1H), 1.97 (d, J = 1.3 Hz, 3H), 1.78 (dd, J = 15.3, 5.4 Hz, 1H), 1.70 (ddd, J = 13.1, 13.1, 3.4 Hz, 1H), 1.58-1.43 (m, 1H), 1.37 (m, 4H), 1.23 (s, 3H), 1.14-1.08 (m, 22H), 1.06-1.02 (m, 24H); ^{13}C NMR (125 MHz, $CDCl_3$) δ 213.4, 197.5, 170.3, 143.6, 141.5, 84.6, 67.6, 63.7, 58.6, 47.0, 41.5, 35.1, 33.9, 32.9, 30.3, 27.1, 24.6, 20.5, 18.2, 18.0, 17.7, 16.7, 12.7, 12.0.

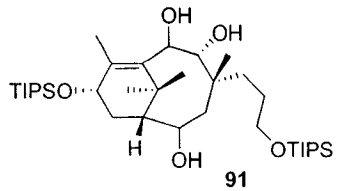

91

Triol **91**: To a solution of diketone **90** (26 mg, 0.039 mmol) dissolved in CH_2Cl_2 (0.5 mL) and cooled to –78°C was added DIBALH (1.0 M solution in CH_2Cl_2, 155 μL, 0.155 mmol). The reaction was stirred at this temperature for 1.5 h. Solid $Na_2SO_4 \cdot 7H_2O$ (150 mg) was then added, and stirring was continued for 2 h. The mixture was subsequently filtered, the solvent removed under reduced pressure, and the crude residue purified by column chromatography (silica, gradient elution from 15:1 to 2:1 hexanes/EtOAc) and gave 13.1 mg (49%) of **91** as a white solid: R_f 0.36 (2:1 hexanes/EtOAc); ^1H NMR (500 MHz, $CDCl_3$, missing peaks) δ 4.57 (s, 1H), 4.50 (br s, 1H), 3.54-3.51 (m, 2H), 2.56 (br s, 1H), 2.54-2.52 (m, 1H), 2.04 (s, 3H), 1.53-1.50 (m, ~5H), 1.49-1.45 (m, ~4H), 1.20-0.99 (m, ~49H); HRMS for $C_{33}H_{65}O_5Si_2$ ($M-C_3H_7^+$) calcd 597.4373, found 597.4345 ($M-C_3H_7^+$).

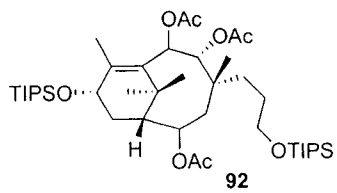

92

Triacetate **92**: Compound **91** (12.5 mg, 0.018 mmol) was dissolved in CH_2Cl_2 (0.5 mL). DMAP (0.1 mg, 0.001 mmol) was then added, followed by Ac_2O (25 μL, 0.22 mmol) and Et_3N (50 μL, 0.36 mmol). The mixture was allowed to stir for 2.5 h, then quenched by the addition of 1 mL of 0.3 M HCl. The aqueous layer was extracted with CH_2Cl_2 (3 x 2 mL). The combined organic fractions were then dried over $MgSO_4$, filtered, and

concentrated. Purification was achieved by chromatography (silica gel, pipette, 15:1 hexanes/EtOAc) and gave 11.8 mg (85%) **92** as a white solid: R_f 0.68 (2:1 hexanes/EtOAc); IR (CH_2Cl_2 film) 2943, 2866, 1742, 1463 cm^{-1}; ^1H NMR (500 MHz, $CDCl_3$) δ 5.96 (br s, 1H), 5.12 (br s, 1H), 4.58 (br s, 1H), 3.74-3.58 (m, 2H), 2.79-2.69 (m, 1H), 2.12 (s, 3H), 2.09 (s, 3H), 2.07 (s, 3H), 2.01 (s, 3H), 1.92-1.82 (m, ~2H), 1.74-1.63 (m, 1H), 1.63-1.44 (m, ~5H), 1.38-1.20 (m, ~5H), 1.14-0.98 (m, ~46H); HRMS for $C_{42}H_{78}O_8Si_2$ (M^+) calcd 766.5237, found 766.5237 (M^+).

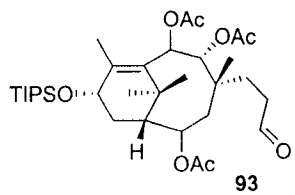

93

Aldehyde **93**: The triacetate **92** (12 mg, 0.015 mmol) was dissolved in CH_3CN (1 mL) at rt in a polypropylene vial. To this was added 1 drop of a 1.1 M solution of HF/pyridine. The mixture was allowed to stir for 3 d and was quenched by the addition of saturated aqueous $NaHCO_3$ (1 mL). The aqueous layer was extracted with Et_2O (3 x 5 mL) and the combined organic layers were then dried over $MgSO_4$, filtered and concentrated under reduced pressure to give a yellow oil (9.1 mg, 100%) which was taken on crude to the next step.

To a solution of the alcohol prepared above in CH_2Cl_2 (0.3 mL) was added 4Å molecular sieves and NMO (5.0 mg, 0.045 mmol), followed by TPAP (0.3 mg, 0.001 mmol). The mixture was stirred at rt for 15-20 min, and was subsequently filtered through a plug of silica with the aid of 35% EtOAc/hexanes. The crude residue was

purified by pipette column (silica gel, gradient elution: 10:1, 9:1, 8:1 hexanes/EtOAc) and gave **93** as a clear colorless oil (6.6 mg, 72%): R_f 0.52 (1:1 hexanes/EtOAc); ^{1}H NMR (500 MHz, $CDCl_3$, partial data) δ 9.79 (s, 1H), 6.00 (br s, 1H), 5.18 (br s, 1H), 4.52 (br s, 1H), 2.75 (br s, 1H), 2.43 (br s, 2H), 2.18 (s, 3H), 2.08 (s, overlapping, 6H), 2.02 (s, 3H) ppm.

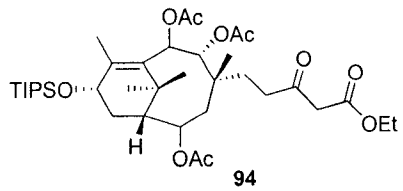

94

β-Keto ester **94**: To a room temperature solution of **93** (6.6 mg, 0.011 mmol) in CH_2Cl_2 (0.2 mL) was added $NbCl_5$ (0.15 mg, 0.001 mmol), followed by ethyl diazoacetate (1.5 μL, 0.13 mmol). The bright yellow reaction was stirred overnight. The crude reaction mixture was filtered through Celite to remove the catalyst, then concentrated under reduced pressure. The crude mixture was purified by column chromatography using a pipette (silica gel, 10:1 hexanes/EtOAc) and gave 7.1 mg (93%) of **94** as a clear colorless oil: R_f 0.31 (1:1 hexanes/EtOAc); ^{1}H NMR (500 MHz, $CDCl_3$, partial data) δ 5.98 (br s, 1H), 5.18 (br s, 1H), 4.55 (br s, 1H), 4.19 (q, J = 7.0 Hz, 2H), 2.75 (br s, 1H), 2.50 (br s, 2H), 2.17 (s, 3H), 2.08 (s, overlapping, 6H), 2.02 (s, 3H) 1.28 (t, J = 7.0 Hz, 3H) ppm; HRMS for $C_{37}H_{62}O_{10}Si$ (M^+) calcd 694.4114, found 694.4116 (M^+).

3.6. References

[1] Lucas, H. *Arch. Pharm.* **1856**, *85*, 145.

[2] Kurono, M.; Nakadaira, Y.; Onuma, S.; Sasaki, K.; Nakanishi, K. *Tetrahedron Lett.* **1963**, *4*, 2153.

[3] a) Itokawa, H. and Kuo-Hsiung Lee, K. H. ed., *Taxus : the genus taxus*, Taylor & Francis, London, New York, NY, 2003. b) Kingston, D. G. I. *Chem. Commun.*, **2001**, 867.

[4] Schiff, P. B.; Fant, J.; Horwitz, S. B. *Nature*, **1979**, *277*, 665.

[5] Holton, R. A.; Biediger, R. J.; Boatman, P. D. in *Taxol®: Science and Applications*, ed. Suffness, M., CRC Press, Boca Raton, FL, 1995, p. 97.

[6] a) Lyseng-Williamson, K. A.; Fenton, C. *Drugs* **2005**, *65*, 2513. b) Crown, J.; O'Leary, M. *Lancet* **2000**, *355*, 1176.

[7] Mehta, G.; Singh, V. *Chem. Rev.* **1999**, *99*, 881.

[8] Zefirova, O. N.; Nurieva, E. V.; Ryzhov, A. N.; Zyk, N. V.; Zefirov, N. S. *Russ. J. Org. Chem.* **2005**, *41*, 329.

[9] Nicolaou, K. C.; Yang, Z.; Liu, J. J.; Ueno, H.; Nantermet, P. G.; Guy, R. K.; Renaud, J.; Couladouros, E. A.; Paulvannan, K.; Sorensen, E. J. *Nature* **1994**, *367*, 630.

[10] Masters, J. J.; Link, J. T.; Snyder, L. B.; Young, W. B. Danishefsky, S. J. *Angew. Chem. Int., Ed. Engl.* **1995**, *34*, 1723.

[11] Morihira, K.; Hara, R.; Kawahara, S.; Nishimori, T.; Nakamura, N.; Kusama, H.; Kuwajima, I. *J. Am. Chem. Soc.* **1998**, *120*, 12980.

[12] a) Takayuki, D.; Fuse, S.; Shigeru, M.; Nakai, K.; Sasuga, D.; Takahashi, T. *Chem. Asian. J.* **2006**, *1*, 370. b) Kress, M. H.; Ruel, R.; Miller, W. H.; Kishi, Y. *Tetrahedron Lett.* **1993**, *34*, 5999. c) Funk, R. L.; Daily, W. J.; Parvez, M. *J. Org. Chem.* **1988**, *53*, 4141. d) Kende, A. S.; Johnson, S.; Sanfilippo, P.; Hodges, J. C.; Jungheim, L. N. *J. Am. Chem. Soc.* **1986**, *108*, 3513.

[13] a) Stork, G.; Manabe, K.; Liu, L. *J. Am. Chem. Soc.* **1998**, *120*, 1337. b) Crich, D.; Natarajan, S.; Crich, J. Z. *Tetrahedron* **1997**, *53*, 7139. c) Bourgeois, D.; Mahuteau, J.; Pancrazi, A.; Nolan, S. P.; Prunet, J. *Angew. Chem. Int. Ed.* **2000**, *39*, 726.

[14] a) Winkler, J. D.; Kim, H. S.; Kim, S.; Ando, K.; Houk, K. N. *J. Org. Chem.* **1997**, *62*, 2957. b) Jackson, R. W.; Shea, K. J. *Tetrahedron Lett.* **1994**, *35*, 1317. c) Lu, Y. F.; Fallis, A. G. *Tetrahedron Lett.* **1993**, *34*, 3367. d) Sakan, K.; Smith, D. A.; Babirad, S.

A.; Fronczek, F. R.; Houk, K. N. *J. Org. Chem.* **1991**, *56*, 2311. e) Yadav, J. S.; Renduchintala, R. *Tetrahedron Lett.* **1991**, *32*, 2629. f) Brown, P. A.; Jenkins, P. R.; Fawcett, J.; Russel, D. R. *J. Chem. Soc. Chem. Commun.* **1984**, *4*, 253.

[15] a) Blechert, S.; Kleine-Klausing, A. *Angew. Chem. Int. Ed.* **1991**, *30*, 412. b) Winkler, J.; Lee, C.; Rubo, L.; Muller, C. L. *J. Org. Chem.* **1989**, *54*, 4491. c) Kojima, T.; Inouye, Y.; Kakisawa, H. *Chem. Lett.* **1985**, *3*, 323.

[16] a) Arseniyadis, S.; Rico Ferreira, M. R.; Quilez del Moral, J.; Martin Hernando, J. I.; Birlirakis, N.; Potier, P. *Tetrahedron: Asymmetry* **1999**, *10*, 193. b) Swindell, C. S.; Patel, B. P.; deSolms, S. J. Springer, J. P. *J. Org. Chem.* **1987**, *52*, 2346.

[17] a) Holton, R. A.; Somoza, C.; Kim H. B.; Liang, F.; Biediger, R. J.; Boatman, P. D.; Shindo, M.; Smith, C. C.; Kim, S.; Nadizadeh, H.; Suzuki, Y.; Tao C.; Vu, P.; Tang, S.; Zhang, P.; Murthi, K. K.; Gentile, L. N.; Liu, J. H. *J. Am. Chem. Soc.* **1994**, *116*, 1597. b) Holton, R. A.; Kim H. B.; Somoza, C.; Liang, F.; Biediger, R. J.; Boatman, P. D.; Shindo, M.; Smith, C. C.; Kim, S.; Nadizadeh, H.; Suzuki, Y.; Tao C.; Vu, P.; Tang, S.; Zhang, P.; Murthi, K. K.; Gentile, L. N.; Liu, J. H. *J. Am. Chem. Soc.* **1994**, *116*, 1599.

[18] a) Wender, P. A.; Badham, N. F.; Conway, S. P.; Floreancig, P. E.; Glass, T. E.; Gränicher, C.; Houze, J. B.; Jänichen, J.; Lee, D.; Marquess, D. G.; McGrane, P. L.; Meng, W.; Mucciaro, T. P.; Mühleback, M.; Natchus, M. G.; Paulsen, H.; Rawlings, D. B.; Satkofsky, J.; Shuker, A. J.; Sutton, J. C.; Taylor, R. E.; Tomooka, K. *J. Am. Chem. Soc.* **1997**, *119*, 2755. b) Wender, P. A.; Badham, N. F.; Conway, S. P.; Floreancig, P. E.; Glass, T. E.; Houze, J. B.; Krauss, N. E.; Lee, D.; Marquess, D. G.; McGrane, P. L.; Meng, W.; Natchus, M. G.; Shuker, A. J.; Sutton, J. C.; Taylor, R. E. *J. Am. Chem. Soc.* **1997**, *119*, 2757.

[19] Trost, B. M.; Fray, M. J. *Tetrahedron Lett.* **1984**, *41*, 4605.

[20] a) Blechert, S.; Müller, R.; Beitzel, M. *Tetrahedron* **1992**, *48*, 6953. b) Neh, H.; Kühling, A.; Blechert, S. *Helv. Chim. Acta* **1989**, *72*, 101.

[21] Ott, M. M.; Little, R. D. *J. Org. Chem.* **1997**, *62*, 1610.

[22] Kobayashi, J.; Ogiwara, A.; Hosoyama, H.; Shigemori, H.; Yoshida, N.; Sasaki, T.; Li, Y.; Iwasaki, S.; Naito, M.; Tsuruo, T. *Tetrahedron* **1994**, *50*, 7401.

[23] Gottesman, M. M.; Fojo, T.; Bates, S. E. *Nat. Rev. Cancer* **2002**, *2*, 48.

[24] a) Zhao, X.; Gu, J.; Yin, D.; Chen, X. *Bioorg. Med. Chem. Lett.* **2004**, *14*, 4767. b) Zhang, S.; Wang, J.; Hirose, K.; Ando, M. *J. Nat. Prod.* **2002**, *65*, 1786. c) Sako, M.; Suzuki, H.; Yamamoto, N.; Hirota, K. *Bioorg. Med. Chem. Lett.* **1999**, *9*, 3403.

[25] a) Banwell, M. G.; McLeod, M. D.; Riches, A. G. *Aust. J. Chem.* **2004**, *57*, 53. b) Banwell, M. G.; Darmos, P.; Hickless, D. C. R. *Aust. J. Chem.* **2004**, *57*, 41. c) Phillips, A. J.; Morris, J. C.; Abell, A. D. *Tetrahedron Lett.* **2000**, *41*, 2723. d) Winkler, J. D.; Bhattacharya, S. K.; Batey, R. A. *Tetrahedron Lett.* **1996**, *37*, 8069.

[26] Giese, S. *Intermolecular Nucleophilic Trapping of Nazarov-Derived Oxyallyl Intermediates and their Application Toward Total Synthesis of Taxinine*, Ph.D. Thesis, University of Utah, 2000.

[27] Mazzola, R. D., Jr. *Torquoselectivity in the Nazarov Cyclization of Facially Biased Dienones and their Application Toward Total Synthesis of Taxinine*, Ph.D. Thesis, University of Utah, 2001.

[28] Mazzola, R. D., Jr.; Giese, S.; Benson, C. L.; West, F. G. *J. Org. Chem.* **2004**, *69*, 220.

[29] Giese, S.; Mazzola, R. D., Jr.; Amann, C. M.; Arif, A. M.; West, F. G. *Angew. Chem. Int. Ed.* **2005**, *44*, 6546.

[30] Mazzola, R. D., Jr.; White, T. D.; Vollmer-Snarr, H. R.; West, F. G. *Org. Lett.* **2005**, *7*, 2799.

[31] a) Banwell, M. G.; McLeod, M. D.; Riches, A. G. *Aust. J. Chem.* **2004**, *57*, 53. b) Mukaiyama, T.; Shiina, I.; Iwadare, H.; Saitoh, M.; Nishimura, T.; Ohkawa, N.; Sakoh, H.; Nishimura, K.; Tani, Y.; Hasegawa, M.; Yamada, K.; Saitoh, K. *Chem. Eur. J.* **1999**, *5*, 121. c) Stork, G.; Manabe, K.; Liu, L. *J. Am. Chem. Soc.* **1998**, *120*, 1337. d) Wender, P. A.; Badham, N. F.; Conway, S. P.; Floreancig, P. E.; Glass, T. E.; Houze, J. B.; Krauss, N. E.; Lee, D.; Marquess, D. G.; McGrane, P. L.; Meng, W.; Natchus, M. G.; Shuker, A. J.; Sutton, J. C.; Taylor, R. E. *J. Am. Chem. Soc.* **1997**, *119*, 2757. e) Holton, R. A.; Somoza, C.; Kim, H.; Liang, F.; Biediger, R. J.; Boatman, P. D.; Shindo, M.; Smith, C. C.; Kim, S.; Nadizadeh, H.; Susuki, Y.; Tao, C.; Vu, P.; Tang, S.; Zhang, P.; Murthi, K. K.; Gentile, L. N.; Liu, J. H. *J. Am. Chem. Soc.* **1994**, *116*, 1597.

[32] Lipshutz, B. H.; Koerner, M.; Parker, D. A. *Tetrahedron Lett.* **1987**, *28*, 945.

[33] Ito, Y.; Saegusa, T. *J. Org. Chem.* **1978**, *43*, 1011.

[34] Nicolaou, K. C.; Zhong, Y. L.; Baran, P. S. *J. Am. Chem. Soc.* **2000**, *122*, 7596.

[35] Walker, D.; Hiebert, J. D. *Chem. Rev.* **1967**, *67*, 153.

[36] For a review of the vinylogous Mukaiyama aldol reaction see: Casiraghi, G.; Zanardi, F.; Appendino, G.; Rassu, G. *Chem. Rev.* **2000**, *100*, 1929.

[37] a) Das Sarma, K.; Zhang, J.; Curran, T. T. *J. Org. Chem.* **2007**, *72*, 3311. b) Saito, S.; Nagahara, T.; Shiozawa, M.; Nakadai, M.; Yamamoto, H. *J. Am. Chem. Soc.* **2003**, *125*,

6200. c) Bella, M.; Piancatelli, G.; Squarcia, A.; Trolli, C. *Tetrahedron Lett.* **2000**, *41*, 3699.

[38] a) Doyle, M. P.; McKervey, M. A.; Ye, T. *Modern Catalytic Methods for Organic Synthesis with Diazo Compounds: from Cyclopropanes to Ylides*; Wiley: New York, 1998. b) Ye, T.; McKervey, A. *Chem. Rev.* **1994**, *94*, 1091.

[39] Adams, J.; Poupart, M. -A.; Grenier, L.; Schaller, C.; Ouimet, N.; Frenette, R. *Tetrahedron Lett.* **1989**, *30*, 1749.

[40] Ballabio, M.; Malatesta, V.; Ruggieri, D.; Temperilli, A. *Gazz. Chim. Ital.* **1988**, *118*, 375.

[41] Taber, D. F.; Ruckle, R. E. *J. Am. Chem. Soc.* **1986**, *108*, 7686.

[42] Ray, C.; Saha, B.; Ghatak, U. R. *Tetrahedron* **1990**, *46*, 2857.

[43] Cane, D. E.; Pulikkottil, J. T. *J. Am. Chem. Soc.* **1984**, *106*, 5295.

[44] Stork, G.; Nakatani, K. *Tetrahedron Lett.* **1988**, *29*, 2283.

[45] Adams, J.; Poupart, M. -A.; Grenier, L.; Schaller, C.; Ouimet, N.; Frenette, R. *Tetrahedron Lett.* **1989**, *30*, 1749.

[46] Wang, P.; Adams, J. *J. Am. Chem. Soc.* **1994**, *116*, 3296.

[47] Nyangulu, J. M.; Nelson, K. M.; Rose, P. A.; Gai, Y.; Loewen, M.; Lougheed, B.; Quail, J. W.; Cutler, A. J.; Abrams, S. R. *Org. Biomol. Chem.* **2006**, *4,* 1400.

[48] Holmquist, C. R.; Roskamp, E. J. *J. Org. Chem.* **1989**, *54*, 3258.

[49] Yadav, J. S.; Subba-Reddy, B. V.; Eeshwaraiah, B.; Reddy, P. N. *Tetrahedron* **2005**, *61*, 875.

4. Studies Toward a Tandem Nazarov Cyclization/Diels-Alder Cycloaddition Reaction

4.1. Introduction

The Nazarov cyclization stands out as a simple and efficient means to access substituted cyclopentenones. Variants of this classic reaction have been reported where the cationic intermediate generated during the course of the cyclization is trapped by a nucleophile in an inter- or intramolecular fashion.[1] This "interrupted" Nazarov reaction is especially useful when the nucleophile employed is a 1,3-diene. These substrates have been shown to react with the oxyallyl cation via [4+3] cycloaddition (Scheme 4.1).[1f,2] In this sequence, linear precursor **1** undergoes cyclization to the allyl cation intermediate, which is then trapped by the pendent 1,3-diene to give tricyclic compounds **2** and **2′** as a 1.3:1 mixture of diastereomers. Overall, this process allows rapid access to complex polycyclic products starting from simple linear precursors. In this respect, tandem reactions are of great synthetic value in organic chemistry.

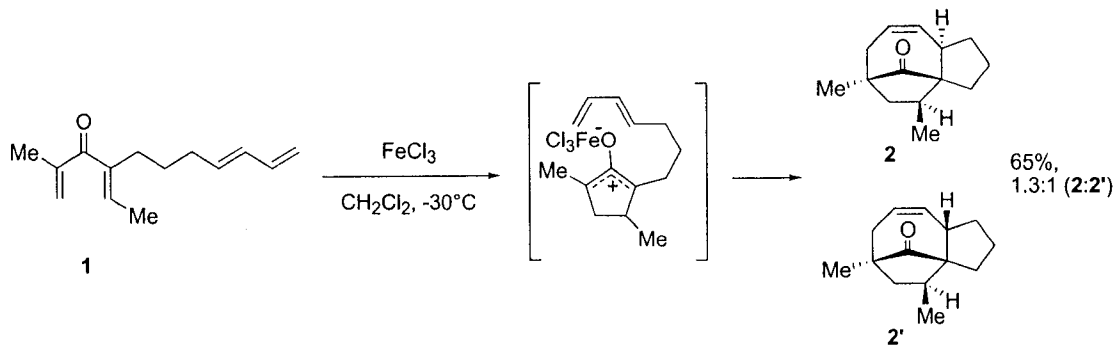

Scheme 4.1. Trapping of the Nazarov intermediate by [4+3] cycloaddition.

4.2. Background

In a subtle variation of the protocol discussed above (Scheme 4.1), a modified version of **1** was prepared where the pendent 1,3-diene side chain was tethered at the β-position of the divinyl ketone (**3**, Scheme 4.2).[3] It was hoped that this substrate would undergo a [4+2] cycloaddition with the oxyallyl cation generated on treatment with Lewis acid in a similar manner as above to give tricyclic product **4** (path a). However, when **3** was treated with anhydrous $FeCl_3$ or $BF_3{\cdot}OEt_2$, complex mixtures were formed and no evidence for the formation of **4** was obtained. It was surmised that the Nazarov cyclization was indeed occurring, but that subsequent approach of the diene moiety to the oxyallyl intermediate resulted in too much strain, preventing the formation of **4**.

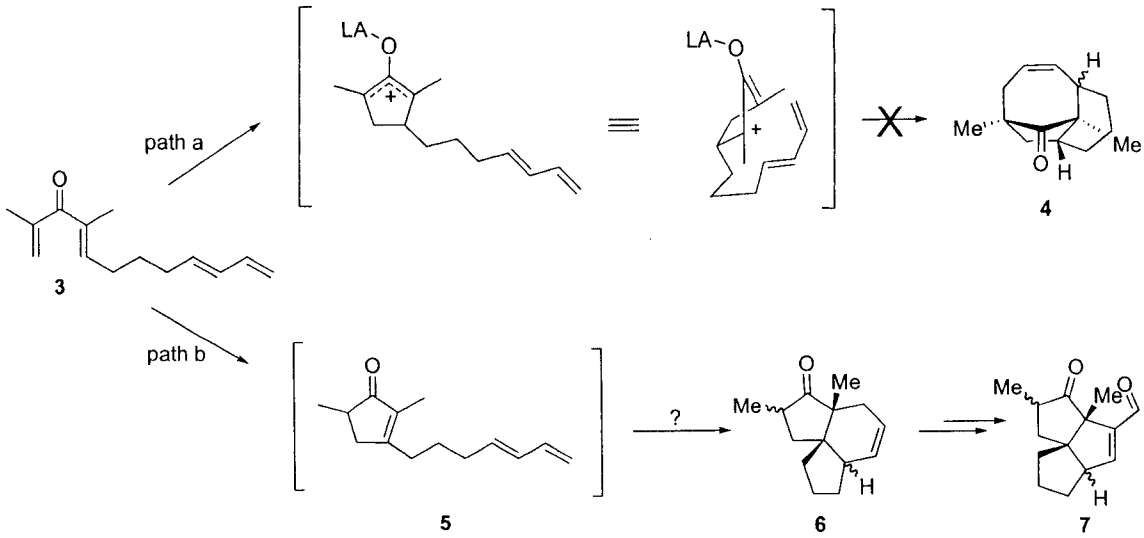

Scheme 4.2. Possible reaction pathways after Nazarov cyclization of tetraenone **3.**

On the other hand, we wondered if it would be possible for substrate **3** to undergo simple Nazarov cyclization, complete with the usual eliminative termination to **5**, then, under appropriate conditions, react with the tethered dienyl moiety in a [4+2] cycloaddition to give **6** (Scheme 4.2, path b). The Diels-Alder reaction is known to be accelerated by Lewis acid catalyst, which might prove useful for the development of a single set of reaction conditions to promote the tandem reaction.[4]

In a further potential application, we hoped to elaborate **6** via oxidative cleavage and subsequent aldol condensation to compound **7**, containing an angularly fused 5,5,5-ring system. This skeletal arrangement is present in numerous natural products, a few of which are depicted in Figure 4.1. Thus in the end, we hoped to utilize this tandem reaction to quickly build up structural complexity from a simple acyclic precursor to gain access to angularly fused triquinanes in only a few steps.

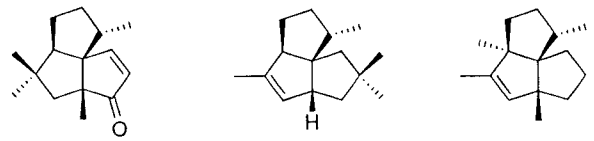

3-oxosilphinene pentalenene isocomene

Figure 4.1. Representative natural products containing angularly fused triquinane cores

4.3. Results and discussion

The requisite dienone **3** was prepared in a previously established nine step sequence with minor modifications along the way (Scheme 4.3).[3] 5-Tetrahydropyran-2-yloxy-pentanal **9** was formed directly by heating neat dihydropyran (**8**) at reflux with catalytic TsOH in the presence of 0.5 equivalents water. Elaboration of **9** to diene **12** was accomplished in moderate yield, but excellent selectivity by reaction with lithium diethyl allylphosphonate in the presence of HMPA[5] and subsequent THP deprotection using CSA. From here, **12** was oxidized to sensitive aldehyde **13** under Moffat-Swern conditions. Immediately after oxidation and without intermediate purification, **13** was reacted with phosphonate **14** to furnish α,β-unsaturated ester **15** in good yield with complete selectivity for the formation of the *E* isomer. DIBALH reduction of **15** provided an allylic alcohol, which was immediately oxidized to the corresponding aldehyde (**17**) using TPAP in the presence of NMO. In the next transformation, 1,2-addition of isopropenyl magnesium bromider took place readily to afford alcohol **18**. The remaining step of the sequence, oxidation of **18** to the corresponding divinyl ketone **3**, could be accomplished in good yield by reaction with buffered Dess-Martin periodinane.

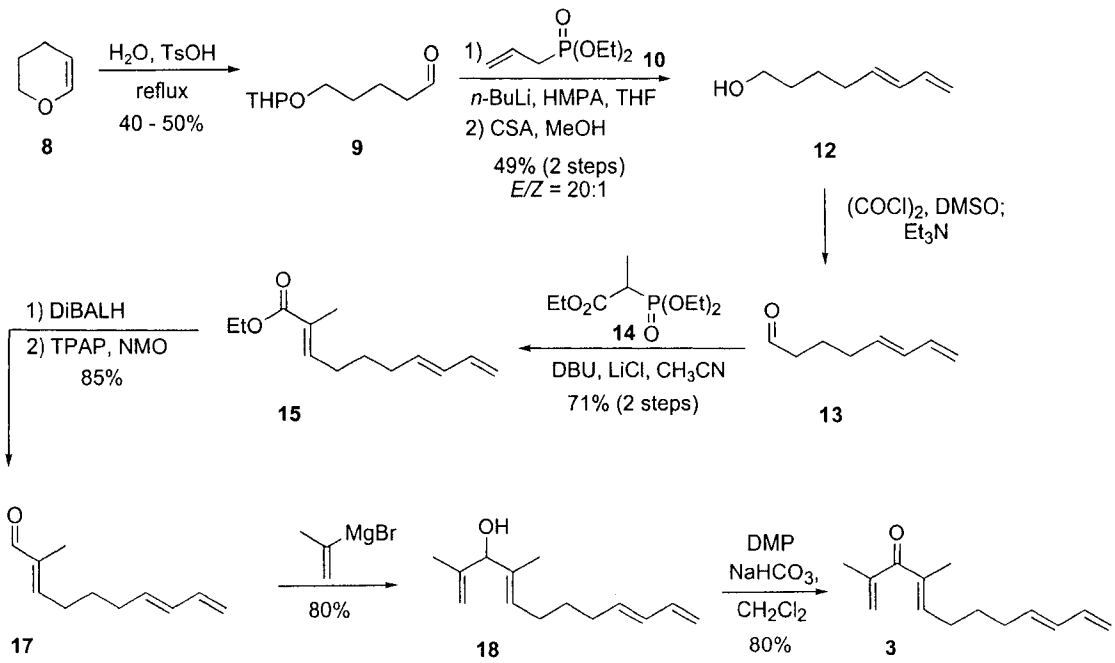

Scheme 4.3. Preparation of tetraenone **3.**

With the desired compound **3** in hand, we next investigated its conversion to cyclopentenone **5**, with the plan that the subsequent [4+2] cycloaddition to give tricyclic **6** would be addressed in a separate step. A search for compatible conditions to effect a one-pot transformation would follow. Preliminary studies had indicated that the Nazarov cyclization of **3** did not occur cleanly in the presence of $BF_3{\cdot}OEt_2$ and $FeCl_3$.[3] However, a separate study on similar substrates had shown that simple Nazarov products predominated on treatment with protic acid, whereas Lewis acids promoted an interrupted process.[6] For our initial purposes, the use of protic acid seemed to be the most promising strategy. Gratifyingly, treatment of a dilute room temperature solution of **3** in CH_2Cl_2 with two equivalents of $TsOH{\cdot}2H_2O$ cleanly led to the formation of cyclopentenones **5** and **5′**, regioisomeric at the newly formed C-C double bond (Scheme 4.4). None of the corresponding [4+3] or [4+2] adducts **4** or **6** were observed.

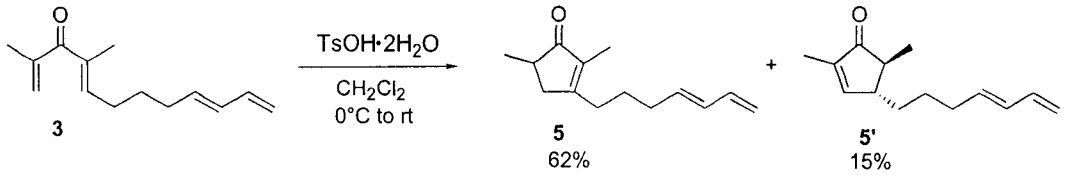

Scheme 4.4. Nazarov cyclization of **3.**

We were encouraged to find that it was possible to effect a clean Nazarov cyclization of **3** to cyclopentenone **5**, the desired thermodynamically more stable isomer. At this point, the next step was to find appropriate conditions to prompt intramolecular cycloaddition to **6**. Diels Alder cycloadditions promoted by Lewis acid catalysis have been shown to occur with greater ease and efficiency than the thermal process for some substrates. Under these conditions, much lower reaction temperatures are often employed, which provides an opportunity to observe increased stereoselectivity.[7] Substrate **5** was a suitable candidate for Lewis acid-promoted cyclization with a coordinating oxygen functionality present on the electron deficient dienophile. We felt that our eventual goal of a tandem Nazarov cyclization/[4+2] cycloaddition reaction would be best served by having both reactions occur with Lewis acidic activation, therefore, a systematic screening of various Lewis acidic conditions was undertaken.

The initial results of the screening were disappointing. When **5** was treated with a wide range of acids ($MeAlCl_2$, $AlCl_3$, $BF_3{\cdot}OEt_2$, $TiCl_4$, $SnCl_4$) at –78°C with gradual warming to room temperature, no reaction occurred at all; only starting material was returned. This observed lack of reactivity is consonant with Fukumoto's report of a similar intramolecular Diels Alder cycloaddition *en route* to 3-oxosilphinene.[8] He found that heating a solution of the Diels Alder substrate in *o*-dichlorobenzene in a sealed tube for 45 hours at 200°C led solely to the product of cyclization in the *exo* mode in moderate

yield, while Lewis acid catalysis did not promote the reaction at all. When these same thermal conditions were applied to our substrate, negligible yields of product were obtained even with heating for up to two weeks.

Spurred by a multitude of reports on the success of [4+2] cycloaddition under microwave irradiation conditions,[9,10] we next sought to apply this protocol to our reluctant substrate. Therefore, **5** was dissolved in *o*-dichlorobenzene and heated to 250°C in a Biotage microwave reactor for 30 minutes. Analysis of the reaction mixture by TLC at that point indicated that a new product was being formed, but significant amounts of starting material still remained. Eventually, it was found that heating for 4 hours in the reactor cleanly converted most of **5** to the product **6**. After purification, **6** was isolated in a yield of 85% as an inseparable mixture of isomers (Scheme 4.5).

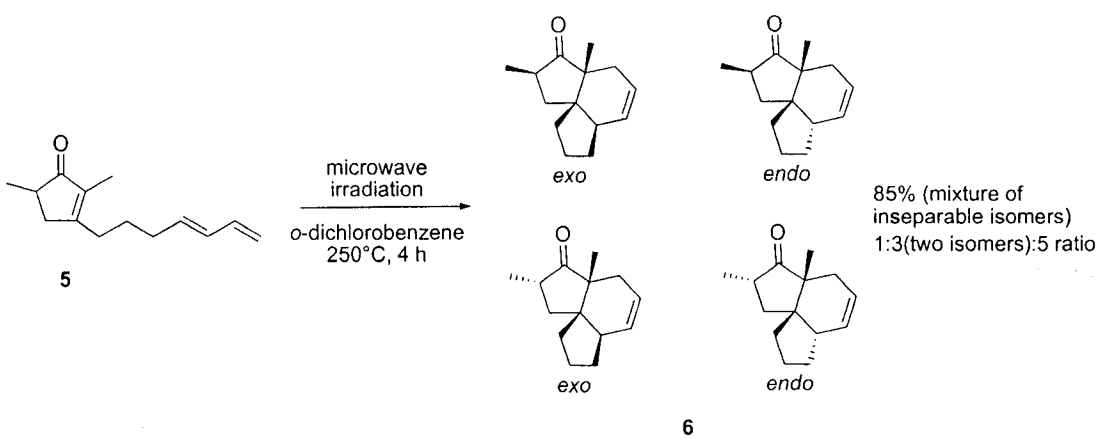

Scheme 4.5. Optimized microwave irradiated Diels Alder cycloaddition of **5.**

There is a potential for formation of four diastereomers during the cycloaddition: the products arising from *exo* and *endo* orientation of the diene and the respective methyl epimers of each. Analysis of the ^{1}H NMR spectrum (alkene region) of the product

formed under microwave irradiation showed that **6** was actually a mixture of four diastereomers in a ratio of 1: 3 (two isomers): 5. The ratios were determined by integration of the diastereomeric alkene protons, and one set contained overlapping peaks that could not be integrated individually. We had hoped the cyclization would occur with a preference for formation of the *exo* diastereomer, (the ratio of methyl epimers was inconsequential); however, the thermal cycloaddition conditions furnished significant quantities of both *exo* and *endo* diastereomers.

At this stage, we decided to revisit the Lewis acid protocol, this time using higher temperatures. Fortunately, this tactic provided promising results (Table 4.1). In entry 1, it was found that cycloadduct **6** could be obtained in 30% yield by refluxing **5** with $AlCl_3$ in CH_3CN. Better yields were obtained on heating at higher temperatures in toluene at reflux (entry 2). Use of other Lewis acids resulted in decomposition of the starting material (entry 3), or no reaction (entries 4,5). With further optimization of the conditions in entry 2 (1.0 eq $AlCl_3$, 0.005 M in toluene), **6** could be formed in 73% yield (Scheme 4.6).

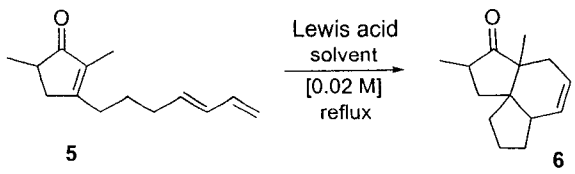

entry	Lewis acid	eq	solvent	yield 6 (%)
1	$AlCl_3$	0.6	CH_3CN	30
2	$AlCl_3$	0.6	toluene	55
3	$MeAlCl_2$	0.6	toluene	decomp
4	Et_2AlCl	0.6	toluene	N/R
5	Me_3Al	0.6	toluene	N/R

Table 4.1. Lewis acid screen for the Diels-Alder cycloaddition of 5 in refluxing solvent.

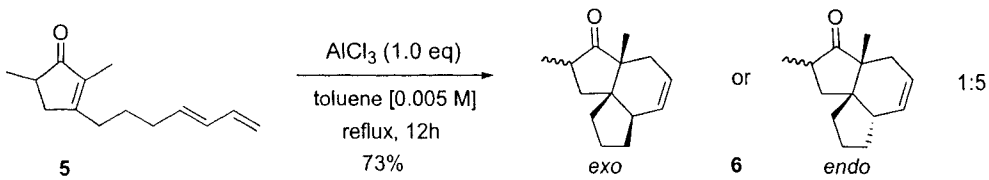

Scheme 4.6. Optimized Lewis acid promoted Diels-Alder cycloaddition of **5.**

We were gratified to find that the reaction provided **6** as a 1:5 mixture of only two diastereomers. These were identical to the major set of isomers formed in the thermal cycloaddition. Fluctuation of the relative ^1H NMR integral ratios for the isomeric alkene protons during the course of work-up and purification led us to believe that these isomers were α methyl epimers. Equilibration of the epimerizable α methyl substituent appeared to be taking place, and the 1:5 ratio reflects the thermodynamic preference of this system. Overlapping signals in the ^1H NMR spectrum precluded any assignment of the stereochemistry of the inseparable isomers, thus it was not clear if the mixture was comprised of *endo* or *exo* diastereomers.

A compelling argument in favor of either diastereomeric transition state could be presented. In the absence of intervening factors, the *endo* mode normally predominates in Diels-Alder reactions.[7] The reason for this is not fully understood,[11] but is most commonly attributed to favorable secondary orbital overlap of the diene with the dienophile.[12] This stabilizing interaction could however, be overwhelmed by non-bonded repulsive forces between the diene and the cyclopentenone, in which case *exo* selectivity would prevail. On the other hand, *exo* approach entails a new set of unfavorable steric interactions between the diene and the vinylic methyl group. Fukomoto's related *exo*-selective reaction demonstrated that these unfavorable interactions did not override the innate *endo* preference of the cycloaddition. Based on Fukumoto's result, we predicted favored *exo* selectivity in **6** (Figure 4.2).

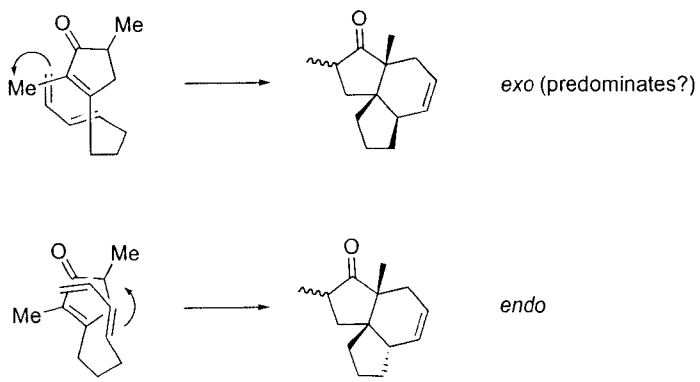

Figure 4.2. Transition states leading to *exo* and *endo* diastereomers.

To provide proof for the relative stereochemistry of **6**, we sought to remove the epimeric stereocenter via C- or O-methylation. This was done with the intent to converge the two inseparable diastereomers to one new product to facilitate characterization by NMR spectroscopy. In the event, tricyclic ketone **6** was treated with KHMDS in THF,

followed by MeI in HMPA. The reaction provided a mixture of what we presume to be O- and C- methylated **19** and **19′** in a combined yield of 88% with an approximate ratio of 2.5:1 (Scheme 4.7).

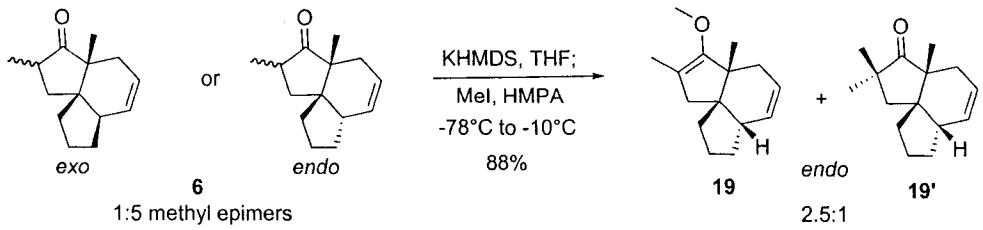

Scheme 4.7. Methylation of diastereomeric **6.**

It was possible to isolate some of the major O-Me isomer **19** in pure form by chromatography and subject it to full spectroscopic characterization for complete structural determination. The ^{1}H NMR spectrum clearly indicated the presence of the O-Me group as a 3H singlet at 3.78 ppm (Figure 4.3). The allylic methyl group resonated at 1.31 ppm, while the angular methyl came at 1.14 ppm. In the ^{13}C NMR spectrum, two alkene peaks were observed at 133 and 127 ppm and were attributed to the cyclohexene olefinic carbons. However, the unsaturated carbons of the enol ether resonated at unexpected chemical shifts of 218 and 87 ppm. This, coupled with the presence of a carbonyl stretch (1749 cm^{-1}) in the IR spectrum made us initially question our assignment of **19**. However, it was noted that the sample was contaminated with a small amount of **19′**, which might explain the presence of the carbonyl band in the IR. The peak in the ^{13}C NMR spectrum at 218 ppm could not be attributed to the impurity, as a second spectrum run on a ~1:1 mixture of **19** and **19′** showed an additional signal at 228 ppm to account for the carbonyl of **19′**.

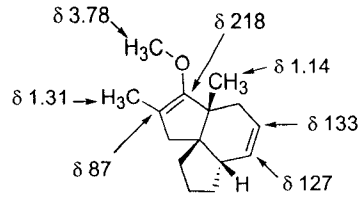

19

Figure 4.3. Selected ^{1}H and ^{13}C resonances in **19.**

Continuing on the assumption that **19** was indeed the structure originally proposed, we sought an explanation for the divergent ^{13}C resonances of the enol ether. Under normal circumstances, the ^{13}C resonances for a cyclopentenol ether would be expected to be well separated and to fall within the ranges of 160-150 ppm and 110-90 ppm.[13] The frequencies observed in **19** can perhaps be rationalized by considering the strain present in this particular five-membered ring because of the two trigonal centers. This may induce a larger contribution of the polar enol ether resonance form of **19** in order to relieve some of the strain by partially pyramidalizing one of the carbons (Figure 4.4). Further, the presence of an adjacent fully substituted carbon may enhance deshielding of the carbon bonded to the O-Me group.

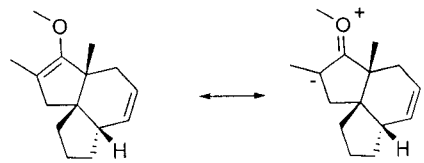

Figure 4.4. Resonance contribution to the structure of **19.**

Compound **19** was identified as the *endo* isomer based on a 2D TROESY experiment. nOe correlations in **19** could be traced from the angular methyl to the allylic

methine proton and one of the allylic methylene protons. A cross peak was also encountered between the two allylic protons. These observed through-space interactions are indicative of the *endo* isomer, in which the allylic methine is in close proximity to the bridgehead methyl. As a further proof of the structure of **19**, the O-Me group was also seen to correlate with both the allylic and bridgehead methyls.

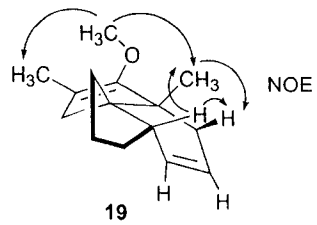

19

Figure 4.5. NOE interactions in **19.**

We had hoped the Diels-Alder cycloaddition of **5** would provide the *exo* product, as its oxidative cleavage and subsequent aldol condensation were expected to be straightforward. Because of the *trans*-fused hydrindane in *endo* **6**, we suspected that its eventual aldol condensation might be problematic (Scheme 4.8). Dialdehyde **20**, generated by oxidative cleavage of *endo* **6**, would be unlikely to cyclize to *cis,trans*-fused angular triquinane **7** because of the geometrical arrangement of the two reacting centers. On the other hand, under appropriate conditions, **20** might be able to equilibrate via epimerization to **21** (which could be obtained directly from oxidative cleavage of *exo* **6**). This should then readily cyclize to *cis,cis*-fused triquinane **7**. If this were possible, then the relative stereochemistry in **6** would not be of consequence since the *exo* and *endo* isomers would eventually converge to the same product.

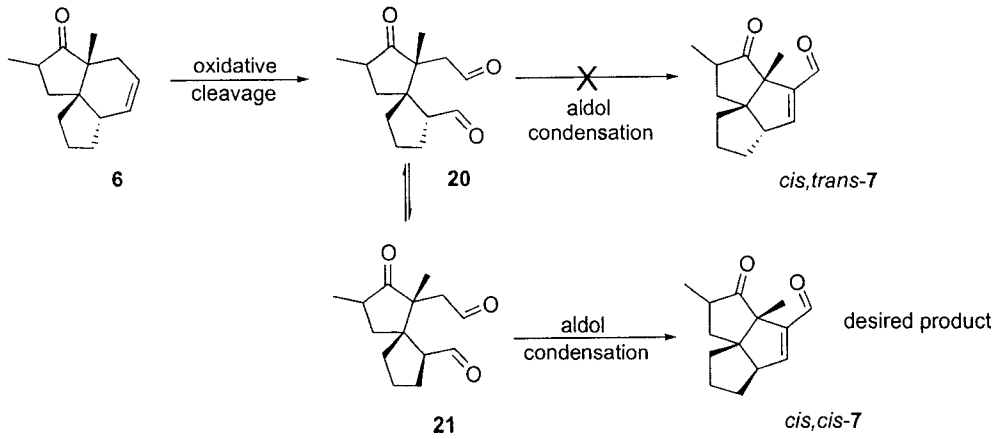

Scheme 4.8. Oxidative cleavage and aldol condensation of **6.**

The first step to test the plausibility of this approach was to find suitable conditions for the oxidative cleavage reaction. The optimization is shown in Table 4.2. Due to the sensitivity of dialdehyde **20**, the effectiveness of the oxidation conditions screened was evaluated based on analysis of the crude ^{1}H NMR spectrum rather than on isolated yields of the pure compound. In all cases the starting material was completely consumed. In entry 1, ozonolysis with reductive dimethylsulfide[14] work up was attempted on **6**, but led to severe decomposition. Cleavage with RuO_4, generated *in situ* by reaction of catalytic $RuCl_3$ and $NaIO_4$[15] indicated the expected dialdehyde peaks in the ^{1}H NMR (9.6 - 9.8 ppm), but the results were inconsistent from trial to trial and decomposition was frequently observed (entry 2). In entry 3, use of the Johnson-Lemieux[16] protocol provided the dialdehyde relatively cleanly; however, some peak broadening in the aliphatic region of the ^{1}H NMR spectra was observed. A two step OsO_4 catalyzed sequence (dihydroxylation and subsequent cleavage in separate step)[17] gave the product without any evidence of decomposition (entry 4). We came across another variant of this protocol, which reported the addition of 2,6-lutidine to minimize

side product formation.[18] Attempted on our substrate (entry 5), the reaction proceeded with clean conversion to the dialdehyde. We also tried substituting pyridine for 2,6-lutidine in the reaction, as it had been reported to cause epimerization in susceptible substrates, and we hoped that this would work to our advantage. Unfortunately, it only led to decomposition (entry 6). Therefore, the most satisfactory conditions were found to be either the two step dihydroxylation/diol cleavage (entry 4) or using 2,6-lutidine as an additive in a one step protocol (entry 5). Interestingly, only one set of dialdehyde peaks was observed in the crude ^{1}H NMR spectra for the products of conditions in entry 4 and entry 5. Therefore, only one isomer was taken on to the next step.

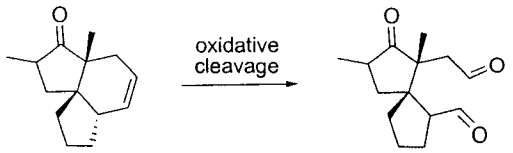

6 **20**

entry	method	result
1	O_3; Me_2S	decomposition
2	$RuCl_3/NaIO_4$	inconsistent
3	$OsO_4/NaIO_4$	prod. present
4	OsO_4/NMO; $NaIO_4$	prod. present
5	$OsO_4/NaIO_4$/2,6-lutidine	prod. present
6	$OsO_4/NaIO_4$/pyridine	decomposition

Table 4.2. Optimization of oxidative cleavage of **6.**

The next step to investigate was the aldol condensation of **20** (or **21**). The crude dialdehyde, generated from either of the two efficient oxidative cleavage protocols above, was exposed to a host of relevant conditions (Scheme 4.9). Unfortunately, though a wide range of procedures were attempted, all led to significant decomposition of the material.

Two notable exceptions were: use of piperidine in the presence of acetic acid as well as pyrrolidine in the presence of molecular sieves. In the crude ^{1}H NMR spectra some decomposition was evident; however, in both cases new aldehyde peaks were observed along with faint peaks in the 6-7 ppm region where the β proton of a cyclopentene carboxaldehyde would be expected to come. On purification of the pyrrolidine reaction (neutral alumina) very little material was isolated, suggesting sensitivity of the compound to the purification method. The only isolated material displayed some broadening of peaks in the aliphatic region of the ^{1}H NMR spectrum, suggestive of decomposition. Despite this, some promising peaks were observed (singlet at 9.62 ppm and broad singlet at 6.62 ppm), and this approach warrants further attention. At this point, lack of material and time constraints prevented further investigation of this reaction.

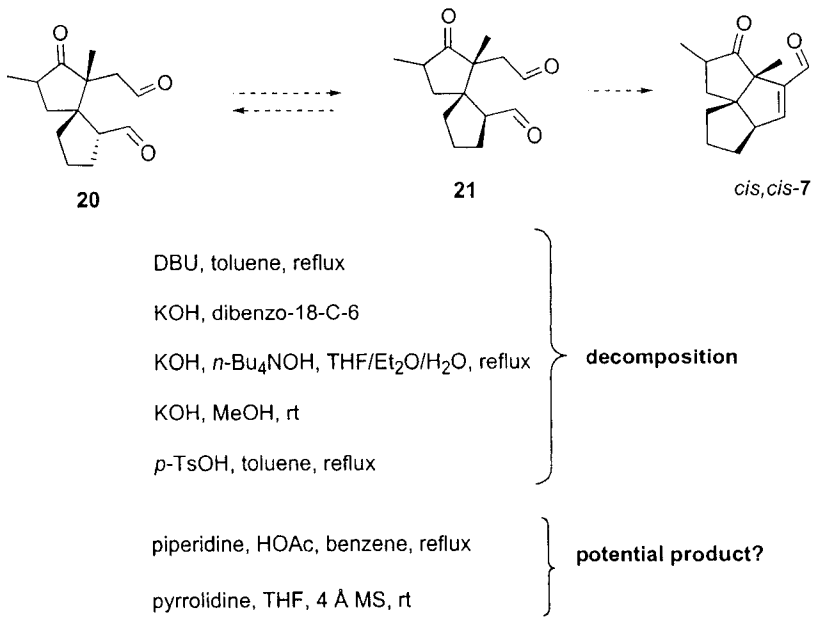

Scheme 4.9. Attempted aldol condensation of **20.**

4.4. Conclusions and Future work

The preliminary results of this project have shown that preparation of angular triquinanes may be feasible using a sequential Nazarov cyclization/Diels Alder cycloaddition protocol. The Nazarov cyclization has been shown to take place smoothly in the presence of protic acid, while the Diels-Alder cycloaddition could be effected thermally under microwave irradiation, or by Lewis acid catalysis. The former provides a mixture of all four potential diastereomers with the epimers of the *endo* cycloadduct being formed in a 1:5 ratio, and with a combined ratio of 3 for the presumed *exo* epimers. On the other hand, Lewis acid catalysis provided only one set of diastereomers (*endo* epimers) in a 1:5 ratio.

The stereochemistry with which the [4+2] cycloaddition proceeds may be inconsequential, provided epimerization is possible once the cyclohexene is cleaved under oxidative conditions. In that case, both the *exo* and *endo* diastereomers would converge to the same intermediate. It has been shown that the oxidative cleavage occurs with ease using OsO_4 and $NaIO_4$ in either a two step sequence or in one step with 2,6-lutidine as an additive. The subsequent aldol condensation has not yet been optimized, but promising results were obtained when the reaction was carried out in the presence of piperidine or pyrrolidine. The starting material and product are prone to decomposition, therefore mild reaction conditions and purification procedures must be explored.

Once the aldol condensation has been optimized, the Nazarov/Diels-Alder reaction should be revisited to examine the possibility of carrying out the sequence in tandem. This could be approached in a number of different ways. For example, the two reactions could be screened for compatible Lewis acidic activation conditions.

Alternatively, the Nazarov cyclization could be promoted by Lewis or Brønsted acid at room temperature, followed by microwave irradiation to induce subsequent [4+2] cycloaddition.

4.5. Experimental

4.5.1. General

Reactions were conducted in oven-dried (120°C) or flame-dried glassware under a positive argon atmosphere unless otherwise stated. Transfer of anhydrous solvents or mixtures was accomplished with oven dried syringes or cannulae. Solvents were distilled before use: CH_2Cl_2, CH_3CN, and HMPA from calcium hydride; toluene from sodium; and tetrahydrofuran (THF) from sodium benzophenone ketyl. Commercial reagents were used as received unless otherwise stated. Thin layer chromatography (TLC) was performed on glass plates precoated with 0.25 mm Kieselgel 60 F_{254} (Merck). Flash chromatography columns were packed with 230-400 mesh silica gel (Silicycle), or ~150 mesh, 58Å, activated neutral Brockmann I, standard grade alumina (Aldrich) as indicated. Microwave irradiation was conducted using a Biotage Initiator.

Proton nuclear magnetic resonance spectra (^{1}H NMR) were recorded at 500 MHz, and the chemical shifts are reported on the δ scale (ppm) upfield from deuterochloroform (δ = 7.27 ppm). Carbon nuclear magnetic resonance spectra (^{13}C NMR) were obtained at 125 MHz. Chemical shifts are reported (ppm) relative to the center line of the triplet for deuterochloroform (δ = 77.23 ppm). Infrared (IR) spectra were measured with a Mattson

Galaxy Series FT-IR 3000 spectrophotometer. Mass spectra were determined on a Kratos Analytical MS-50 (EI). Elemental analysis was obtained at the University of Alberta on a Carlo Erba CHNS-O EA 1108 Elemental Analyzer.

4.5.2. Substrate syntheses and characterization

Intermediates in the preparation of compound **3** have been previously synthesized and partially characterized.[3] The previous procedures were followed, and spectral data were consistent with those reported. Any data required for complete characterization of the intermediates that was missing in the original source is reported here.

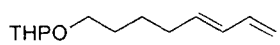

11

2-((*E*)-Octa-5,7-dienyloxy)-tetrahydro-2*H*-pyran (**11**): HRMS for $C_{13}H_{22}O_2$ (M^+) calcd 210.1621, found 210.1620 (M^+).

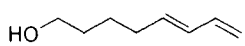

12

(*E*)-Octa-5,7-dien-1-ol (**12**): IR (neat) 3331, 3086, 3037, 3008, 2935, 1653, 1603 cm^{-1}; HRMS for $C_8H_{14}O$ (M^+) calcd 126.1045, found 126.1043 (M^+).

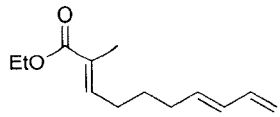

15

(2*E*,7*E*)-Ethyl 2-methyl deca-2,7,9-trienoate (**15**): IR (neat) 3086, 2981, 2932, 2864, 1710, 1650, 1603 cm^{-1}; HRMS for $C_{13}H_{20}O_2$ (M^+) calcd 208.1464, found 208.1461 (M^+).

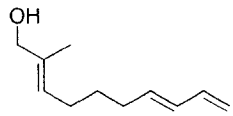

16

(2*E*,7*E*)-2-methyl deca-2,7,9-triene-1-ol (**16**): IR (neat) 3342, 3086, 2926, 2857, 1652, 1603 cm^{-1}; HRMS for $C_{11}H_{18}O$ (M^+) calcd 166.1358, found 166.1352 (M^+).

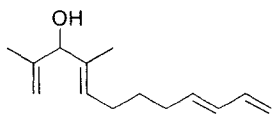

18

(4*E*,9*E*)-2,4-dimethyldodeca-1,4,9,11-tetraen-3-ol (**18**): IR (neat) 3386, 3086, 2972, 2924, 2857, 1652, 1603 cm^{-1}; HRMS for $C_{14}H_{22}O$ (M^+) calcd 206.1672, found 206.1656 (M^+); Anal. calcd for $C_{14}H_{22}O$: C, 81.49; H, 10.75. Found: C, 81.01; H, 10.75.

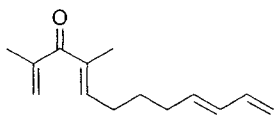

3

(4*E*,9*E*)-2,4-dimethyldodeca-1,4,9,11-tetraen-3-one (**3**): IR (neat) 2927, 2872, 1703, 1454 cm^{-1}; HRMS for $C_{14}H_{20}O$ (M^+) calcd 204.1515, found 204.1513 (M^+);

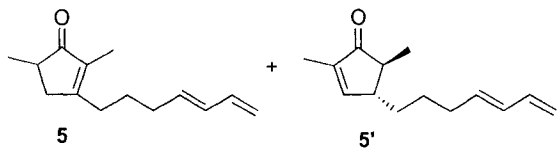

5 5'

Cyclopentenones **5** and **5′**: To a 0°C solution of **3** (242 mg, 1.20 mmol) in CH_2Cl_2 (120 mL) was added $TsOH{\cdot}H_2O$ (450 mg, 2.40 mmol). The mixture was stirred for 30 min, then warmed to rt and stirred for 2 h. The reaction was quenched by the addition of H_2O (10 mL), and the aqueous layer extracted with CH_2Cl_2 (3 x 10 mL). The combined organic extracts were dried ($MgSO_4$), filtered, and concentrated under reduced pressure. Purification by column chromatography (silica, 10:1 hexanes/EtOAc) gave recovered **3** (36 mg, 15%), enone **5** (151mg, 62%) and enone **5′** (36mg, 15%):

Enone **5**: clear colorless oil; R_f 0.33 (5:1 hexanes/EtOAc); IR (neat) 2928, 2869, 1699, 1646, 1457 cm^{-1}; ^1H NMR (500 MHz, $CDCl_3$) δ 6.34 (ddd, J = 16.6, 10.3, 10.3 Hz, 1H), 6.06 (dd, J = 14.5, 10.3 Hz, 1H), 5.69 (dt, J = 14.5, 7.0 Hz, 1H), 5.12 (d, J = 16.9 Hz, 1H), 4.99 (d, J = 10.2 Hz, 1H), 2.78-2.71 (m, 1H), 2.41 (t, J = 7.6 Hz, 2H), 2.36 (dqd, J = 7.4, 7.4, 2.4 Hz, 1H), 2.13 (dt, J = 7.4, 7.4 Hz, 2H), 2.10-2.06 (m, 1H), 1.68 (s, 3H), 1.68-1.60 (m, 2H), 1.16 (d, J = 7.5 Hz, 3H); ^{13}C NMR (500 MHz, $CDCl_3$) δ 212.5, 171.2, 136.9, 135.1, 133.8, 131.9, 115.4, 39.4, 38.3, 32.3, 30.5, 26.7, 16.7, 8.2; HRMS for $C_{14}H_{20}O$ (M^+) calcd 204.1515, found 204.1511 (M^+).

Enone **5′**: clear colorless oil; R_f 0.47 (5:1 hexanes/EtOAc); IR (neat) 3085, 2963, 2927, 1705, 1639, 1603, 1455 cm^{-1}; ^1H NMR (500 MHz, $CDCl_3$) δ 7.16 (s, 1H), 6.30 (ddd, J = 17.0, 10.3, 10.3 Hz, 1H), 6.06 (dd, J = 14.7, 10.4 Hz, 1H), 5.69 (dt, J = 14.7, 7.0, Hz, 1H), 5.10 (d, J = 17.0 Hz, 1H), 4.98 (d, J = 10.3 Hz, 1H), 2.34-2.29 (m, 1H), 2.14 (dt, J =

7.1, 7.1 Hz, 2H), 1.95 (qd, J = 7.5, 2.4 Hz, 1H), 1.76 (dd, J = 1.5, 1.5 Hz, 3H), 1.58-1.41 (m, 4H), 1.18 (d, J = 7.5 Hz, 3H); ^{13}C NMR (500 MHz, $CDCl_3$) δ 212.0, 159.9, 140.1, 137.1, 134.5, 131.5, 115.1, 47.8, 46.9, 34.0, 32.6, 27.3, 15.7, 10.2; HRMS for $C_{14}H_{20}O$ (M^+) calcd 204.1515, found 204.1509 (M^+).

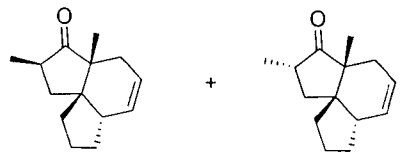

6

Lewis acid promoted formation of cyclohexene **6**: To a solution of **5** (20 mg, 0.10 mmol) in toluene (20 mL) was added $AlCl_3$ (13 mg, 0.10 mmol). The mixture was heated to reflux for 12 h, then quenched by the addition of H_2O (5 mL), and the aqueous layer extracted with Et_2O (3 x 5 mL). The combined organic fractions were dried over $MgSO_4$, filtered, then concentrated under reduced pressure. The crude reside was purified by column chromatography (silica treated with 1% Et_3N, 20:1 hexanes/EtOAc) to give a 1:5 ratio of inseparable *endo* epimers of **6** (14.6 mg, 73% yield) as a clear colorless oil:

Major *endo* diastereomer (impure): R_f 0.65 (2:1 hexanes/EtOAc); IR (CH_2Cl_2 film) 3017, 2958, 2929, 2872, 1737, 1454 cm^{-1}; ^1H NMR (500 MHz, $CDCl_3$) δ 5.83 (dddd, J = 10.0, 4.0, 1.9, 1.9 Hz, 1H), 5.63 (dddd, J = 10.5, 4.3, 3.2, 3.2 Hz, 1H), 2.28 (ddq, J = 12.0, 8.6, 7.0 Hz, 1H), 2.14-1.88 (m, 2H), 1.98-1.88 (m, 1H), 1.84-1.74 (m, 3H), 1.70 (dd, J = 12.4, 8.6 Hz, 1H), 1.46-1.30 (m, 4H), 1.17 (d, J = 7.0 Hz, 3H), 1.01 (s, 3H); HRMS for $C_{14}H_{20}O$ (M^+) calcd 204.1515, found 204.1514 (M^+).

Minor *endo* diastereomer (impure): R_f 0.65 (2:1 hexanes/EtOAc); ^{1}H NMR (500 MHz, $CDCl_3$, selected peaks) δ 5.91-5.86 (m, 1H), 5.70 (dddd, J = 10.6, 4.3, 3.1, 3.1 Hz, 1H), 2.53 (ddq, J = 14.7, 4.3, 7.0 Hz, 1H), 1.13 (d, J = 8.2 Hz, 3H), 1.02 (s, 3H).

Formation of **6** under microwave irradiation: Compound **5** (20 mg, 0.10 mmol) was dissolved in *o*-dichlorobenzene (1 mL) in a 2 mL process vial equipped with a stir bar. The system was then flushed with Ar for 5 min before capping the vial and placing it in the microwave reactor. The reaction temperature was set to 250°C, the absorption level to normal, and the time was set to 4 h. At reaction completion, the vial was allowed to cool to room temperature, the solvent removed under reduced pressure with heating, and the crude reaction purified by column chromatography as above. The product was isolated as a clear colorless oil comprised of an inseparable mixture of four diastereomers. The ^{1}H NMR spectrum showed a new set of isomeric alkene peaks (presumed *exo* epimers, overlapping signals) in addition to those from the Lewis acid catalyzed reaction above. The ratio of the *endo* epimers to the combined *exo* epimers was found to be 1:5:3.

Presumed *exo* isomers: R_f 0.65 (2:1 hexanes/EtOAc); ^{1}H NMR (500 MHz, $CDCl_3$, overlapping chemical shifts in the alkene region of the two new isomers) δ 5.82-5.40 (m), 5.52-5.47 (m).

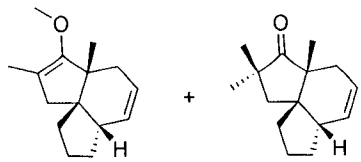

19 19'

Tricycles **19** and **19′**: To a –78°C solution of KHMDS (50 mg, 0.24 mmol), in THF (0.75 mL) was added a solution of **6** (12.5 mg, 0.61 mmol) in THF (0.75 mL) via cannula. After stirring for 1 h, a solution of MeI (30 μL, 0.49 mmol) in HMPA (0.25 mL) was added. The mixture was slowly warmed to –10°C over 2h, quenched with H_2O (1 mL) and extracted with Et_2O (3 x 2 mL). The combined organic extracts were dried ($MgSO_4$), filtered and concentrated. Purification by column chromatography (silica treated with 1% Et_3N, 30:1 hexanes/EtOAc) gave **19** (4 mg) and a 1.2:1 mixture of **19** and **19′** (7 mg) (88% total, 1:2.5 ratio):

Compound **19**: Clear colorless oil; R_f 0.50 (10:1 hexanes/EtOAc); IR (neat) 3030, 2959, 2875, 1749 (impurity), 1454 cm^{-1}; ^1H NMR (500 MHz, $CDCl_3$) δ 5.90 (ddd, J = 9.3, 2.9, 2.9 Hz, 1H), 5.74 (ddd, J = 9.3, 6.1, 3.1 Hz, 1H), 3.78 (s, 3H), 2.37 (ddd, J = 16.7, 6.1, 1.0 Hz, 1H), 2.12-2.04 (m, 1H), 1.90-1.87 (m, 2H), 1.86-1.72 (m, 4H), 1.56-1.48 (m, 2H), 1.46-1.34 (m, 1H), 1.31 (s, 3H), 1.14 (s, 3H) ^{13}C NMR (500 MHz, $CDCl_3$) δ 218.4, 132.7, 127.3, 86.8, 63.1, 52.0, 50.8, 44.6, 39.5, 37.1, 32.6, 25.3, 21.0, 20.6, 19.0; HRMS for $C_{15}H_{22}O$ ($M+1^+$) calcd 219.1750, found 219.1746 ($M+1^+$).

Compound **19′**: R_f 0.55 (10:1 hexanes/EtOAc); ^1H NMR (500 MHz, $CDCl_3$, selected peaks) δ 2.30 (ddd, J = 17.5, 6.1, 1.5 Hz, 1H), 1.55 (s, 3H), 1.07 (s, 3H), 1.06 (s, 3H).

4.6. References

[1] For some recent examples see: a) Rostami, A.; Wang, Y.; Arif, A. M.; McDonald, R.; West, F. G. *Org. Lett.* **2007**, *9*, 703. b) Janka, M.; He, W.; Haedicke, I. E.; Fronczek, F. R.; Frontier, A. J.; Eisenberg, R. *J. Am. Chem. Soc.* **2006**, *128*, 5312. c) Grant, T. N.; West, F. G. *J. Am. Chem. Soc.* **2006**, *128*, 9348. d) Dhoro, F.; Tius, M. A. *J. Am. Chem. Soc.* **2005**, *127*, 12472. e) White, T. D.; West, F. G. *Tetrahedron Lett.* **2005**, *46*, 5629. f) Wang, Y.; Schill, B. D.; Arif, A. M.; West, F. G. *Org. Lett.* **2003**, *5*, 2747. g) Browder, C. C.; Marmsäter, F. P.; West, F. G. *Org. Lett.* **2001**, *3*, 3033. h) Giese, S.; West, F. G. *Tetrahedron* **2000**, *56*, 10221.

[2] a) Yungai, A.; West, F. G. *Tetrahedron Lett.* **2004**, *45*, 5445. b) Wang, Y.; Arif, A. M.; West, F. G. *J. Am. Chem. Soc.* **1999**, *121*, 876.

[3] Wang, Y. *A Novel (4+3) Cycloaddition of the Nazarov Oxyallyl Intermediate.* Ph.D. Thesis, University of Utah, 1999.

[4] Roush, W. R. In *Comprehensive Organic Synthesis*; Trost, B. M., Fleming, I., Eds.; Pergamon: Oxford, 1991; Vol. 5, 513.

[5] Wang, Y.; West, F. G. *Synthesis* **2002**, 99.

[6] Bender J. A. *[4+4]-Photocycloadditions of 2-Pyrones with Tethered Furans and Lewis Acid Initiated Cycloisomerizations*. Ph.D. Thesis, University of Utah, 1997.

[7] Oppolzer, W. In *Comprehensive Organic Synthesis*; Trost, B. M., Fleming, I., Eds.; Pergamon: Oxford, 1991; Vol. 5, 315.

[8] Ihara, M.; Kawaguchi, A.; Ueda, H.; Chihiro, M.; Fukumoto, K.; Kametani, T. *J. Chem. Soc. Perkin Trans. 1* **1987**, 1331.

[9] For a review on microwave irradiation in organic chemistry see: Lidström, P.; Tierney, J.; Wathey, B.; Westman, J. *Tetrahedron* **2001**, *57*, 9225.

[10] For selected examples see: a) Wu, J.; Sun, L.; Dai, W. M. *Tetrahedron* **2006**, *62*, 8360. b) Sarotti, A. M.; Joullié, M. M.; Spanevello, R. A.; Suárez, A. G. *Org. Lett.* **2006**, *8*, 5561. c) Cook, S. P.; Polara, A.; Danishefsky, S. J. *J. Am. Chem. Soc.* **2006**, *128*, 16440.

[11] Imade, M.; Hirao, H.; Omoto, K.; Fujimoto, H. *J. Org. Chem.* **1999**, *64*, 6697.

[12] Hoffmann, R.; Woodward, R. B. *J. Am. Chem. Soc.* **1965**, *87*, 4388.

[13] Paquette, L. A.; Borrelly, S. *J. Org. Chem.* **1995**, *60*, 6912.

[14] Sternbach, D. D.; Hughes, J. W.; Burdi, D. F.; Banks, B. A. *J. Am. Chem. Soc.* **1985**, *107*, 2149.

[15] Yang, D.; Zhang, C. *J. Org. Chem.* **2001**, *66*, 4814.

[16] Pappo, R.; Allen, D. S., Jr.; Lemieux, R. U.; Johnson, W. S. *J. Org. Chem.* **1956**, *21*, 478.

[17] For selected examples of the two step OsO_4 procedure for oxidative olefin cleavage see: a) Francavilla, C.; Chen, W.; Kinder, F. R. Jr. *Org Lett.* **2003**, *5*, 1233. b) Taylor, R. E.; Chen, Y.; Beatty, A. *J. Am. Chem. Soc.* **2003**, *125*, 26.

[18] Yu, W.; Mei, Y.; Kang, Y.; Hua, Z.; Jin, Z. *Org Lett.* **2004**, *6*, 3217.

5. Conclusion

We have presented here three studies involving electrocyclization reactions and their application to the formation of complex cyclic structures. Chapter two reported the development of a highly diastereoselective 6π electrocyclization of 1,3,5-hexatrienes encased in bridged bicyclic skeletons. The required hexatrienes were prepared via Zn-mediated *cis*-reduction of dienyne precursors, which were themselves available through Pd-catalyzed cross coupling of the corresponding bicyclic vinyl triflates and substituted enynes. In most cases, the electrocyclization reactions took place readily following reduction of the dienyne substrates and provided moderate to excellent yields of the cyclohexadienes with complete *exo* diastereoselectivity. Thus, a method has been developed to access unique tricyclic structures with excellent stereoselectivity. Further, the study highlights differences in torquoselectivity observed in the cationic 4π and 6π electrocyclizations of substrates tethered through similar bicyclic manifolds.

Our continued efforts toward the total synthesis of the complex natural product taxinine were then outlined in Chapter three. The key steps of the synthesis include an *endo*-selective Nazarov cyclization of a dienone encased in a bicyclo[3.2.1]octene

skeleton, followed by an oxidative fragmentation to reveal the central eight-membered taxane ring. Previous studies in the group had ascertained the potential of this methodology to access highly advanced taxoid intermediates containing the bicyclic A/B ring system or the complete tricyclic core. However, these routes did not provide the ultimate product because of difficulties experienced with reactivity of key intermediates. In particular, annulation of the six-membered C-ring from a highly functionalized bicyclic A/B ring system remained a challenge. In this study, we attempted to facilitate C-ring closure through the installation of a functional group handle prior to revelation of the key eight-membered ring to which the C-ring was to be appended. Unfortunately, this approach ultimately compromised the reactivity of the subsequent intermediates needed to access the oxidative fragmentation precursor. In a second study aimed at C-ring closure via intramolecular C-H insertion of a metal- carbenoid species, we gained some insight into reactivity and conformational preferences of the advanced taxane A/B ring system. The key ring-closure reaction was however not attempted due to material shortage. At this stage, the C-ring closure strategy still appears to be promising. Future endeavors should focus on modification of the advanced bicyclic ring system so as to induce a favorable conformational change in the eight-membered ring allowing access to the required ring closure precursors.

In Chapter four we describe our work on the development of a tandem Nazarov cyclization/Diels-Alder cycloaddition reaction to build complex tricyclic products in only one step. Thus far, we have found the desired product to be readily accessible in a two step sequence. The potential for the sequence to be carried out in one pot has not yet been investigated. We instead focused on elaboration of the Nazarov/Diels-Alder

product to an angular triquinane via oxidative cleavage and aldol condensation. Preliminary investigations have shown this sequence to be a potential entry into these types of structures, and further investigation is warranted.

Electrocyclization reactions constitute a valuable class of carbon-carbon bond forming reactions. Our investigations, ranging from important methodological studies to applications in total synthesis, have shown these reactions to be an excellent way to provide complex cyclic products from simple starting materials with excellent selectivity.

Appendices

Appendix A: Selected NMR Spectra (Chapter 2)

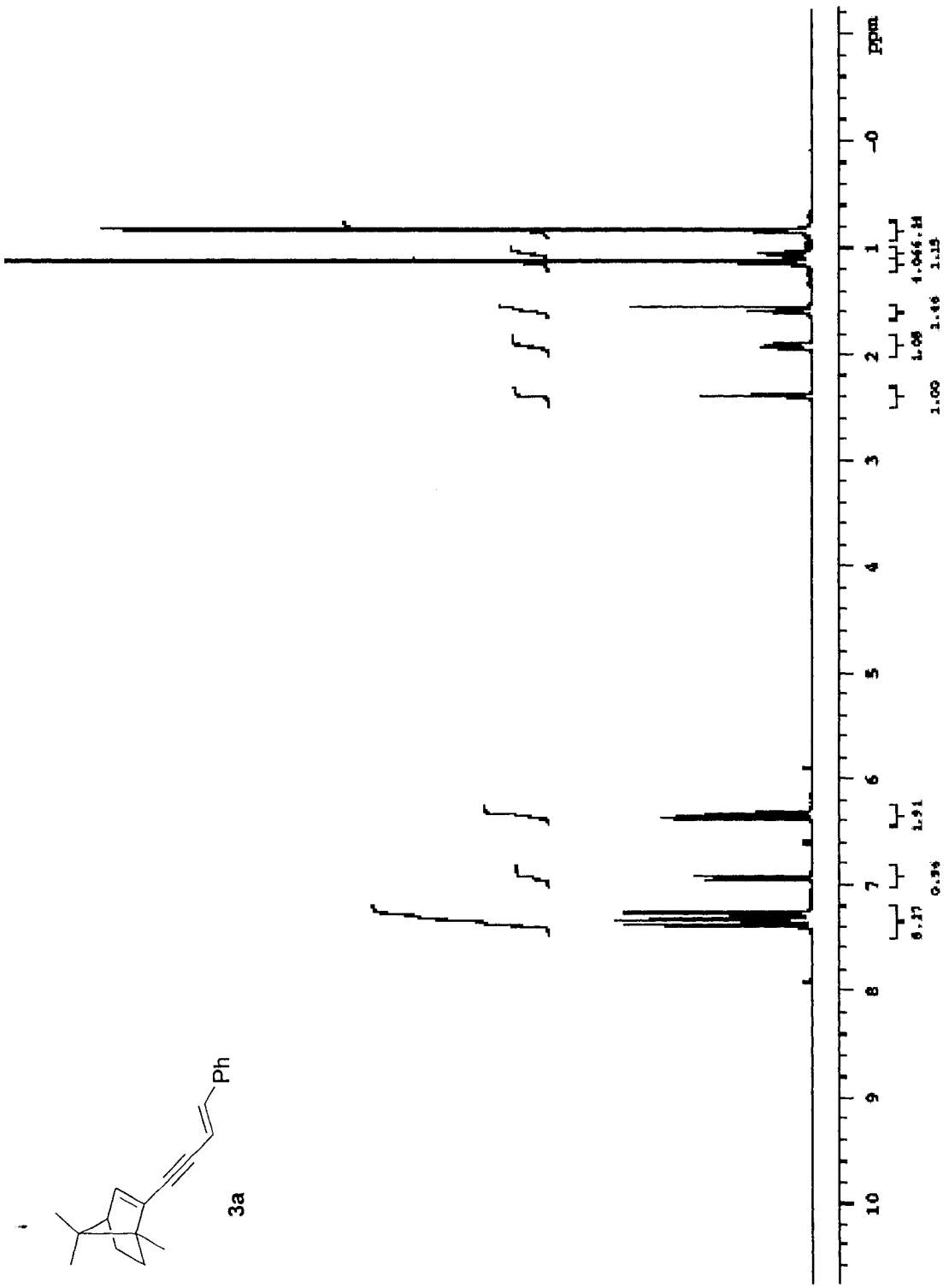

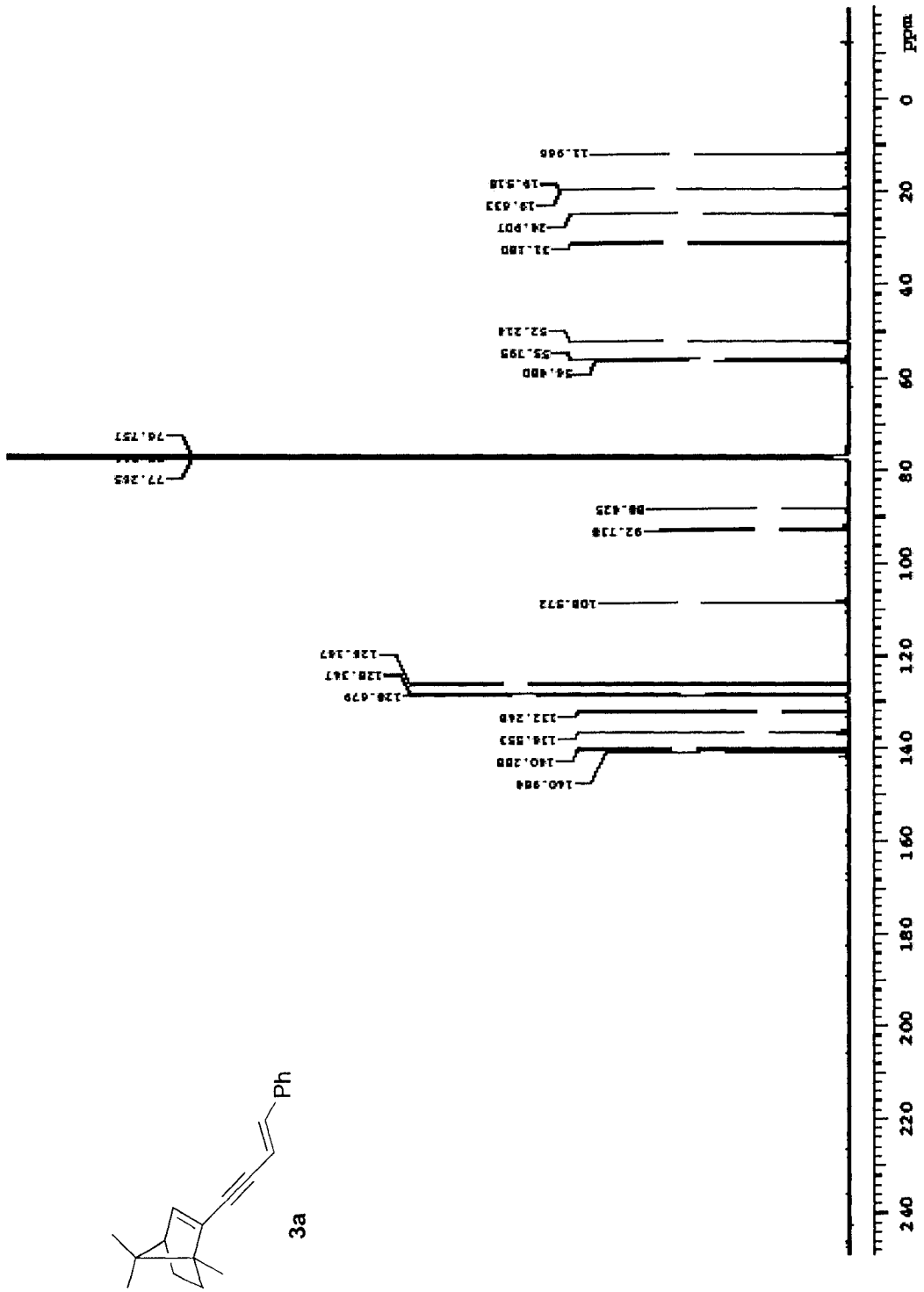

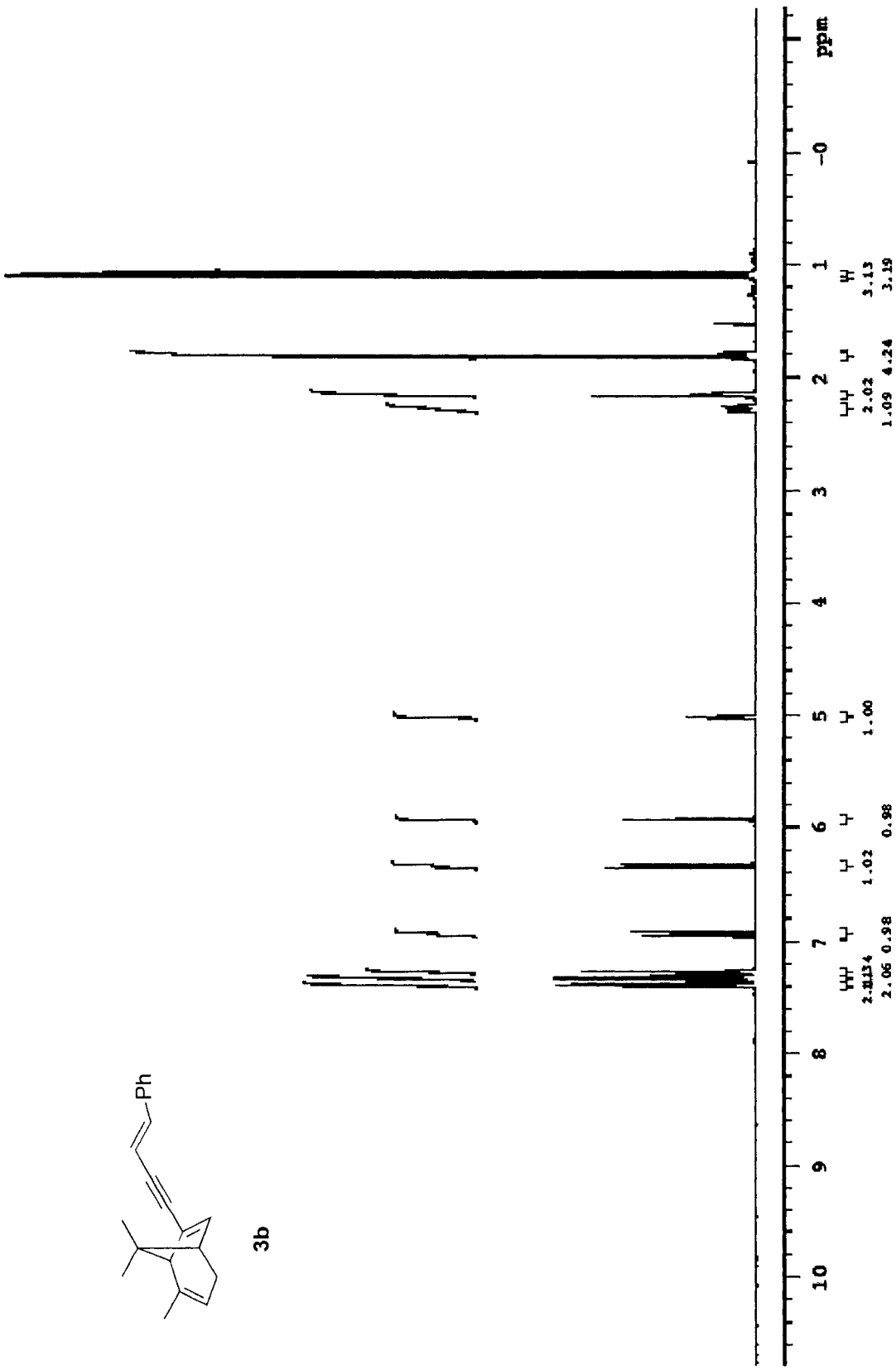

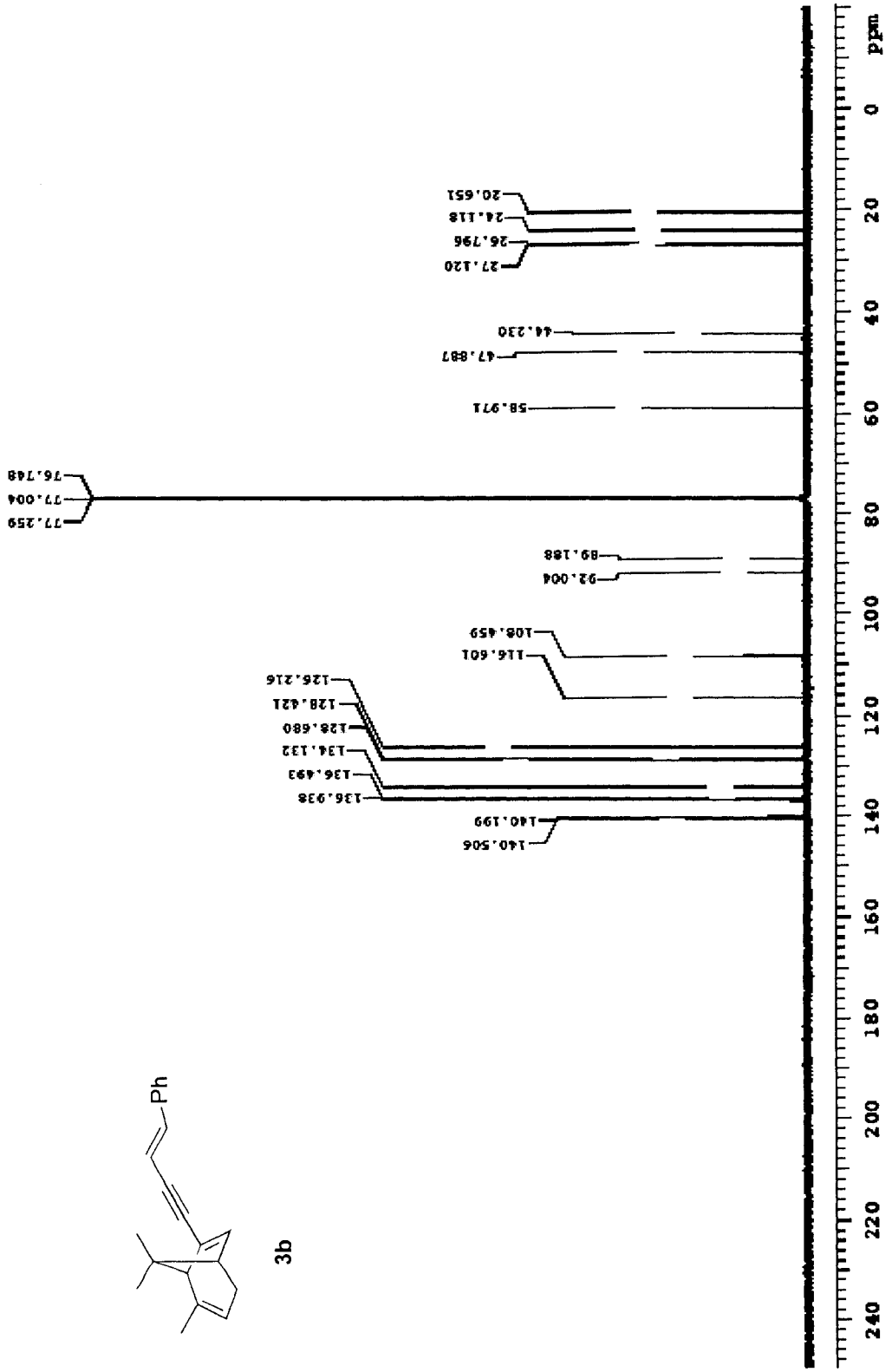

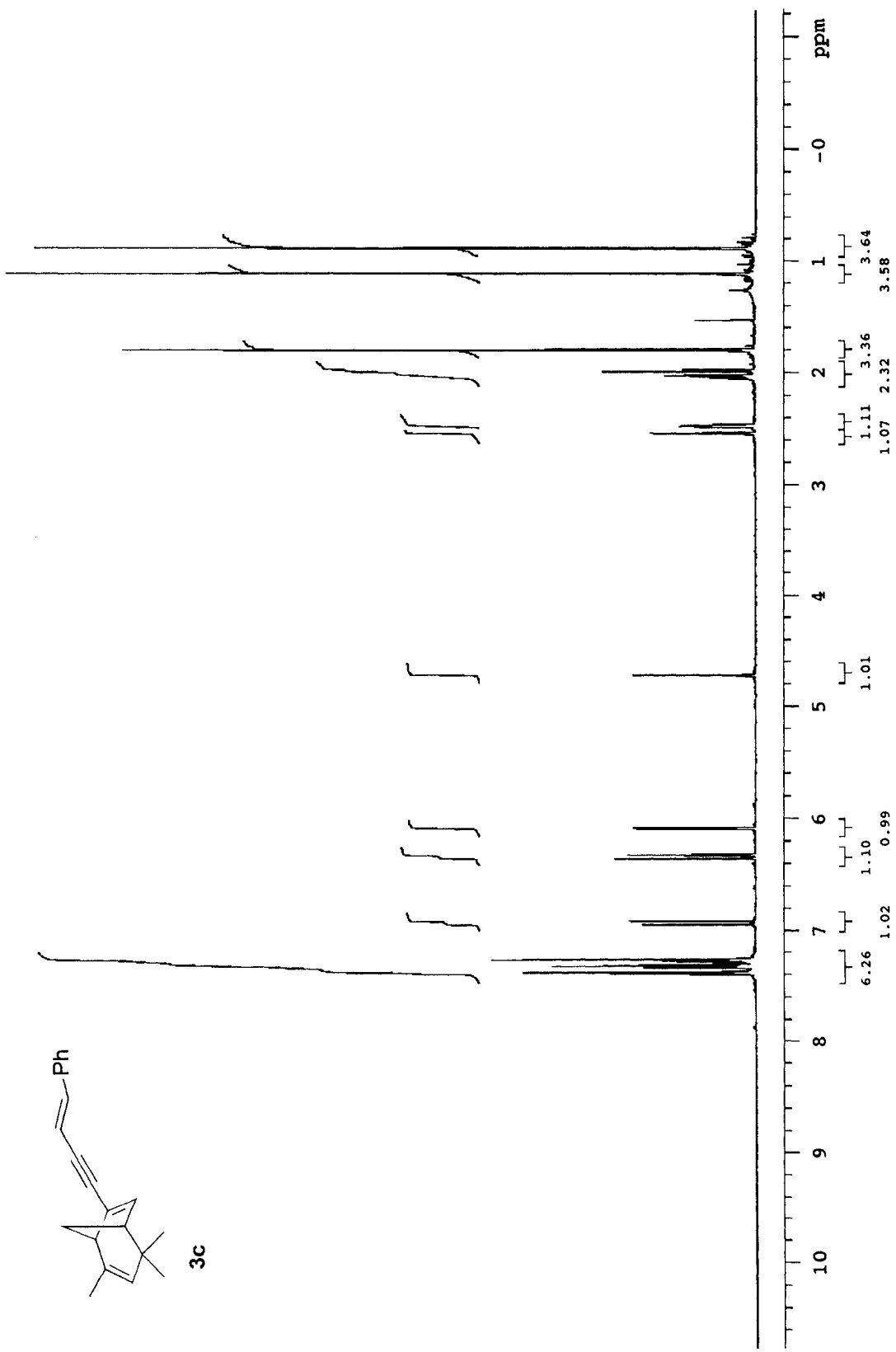

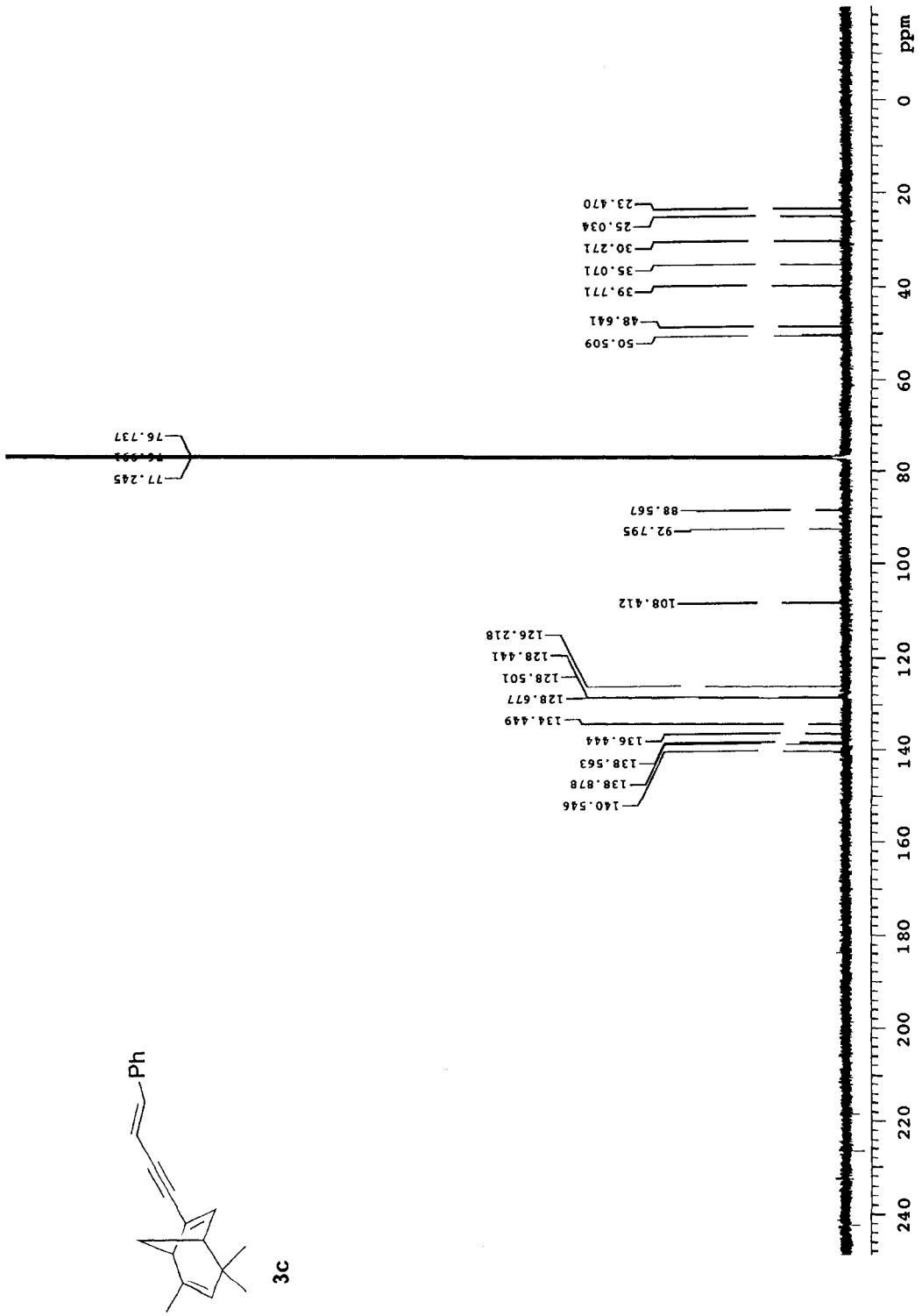

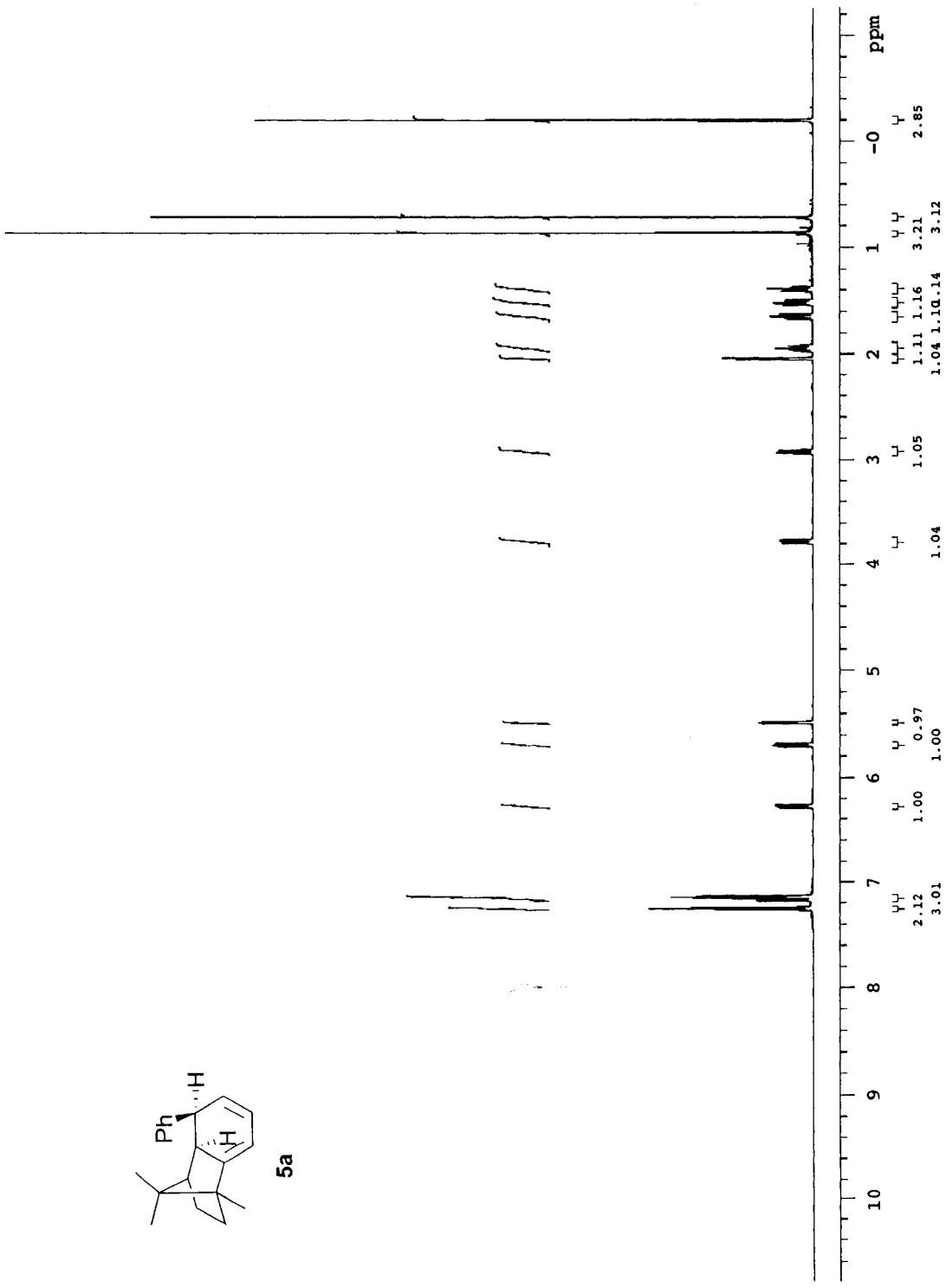

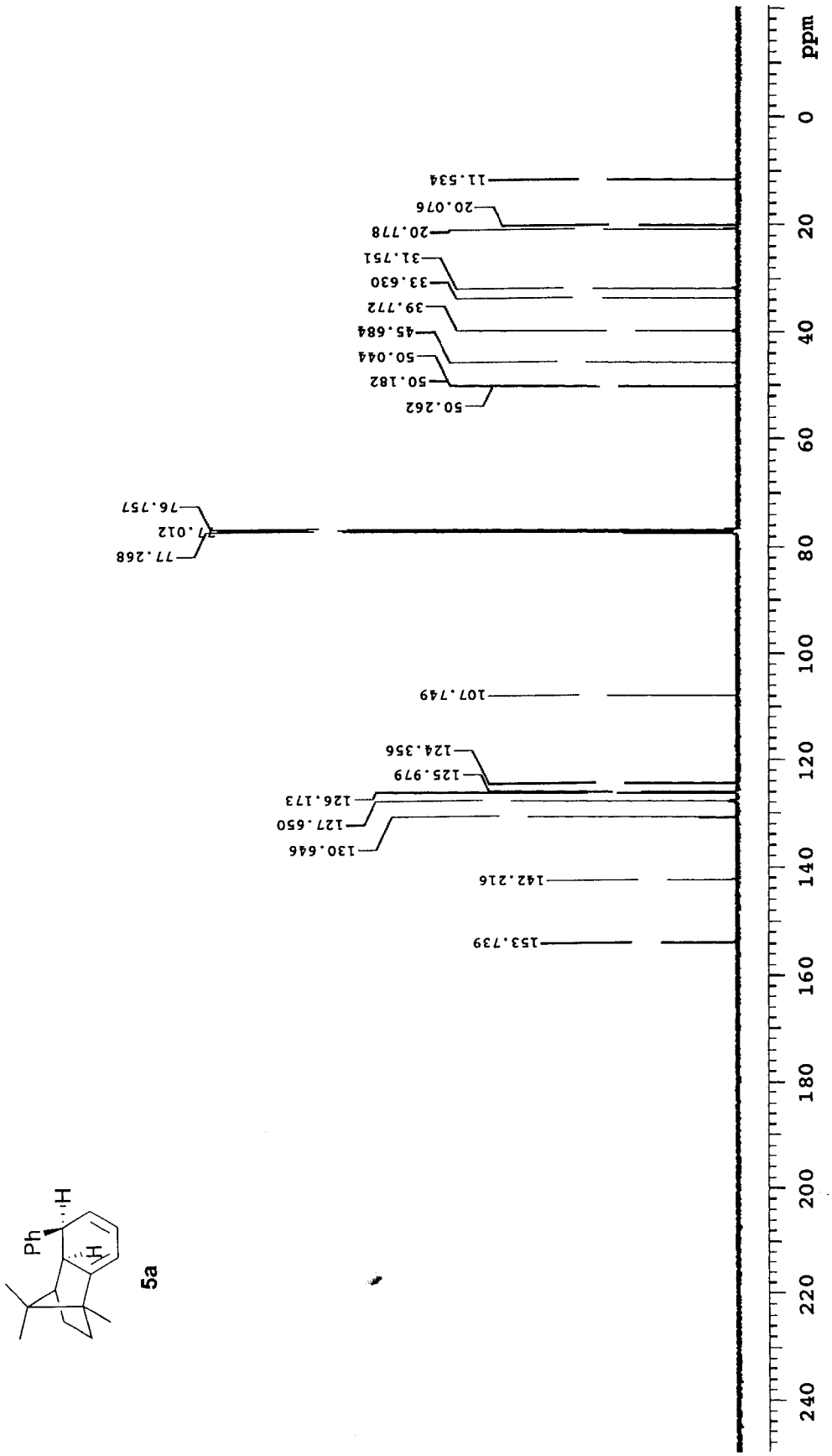

5a

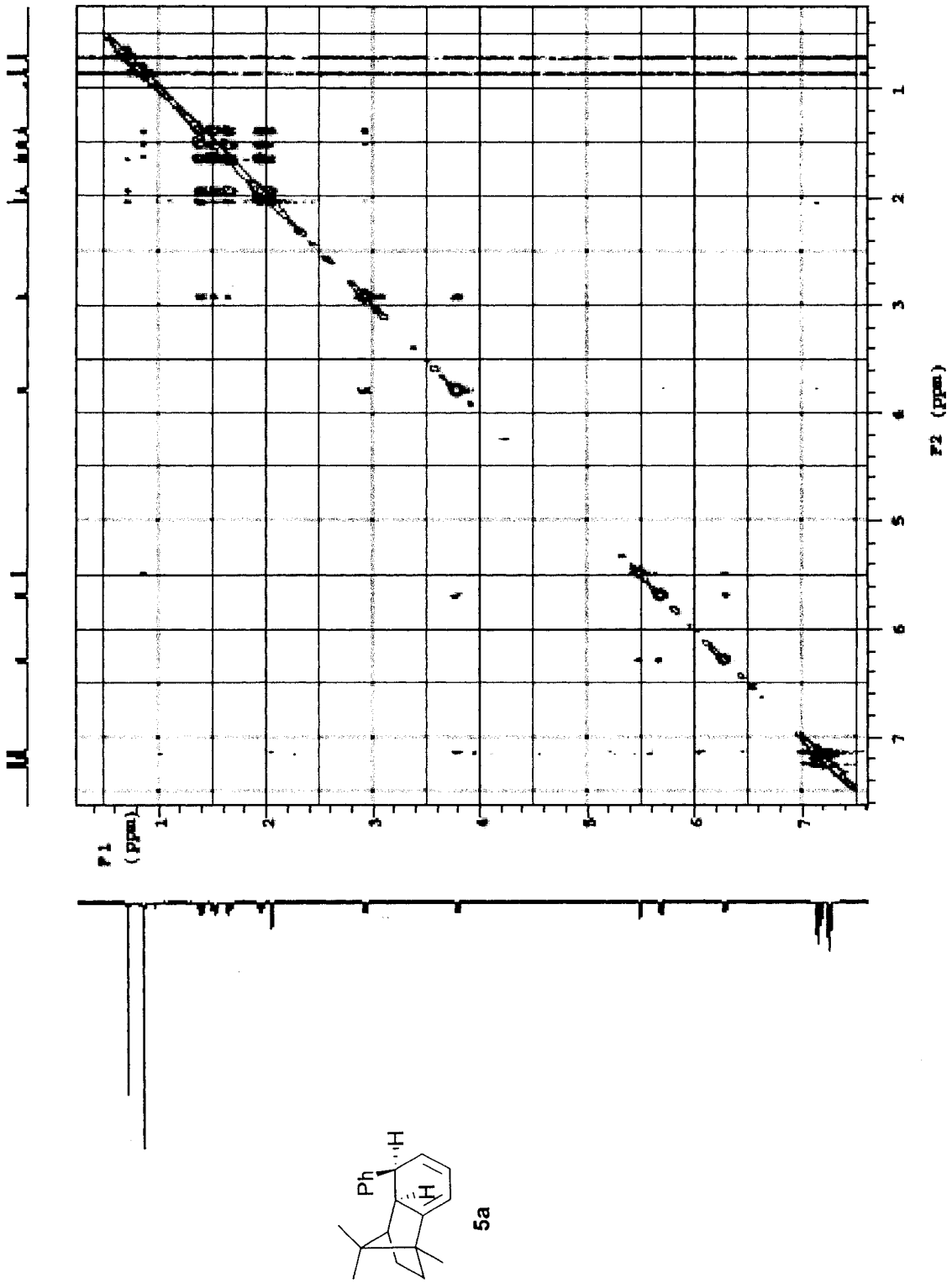

5a

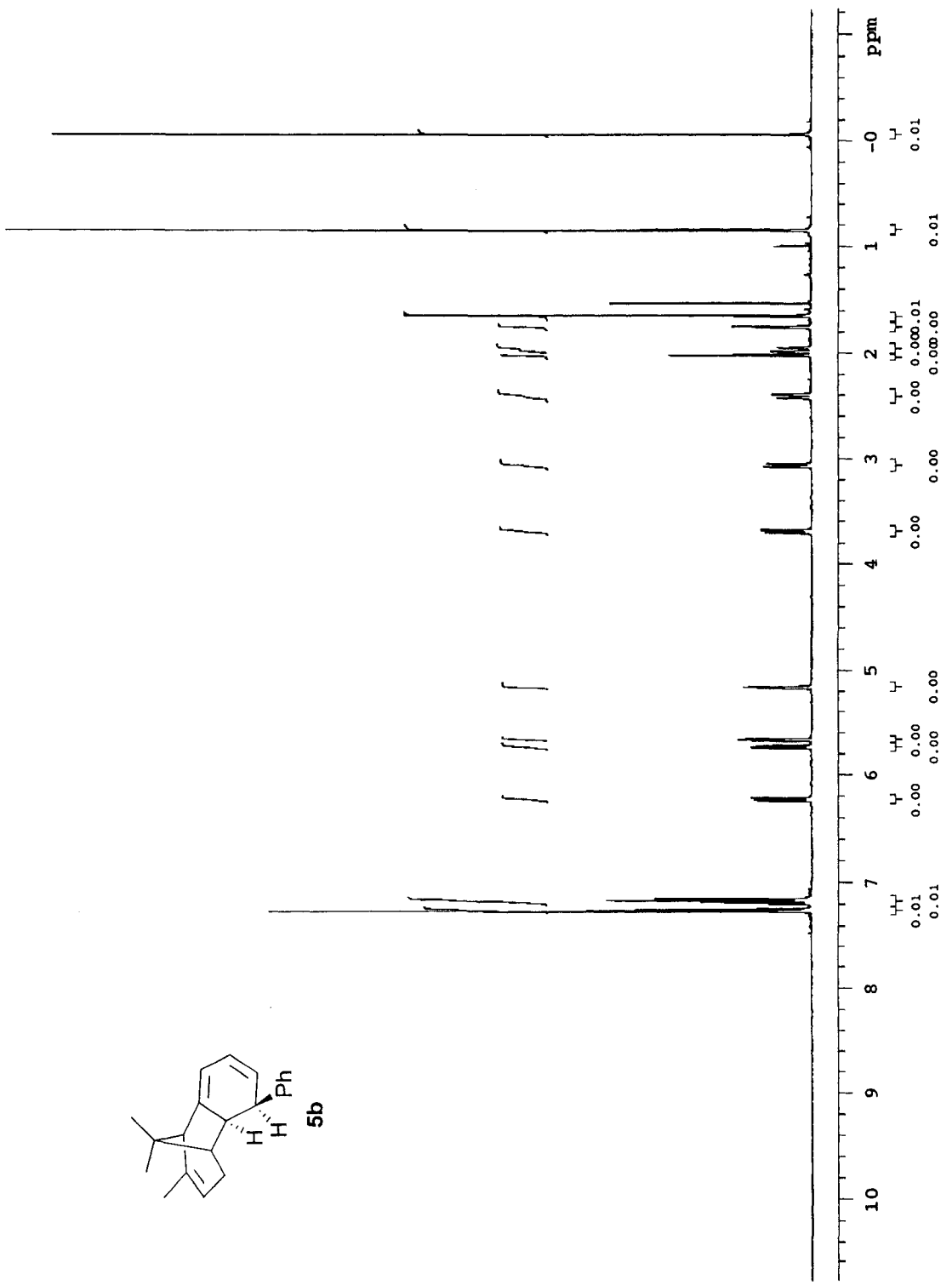

5b

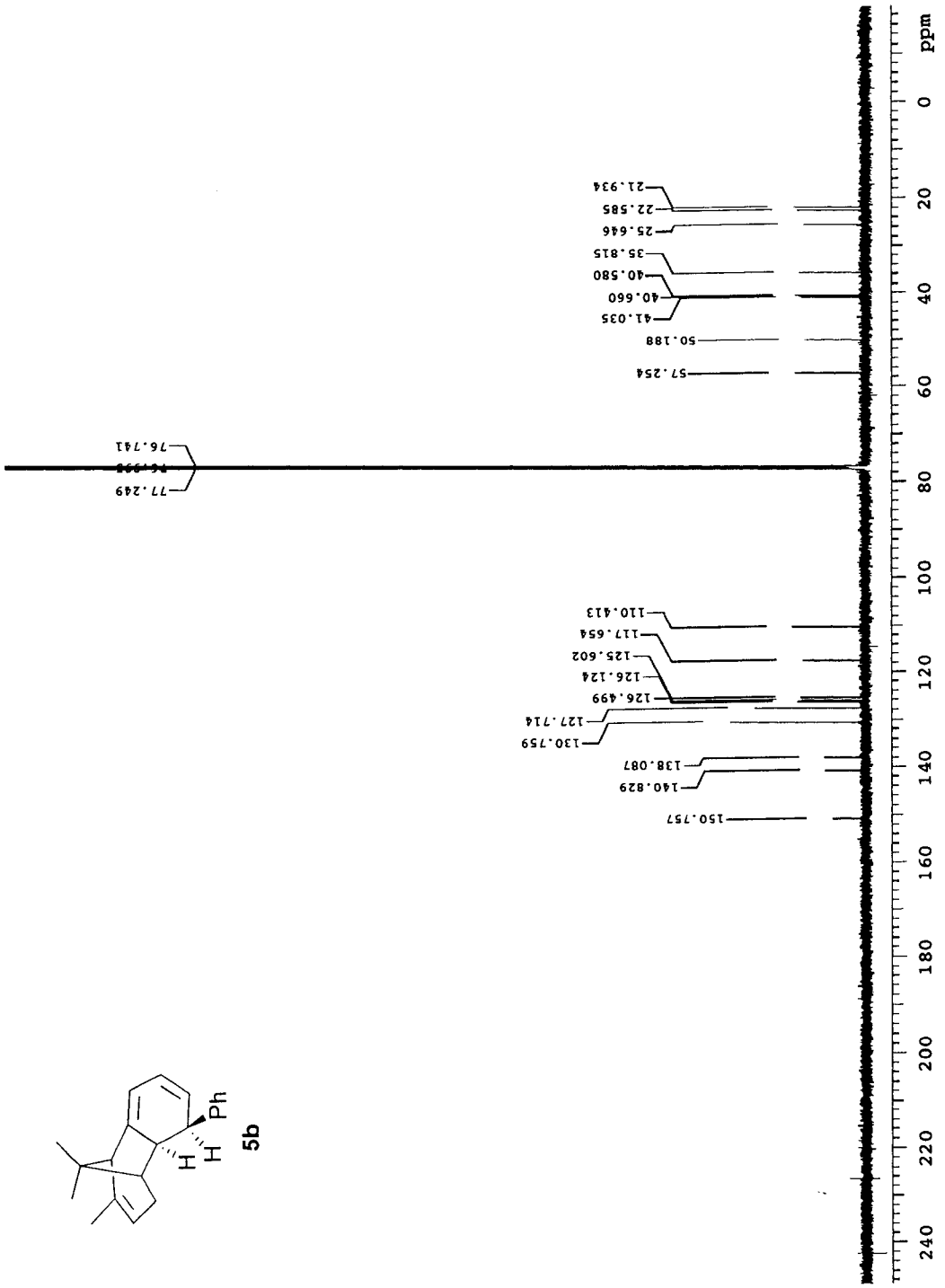

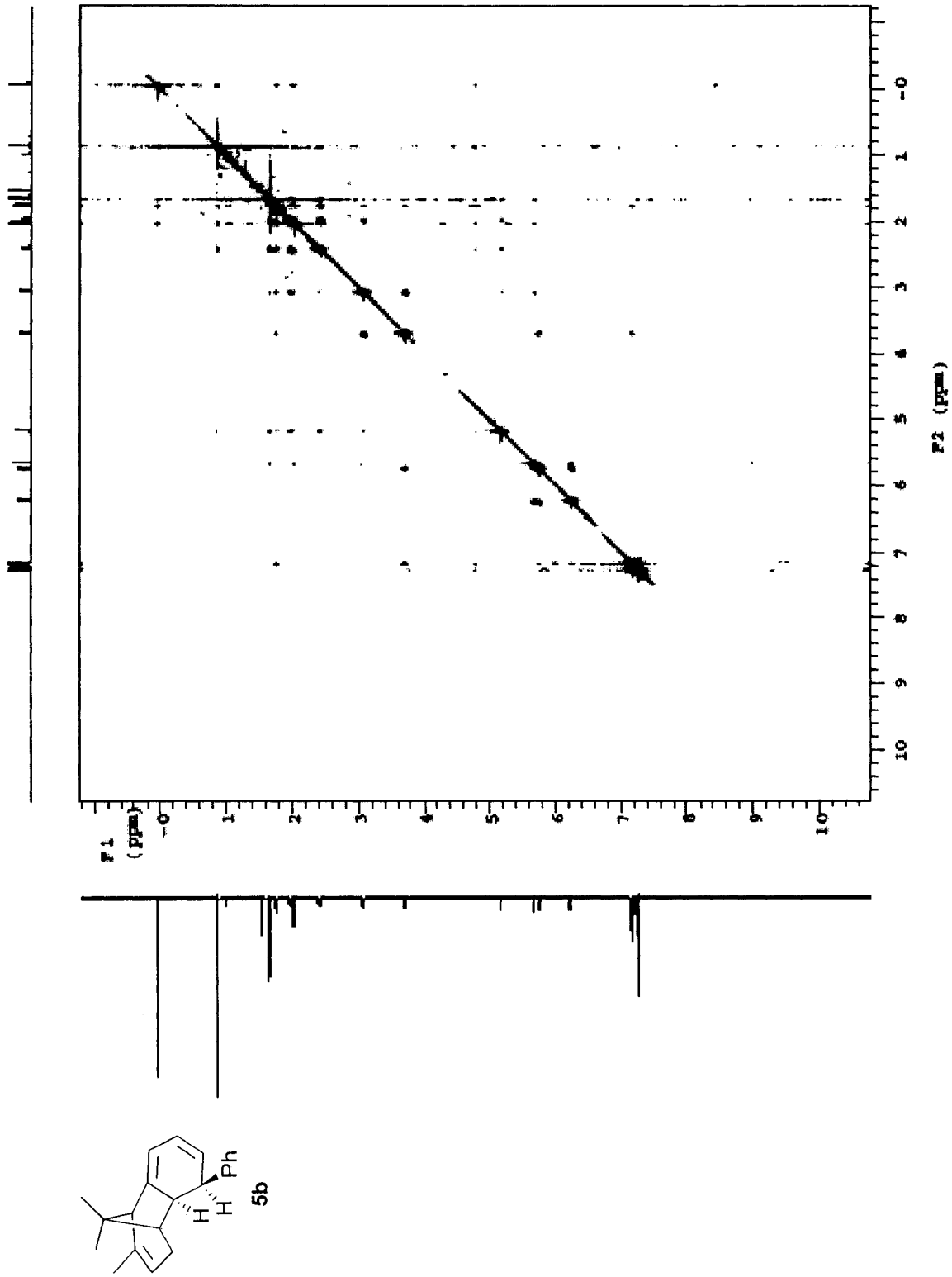

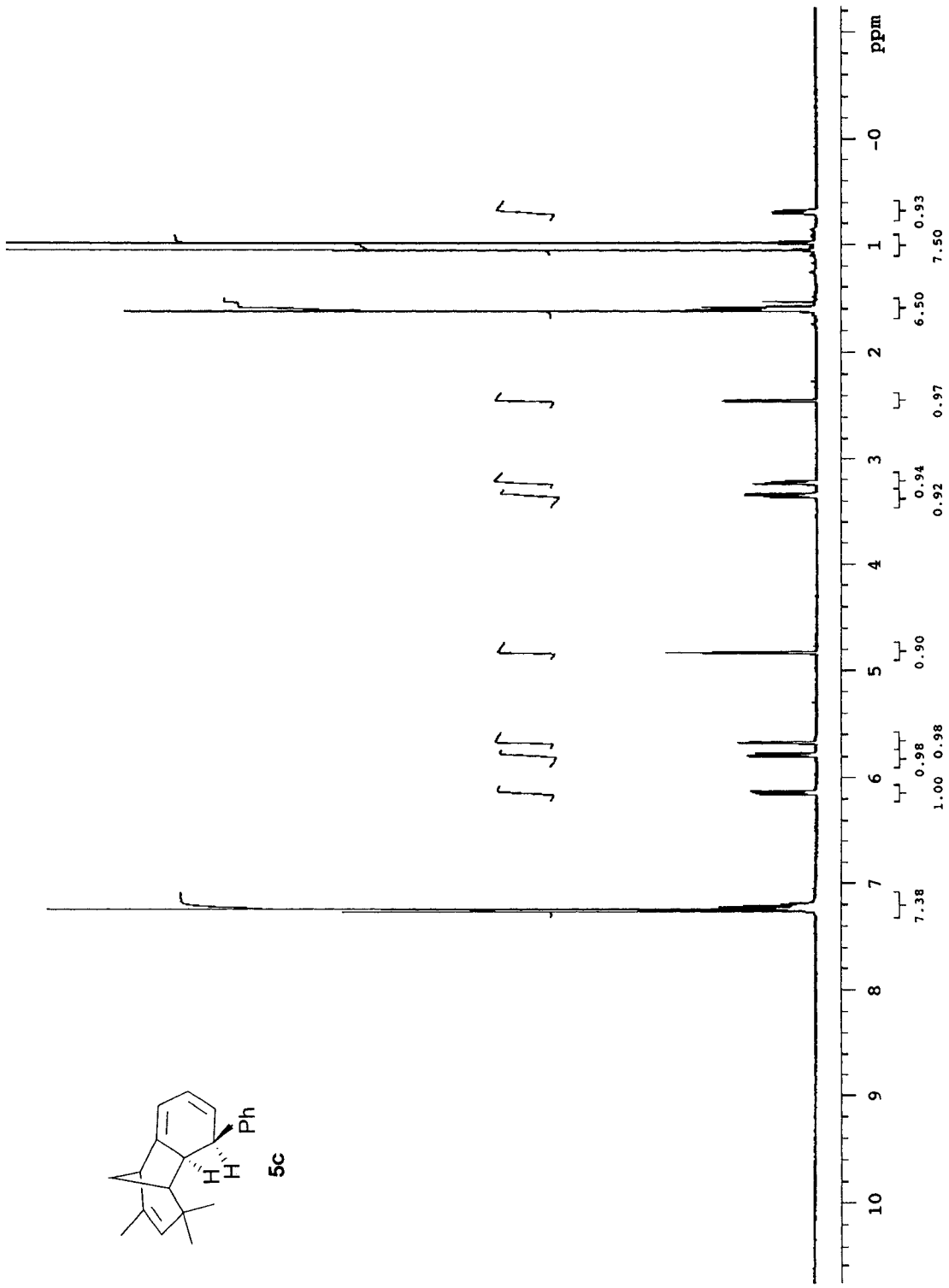

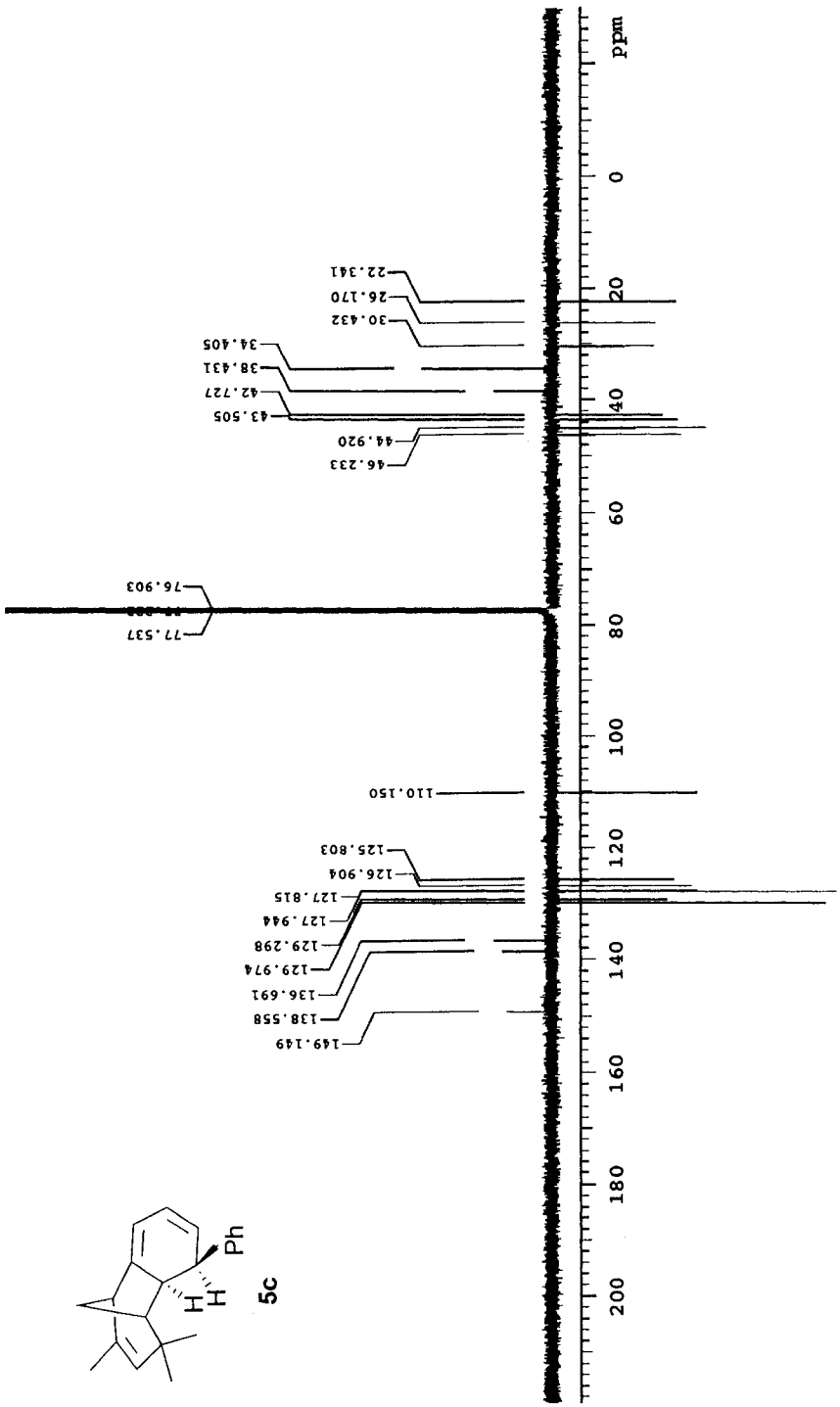

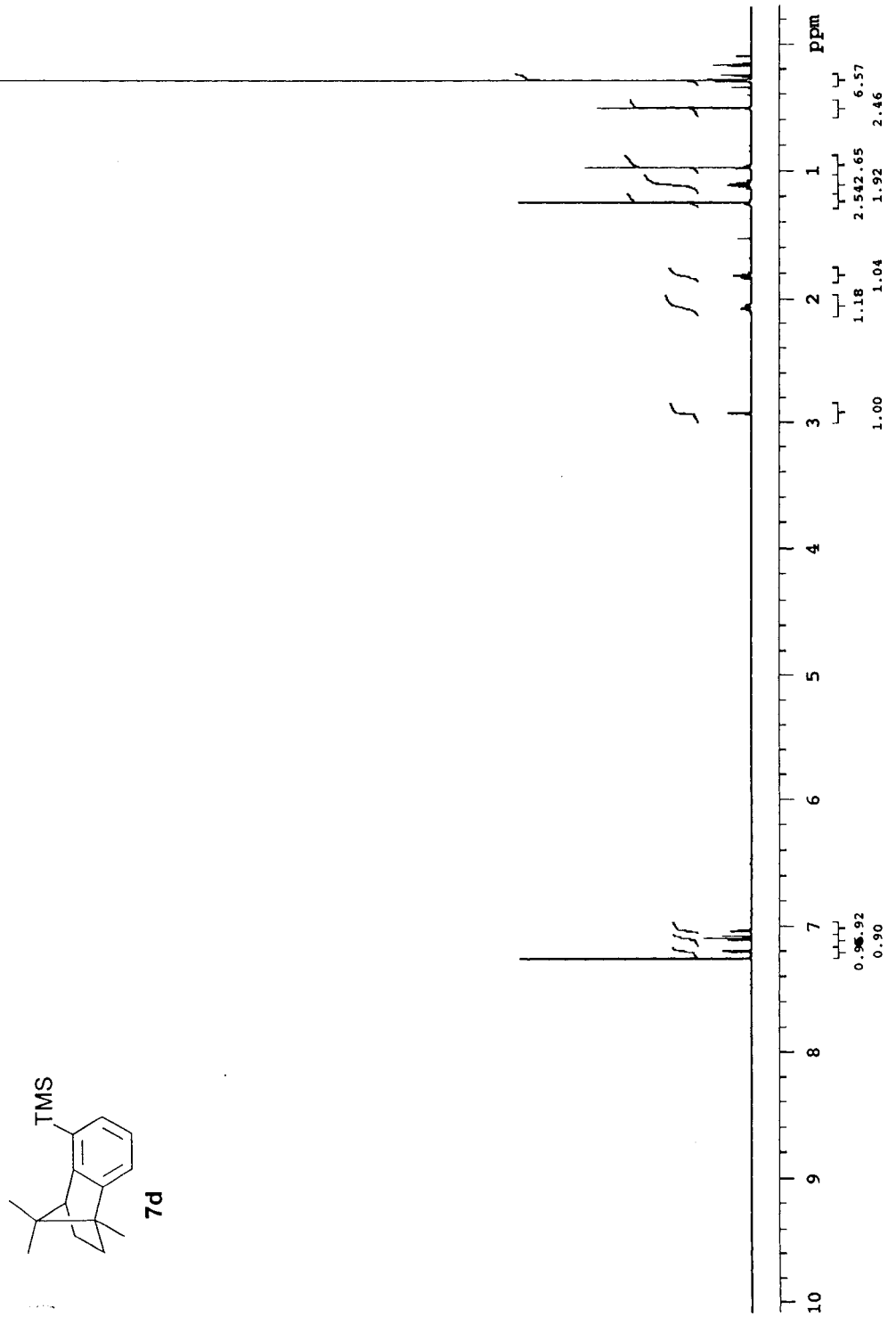

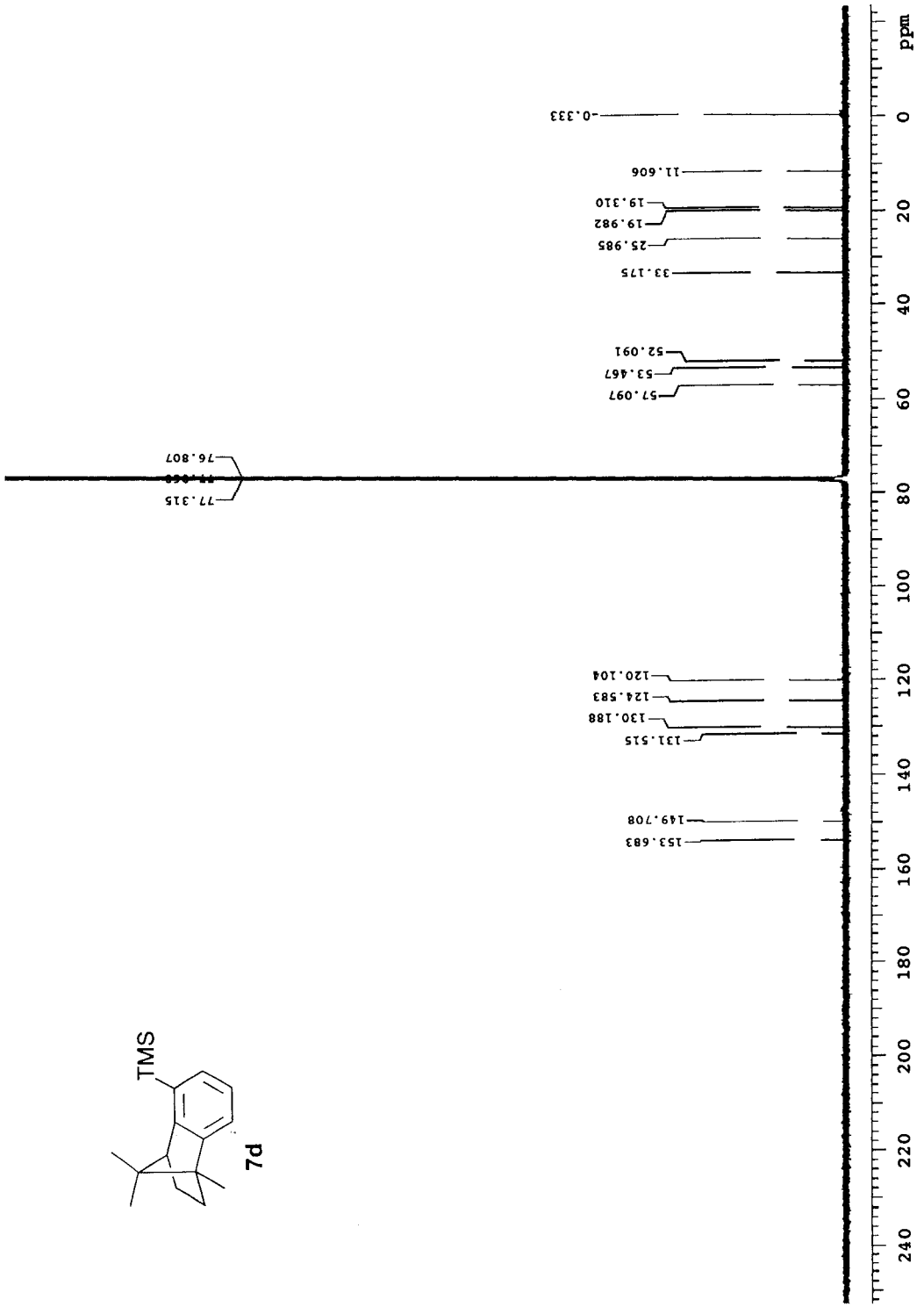

Appendix B: Selected NMR Spectra (Chapter 3)

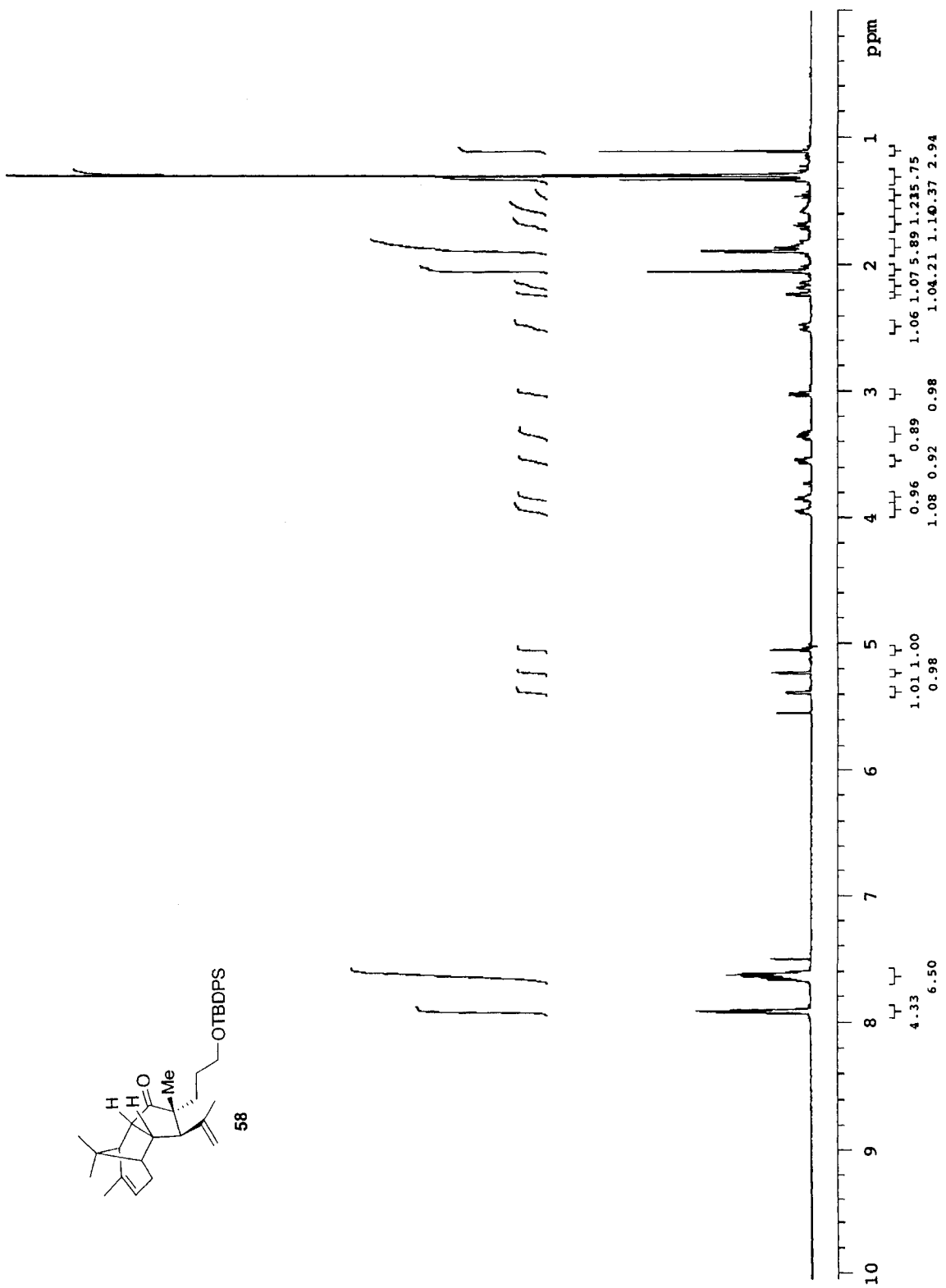

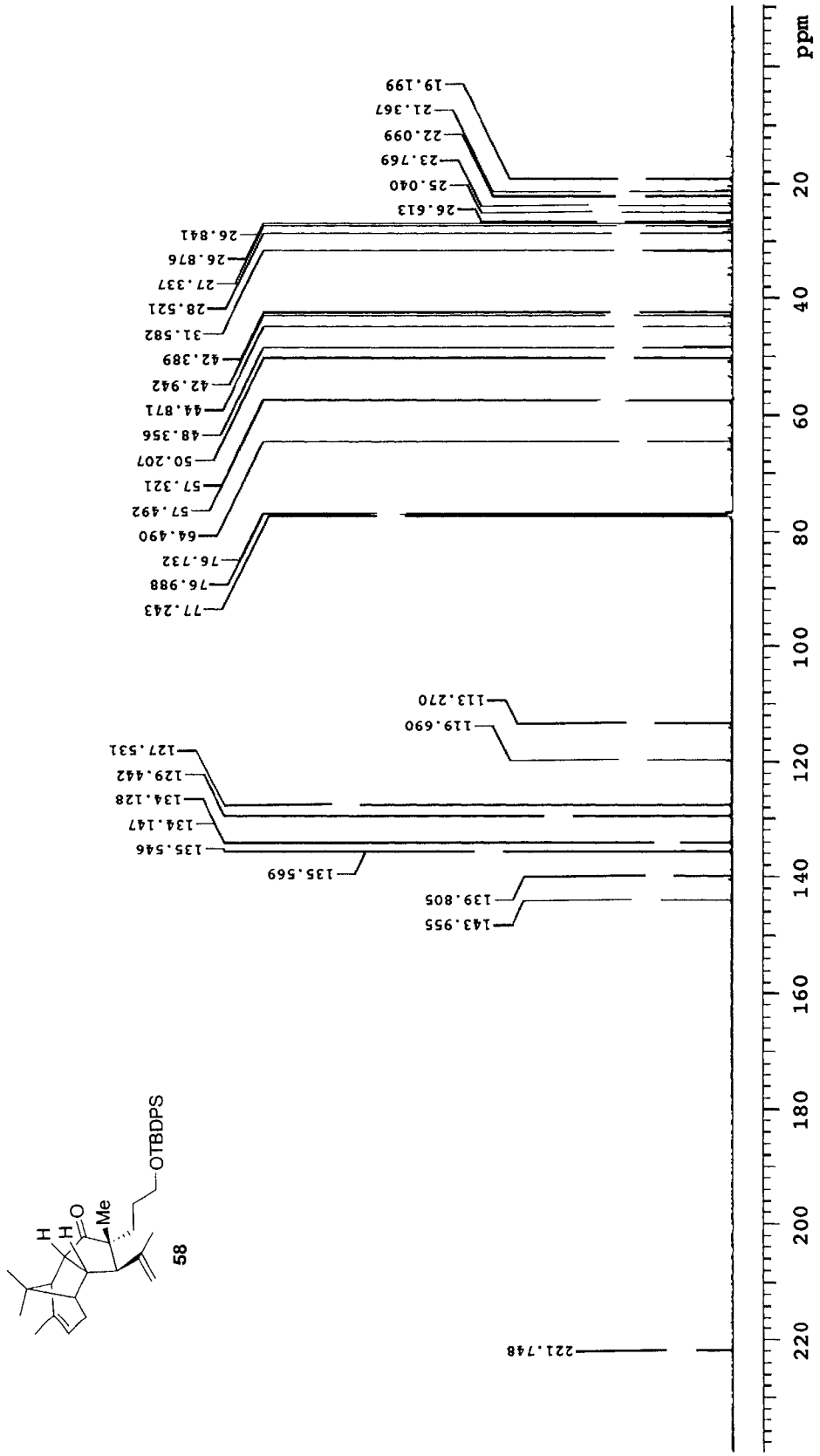

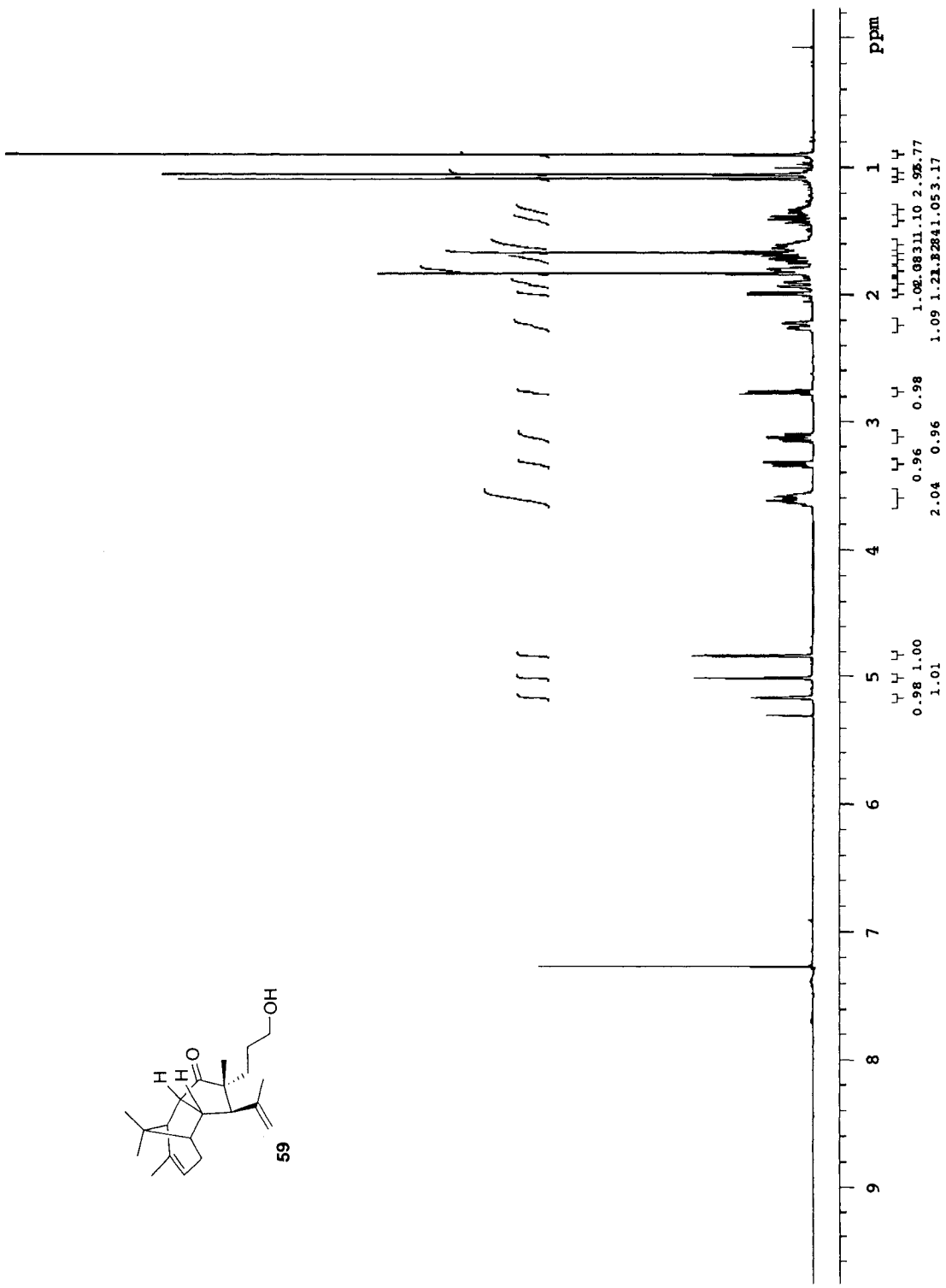

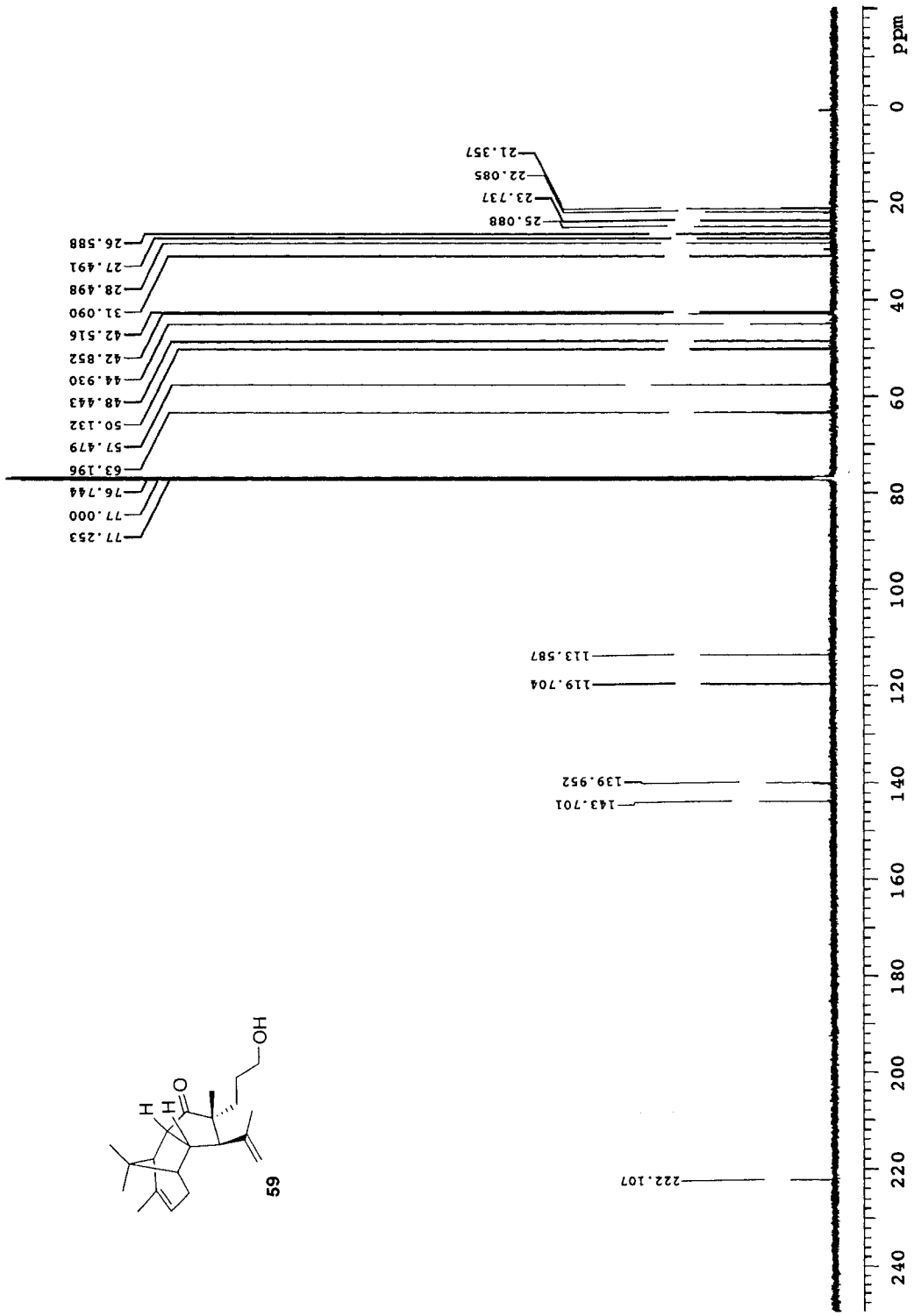

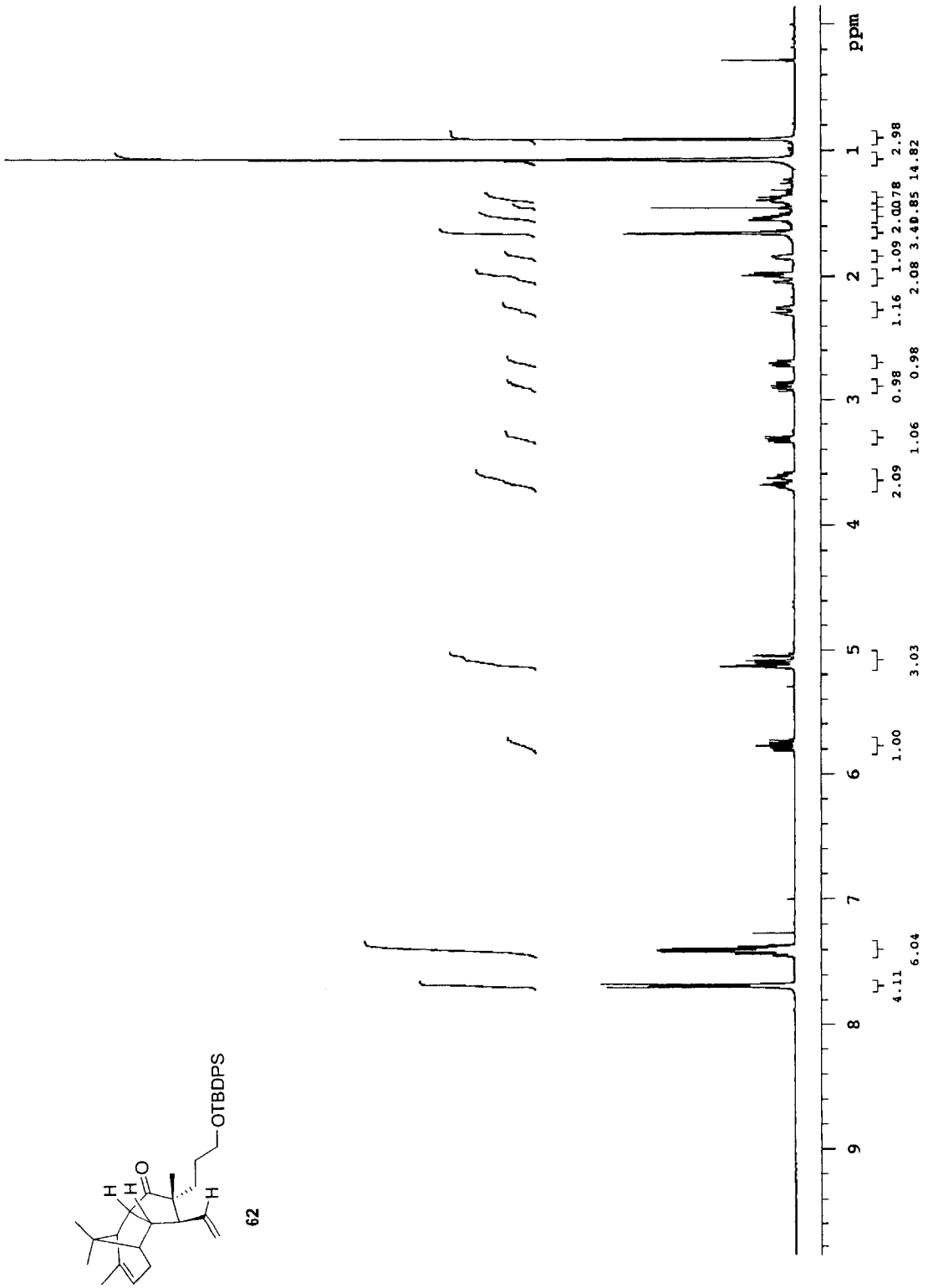

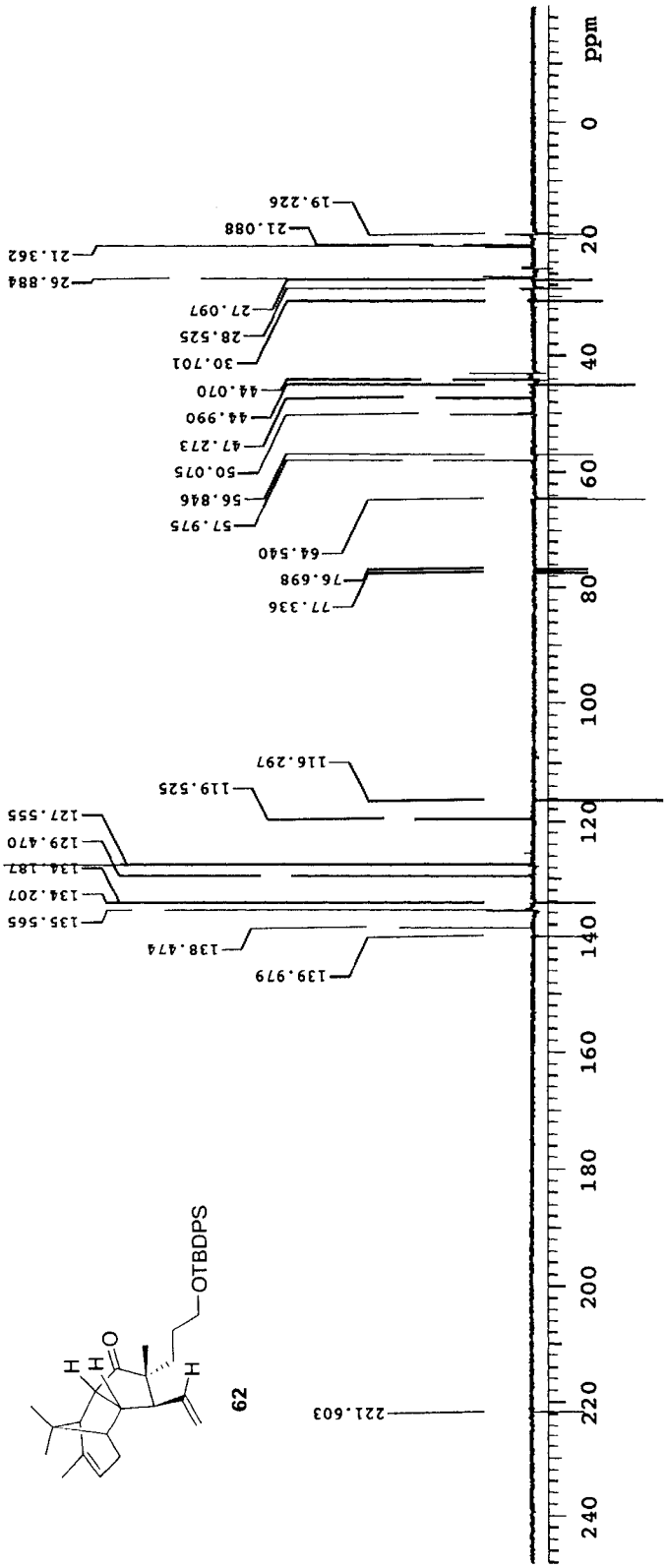

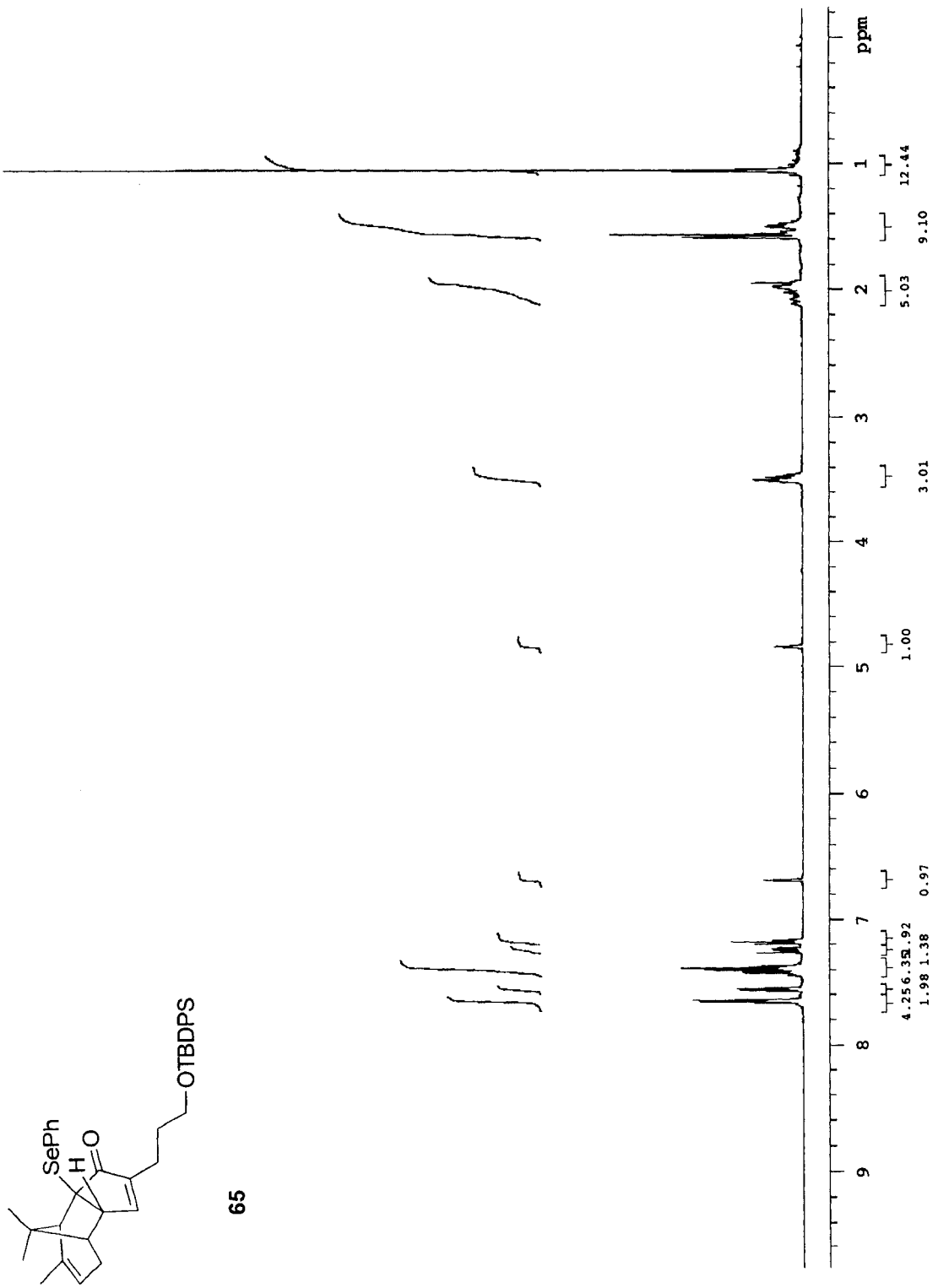

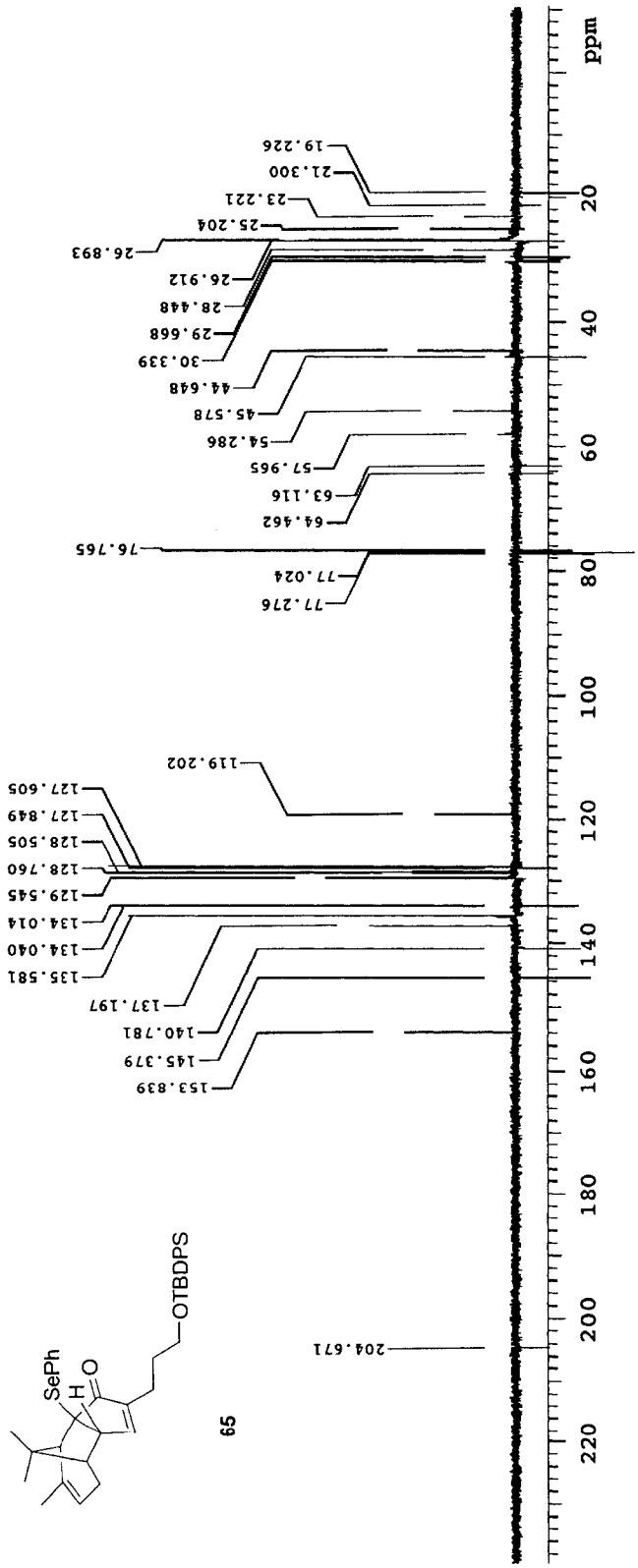

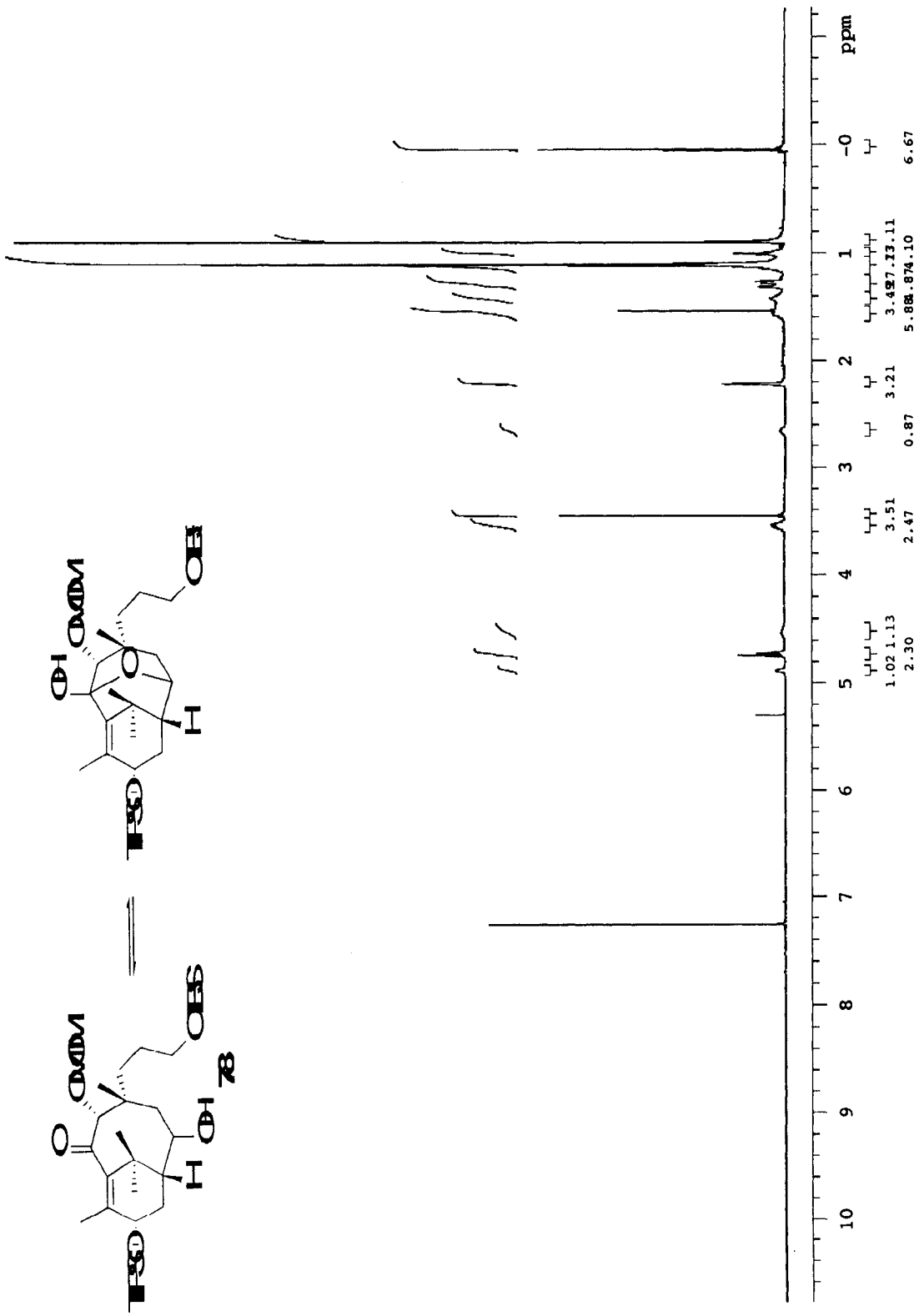

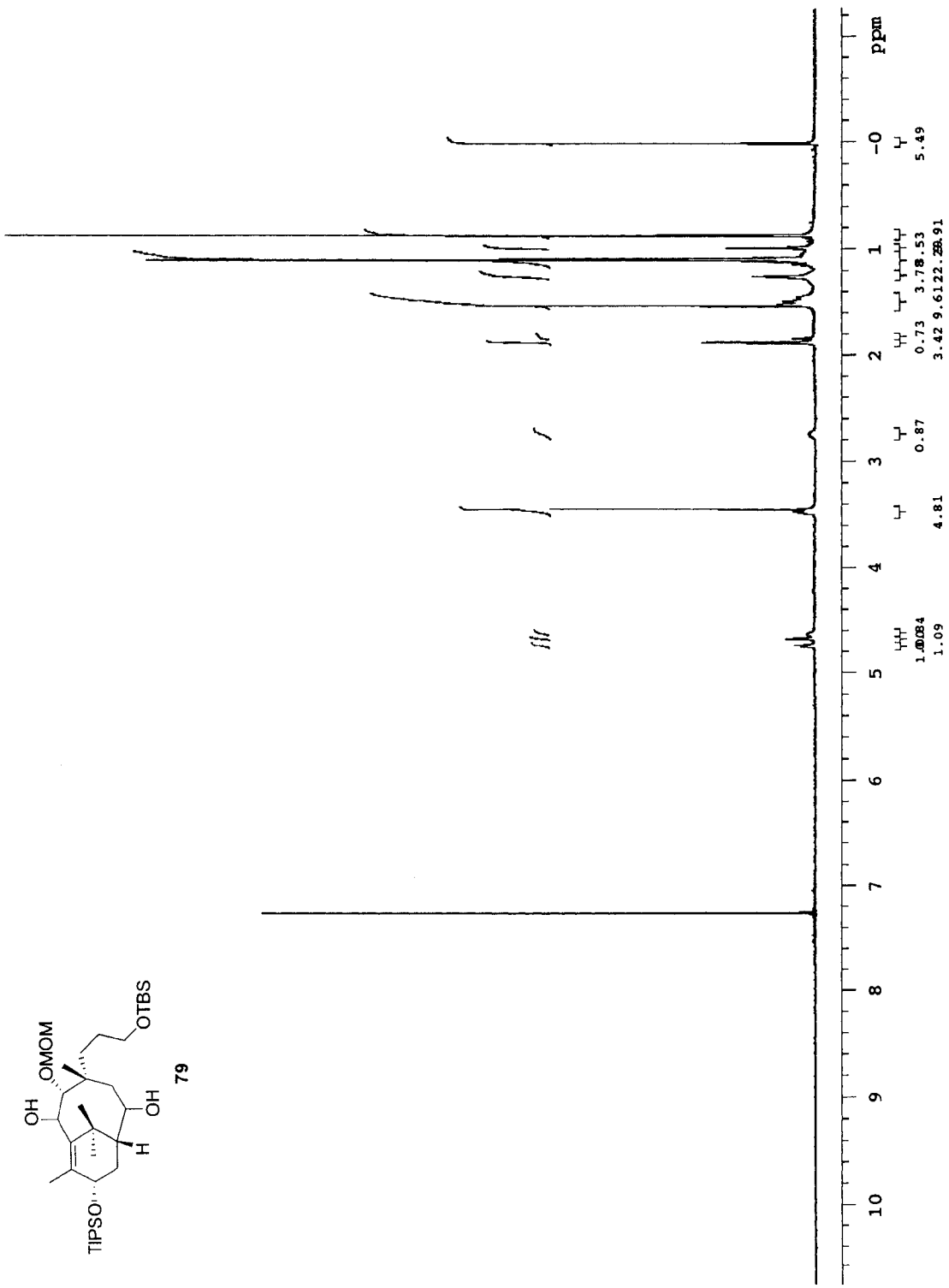

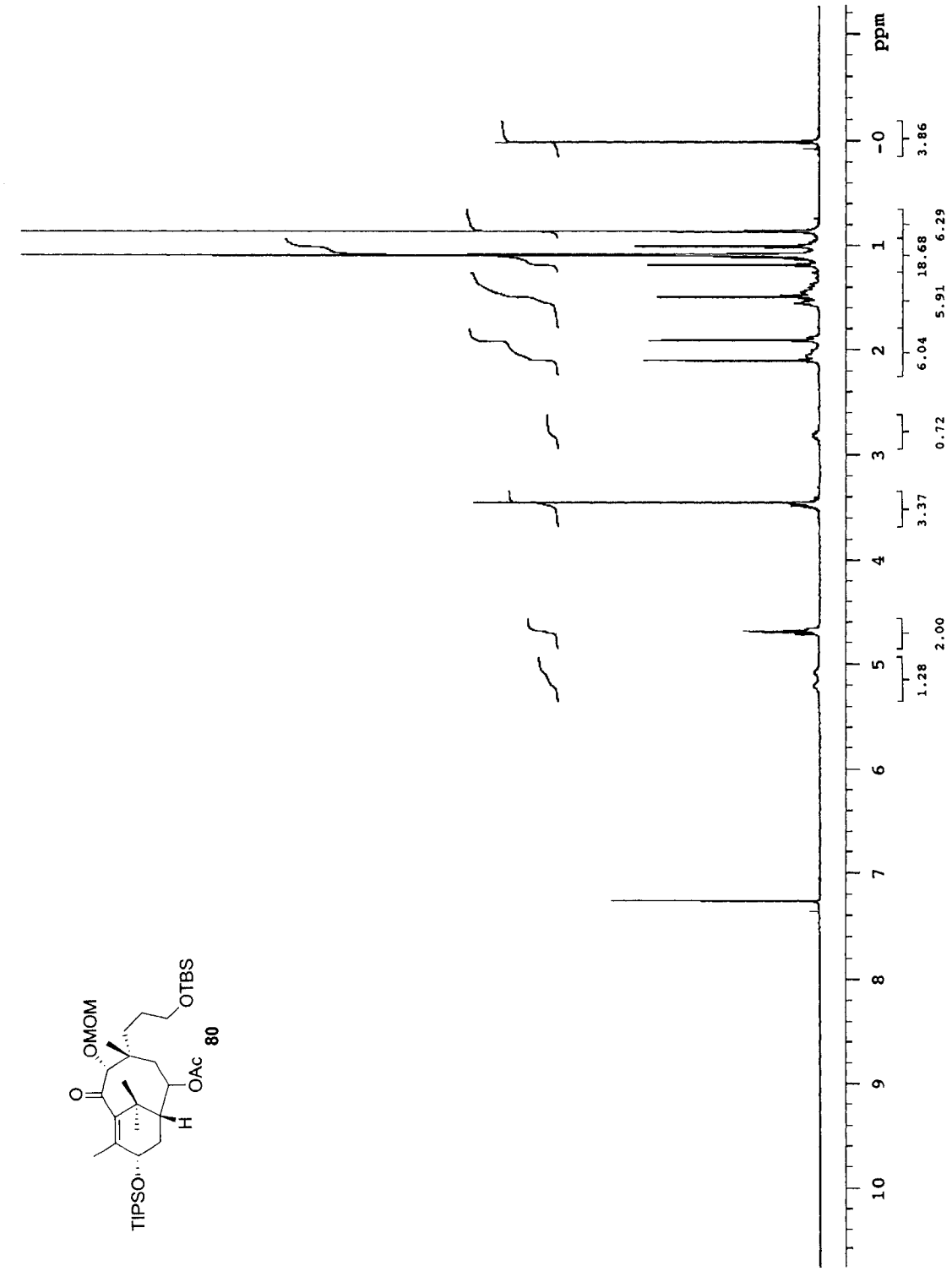

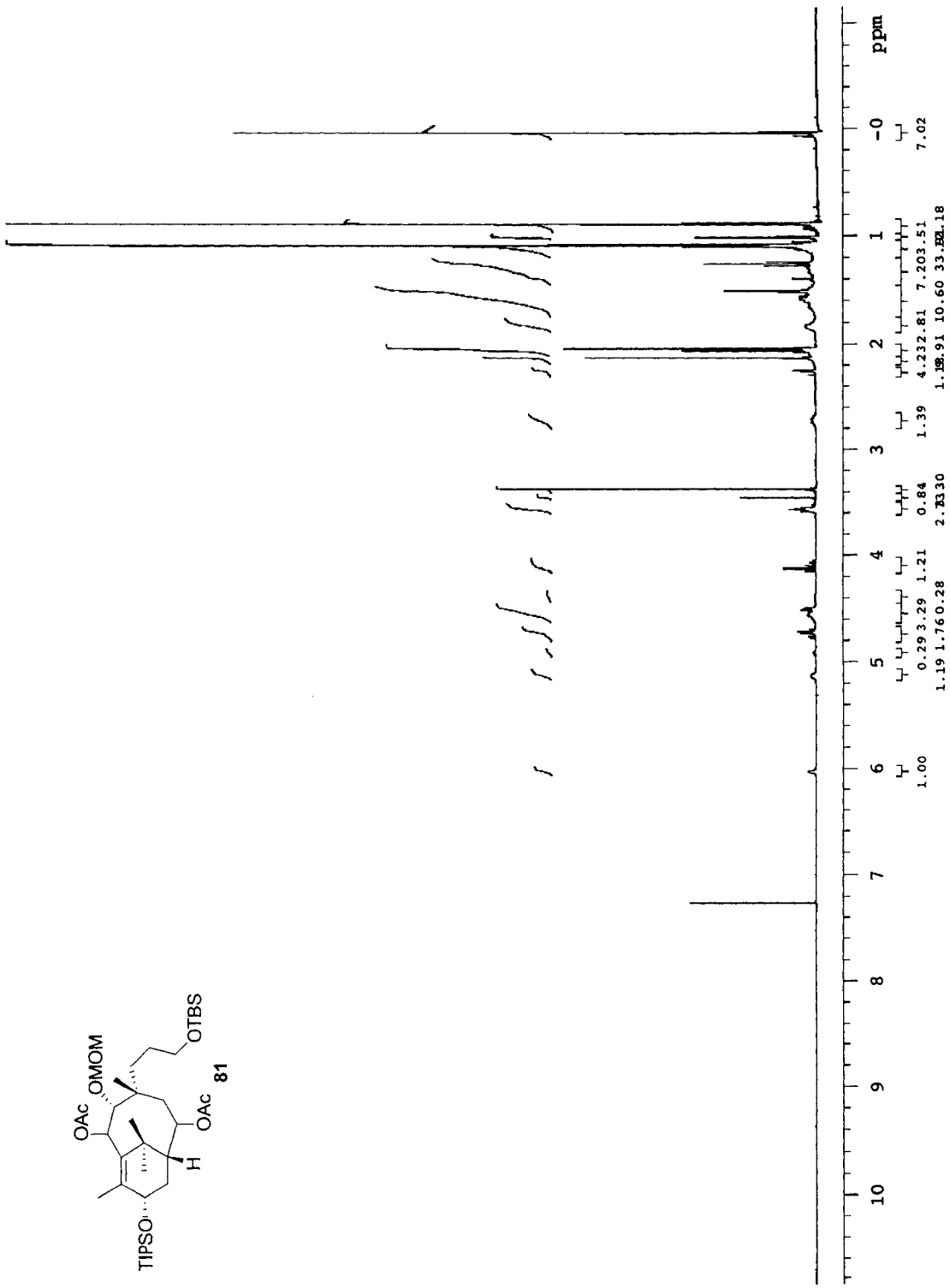

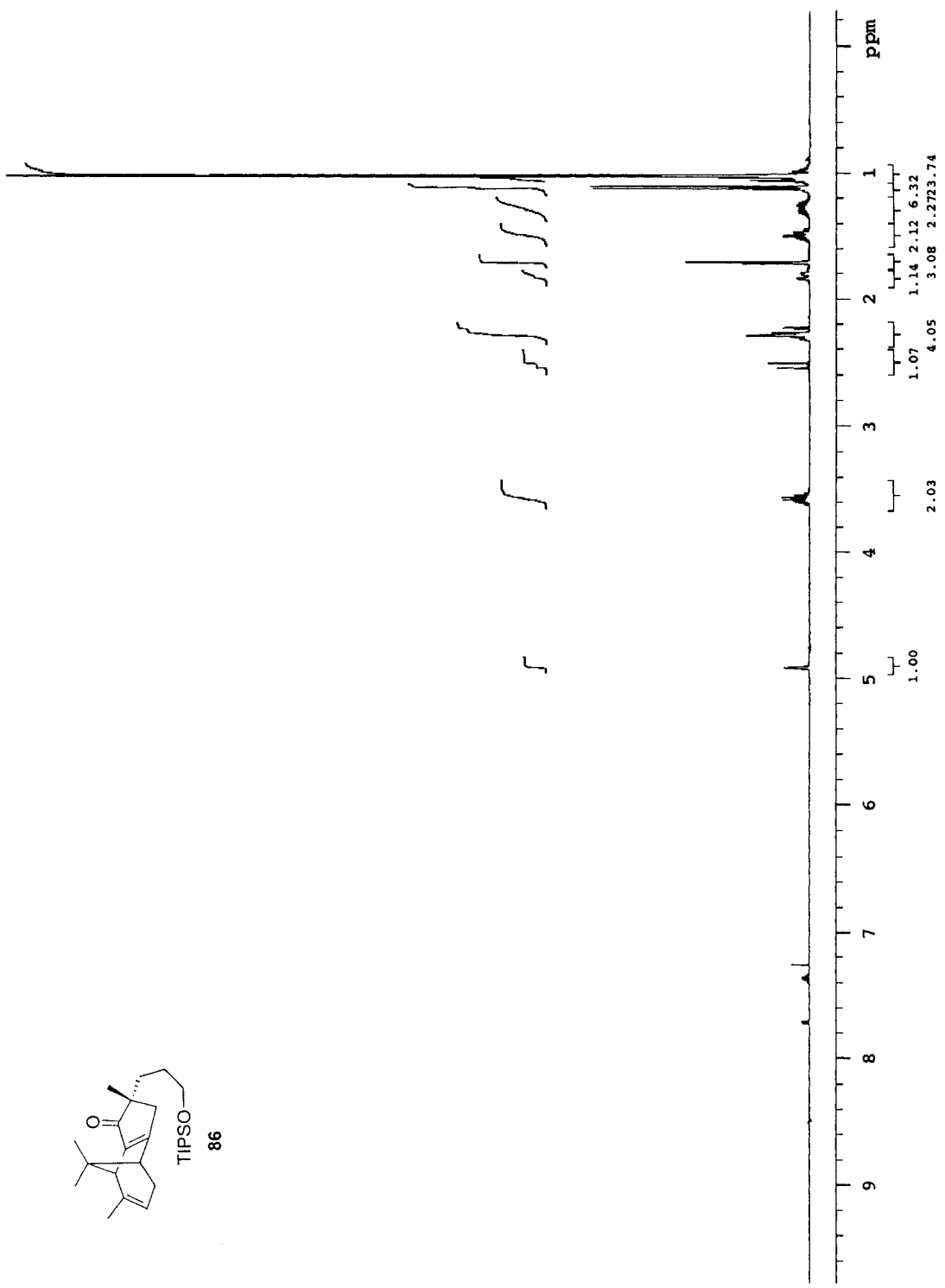

86

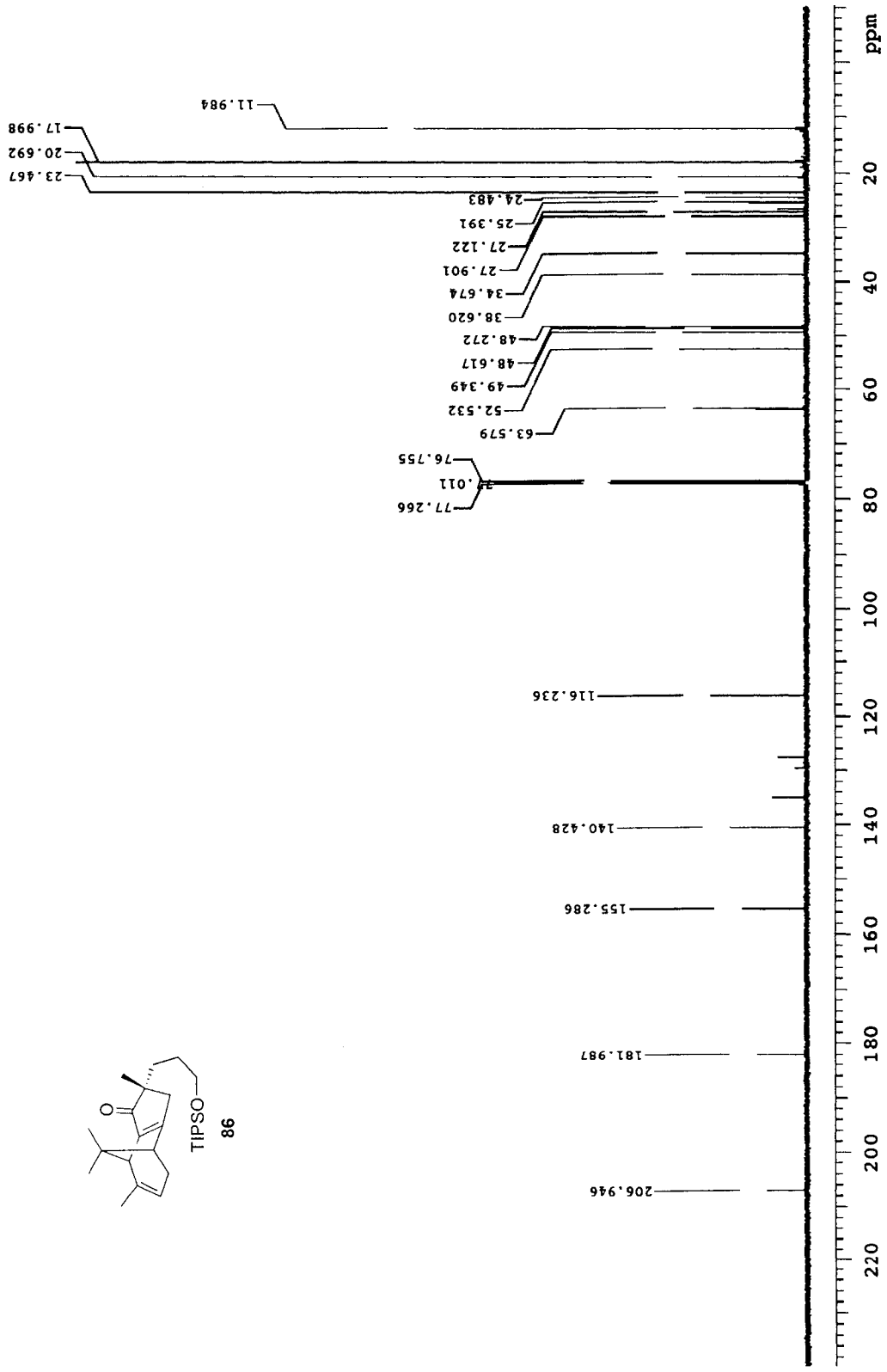

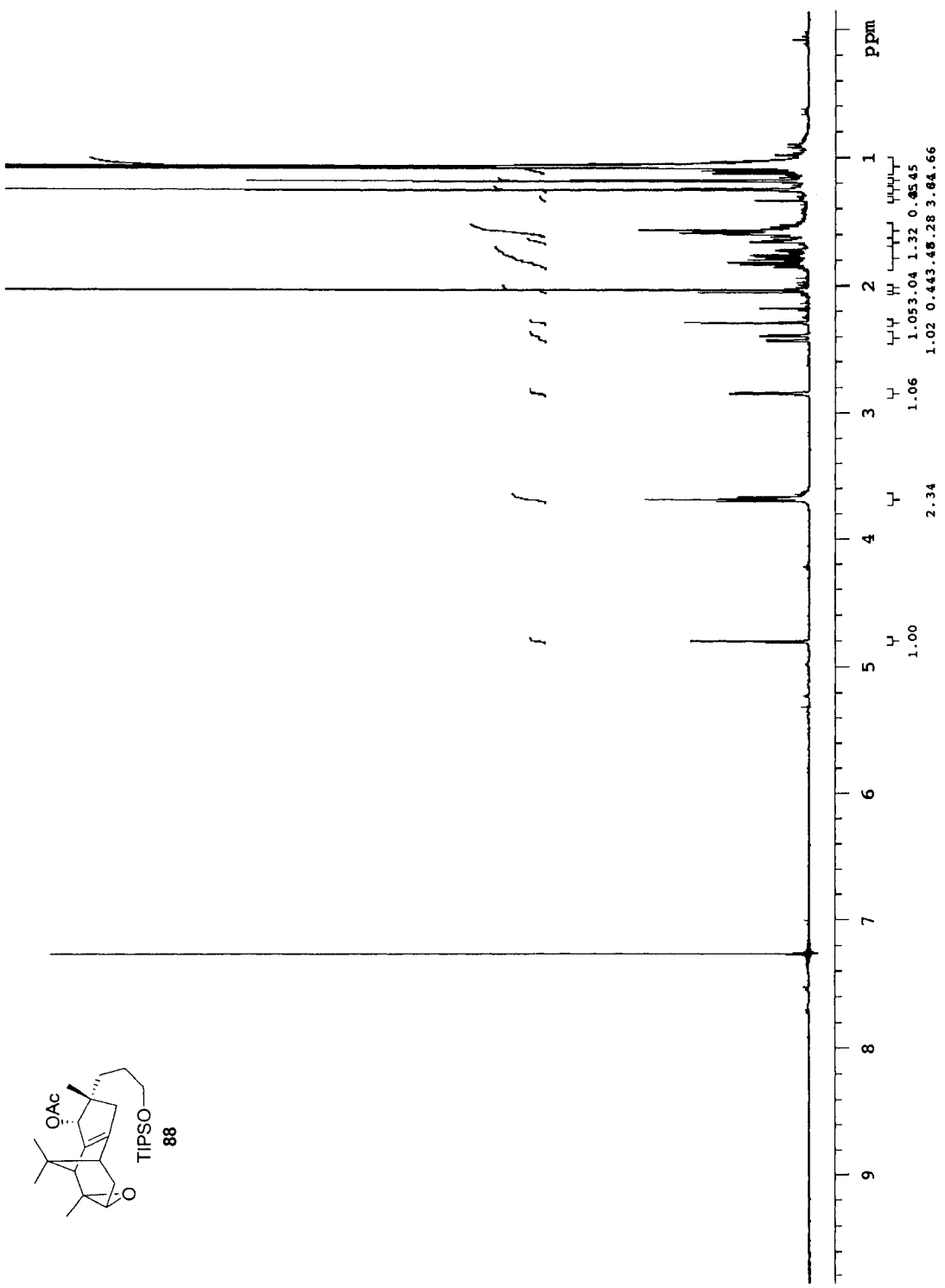

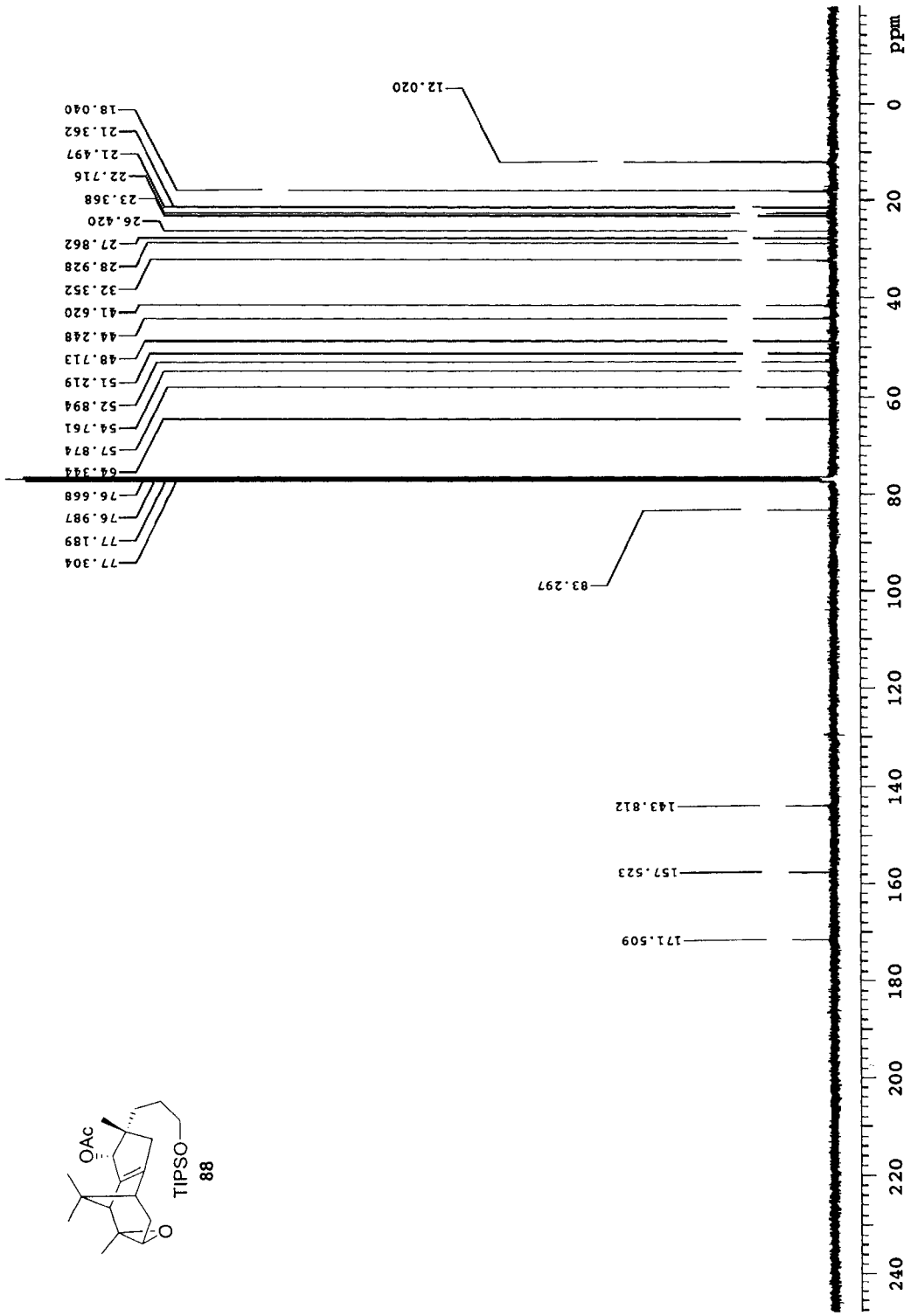

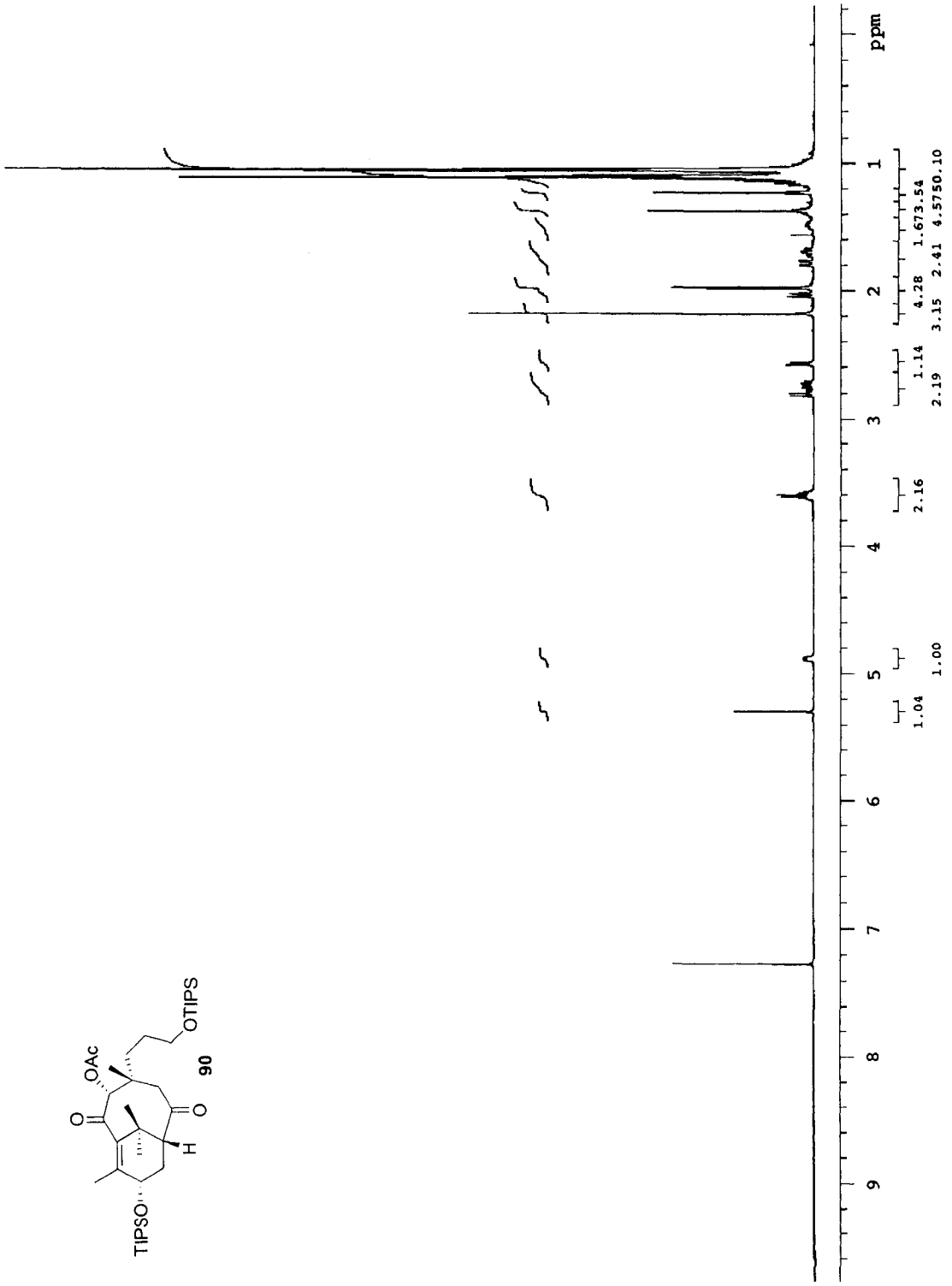

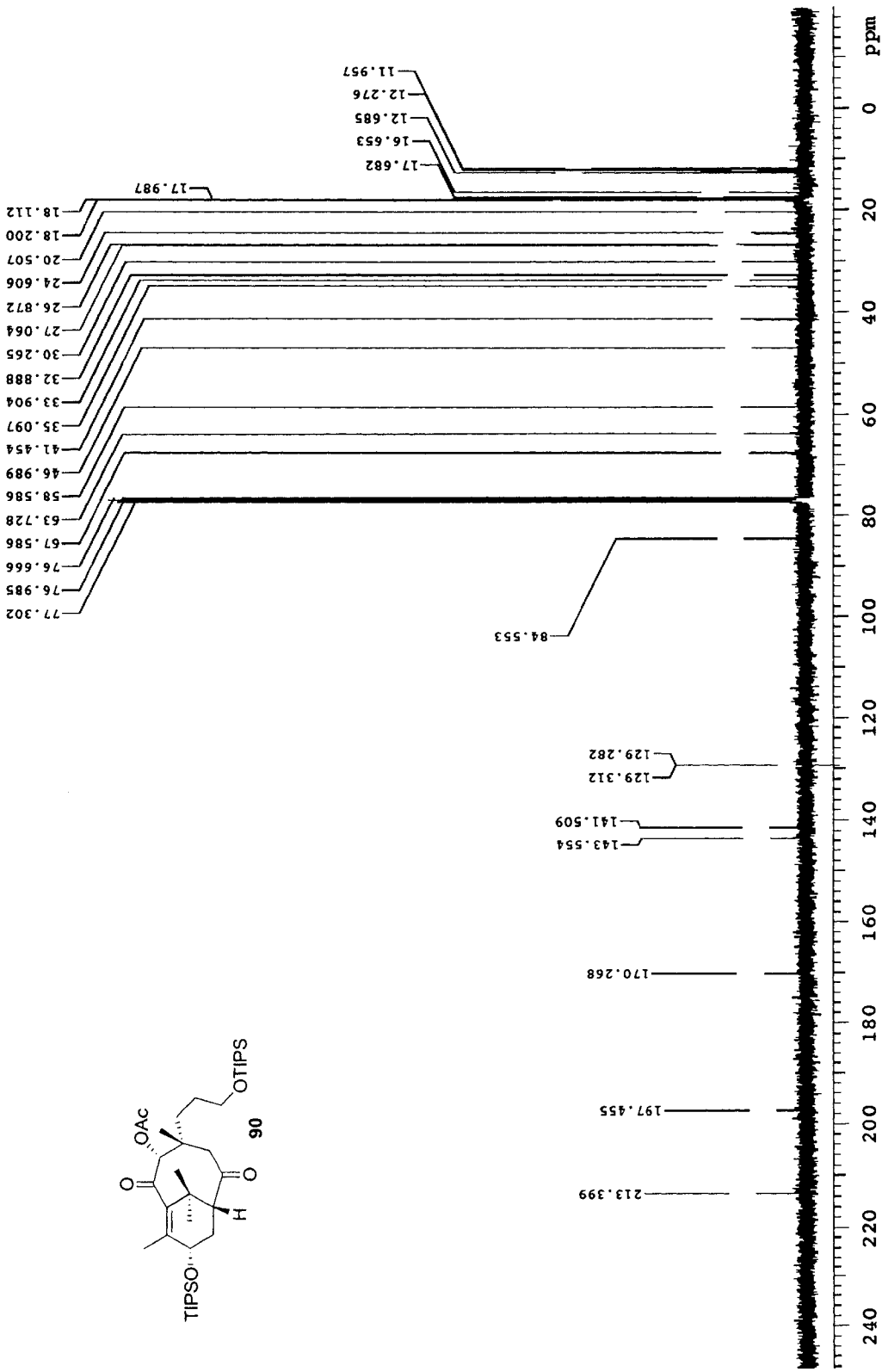

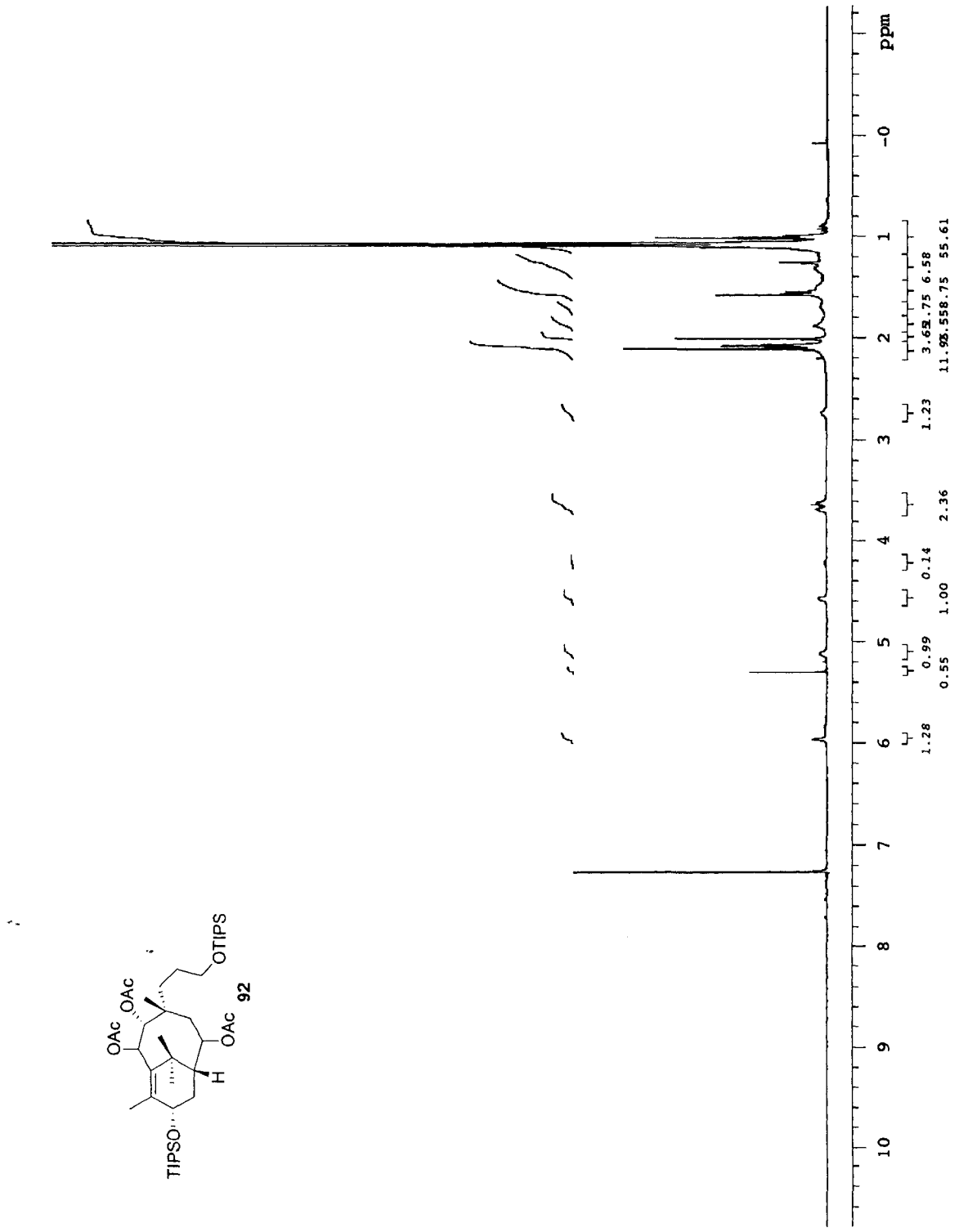

Appendix C: Selected NMR Spectra (Chapter 4)

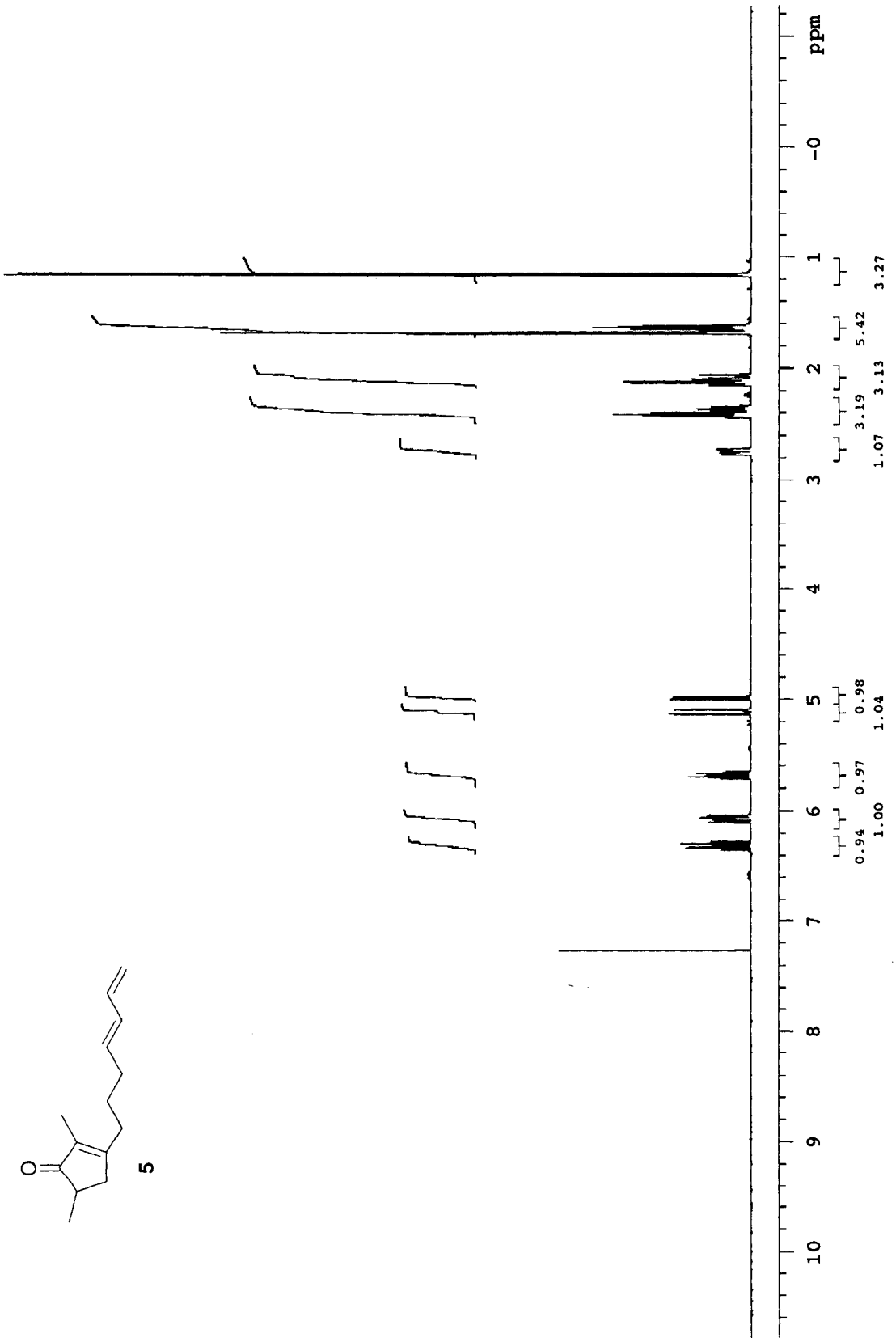

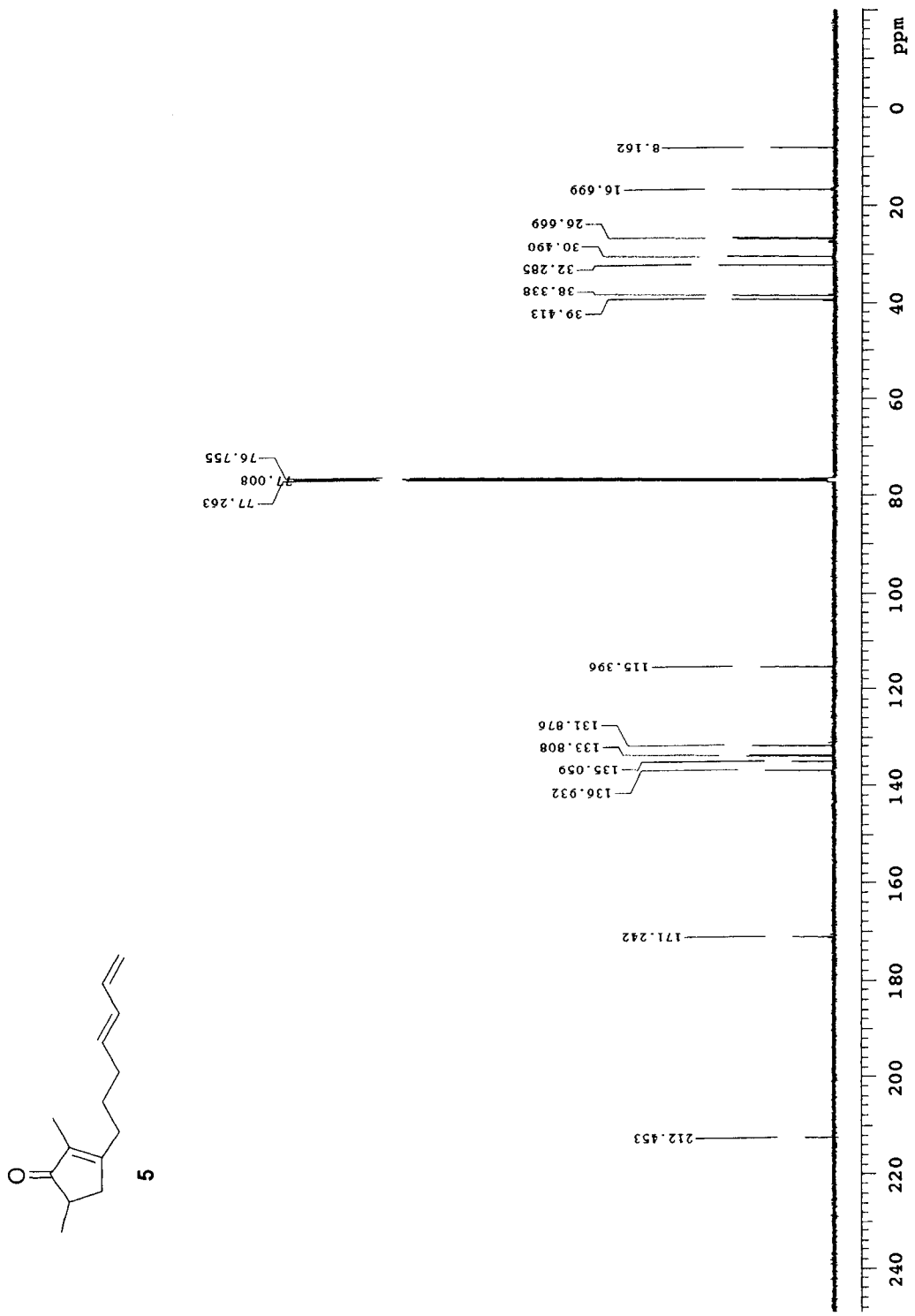

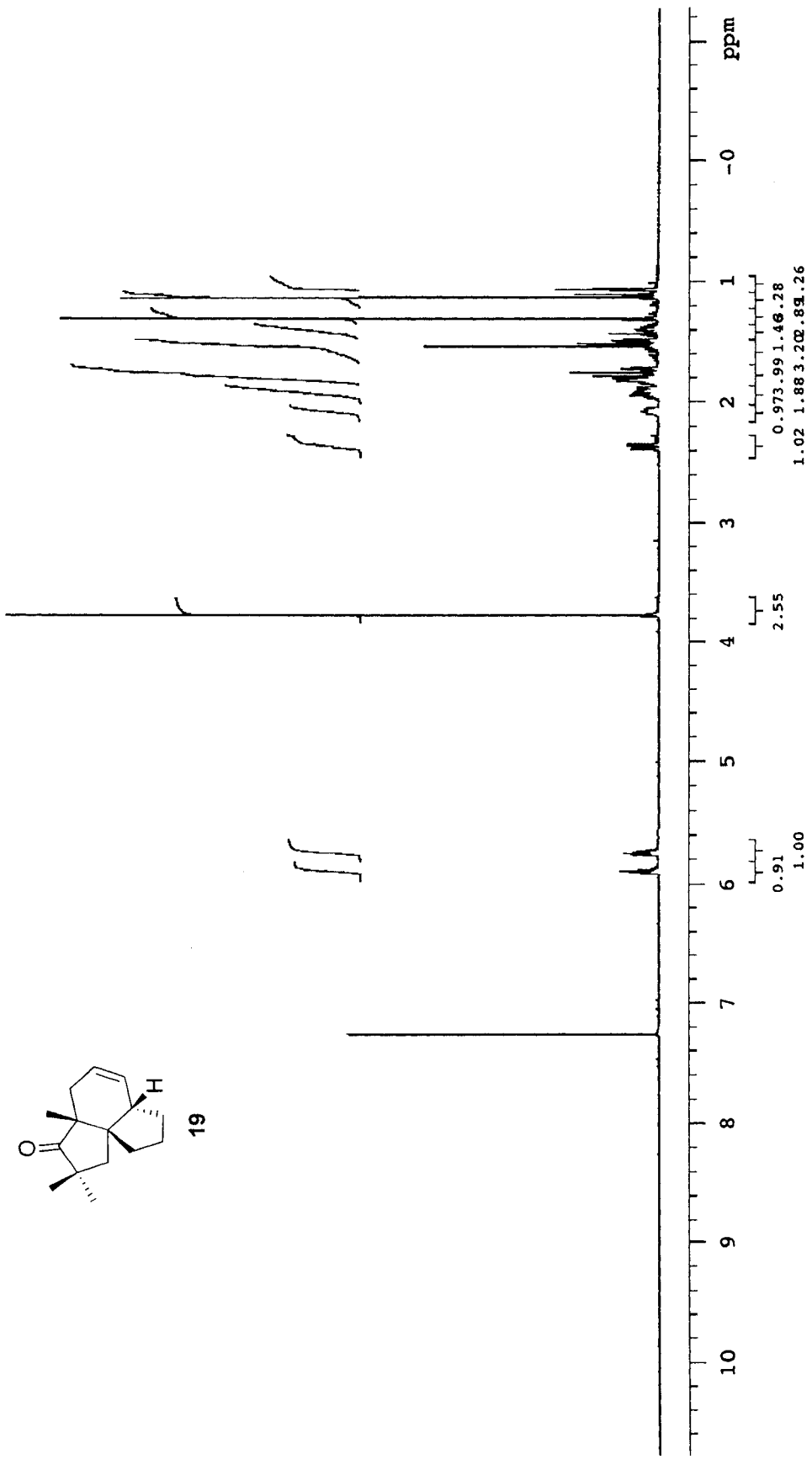

19

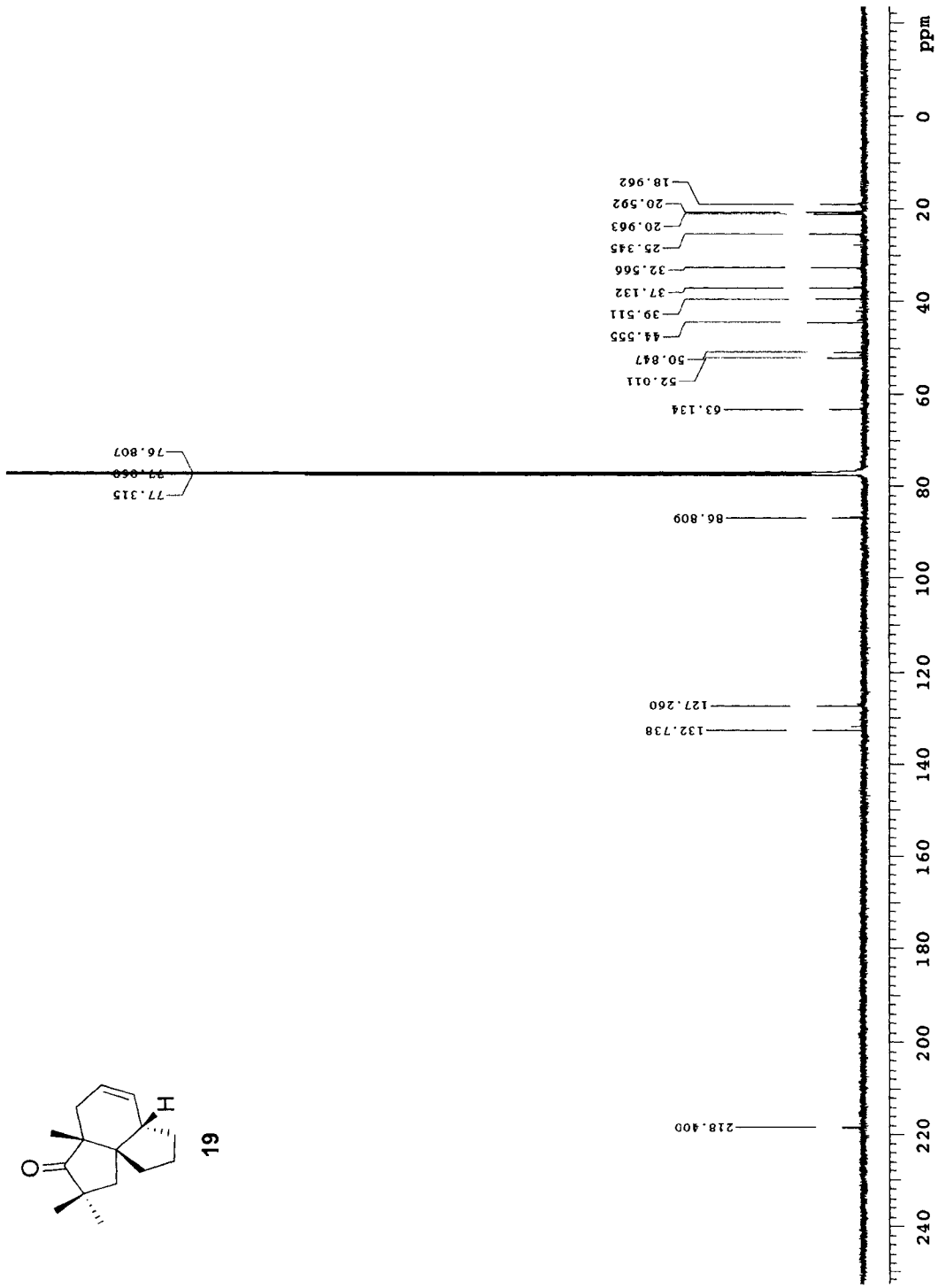

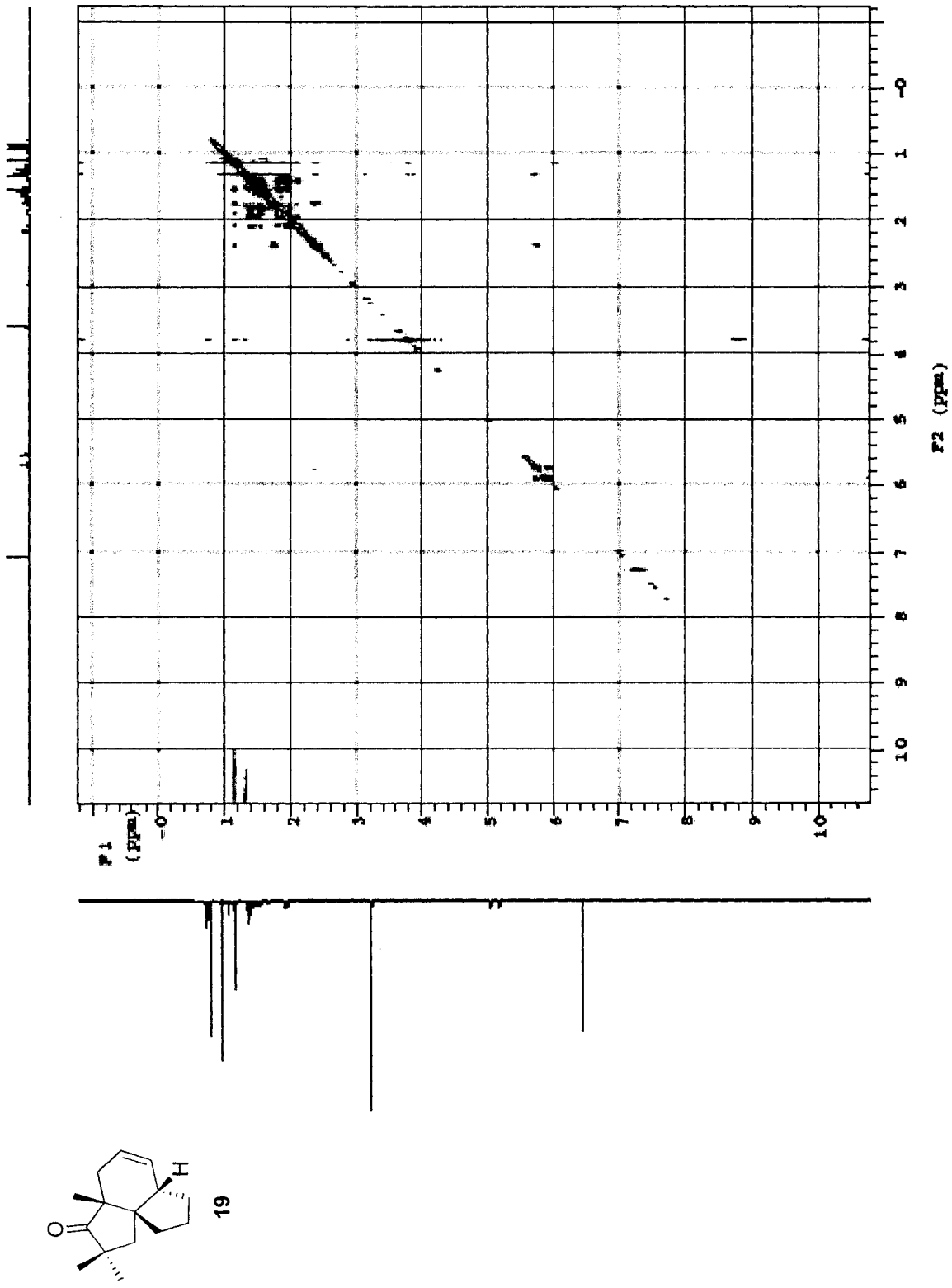

19

Appendix D: X-ray crystallographic data for compound 58a (Chapter 3)

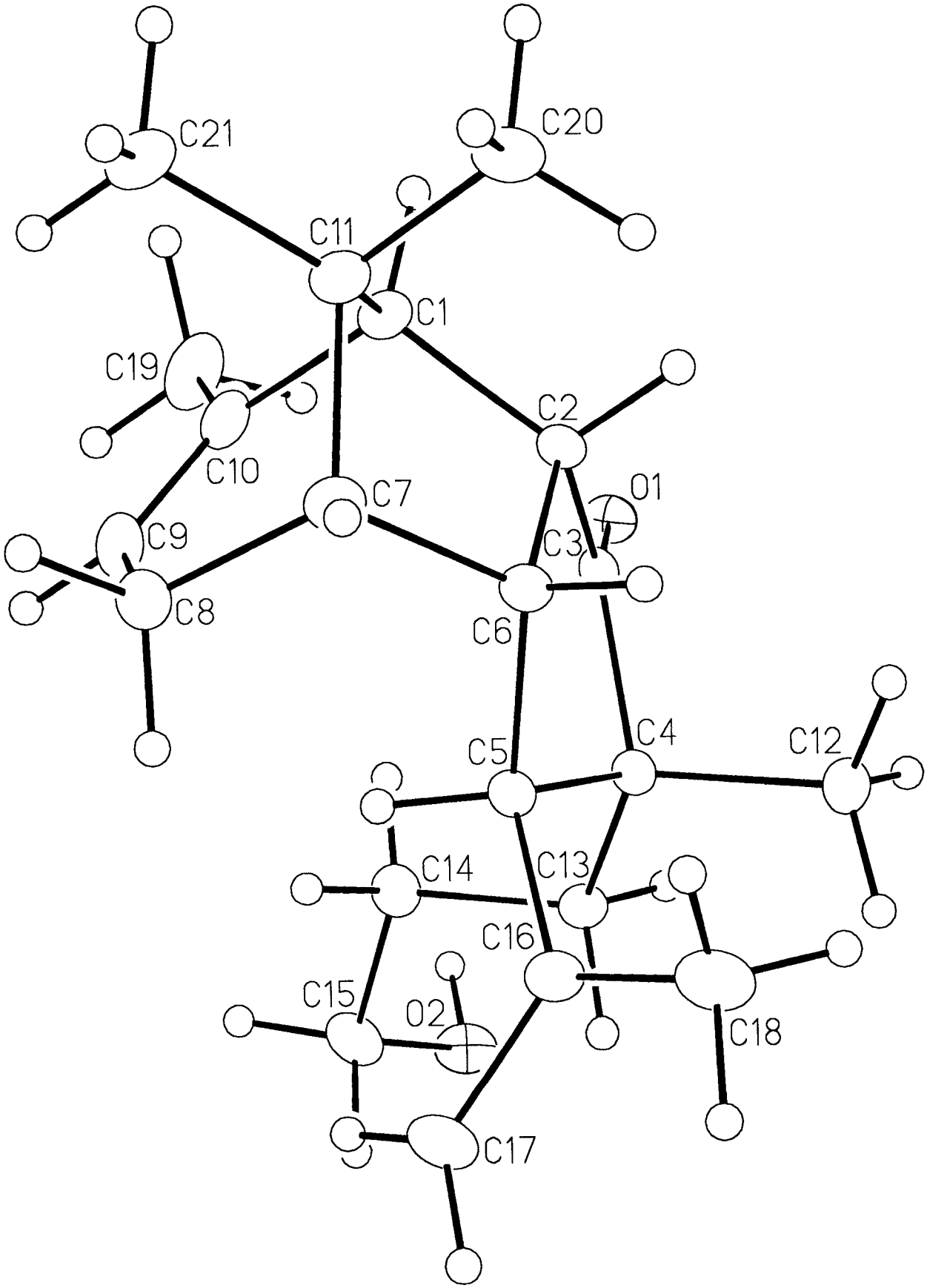

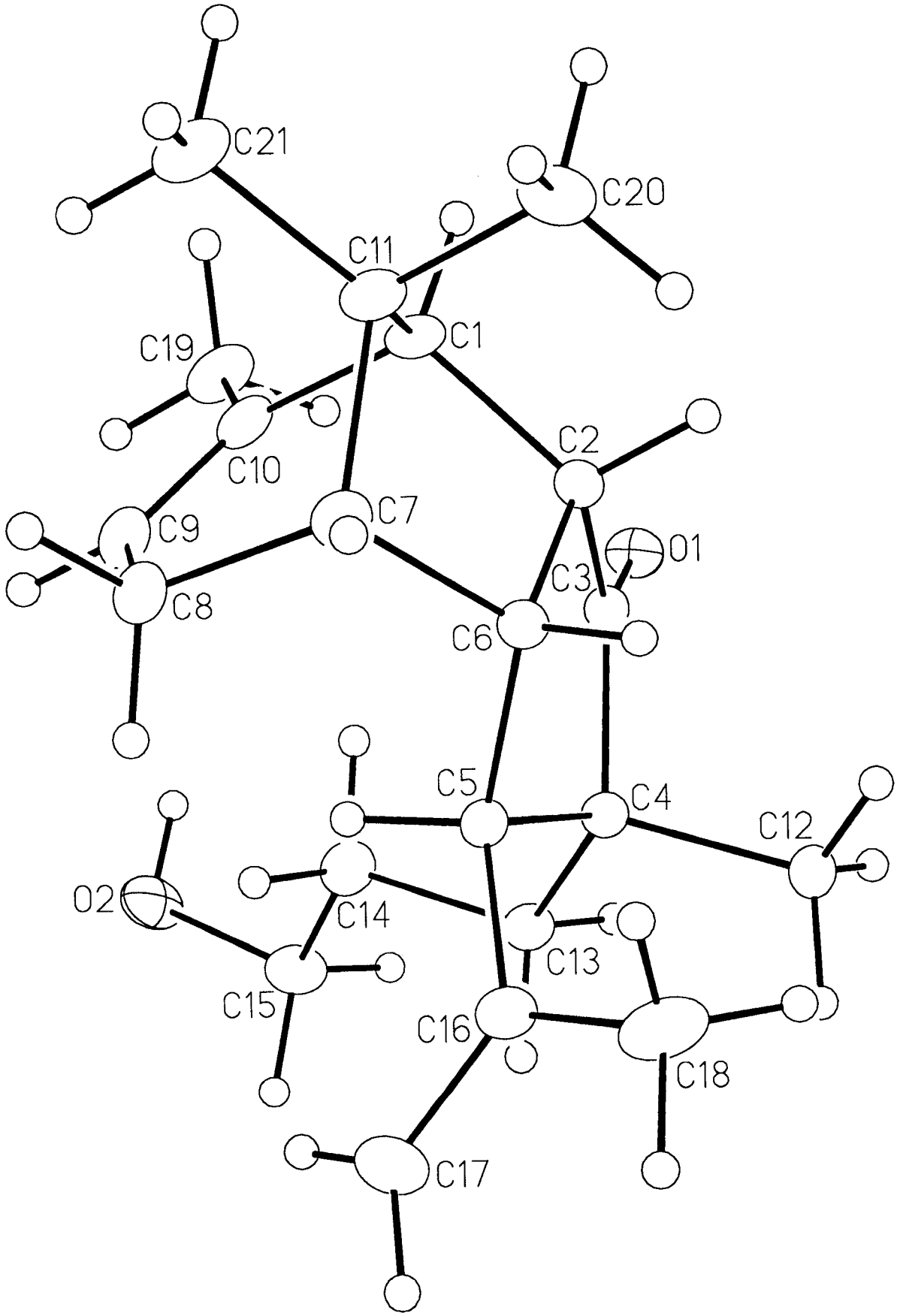

List of Tables

Table 1. Crystallographic Experimental Details

Table 2. Atomic Coordinates and Equivalent Isotropic Displacement Parameters

Table 3. Selected Interatomic Distances

Table 4. Selected Interatomic Angles

Table 5. Torsional Angles

Table 6. Anisotropic Displacement Parameters

Table 7. Derived Atomic Coordinates and Displacement Parameters for Hydrogen Atoms

Table 1. Crystallographic Experimental Details

A. Crystal Data	
formula	$C_{21}H_{32}O_2$
formula weight	316.47
crystal dimensions (mm)	0.58 × 0.26 × 0.22
crystal system	monoclinic
space group	$P2_1$ (No. 4)
unit cell parameters[a]	
a (Å)	11.4752 (11)
b (Å)	9.2954 (9)
c (Å)	17.6872 (17)
β (deg)	94.605 (2)
V (Å^3)	1880.5 (3)
Z	4
ρ_{calcd} (g cm^{-3})	1.118
μ (mm^{-1})	0.069
B. Data Collection and Refinement Conditions	
diffractometer	Bruker PLATFORM/SMART 1000 CCD[b]
radiation (λ [Å])	graphite-monochromated Mo Kα (0.71073)
temperature (°C)	–80
scan type	ω scans (0.3°) (20 s exposures)
data collection 2θ limit (deg)	52.82
total data collected	14551 ($-14 \le h \le 14$, $-11 \le k \le 11$, $-22 \le l \le 22$)
independent reflections	7680 (R_{int} = 0.0250)
number of observed reflections (*NO*)	7075 [$F_o^2 \ge 2\sigma(F_o^2)$]
structure solution method	direct methods (*SHELXS–86*[c])
refinement method	full-matrix least-squares on F^2 (*SHELXL–93*[d])
absorption correction method	multi-scan (*SADABS*)
range of transmission factors	0.9849–0.9608
data/restraints/parameters	7680 [$F_o^2 \ge -3\sigma(F_o^2)$] / 0 / 415
Flack absolute structure parameter[e]	0.0(8)
goodness-of-fit (*S*)[f]	1.029 [$F_o^2 \ge -3\sigma(F_o^2)$]
final R indices[g]	
R_1 [$F_o^2 \ge 2\sigma(F_o^2)$]	0.0406
wR_2 [$F_o^2 \ge -3\sigma(F_o^2)$]	0.1082
largest difference peak and hole	0.223 and –0.184 e Å^{-3}

[a]Obtained from least-squares refinement of 4703 reflections with 4.96° < 2θ < 52.72°.

[b]Programs for diffractometer operation, data collection, data reduction and absorption

correction were those supplied by Bruker.

(continued)

Table 1. Crystallographic Experimental Details (continued)

[c]Sheldrick, G. M. *Acta Crystallogr.* **1990**, *A46*, 467–473.

[d]Sheldrick, G. M. *SHELXL-93*. Program for crystal structure determination. University of Göttingen, Germany, 1993. Refinement on F_o^2 for all reflections (all of these having $F_o^2 \geq -3\sigma(F_o^2)$). Weighted R-factors wR_2 and all goodnesses of fit S are based on F_o^2; conventional R-factors R_1 are based on F_o, with F_o set to zero for negative F_o^2. The observed criterion of $F_o^2 > 2\sigma(F_o^2)$ is used only for calculating R_1, and is not relevant to the choice of reflections for refinement. R-factors based on F_o^2 are statistically about twice as large as those based on F_o, and R-factors based on ALL data will be even larger.

[e]Flack, H. D. *Acta Crystallogr.* **1983**, *A39*, 876–881; Flack, H. D.; Bernardinelli, G. *Acta Crystallogr.* **1999**, *A55*, 908–915; Flack, H. D.; Bernardinelli, G. *J. Appl. Cryst.* **2000**, *33*, 1143–1148. The Flack parameter will refine to a value near zero if the structure is in the correct configuration and will refine to a value near one for the inverted configuration. In this case the presence of only light atoms (carbon, hydrogen, and oxygen) implies that the X-ray data alone cannot be used to unambiguously assign absolute stereochemistry. The known stereochemistry of the precursor compound was used to establish the configuration reported herein.

[f]$S = [\Sigma w(F_o^2 - F_c^2)^2/(n - p)]^{1/2}$ (n = number of data; p = number of parameters varied; $w = [\sigma^2(F_o^2) + (0.0613P)^2 + 0.2293P]^{-1}$ where $P = [\mathrm{Max}(F_o^2, 0) + 2F_c^2]/3$).

[g]$R_1 = \Sigma||F_o| - |F_c||/\Sigma|F_o|$; $wR_2 = [\Sigma w(F_o^2 - F_c^2)^2/\Sigma w(F_o^4)]^{1/2}$.

Table 2. Atomic Coordinates and Equivalent Isotropic Displacement Parameters

(a) atoms of molecule A

Atom	*x*	*y*	*z*	U_{eq}, Å^2
O1	-0.00933(10)	0.23710(13)	0.01511(7)	0.0333(3)*
O2	-0.16287(12)	0.63919(14)	-0.12885(8)	0.0438(3)*
C1	-0.14676(14)	0.0614(2)	0.13393(9)	0.0322(4)*
C2	-0.12957(13)	0.03657(18)	0.04899(9)	0.0268(3)*
C3	-0.09384(13)	0.16081(17)	0.00109(9)	0.0263(3)*
C4	-0.17564(13)	0.16978(16)	-0.07127(9)	0.0260(3)*
C5	-0.29152(13)	0.10742(17)	-0.04454(9)	0.0266(3)*
C6	-0.25229(13)	-0.01078(18)	0.01369(9)	0.0279(3)*
C7	-0.32707(14)	-0.03165(19)	0.08298(10)	0.0337(4)*
C8	-0.39690(15)	0.1012(2)	0.10175(11)	0.0430(4)*
C9	-0.31790(18)	0.2225(2)	0.12914(11)	0.0447(5)*
C10	-0.20401(17)	0.2065(2)	0.14503(10)	0.0381(4)*
C11	-0.23279(15)	-0.0624(2)	0.14892(9)	0.0352(4)*
C12	-0.12070(16)	0.07064(19)	-0.12869(10)	0.0350(4)*
C13	-0.18649(15)	0.32264(17)	-0.10395(9)	0.0297(3)*
C14	-0.22360(17)	0.43905(19)	-0.04986(10)	0.0367(4)*
C15	-0.25493(16)	0.57986(19)	-0.09030(12)	0.0400(4)*
C16	-0.38319(14)	0.0629(2)	-0.10695(9)	0.0336(4)*
C17	-0.46765(19)	0.1608(3)	-0.12959(13)	0.0580(6)*
C18	-0.3823(2)	-0.0781(2)	-0.14110(13)	0.0521(5)*
C19	-0.1259(2)	0.3263(3)	0.17553(13)	0.0567(6)*
C20	-0.17746(18)	-0.2105(2)	0.14094(12)	0.0444(5)*
C21	-0.27825(17)	-0.0554(3)	0.22826(10)	0.0463(5)*

(b) atoms of molecule B

Atom	*x*	*y*	*z*	U_{eq}, Å^2
O1	-0.00140(10)	-0.14848(14)	0.46502(7)	0.0375(3)*
O2	0.14593(15)	-0.64921(15)	0.40585(9)	0.0542(4)*
C1	0.20931(15)	-0.0492(2)	0.58204(9)	0.0350(4)*
C2	0.16442(14)	0.00454(18)	0.50208(9)	0.0295(3)*
C3	0.09076(14)	-0.09500(17)	0.45061(9)	0.0284(3)*
C4	0.14494(14)	-0.11134(17)	0.37474(9)	0.0279(3)*
C5	0.27672(14)	-0.07769(18)	0.39656(8)	0.0284(3)*
C6	0.27832(14)	0.03206(18)	0.46259(9)	0.0292(3)*
C7	0.38013(15)	0.02031(19)	0.52668(9)	0.0343(4)*
C8	0.43691(15)	-0.1283(2)	0.53236(11)	0.0397(4)*
C9	0.35206(17)	-0.2394(2)	0.55571(10)	0.0409(4)*
C10	0.24816(17)	-0.2059(2)	0.57921(9)	0.0385(4)*
C11	0.31594(16)	0.0501(2)	0.59937(10)	0.0397(4)*

Table 2. Atomic Coordinates and Displacement Parameters (continued)

(b) atoms of molecule B

Atom	*x*	*y*	*z*	U_{eq}, Å^2
C12	0.08585(15)	0.00302(19)	0.32163(10)	0.0332(4)*
C13	0.12154(16)	-0.26060(19)	0.33976(10)	0.0333(3)*
C14	0.1570(2)	-0.3889(2)	0.39093(11)	0.0436(4)*
C15	0.1262(2)	-0.5323(2)	0.35480(11)	0.0457(5)*
C16	0.34822(15)	-0.0364(2)	0.33129(9)	0.0373(4)*
C17	0.4008(2)	-0.1371(3)	0.29422(13)	0.0579(6)*
C18	0.3601(2)	0.1186(3)	0.30998(12)	0.0561(6)*
C19	0.1657(2)	-0.3179(3)	0.60517(11)	0.0515(5)*
C20	0.2807(2)	0.2084(2)	0.60316(12)	0.0501(5)*
C21	0.3853(2)	0.0123(3)	0.67461(11)	0.0540(6)*

Anisotropically-refined atoms are marked with an asterisk (*). The form of the anisotropic displacement parameter is: $\exp[-2\pi^2(h^2a^{*2}U_{11} + k^2b^{*2}U_{22} + l^2c^{*2}U_{33} + 2klb^*c^*U_{23} + 2hla^*c^*U_{13} + 2hka^*b^*U_{12})]$.

Table 3. Selected Interatomic Distances (Å)

(a) involving atoms of molecule A

Atom1	Atom2	Distance
O1	C3	1.2109(19)
O1	H2OA[a]	2.015†
O2	C15	1.414(2)
C1	C2	1.548(2)
C1	C10	1.519(3)
C1	C11	1.553(2)
C2	C3	1.508(2)
C2	C6	1.557(2)
C3	C4	1.527(2)
C4	C5	1.558(2)
C4	C12	1.543(2)
C4	C13	1.535(2)
C5	C6	1.548(2)
C5	C16	1.520(2)
C6	C7	1.564(2)
C7	C8	1.523(3)
C7	C11	1.552(2)
C8	C9	1.503(3)
C9	C10	1.323(3)
C10	C19	1.502(3)
C11	C20	1.527(3)
C11	C21	1.537(2)
C13	C14	1.528(2)
C14	C15	1.521(2)
C16	C17	1.366(3)
C16	C18	1.444(3)

[a]Located at $\bar{x}, -1/2 + y, \bar{z}$.
†Nonbonded distance.

(b) involving atoms of molecule B

Atom1	Atom2	Distance
O1	C3	1.214(2)
O1	H2OB[b]	2.094†
O2	C15	1.420(2)
C1	C2	1.549(2)
C1	C10	1.525(3)
C1	C11	1.544(2)
C2	C3	1.509(2)
C2	C6	1.552(2)
C3	C4	1.531(2)
C4	C5	1.562(2)
C4	C12	1.539(2)
C4	C13	1.534(2)
C5	C6	1.550(2)
C5	C16	1.518(2)
C6	C7	1.565(2)
C7	C8	1.527(3)
C7	C11	1.557(3)
C8	C9	1.500(3)
C9	C10	1.331(3)
C10	C19	1.503(3)
C11	C20	1.528(3)
C11	C21	1.536(3)
C13	C14	1.532(3)
C14	C15	1.508(3)
C16	C17	1.317(3)
C16	C18	1.498(3)

[b]Located at $\bar{x}, 1/2 + y, 1 - \bar{z}$.

Table 4. Selected Interatomic Angles (deg)

(a) within molecule A				*(b) within molecule B*			
Atom1	Atom2	Atom3	Angle	Atom1	Atom2	Atom3	Angle
C2	C1	C10	110.36(14)	C2	C1	C10	110.79(14)
C2	C1	C11	100.79(13)	C2	C1	C11	100.86(14)
C10	C1	C11	110.38(14)	C10	C1	C11	110.40(15)
C1	C2	C3	119.49(14)	C1	C2	C3	118.84(14)
C1	C2	C6	104.46(12)	C1	C2	C6	103.52(13)
C3	C2	C6	105.60(12)	C3	C2	C6	106.31(13)
O1	C3	C2	125.63(14)	O1	C3	C2	125.43(14)
O1	C3	C4	124.60(14)	O1	C3	C4	124.43(14)
C2	C3	C4	109.63(13)	C2	C3	C4	110.03(13)
C3	C4	C5	101.97(12)	C3	C4	C5	102.52(12)
C3	C4	C12	105.24(13)	C3	C4	C12	106.04(13)
C3	C4	C13	113.07(13)	C3	C4	C13	111.90(13)
C5	C4	C12	112.41(13)	C5	C4	C12	112.50(13)
C5	C4	C13	114.40(13)	C5	C4	C13	114.54(13)
C12	C4	C13	109.27(13)	C12	C4	C13	108.92(13)
C4	C5	C6	104.85(12)	C4	C5	C6	105.70(12)
C4	C5	C16	116.01(13)	C4	C5	C16	115.74(13)
C6	C5	C16	115.94(14)	C6	C5	C16	115.60(14)
C2	C6	C5	105.75(12)	C2	C6	C5	105.74(13)
C2	C6	C7	104.85(12)	C2	C6	C7	105.62(13)
C5	C6	C7	117.45(13)	C5	C6	C7	117.57(13)
C6	C7	C8	113.69(14)	C6	C7	C8	113.61(14)
C6	C7	C11	102.62(12)	C6	C7	C11	102.15(13)
C8	C7	C11	109.43(15)	C8	C7	C11	109.53(15)
C7	C8	C9	111.37(15)	C7	C8	C9	110.97(15)
C8	C9	C10	122.96(19)	C8	C9	C10	122.85(18)
C1	C10	C9	120.17(17)	C1	C10	C9	120.36(17)
C1	C10	C19	116.91(17)	C1	C10	C19	117.27(18)
C9	C10	C19	122.9(2)	C9	C10	C19	122.36(19)
C1	C11	C7	98.59(13)	C1	C11	C7	98.60(13)
C1	C11	C20	112.19(14)	C1	C11	C20	112.08(16)
C1	C11	C21	113.03(15)	C1	C11	C21	112.50(17)
C7	C11	C20	111.50(16)	C7	C11	C20	110.61(16)
C7	C11	C21	114.26(14)	C7	C11	C21	115.34(16)
C20	C11	C21	107.26(15)	C20	C11	C21	107.63(17)
C4	C13	C14	115.98(13)	C4	C13	C14	115.86(14)
C13	C14	C15	112.48(15)	C13	C14	C15	113.30(15)
O2	C15	C14	113.88(15)	O2	C15	C14	112.78(16)
C5	C16	C17	117.73(17)	C5	C16	C17	119.70(19)
C5	C16	C18	121.53(16)	C5	C16	C18	120.01(16)
C17	C16	C18	120.74(17)	C17	C16	C18	120.28(19)

Table 5. Torsional Angles (deg)

(a) within molecule A					*(b) within molecule B*				
Atom1	Atom2	Atom3	Atom4	Angle	Atom1	Atom2	Atom3	Atom4	Angle
C10	C1	C2	C3	38.55(19)	C10	C1	C2	C3	40.2(2)
C10	C1	C2	C6	-79.15(16)	C10	C1	C2	C6	-77.33(16)
C11	C1	C2	C3	155.22(13)	C11	C1	C2	C3	157.10(14)
C11	C1	C2	C6	37.52(15)	C11	C1	C2	C6	39.58(16)
C2	C1	C10	C9	78.36(19)	C2	C1	C10	C9	79.4(2)
C2	C1	C10	C19	-102.64(18)	C2	C1	C10	C19	-101.68(18)
C11	C1	C10	C9	-32.2(2)	C11	C1	C10	C9	-31.5(2)
C11	C1	C10	C19	146.82(16)	C11	C1	C10	C19	147.45(15)
C2	C1	C11	C7	-52.29(15)	C2	C1	C11	C7	-53.32(16)
C2	C1	C11	C20	65.22(17)	C2	C1	C11	C20	63.14(18)
C2	C1	C11	C21	-173.34(14)	C2	C1	C11	C21	-175.41(16)
C10	C1	C11	C7	64.37(16)	C10	C1	C11	C7	63.87(17)
C10	C1	C11	C20	-178.12(15)	C10	C1	C11	C20	-179.67(15)
C10	C1	C11	C21	-56.69(19)	C10	C1	C11	C21	-58.2(2)
C1	C2	C3	O1	54.5(2)	C1	C2	C3	O1	58.6(2)
C1	C2	C3	C4	-129.54(14)	C1	C2	C3	C4	-125.20(15)
C6	C2	C3	O1	171.63(15)	C6	C2	C3	O1	174.63(16)
C6	C2	C3	C4	-12.43(16)	C6	C2	C3	C4	-9.15(17)
C1	C2	C6	C5	116.71(14)	C1	C2	C6	C5	114.98(14)
C1	C2	C6	C7	-8.06(16)	C1	C2	C6	C7	-10.34(17)
C3	C2	C6	C5	-10.14(16)	C3	C2	C6	C5	-10.98(16)
C3	C2	C6	C7	-134.91(13)	C3	C2	C6	C7	-136.30(13)
O1	C3	C4	C5	-154.49(15)	O1	C3	C4	C5	-158.64(16)
O1	C3	C4	C12	88.01(18)	O1	C3	C4	C12	83.21(19)
O1	C3	C4	C13	-31.2(2)	O1	C3	C4	C13	-35.4(2)
C2	C3	C4	C5	29.52(15)	C2	C3	C4	C5	25.10(16)
C2	C3	C4	C12	-87.98(14)	C2	C3	C4	C12	-93.05(15)
C2	C3	C4	C13	152.83(13)	C2	C3	C4	C13	148.32(14)
C3	C4	C5	C6	-34.89(15)	C3	C4	C5	C6	-31.25(15)
C3	C4	C5	C16	-164.15(14)	C3	C4	C5	C16	-160.58(14)
C12	C4	C5	C6	77.33(16)	C12	C4	C5	C6	82.23(15)
C12	C4	C5	C16	-51.94(18)	C12	C4	C5	C16	-47.10(19)
C13	C4	C5	C6	-157.29(13)	C13	C4	C5	C6	-152.68(13)
C13	C4	C5	C16	73.44(18)	C13	C4	C5	C16	77.99(18)
C3	C4	C13	C14	-55.01(19)	C3	C4	C13	C14	-53.5(2)
C5	C4	C13	C14	61.14(19)	C5	C4	C13	C14	62.58(19)
C12	C4	C13	C14	-171.85(15)	C12	C4	C13	C14	-170.46(15)
C4	C5	C6	C2	28.30(16)	C4	C5	C6	C2	26.55(16)
C4	C5	C6	C7	144.83(14)	C4	C5	C6	C7	144.11(14)

Table 5. Torsional Angles (continued)

(a) within molecule A					*(b) within molecule B*				
Atom1	Atom2	Atom3	Atom4	Angle	Atom1	Atom2	Atom3	Atom4	Angle
C16	C5	C6	C2	157.61(13)	C16	C5	C6	C2	155.96(14)
C16	C5	C6	C7	-85.86(18)	C16	C5	C6	C7	-86.47(18)
C4	C5	C16	C17	-94.5(2)	C4	C5	C16	C17	-89.4(2)
C4	C5	C16	C18	86.0(2)	C4	C5	C16	C18	91.4(2)
C6	C5	C16	C17	141.86(18)	C6	C5	C16	C17	146.22(18)
C6	C5	C16	C18	-37.7(2)	C6	C5	C16	C18	-32.9(2)
C2	C6	C7	C8	93.57(16)	C2	C6	C7	C8	95.45(17)
C2	C6	C7	C11	-24.49(17)	C2	C6	C7	C11	-22.42(17)
C5	C6	C7	C8	-23.4(2)	C5	C6	C7	C8	-22.2(2)
C5	C6	C7	C11	-141.51(14)	C5	C6	C7	C11	-140.05(15)
C6	C7	C8	C9	-66.37(19)	C6	C7	C8	C9	-65.2(2)
C11	C7	C8	C9	47.70(19)	C11	C7	C8	C9	48.33(19)
C6	C7	C11	C1	47.27(16)	C6	C7	C11	C1	46.35(16)
C6	C7	C11	C20	-70.77(17)	C6	C7	C11	C20	-71.23(17)
C6	C7	C11	C21	167.41(15)	C6	C7	C11	C21	166.35(16)
C8	C7	C11	C1	-73.77(16)	C8	C7	C11	C1	-74.38(16)
C8	C7	C11	C20	168.19(14)	C8	C7	C11	C20	168.03(15)
C8	C7	C11	C21	46.4(2)	C8	C7	C11	C21	45.6(2)
C7	C8	C9	C10	-9.2(2)	C7	C8	C9	C10	-9.5(2)
C8	C9	C10	C1	1.6(3)	C8	C9	C10	C1	1.2(3)
C8	C9	C10	C19	-177.33(17)	C8	C9	C10	C19	-177.72(17)
C4	C13	C14	C15	-168.91(14)	C4	C13	C14	C15	177.07(17)
C13	C14	C15	O2	-58.8(2)	C13	C14	C15	O2	-172.60(18)

Table 6. Anisotropic Displacement Parameters (U_{ij}, Å^2)

(a) atoms of molecule A

Atom	U_{11}	U_{22}	U_{33}	U_{23}	U_{13}	U_{12}
O1	0.0263(5)	0.0351(6)	0.0382(6)	0.0065(5)	0.0017(5)	-0.0057(5)
O2	0.0465(7)	0.0364(7)	0.0468(7)	0.0079(6)	-0.0069(6)	-0.0094(6)
C1	0.0287(8)	0.0402(9)	0.0278(8)	0.0066(7)	0.0020(6)	-0.0044(7)
C2	0.0228(7)	0.0270(7)	0.0303(8)	0.0039(6)	0.0008(6)	0.0006(6)
C3	0.0232(7)	0.0272(8)	0.0293(7)	0.0015(6)	0.0069(6)	0.0046(6)
C4	0.0281(7)	0.0230(7)	0.0271(7)	0.0020(6)	0.0040(6)	0.0019(6)
C5	0.0258(7)	0.0258(7)	0.0282(7)	0.0021(6)	0.0022(6)	0.0011(6)
C6	0.0269(7)	0.0264(8)	0.0300(8)	0.0043(6)	0.0009(6)	-0.0015(6)
C7	0.0275(8)	0.0391(9)	0.0345(8)	0.0088(7)	0.0028(6)	-0.0089(7)
C8	0.0287(8)	0.0605(12)	0.0412(10)	0.0095(9)	0.0117(7)	0.0032(8)
C9	0.0473(11)	0.0474(11)	0.0418(10)	0.0004(8)	0.0189(8)	0.0071(9)
C10	0.0463(10)	0.0403(10)	0.0293(8)	-0.0016(7)	0.0133(7)	-0.0055(8)
C11	0.0312(8)	0.0422(10)	0.0325(8)	0.0106(7)	0.0034(6)	-0.0052(7)
C12	0.0417(9)	0.0305(8)	0.0338(9)	0.0009(7)	0.0090(7)	0.0031(7)
C13	0.0347(8)	0.0250(8)	0.0292(8)	0.0043(6)	0.0014(6)	0.0004(6)
C14	0.0431(9)	0.0277(8)	0.0399(9)	0.0020(7)	0.0065(7)	0.0029(7)
C15	0.0371(9)	0.0255(8)	0.0563(11)	0.0035(8)	-0.0028(8)	0.0021(7)
C16	0.0301(8)	0.0371(9)	0.0331(8)	0.0039(7)	-0.0012(6)	-0.0038(7)
C17	0.0535(12)	0.0566(13)	0.0595(13)	-0.0140(11)	-0.0224(10)	
	0.0218(11)					
C18	0.0529(12)	0.0387(10)	0.0608(12)	-0.0073(10)	-0.0210(10)	0.0005(9)
C19	0.0704(15)	0.0527(13)	0.0493(12)	-0.0136(10)	0.0193(10)	-
0.0190(11)						
C20	0.0445(11)	0.0418(10)	0.0468(11)	0.0185(9)	0.0030(8)	-0.0009(8)
C21	0.0411(10)	0.0631(13)	0.0352(9)	0.0143(9)	0.0060(7)	-0.0125(9)

(b) atoms of molecule B

Atom	U_{11}	U_{22}	U_{33}	U_{23}	U_{13}	U_{12}
O1	0.0343(6)	0.0427(7)	0.0358(6)	-0.0054(5)	0.0048(5)	-0.0059(5)
O2	0.0801(11)	0.0285(6)	0.0572(8)	0.0017(6)	0.0259(8)	0.0054(7)
C1	0.0399(9)	0.0417(10)	0.0235(8)	-0.0052(7)	0.0024(6)	-0.0057(8)
C2	0.0321(8)	0.0272(8)	0.0291(8)	-0.0040(6)	0.0017(6)	0.0002(6)
C3	0.0304(8)	0.0271(8)	0.0272(7)	-0.0013(6)	-0.0007(6)	0.0019(7)
C4	0.0330(8)	0.0252(8)	0.0252(7)	-0.0026(6)	0.0005(6)	0.0000(6)
C5	0.0313(8)	0.0285(8)	0.0252(7)	-0.0007(6)	0.0001(6)	0.0016(6)
C6	0.0325(8)	0.0264(8)	0.0285(8)	-0.0023(6)	0.0012(6)	-0.0012(6)
C7	0.0351(8)	0.0349(9)	0.0323(9)	-0.0025(7)	-0.0014(7)	-0.0084(7)
C8	0.0327(9)	0.0471(10)	0.0377(9)	0.0017(8)	-0.0063(7)	0.0021(8)

C9	0.0475(10)	0.0371(10)	0.0365(9)	0.0045(8)	-0.0064(8)	0.0037(8)
C10	0.0474(10)	0.0416(10)	0.0251(8)	0.0056(7)	-0.0055(7)	-0.0053(8)

Table 6. Anisotropic Displacement Parameters (continued)

(b) atoms of molecule B

Atom	U_{11}	U_{22}	U_{33}	U_{23}	U_{13}	U_{12}
C11	0.0441(10)	0.0457(10)	0.0283(8)	-0.0078(8)	-0.0026(7)	-0.0070(9)
C12	0.0348(8)	0.0315(8)	0.0325(8)	-0.0003(7)	-0.0020(7)	0.0030(7)
C13	0.0413(9)	0.0295(8)	0.0287(8)	-0.0047(7)	0.0003(6)	-0.0019(7)
C14	0.0622(12)	0.0296(9)	0.0382(9)	-0.0019(8)	-0.0009(8)	0.0001(9)
C15	0.0673(13)	0.0292(9)	0.0420(10)	-0.0050(8)	0.0137(9)	-0.0061(9)
C16	0.0310(8)	0.0512(11)	0.0297(8)	-0.0028(8)	0.0017(6)	-0.0026(8)
C17	0.0489(12)	0.0772(16)	0.0498(11)	-0.0065(11)	0.0167(9)	0.0078(12)
C18	0.0682(14)	0.0638(14)	0.0381(10)	0.0037(10)	0.0146(10)	-0.0239(12)
C19	0.0650(13)	0.0528(12)	0.0363(10)	0.0124(9)	0.0018(9)	-0.0158(11)
C20	0.0556(12)	0.0470(12)	0.0470(11)	-0.0224(9)	0.0002(9)	-0.0079(9)
C21	0.0555(12)	0.0692(15)	0.0352(10)	-0.0062(10)	-0.0096(9)	-0.0135(11)

The form of the anisotropic displacement parameter is:

$\exp[-2\pi^2(h^2a^{*2}U_{11} + k^2b^{*2}U_{22} + l^2c^{*2}U_{33} + 2klb^*c^*U_{23} + 2hla^*c^*U_{13} + 2hka^*b^*U_{12})]$

Table 7. Derived Atomic Coordinates and Displacement Parameters for Hydrogen Atoms

(a) atoms of molecule A

Atom	*x*	*y*	*z*	U_{eq}, Å^2
H2OA	-0.1103	0.6696	-0.0971	0.053
H1A	-0.0715	0.0518	0.1662	0.039
H2A	-0.0732	-0.0444	0.0444	0.032
H5A	-0.3274	0.1857	-0.0154	0.032
H6A	-0.2454	-0.1047	-0.0132	0.033
H7A	-0.3802	-0.1164	0.0745	0.040
H8AA	-0.4457	0.1323	0.0560	0.052
H8AB	-0.4497	0.0767	0.1415	0.052
H9A	-0.3512	0.3149	0.1353	0.054
H12A	-0.0484	0.1142	-0.1439	0.042
H12B	-0.1758	0.0578	-0.1735	0.042
H12C	-0.1030	-0.0231	-0.1052	0.042
H13A	-0.1100	0.3504	-0.1218	0.036
H13B	-0.2439	0.3207	-0.1488	0.036
H14A	-0.2920	0.4045	-0.0243	0.044
H14B	-0.1591	0.4564	-0.0103	0.044
H15A	-0.3230	0.5634	-0.1273	0.048
H15B	-0.2786	0.6506	-0.0526	0.048
H17A	-0.5267	0.1364	-0.1682	0.070
H17B	-0.4674	0.2533	-0.1067	0.070
H18A	-0.4476	-0.0863	-0.1801	0.063
H18B	-0.3901	-0.1515	-0.1021	0.063
H18C	-0.3084	-0.0923	-0.1643	0.063
H19A	-0.1723	0.4139	0.1801	0.068
H19B	-0.0649	0.3438	0.1409	0.068
H19C	-0.0895	0.2994	0.2256	0.068
H20A	-0.2345	-0.2852	0.1510	0.053
H20B	-0.1089	-0.2195	0.1774	0.053
H20C	-0.1535	-0.2219	0.0893	0.053
H21A	-0.3147	0.0385	0.2353	0.056
H21B	-0.2129	-0.0686	0.2668	0.056
H21C	-0.3361	-0.1316	0.2332	0.056

Table 7. Derived Parameters for Hydrogen Atoms (continued)

(b) atoms of molecule B

Atom	*x*	*y*	*z*	U_{eq}, Å^2
H2OB	0.1016	-0.6416	0.4412	0.065
H1B	0.1494	-0.0351	0.6194	0.042
H2B	0.1220	0.0976	0.5069	0.035
H5B	0.3121	-0.1683	0.4185	0.034
H6B	0.2765	0.1318	0.4414	0.035
H7B	0.4404	0.0960	0.5201	0.041
H8BA	0.4644	-0.1549	0.4826	0.048
H8BB	0.5056	-0.1255	0.5699	0.048
H9B	0.3734	-0.3380	0.5536	0.049
H12D	0.0040	-0.0235	0.3089	0.040
H12E	0.1266	0.0087	0.2751	0.040
H12F	0.0894	0.0967	0.3471	0.040
H13C	0.0370	-0.2684	0.3242	0.040
H13D	0.1638	-0.2677	0.2932	0.040
H14C	0.2424	-0.3853	0.4042	0.052
H14D	0.1178	-0.3805	0.4386	0.052
H15C	0.0428	-0.5314	0.3355	0.055
H15D	0.1735	-0.5465	0.3110	0.055
H17C	0.4465	-0.1117	0.2538	0.070
H17D	0.3930	-0.2353	0.3079	0.070
H18D	0.4090	0.1263	0.2672	0.067
H18E	0.3966	0.1722	0.3534	0.067
H18F	0.2826	0.1588	0.2955	0.067
H19D	0.2000	-0.4136	0.6002	0.062
H19E	0.0914	-0.3126	0.5739	0.062
H19F	0.1518	-0.3004	0.6584	0.062
H20D	0.3506	0.2675	0.6143	0.060
H20E	0.2274	0.2214	0.6432	0.060
H20F	0.2414	0.2376	0.5543	0.060
H21D	0.4518	0.0782	0.6831	0.065
H21E	0.4141	-0.0867	0.6724	0.065
H21F	0.3345	0.0214	0.7163	0.065